UNIVERSITY OF NIŠ Faculty of Technology, Leskovac

PROCEEDINGS

16th INTERNATIONAL SYMPOSIUM "NOVEL TECHNOLOGIES AND SUSTAINABLE DEVELOPMENT" UNIVERSITY OF NIŠ
Faculty of Technology, Leskovac

PROCEEDINGS 16th INTERNATIONAL SYMPOSIUM "NOVEL TECHNOLOGIES AND SUSTAINABLE DEVELOPMENT" Leskovac. 2025.

Faculty of Technology, Leskovac

Publisher: Faculty of Technology, Leskovac For the Publisher: Prof. Dragiša Savić

Editor: Prof. Dragan Đorđević, Full Professor, Faculty of Technology, Leskovac

СІР - Каталогизација у публикацији Народна библиотека Србије, Београд

6(082)(0.034.2)

INTERNATIONAL Symposium "Novel Technologies and Sustainable Development" (16; 2025; Leskovac)

Proceedings [Elektronski izvor] / 16th International Symposium "Novel Technologies and Sustainable Development" Leskovac, October, 17-18, 2025.; editor Dragan Đorđević. - Leskovac: Faculty of Technology, 2025 (Leskovac: Faculty of Technology). - 1 elektronski optički disk (CD-ROM); 12 cm

Sistemski zahtevi: Nisu navedeni. - Nasl. sa naslovne strane dokumenta. - Na vrhu nasl. str.: University of Niš. - Tiraž 30. - Bibliografija uz svaki rad.

ISBN 978-86-89429-63-3

а) Технологија -- Зборници b) Технолошки прогрес -- Привредни развој -- Зборници

COBISS.SR-ID 176444425

Printing by: Faculty of Technology, Leskovac

Impression: 30

Proofreader: Jovana Nikolić

Paging and graphical design: Vesna Marinković

ISBN 978-86-89429-63-3 DOI: 10.46793/NoveITSD16

All papers are licensed under a CC BY 4.0 Attribution 4.0 International License





16th International Symposium "Novel Technologies and Sustainable Development" Organized by: Faculty of Technology, Leskovac

The Programme Committee:

Prof. Olivera Stamenković, Full professor, Faculty of Technology, Leskovac, Serbia

Prof. Goran Nikolić, Full professor, Faculty of Technology, Leskovac, Serbia

Dr Saša Savić, Assistant professor, Faculty of Technology, Leskovac, Serbia

Dr Marija Miladinović, Assistant professor, Faculty of Technology Leskovac, Serbia

Dr Miloš Kostić, Senior Research Associate, Faculty of Sciences and Mathematics, Niš, Serbia

Prof. Mirjana Kijevčanin, Full professor, Faculty of Technology and Metallurgy, Belgrade, Serbia

Prof. Zita Šereš, Full professor, Faculty of Technology, Novi Sad, Serbia

Dr Nataša Đurišić Mladenović, Associate professor, Faculty of Technology, Novi Sad, Serbia

Dr Branko Matović, Principal Research Fellow, Tehe Institute for Nuclear sciences Vinca, National Institute of the Republic of Serbia. Belgrade. Serbia

Dr Jasna Stajić Trošić, Principal Research Fellow, Institute for Chemistry, Technology and Metallurgy,

National Institute of the Republic of Serbia, Belgrade, Serbia

Prof. Borislav Malinović, Full professor, Faculty of Technology, Banja Luka, Bosnia and Herzegovina

Prof. Anita Tarbuk, Full professor, Faculty of Textile technology, Zagreb, Croatia

Dr Karmina Miteva, Associate profesor, Faculty of Technology and Metallurgy, Skopje, Republic of Northern Macedonia

Dr Luca Polleto, Senior research scientist, National Council of Research of Italy, Institute of Photonics and Nanotechnologies, Padova, Italy

Dr Farzam Fotovat, Associate profesor, Sharif University of Technology, Teheran, Iran

Dr Marcela Elisabeta Barbinta-Patrascu, Associate profesor, Faculty of Physics, Univetsity of Bucharest, Bucharest, Romania

Dr Ljubica Tasić, Associate profesor, Instituteof Chemistry, University of Campinas. Sao Paolo, Brasil

Dr Dejan Nikolić, Research associate professor, Center for Botanical Dietary Supplements Research, State University of Illinois, Chicago, USA

Prof. Irena Žižović, Full Professor, Faculzy of Chemistry Wroclaw University of Sciece and Technology, Wroclaw, Poland

Dr Zou Xiaobo, Full Professor, School of Food and Biological Engineering, Jiangsu, China

Dr Zhang Di, Associate Professor, School of Food and Biological Engineering, Jiangsu, China

Dr Hristo Najdenski, Corresponding Member of BAS, Insitute of Microbiology "Stefan Angelov", Sofia, Bulgaria

Dr Igor Jordanov, Full Professor, Faculty of Technology and Metallurgy, Skopje, North Macedonia

Dr Dani Djordjevic, Associate Professor, Faculty of Veterinary Hygiene and Ecology, Universuty of Veterinary Sciemces, Brno, Czech Republic

The Organizing Committee:

Prof. Dragiša Savić, Full Professor, Faculty of Technology, Leskovac, Serbia

Goran Cvetanović, Mayor, Leskovac, Serbia

Goran Jović, Director of the Regional Chamber of Commerce and Industry of Jablanica and Pćinja District, Leskovac, Serbia

Igor Denić, Director, DCP Hemigal, Leskovac, Serbia

Radojica Ristić, Director, NEVENA COLOR, Ltd, Leskovac, Serbia

Aleksandar Stanković, ELIXIR, Ltd, Prahovo, Serbia

Dr Petar Stojanović, Director, DUNAV, Grocka, Serbia

Dr Predrag Stamenković, Director, Academy of South Serbia, Leskovac, Serbia

Prof. Dušan Traiković. Full Professor, Faculty of Technology, Leskovac, Serbia

Dr Ivan Savić, Associate Professor, Faculty of Technology, Leskovac, Serbia

Prof. Zoran Kostić, Full Professor, Faculty of Technology, Leskovac, Serbia

Dr Milan Kostić, Assistant Professor, Faculty of Technology, Leskovac, Serbia

Dr Biliana Đođević, Assistant, Faculty of Technology, Leskovac, Serbia

Čedomir Dimić, Junior Research Assistant, Faculty of Technology, Leskovac, Serbia

Dejan Ranđelović, Faculty of Technology, Leskovac, Serbia

Miloš Stevanović, Faculty of Technology, Leskovac, Serbia

Jovana Nikolić, Faculty of Technology, Leskovac, Serbia

CONTENS

Section: FOOD ENGINEERING Slađana Stanojević, Danijel Milinčić, Mirjana Pešić COMPOSITION OF CARBOHYDRATES IN FRESH WHEY AS WASTE IN TOFU PROCESSING 9 Section: MATERIALS ENGINEERING Sandra Bulatović, Natalija Nedić, Tamara Tadić, Bojana Marković, Aleksandra Žerađanin, Aleksandra Nastasović GMA/Ag COMPOSITE AS ANTIMICROBIAL AGENT 21 Section: ENVIRONMENTAL ENGINEERING Bojana Marković, Tamara Tadić, Sandra Bulatović, Natalija Nedić, Aleksandra Nastasović DISPERSIVE SOLID-PHASE MICROEXTRACTION BASED ON AMINO-FUNCTIONALIZED POLYMER FOR PRECONCENTRATION OF AZO DYE 31 FROM AQUEOUS SAMPLES Jovana Ilić Pajić, Jasna Stajić-Trošić, Mirko Stijepović, Srdjan Perišić, Vladimir Stijepović, Aleksandar Grujić RECYCLING AND REUSE OF ORGANIC SOLVENTS FROM WASTE PAINTS 42 Section: TEXTILE ENGINEERING Anita Tarbuk, Lea Botteri, Stefana Begović THE INFLUENCE OF ENZYMATIC PRE-TREATMENT ON THE ADSORPTION OF COTTON-POLYESTER BLENDED FABRIC 59 Sandra Flinčec Grgac, Franka Žuvela Bošnjak, Ana Palčić, Tanja Krivec APPLICATION OF IN-SITU HYDROTHERMAL SYNTHESIS FOR THE FUNCTIONALISATION OF COTTON/POLYESTER FABRIC WITH THE INCLUSION COMPLEX OF B-CYCLODEXTRIN AND ESSENTIAL TEATREE 70 OIL Suzana Đorđević, Sandra Stojanović, Slađana Antić EFFICIENCY OF COTTON FABRIC DESIZING USING DIFFERENT **METHODS** 82 Suzana Đorđević, Anita Tarbuk, Nikola Stojanović, Tihana Dekanić, Dragan Đorđević SIZING OF COTTON YARN WITH A COPOLYMER OF ACRYLAMIDE AND **ACRYLIC ACID** 94 Marija Kodrić, Shahidul Islam, Zorica Eraković, Predrag Tasić, Dragan Đorđević COLOURABILITY AND FASTNESS OF COLOURED POLYESTER KNITTED FABRIC AFTER PRETREATMENT 105 Shahidul Islam, Md. Rahamatolla, Marija Kodric, Sanjay Belowar MECHANISTIC INSIGHTS INTO THE CHEMISORPTION OF INDUSTRIAL DYES ON TI3C2 MXENE SURFACE FOR WASTE WATER TREATMENT 117 APPLICATION: A THEORETICAL APPROACH

| Jelena Jovićević Pavković, Dragan Djordjević | |
|---|-----|
| DYEING KINETICS OF MULTI-COMPONENT TEXTILE YARN WITH BASIC | |
| DYE | 133 |
| Jelena Jovićević Pavković, Dragan Đorđević | |
| DECOLORIZATION OF AQUEOUS SOLUTION OF TEXTILE DYE USING | |
| VOLCANIC ASH-BASED ADSORBENT | 143 |
| Predrag Tasić, Dušan Trajković, Nenad Ćirković, Jelka Geršak | |
| COMPRESSIBLE PROPERTIES OF MEN'S SOCKS MADE FROM | |
| DIFFERENT FIBERS IN PLAIN JERSEY | 153 |
| Predrag Tasić, Dusan Trajković, Jovan Stepanović, Jelka Geršak | |
| THERMAL, PHYSIOLOGICAL, AND THERMOGRAPHIC ANALYSIS OF | |
| MEN'S BAMBOO SOCKS IN A RIGHT-LEFT KNIT STRUCTURE | 163 |
| Sandra Stojanović, Dušan Trajković, Suzana Đorđević, | |
| Slađana Antić, Tanja Nikolić, Svetomir Golubović | |
| ANALYSIS OF SURFACE PROPERTY CHANGES ON THE REVERSE SIDE | |
| OF KNITTED FABRICS AFTER PRINTING | 175 |
| Slađana Antić, Suzana Đorđević, Sandra Stojanović, Tanja Nikolić, | |
| Svetomir Golubović | |
| THE INFLUENCE OF RELATIVE AIR HUMIDITY ON THE ELECTRICAL | |
| RESISTIVITY OF WOVEN FABRICS INTENDED FOR OUTERWEAR | 187 |
| Ferhan Gebes, İlter Sevilen, Kenan Yıldırım | |
| EFFECT OF TOW BREAK CONDITIONS ON THE PROPERTIES OF HIGH- | |
| BULK ACRYLIC YARN | 198 |
| Section: TECHNOLOGY AND SUSTAINABLE DEVELOPMENT | |
| OCCION. I CONTOCCOT AND GOSTAMABLE DEVELOT MENT | |
| Drago Cvijanović, Aleksandra Vujko, Božo Ilić | |
| HOSPITALITY 4.0 IN THE WESTERN BALKANS: TECHNOLOGICAL | |
| INNOVATION FOR A SUSTAINABLE FUTURE | 209 |
| | |
| REVIEWERS | 221 |



UDK 633.34 + 637.344 : 577.114 DOI: 10.46793/NovelTDS16.009S

COMPOSITION OF CARBOHYDRATES IN FRESH WHEY AS WASTE IN TOFU PROCESSING

Slađana Stanojević* D, Danijel Milinčić D, Mirjana Pešić D
University of Belgrade, Faculty of Agriculture, Department of Chemistry and
Biochemistry, Belgrade, Serbia

Soy whey is generated as a process waste while preparing tofu from soy milk, causing environmental pollution and also representing an economic burden for the soybean processing industry. On the other hand, literature data indicate that fresh tofu whey is characterized by a high content of total proteins with all essential amino acids present. a favorable residual activity of trypsin inhibitors, and a low content of lectins. This indicates a good nutritional value of tofu whey. Therefore, its potential valorization is of importance to the soy industry. The present investigation aims to determine the carbohydrate composition of tofu whey, which was obtained in the process of preparing tofu, from six soybean genotypes, using the hydrothermal-cooking-method, with the application of the chymosin-pepsin rennet. High-performance liquid chromatography (HPLC) was used. The presence of monosaccharide arabinose (0.39-1.73%) and disaccharide sucrose (2.19-4.60%) was registered. The presence of pentosearabinose was expected, since it can be part of glycoproteins, so it was probably separated from the protein part of the molecule, since some of the soybean proteins are glycoproteins. In addition, arabinose is part of the disaccharide vicianoze, which is part of the soybean saponins. The presence of sucrose indicates that the weakly acidic environment of the whey was not sufficient to hydrolyze this disaccharide (to glucose and fructose). The results indicate that tofu whey can be potentially useful for application as a cheap, functional, and nutritional food additive, enabling sustainable production through the recycling of waste.

Keywords: tofu whey, HPLC, arabinose, sucrose, sustainable production

E-mail address: sladjas@agrif.bg.ac.rs



^{*} Author address: Slađana Stanojević, University of Belgrade, Faculty of Agriculture, Department of Chemistry and Biochemistry, Institute of Food Technology and Biochemistry; Nemanjina 6, 11080 Zemun; P.O.Box 14, Serbia. Tel/Fax: +381 112199711

INTRODUCTION

The most commonly used soy food products in the world are soy milk and tofu. In the process of soy milk production, two by-products are also produced: soy soaking water whey (which is separated after soaking soybeans) and okara (the solid part of soybean seeds that remains after milk extraction). Further processing of soy milk into soy cheese - tofu produces another by-product/waste, which is tofu whey. Tofu whey is a pale yellowish liquid that is separated after pressing tofu, which has a specific aroma/taste.

These by-products in the tofu production process represent a serious problem in terms of waste disposal. They represent organic waste that is very suitable for the development of many microorganisms. Today, more and more attention is paid to finding opportunities for the further use of this waste according to the principles of the circular economy and sustainable waste treatment [1-3].

In our previous research, we characterized soy milk and tofu produced using the hydrothermal cooking method (HTC) using chymosin-pepsin rennet [4]. In addition, we investigated the characteristics of soaking water whey [5] and okara [6-8] and their potential for use.

Also, in our previous work, we examined the major storage protein composition and the activity of bioactive proteins of fresh tofu whey [9]. Our research results, as well as literature data, indicate that fresh tofu whey is characterized by significant nutritional value. It has been found that tofu whey contains a high content of total proteins (22.67-28.00%), with a wide spectrum of amino acids, with all essential amino acids present (phenylalanine 7.23 mg/L, histidine 4.27 mg/L, isoleucine 4.40 mg/L, leucine 6.12 mg/L, lysine 8.49 mg/L, methionine 2.77 mg/L, tryptophan 12.84 mg/L, valine 5.26 mg/L, threonine 5.39 mg/L) [9, 10]. It was found that basic 7S globulin is the dominant fraction of the 7S protein fraction of tofu whey, followed by β -conglycinin and γ -conglycinin [9]. The presence of isoflavones (50.84 mg of total isoflavones/L; with dominant genistin 25.99 mg/L and daidzin 17.66 mg/L), as well as the presence of organic acids (4.77 g of total organic acids/L), was registered in tofu whey [10].

In our earlier research for the preparation of tofu, the hydrothermal cooking method (HTC) using chymosin-pepsin rennet as a coagulant [4] was used, and the research results indicated that the applied heat treatment significantly reduced the activity of proteins with potential antinutritional properties, such as trypsin inhibitors and lectins in the tofu whey. These phytochemicals can have adverse antinutritional effects after consuming a raw soybean meal (e.g., a disorder of vitamin and amino acid metabolism, adverse changes in the digestive tract, pancreatic hypertrophy and hyperplasia, and disturbance of mineral composition in the body) [11]. That is why the activity of trypsin inhibitors must be reduced. But on the other hand, they are high in sulfur-containing amino acids (with which soy proteins are in deficit), [12] so that their presence is desirable. To improve the nutritional quality of soy foods, trypsin inhibitors are generally inactivated by heat treatment [13-16], with the aim of balancing their content and activity (to preserve content and reduce activity). Namely, residual activity of trypsin inhibitors (1.95-3.76%) and a low content of lectins (5.04-5.48% of total extracted proteins) were found, as well as low urease index activity of the fresh tofu



whey, which indicates that the heat HTC treatment was adequate to inactivate antinutritional factors [9]. So, this very low residual TIA of tofu whey suggested that tofu whey obtained by hydrothermal cooking could be applied in human consumption, because it features <20% of soybean trypsin inhibitor activity. Friedman and Brandon [17] reported that the commercial soy food can retain at most 20% of the activity of trypsin inhibitors, without any unwanted consequences on the body. In addition, literature data indicate that, given that trypsin inhibitors are more thermostable than lectins, achieving a satisfactory level of residual trypsin inhibitory activity leads to a satisfactory level of lectin content [17].

Since the application of the HTC process (short time/high temperature/under pressure) is significantly different from the traditional method of obtaining tofu (heating sovbeans without pressure and using acids, glucono-δ-lactone, or salts (MgCl₂, MgSO₄, CaCl₂ and CaSO₄) as the coagulating agents), it can be expected that the characteristics of the obtained products and by-products will also differ after applying different processing conditions. The aim of this study was to determine the carbohydrate composition of tofu whey, which was obtained in the process of preparing tofu, from six soybean genotypes, using the hydrothermal-cooking-method, with the application of the chymosin-pepsin rennet. Namely, we believe that the knowledge of the characteristics of fresh tofu whey, which has not vet been studied, will help to better understand the possible utilization of this by-product obtained using the HTC process. The results obtained in this study complement our previous work on the nutritional and non-nutritive characteristics of products and by-products obtained by the HTC process [3-9, 18-21], so the results of these studies can potentially provide an opportunity for the production of soy-food (soy milk and tofu) according to the principles of sustainable production and circular economy.

MATERIALS AND METHODS

Materials

For tofu preparation, six commercial soybean genotypes were used: Novosađanka, Balkan and Krajina (selected by the Institute of Field and Vegetable Crops, Novi Sad, Serbia), Lana, Nena and ZPS-015 (selected by the Maize Research Institute Zemun Polje, Belgrade, Serbia), Commercial chymosin-pepsin rennet was used as the coagulating agent (Rennet workshop, Idealka," Novo Selo, Serbia).

Tofu processing and separation of tofu whey

Tofu was made using the method described by Stanojević et al [4], using a hydrothermal cooking method that includes short time/high temperature/under pressure, by applying the chymosin-pepsin as the coagulating agent. Briefly, soybeans (soybeans/water ratio = 1/6) were soaked in water for 14 h, at 5–7 °C. Soaked soybeans were cooked by the hot-grind method with a steam injection system - 8 min/at 110 °C/1.8 bar, (SoyaCow VS 30/40, model SM-30, Russia). The slurry was filtered to separate soy milk and okara, and then soy milk was cooled at room temperature, and commercial chymosin-pepsin rennet was added (10 mL rennet/L soy milk). The tofu curd was pressed mechanically (35 min), and the obtained fresh tofu whey samples were stored at 4 °C before further analysis.



High-performance liquid chromatography (HPLC)

The characterization of carbohydrates using the HPLC technique was performed on a Waters chromatographic device (Waters Chomatography Div., Millipore, Milford, USA), which consists of a solvent and sample delivery system - Waters 600E System Controller and a detector - Waters 410 Differential Refractometer, on a column - Carbohydrate Analysis (Waters Chomatography Div., Millipore, Milford, USA) for the analysis of monosaccharides and disaccharides, while for the analysis of oligosaccharides (raffinose and stachyose) used Shugar-PAKTM - column of the same manufacturer. As a protective column, a GuardPakTM and RadialPakTM pre-column with ResolveTM Silica filling from the same manufacturer was used. As a mobile phase, a solution of acetonitrile/water in the ratio 83/17 (v/v) was used, for monosaccharides, and for polysaccharides, a solution of acetonitrile/water in a ratio of 65/35 (v/v). The column was calibrated by passing the mobile phase, with a gradual increase in the flow rate of 0.5 - 2 mL/min over a period of 5 hours.

In order to characterize monosaccharides and disaccharides, the standard solution contained: monosaccharides: xylose, arabinose, mannose, glucose, fructose; disaccharides: sucrose, maltose (Sigma, USA). The standards were dissolved in redistilled water, so that the standard mixture contained each of the listed monosaccharides and disaccharides at a concentration of 0.1%. Before application, they were filtered on a 0.25 μ m filter (Nucleopore, Corp., Pleasanton, CA, USA). 10 μ l of the standard solution was applied to the column and eluted for 25 minutes, at a flow rate of 2 mL/min and a temperature of 30°C.

The examined samples were mixed with 95% ethanol in the ratio sample: ethanol = 1:5 v/v; 1 hour, in a water bath (T=50°C), and then filtered (Whatman 42) while washing the precipitate (2 times) with 95% ethanol (supernatant:ethanol=1:1 v/v). After that, the samples were evaporated to dryness under vacuum (Devarot, Type-D-3, Elektromedicina, Ljubljana, Slovenia), then dissolved in an ultrasonic bath (Sonic, Italy) with redistilled water (initial sample: redest. $H_2O=1:4$ v/v). The extract was then filtered (Whatman 4) and frozen until use. Before injection into the HPLC device, all samples were filtered on a 0.25 μ m filter (Nucleopore, Corp., Pleasanton, CA, USA) and applied to the column in the amount of 20μ l. Chromatography was performed under identical conditions for samples and standards; flow rate - 2ml/min, at 30°C, 25 min.

Statistical analysis

The experiments were performed in triplicate, and all results are presented as mean values with standard deviations. The significance of the differences between the means was determined using a t-test procedure at P<0.05. The data were analyzed using the Statistica software version 7.0 (StatSoft Co., Tulsa, OK, USA).

RESULTS AND DISCUSSION

The presence of the monosaccharide- arabinose (0.39-1.73%; Table 1) was registered in the tofu whey obtained from all investigated soybean varieties. The presence of this pentose could be expected, considering that it very often enters into the composition of glycoproteins. So, during the production process, it was probably released from the protein part of the molecule, considering that some of the main proteins of soybeans



are precisely glycoproteins. On the other hand, arabinose is included in the composition of disaccharide vicianose, which is included in the composition of saponins [22], and saponins are present in non-defatted soybean flour with about 0.6-6.2% [23,24].

Table 1. Carbohydrate composition of tofu whey obtained using the HTC procedure*

| Rt (min) | 8.11 | 17.13 |
|--------------|------------------------|------------------------|
| genotype | arabinose | sucrose |
| Nena | 1.27±0.01 ^b | 4.60±0.20 ^a |
| Krajina | 1.13±0.02° | 4.25±0.22 ^b |
| Balkan | 1.73±0.03 ^a | 3.77±0.12° |
| Novosadjanka | 0.39±0.01 ^f | 2.19±0.12 ^e |
| ZPS-015 | 0.54±.0.02e | 3.20±0.11 ^d |
| Lana | 0.71±0.01 ^d | 3.31±0.11 ^d |

*Means in the same column with different roman letters are significantly different (P<0.05). HTC - hydrothermal cooking method. Rt (min) - retention time.

Tofu whey also contained sucrose (2.19-4.60%; Table 1). The presence of this disaccharide may also be a consequence of its relatively large participation in defatted soybean flour (4.45%; or even from 6.1% to 12.4% [25,26]). On the other hand, considering that whey is characterized by a slightly acidic medium (pH 4.02; [10]), it is evident that the acidity is not sufficient to cause sucrose hydrolysis, since it is known that it undergoes acid hydrolysis to glucose and fructose.

The results obtained indicate a greater dependence of the genotype type in terms of sucrose content than arabinose. Namely, although a statistically significant difference was registered in the arabinose content of all tested genotypes, it can still be seen that the values are relatively approximate (0.39-0.71% for the Novosađanka, ZPS-15, and Lana genotypes and 1.13-1.73% for the Nena, Krajina, and Balkan genotypes). On the other hand, the influence of the genotype type is significant in terms of sucrose content. Namely, the highest sucrose content was registered in tofu whey obtained from the Nena genotype (4.60%), while the lowest sucrose content was registered in tofu whey obtained from the Novosađanaka genotype (2.19%).

The Novosađanka genotype was selected as high-protein (58.02% total protein, [4]) so that the high total protein content may be a reason for the lower carbohydrate content in products obtained from soybeans of the Novosađanka genotype. Namely, Hymowitz et al. [27] evaluated 60 soybean lines for protein content, total sugar, and individual sugar content. Their results suggested that total sugar content and individual sugar content are negatively correlated with protein content. These results indicate that the soybean genotype may have an impact on the carbohydrate composition of tofu whey. Also, the presence of only these two sugars in tofu whey may be due to the significant retention of carbohydrates in okara as well as the conditions of the applied HTC procedure for preparing tofu, which differ significantly from the conditions of traditional soybean processing. Namely, the okara obtained after the same conditions of HTC processing contains 7.02-8.21% carbohydrates [7]. In addition, using the traditional method of obtaining soy milk and calcium sulfate as a coagulant in obtaining tofu, Chua and colleagues [10] registered: fructose 0.4 g/L, glucose 0.14 g/L, sucrose



111.72 g/L, and raffinose 0.30 g/L in tofu whey. Such results indicate that, in addition to the soybean genotype, the processing method has a significant effect on the characteristics of tofu whey. The results obtained in this study complement our previous work on examining the characteristics of soybean products and by-products obtained using the HTC process and indicate the specificity of the applied technological process.

CONCLUSION

Carbohydrate composition of tofu whey obtained from all tested soybean genotypes, using the HTC procedure, was characterized by the presence of monosaccharide arabinose and disaccharide sucrose. This result could be expected considering the carbohydrate composition of okara and the specificity of the applied technological process. In addition to other favorable characteristics of the composition of tofu whey (protein content and composition, as well as biologically active components), it can be assumed that tofu whey can potentially be used as a nutritional additive. Its distribution can reduce the production of organic waste in soybean processing.

Acknowledgment

This work was supported by the Ministry of Science, Technological Development and Innovation of the Republic of Serbia, Grant Nos 451-03-137/2025-03/200116.

References

- [1] Choi SI, Kim GY, Jung KJ, Bae HJ. Soybean waste (okara) as a valorization biomass for the bioethanol production. *Energy*. 2015, 93, 1742-1747. https://doi.org/10.1016/j.energy.2015.09.093
- [2] Belen F, Sanchez J, Hernandez E J, Auleda M, Raventos M. One option for the management of wastewater from tofu production: freeze concentration in a falling-film system. Journal of Food Engineering. 2012, 110, 364-373. https://doi.org/10.1016/j.jfoodeng.2011.12.036.
- [3] Pešić MB, Pešić MM, Bezbradica J, Stanojević AB, Ivković P, Milinčić DD, Demin M, Kostić AŽ, Dojčinović B, Stanojević SP. Okara-enriched gluten-free bread: nutritional, antioxidant and sensory properties. *Molecules*. 2023, 28, 4098. https://doi.org/10.3390/molecules28104098
- [4] Stanojevic PS, Barac BM, Pesic BM, Vucelic-Radovic VB. Assessment of soy genotype and processing method on quality of soybean tofu. *Journal of Agricultural and Food Chemistry*. 2011, 59,7368-7376. https://doi.org/10.1021/jf2006672
- [5] Stanojevic PS, Barać BM, Kostić ŽA, Pešić BM. Trypsin inhibitor content and activity of soaking water whey as waste in soy milk processing. *Journal of Environmental Science and Health, Part B*. 2021, 58(1), 10-20. https://doi.org/10.1080/03601234.2021.1874232
- [6] Stanojevic PS, Barac BM, Pesic BM, Vucelic-Radovic VB. Composition of proteins in okara as a byproduct in hydrothermal processing of soy milk. *Journal of Agricultural and Food Chemistry*. 2012, 60, 9221-9228. https://doi.org/10.1021/jf3004459



- [7] Stanojevic PS, Barac BM, Pesic BM, Jankovic SV, Vucelic-Radovic VB. Bioactive proteins and energy value of okara as a byproduct in hydrothermal processing of soy milk. *Journal of Agricultural and Food Chemistry*. 2013, 61, 9210–9219. https://doi.org/10.1021/jf4012196
- [8] Stanojevic PS, Barac BM, Pesic BM, Zilic MS, Kresovic MM, Vucelic-Radovic VB. mineral elements, lipoxygenase activity, and antioxidant capacity of okara as a byproduct in hydrothermal processing of soy milk. *Journal of Agricultural and Food Chemistry*. 2014, 62, 9017-9023. https://doi.org/10.1021/if501800s
- [9] Stanojevic PS, Barac BM, Kostić ŽA, Pešić BM. Composition of proteins in fresh whey as waste in tofu processing. *Journal of Environmental Science and Health, Part B.* 2023, 58(1), 10-20. https://doi.org/10.1080/03601234.2022.2162300
- [10] Chua J-Y, Lu Y, Liu S-Q. Evaluation of five commercial non-Saccharomyces yeasts in fermentation of soy (tofu) whey into an alcoholic beverage. Food Microbiology. 2018, 76, 533-542. https://doi.org/10.1016/j.fm.2018.07.016
- [11] Liener IE. Factor affecting the nutritional quality of soya products. *Journal of the American Oil Chemists' Society*. 1981, 58, 406-415. https://link.springer.com/article/10.1007/BF02582390
- [12] Koide T, Ikenaka T. Studies on soybean trypsin-inhibitors. 3. Amino acid sequence of the carboxyl-terminal region and the complete amino acid sequence of the soybean trypsin inhibitor (Kunitz). *European Journal of Biochemistry*. 1973, 32(3), 417-431. https://doi.org/10.1111/j.1432-1033.1973.tb02624.x
- [13] Stanojević PS, Vucelić-Radović VB, Barać BM, Pešić BM. The effect of autoclaving on soluble protein composition and trypsin inhibitor activity of cracked soybeans. *Acta Periodica Technologica*. 2004,35, 48-57. https://doi.org/10.2298/APT0435049S
- [14] Barać M, Stanojević S. The effect of microwave roasting on soybean protein composition and components with trypsin inhibitor activity. *Acta Alimentaria*. 2005, 34, 23-31. https://doi.org/10.1556/AAlim.34.2005.1.5
- [15] Stanojević PS, Barać BM, Pešić BM, Vucelić-Radović VB. The Influence of soybean genotypes and HTC processing method on trypsin inhibitor activity of soymilk. *Journal of Agricultural Sciences (Belgrade)*.2016, 61, 271-279. https://doi.org/10.2298/JAS1603271S
- [16] Brinda HV, Sai KV, Vijaya R. Inactivation methods of soybean trypsin inhibitor -A Review. *Trends in Food Science Technology*. 2017, 64, 115-125. https://doi.org/10.1016/j.tifs.2017.02.003
- [17] Friedman M, Brandon LD. Nutritional and health benefits of soy protein. *Journal of Agricultural and Food Chemistry*. 2001, 49, 1069–1086. https://doi.org/10.1021/jf0009246
- [18] Stanojević PS, Barać BM, Pešić BM, Vucelić-Radović V B. The Influence of soybean genotypes and HTC processing method on trypsin inhibitor activity of soymilk. Journal of Agricultural Science. 2016, 61, 271-279. https://www.researchgate.net/publication/310433046
- [19] Stanojevic PS, Barać BM, Pešić BM, Vucelić-Radović VB. Protein composition and textural properties of inulinenriched tofu produced by hydrothermal process.



- *LWT-Food Science and Technology.* 2020, 126, 109309. https://doi.org/10.1016/j.lwt.2020.109309
- [20] Stanojevic PS, Barać BM, Pešić BM, Vucelić-Radović VB. Distribution of β-amylase and lipoxygenase in soy protein products obtained during tofu production. *Chemical Industry*. 2017, 71, 119-126. https://doi.org/10.2298/HEMIND150525021S
- [21] Stanojevic PS, Barać BM, Pešić BM, Vucelić-Radović VB. Energy value and bioactive proteins of inulin-enriched tofu produced by hydrothermal process with chymosin-pepsin rennet. *International Journal of Food Science and Technology*. 2021, 56, 5560-5568. https://doi.org/10.1111/ijfs.15132
- [22] Džamić M. *Biochemistry*. University of Belgrade, IRO "Građevinska knjiga", Belgrade, pp. 342-343. 1984, on Serbian.
- [23] Rackis JJ. Biological and physiological factors in soybeans. *Journal of the American Oil Chemists' Society.* 1974, 51(1), 161A-174A. https://doi.org/10.1007/BF02542123
- [24] Sun H, Meng X, Han Y, Li X, Li X, Li Y. Soybean saponin content detection based on spectral and image information combination. *Journal of Spectroscopy.* 2024, Article ID 7599132. https://doi.org/10.1155/2024/7599132
- [25] Murai T, Naeve S, Annor GA. Regional variability in sugar and amino acid content of U.S. soybeans and the impact of autoclaving on reducing sugars and free lysine. *Foods*. 2024, 13, 1884. https://doi.org/10.3390/foods13121884
- [26] Maughan P, Maroof MS. Buss G. Identification of quantitative trait loci controlling sucrose content in soybean (*Glycine max*). *Molecular Breeding*. 2000, 6, 105–111. https://doi.org/10.1023/A:1009628614988
- [27] Hymowitz T, Collins FI, Panczner J, Walker WM. Relationship between the content of oil, protein and sugar in soybean seed. *Agronomy Journal*. 1972, 64, 613-616. https://doi.org/10.2134/agronj1972.00021962006400050019x

Izvod

SASTAV UGLJENIH HIDRATA U SVEŽOJ SURUTCI DOBIJENOJ KAO OTPAD U PRERADI TOFU-a

Slađana Stanojević ID, Danijel Milinčić ID, Mirjana Pešić ID
Univerzitet u Beogradu, Poljoprivredni fakultet, Katedra za hemiju i biohemiju,
Beograd, Srbija

Sojina surutka nastaje kao otpad iz procesa pripreme tofua od sojinog mleka, što uzrokuje zagađenje životne sredine i predstavlja ekonomski teret za proces prerade soje. S druge strane, literaturni podaci ukazuju da se sveža tofu surutka karakteriše visokim sadržajem ukupnih proteina sa prisutnim svim esencijalnim aminokiselinama, povoljnom rezidualnom aktivnošću inhibitora tripsina i niskim sadržajem lektina. Ovo ukazuje na dobru nutritivnu vrednost tofu surutke. Stoga je njena potencijalna



valorizacija važna za industriju prerade soje. Cilj ovog istraživanja je da se utvrdi sastav ugljenih hidrata tofu surutke, koja je dobijena u procesu pripreme tofua, od šest genotipova soje, primenom metode hidrotermčkog kuvanja, uz primenu himozinpepsinskog sirila. Korišćena je visokoefikasna tečna hromatografija (HPLC). Registrovano je prisustvo monosaharida arabinoze (0,39-1,73%) i disaharida saharoze (2,19-4,60%). Prisustvo pentoze - arabinoze bilo je očekivano, s obzirom da može biti deo glikoproteina, pa je verovatno odvojena od proteinskog dela molekula, s obzirom da su neki od sojinih proteina glikoproteini. Pored toga, arabinoza je deo disaharida vicinoze, koji je deo sojinih saponina. Prisustvo saharoze ukazuje na to da slabo kisela sredina surutke nije bila dovoljna da hidrolizuje ovaj disaharid (do glukoze i fruktoze). Rezultati ukazuju da tofu surutka može biti potencijalno korisna za primenu kao jeftin, funkcionalni i nutritivni aditiv u pripremi hrane i da može omogućiti održivu proizvodnju kroz reciklažu otpada.

Ključne reči: tofu surutka, HPLC, arabinoza, saharoza, održiva proizvodnja



Section: MATERIALS ENGINEERING

UDK 678.7:669.22:579:543.4 DOI: 10.46793/NovelTDS16.021B

GMA/Ag COMPOSITE AS ANTIMICROBIAL AGENT

Sandra Bulatović* <u>ID</u>, Natalija Nedić <u>ID</u>, Tamara Tadić <u>ID</u>, Bojana Marković <u>ID</u>, Aleksandra Žerađanin <u>ID</u>, Aleksandra Nastasović <u>ID</u>

University of Belgrade, Institute of Chemistry, Technology and Metallurgy (ICTM), National Institute of the Republic of Serbia, Belgrade, Serbia

Silver, a precious metal used across various industries, can be released into the environment as a byproduct of industrial activities, potentially leading to environmental pollution. Consequently, removing silver from wastewater is crucial for enhancing environmental quality. Porous synthetic polymers (composites), with their high specific surface area and unique physico-chemical properties, have garnered interest as effective sorbents in environmental protection. Glycidyl methacrylate (GMA)-based composites are widely used in various applications such as sorbents (of metals, organic compounds, etc.), enzyme supports, and in biomedicine. The main objectives of this study were the synthesis, characterization, and investigation of the antimicrobial activity of a novel GMA/Ag composite. For the synthesis of the composite, GMA as the monomer, and the crosslinker trimethylolpropane trimethacrylate (TMPTMA) were used, followed by functionalization with diethylenetriamine (DETA). Silver was incorporated into the composite by sorption from 0.1 M AqNO₃ solution at pH 5, and 25°C, for 24h. The synthesized composite was characterized using Fourier-transform infrared spectroscopy (FTIR), and Scanning Electron Microscopy (SEM). The antimicrobial activity of the GMA/Ag composite was assessed using the agar-well diffusion method against different microorganisms, including representatives of Gram-negative (Escherichia coli) and Gram-positive bacteria (Staphylococcus aureus), yeast (Candida albicans), and fungi (Aspergillus niger). The results of antimicrobial tests indicated that the GMA/Ag composite displayed good antimicrobial activity against the analyzed microbes, and it can potentially be used for biomedical applications, in the food and pharmaceutical industries, in the treatment of wastewater, etc.

Keywords: GMA/Ag composite, FTIR, SEM, antimicrobial activity.

e-mail address: sandra.bulatovic@ihtm.bg.ac.rs



^{*} Author address: Sandra Bulatović, University of Belgrade, Institute of Chemistry, Technology and Metallurgy (ICTM), National Institute of the Republic of Serbia, Njegoševa 12, Belgrade, Serbia

INTRODUCTION

Silver is being increasingly utilized across diverse industries, such as jewelry, photography, catalysis, electronics, biomedicine, and chemical manufacturing, owing to its exceptional physicochemical properties [1]. However, increasing demand and improper handling have led to the generation of silver-containing wastewater [2]. According to the World Health Organization (WHO), silver(I) ions in aquatic environments are classified as hazardous substances, making their removal from wastewater a critical step prior to discharge [3]. Silver(I) ions interact with biomolecules, causing toxic responses comparable to those induced by other heavy metals and persistent organic pollutants. Their bioaccumulation presents significant environmental and health risks, as silver can be transferred through the aquatic food chain [4]. Accordingly, the U.S. Environmental Protection Agency has set the maximum allowable silver concentration in drinking water at 0.1 mg/L [2]. Among various water treatment methods, sorption is recognized for its simplicity, cost-effectiveness, and environmental sustainability [3]. Owing to its low energy requirements and minimal secondary pollution, it has attracted considerable attention for the removal of metals from wastewater [2]. The glycidyl methacrylate (GMA)-based composites serve as efficient chelating agents that efficiently bind metal ions, facilitating their removal from aqueous solutions, and thereby contributing to the reduction of toxic metal concentrations in the environment [5]. These porous synthetic polymers, characterized by high specific surface area and unique physicochemical properties, are widely used not only as sorbents but also as reactive composites. Because the GMA molecule contains an epoxide group susceptible to nucleophilic and electrophilic ring-opening reactions, various functional groups can be introduced to tailor polymer properties for diverse applications [6]. In this study, an amino-functionalized GMA composite was used for silver(I) ion sorption. Incorporating metal ions into polymers enables the creation of biocidal materials with expanded applications. Silver is well known for its antimicrobial properties, acting through various mechanisms, including protein denaturation, and disrupting the bacterial respiratory chain by interfering with membrane-bound respiratory proteins. Additionally, silver alters membrane permeability and generates reactive oxygen species (ROS), leading to oxidative stress and eventual microbial cell death [7].

The aim of this study was to investigate the application of an amino-functionalized composite based on glycidyl methacrylate (GMA) as a potential sorbent for silver(I) ions, which was synthesized and characterized by Fourier Transform Infrared Spectroscopy (FTIR) and Scanning Electron Microscopy (SEM) analyses. Additionally, the antimicrobial efficiency after sorption of silver(I) ions was evaluated. This approach aims to achieve a dual purpose: removal of silver(I) ions from wastewater and imparting antimicrobial activity to the analyzed GMA/Ag composite.

MATERIALS AND METHODS

Materials and instrumentation

For the synthesis of the GMA composite, the following reagents were used: glycidyl methacrylate (GMA, p.a., Merck, Germany), trimethylolpropane trimethacrylate



(TMPTMA, p.a., Sigma-Aldrich, Germany), 2,2'-azobisisobutyronitrile (AIBN, 98%, Sigma-Aldrich, Germany), cyclohexanol (Cy6, p.a., Merck, Germany), and tetradecanol (C₁₄, p.a., Merck, Germany). The GMA composite sample was functionalized with diethylenetriamine (DETA, p.a., Merck, Germany) in toluene (p.a., Sigma-Aldrich, Germany). A solution of AgNO₃ in deionized water was used for Ag (I) sorption. Mueller-Hinton agar for bacteria (casein hydrolysate 17.5 g/L, meat extract 2 g/L, starch 1.5 g/L, agar 17 g/L) and Sabouraud Dextrose agar for yeast and fungi (agar 15 g/L, glucose 4%, D (+)-glucose 40 g/L, peptone 10 g/L) were used for the determination of antimicrobial activity.

GMA/Ag composite was characterized with a Nicolet SUMMIT FTIR Spectrometer (Thermo Fisher Scientific, Waltham, MA, USA), in ATR mode, in the range 4000–500 cm⁻¹ and Scanning Electron Microscopy with Energy-Dispersive X-ray Spectroscopy (SEM-EDS) (JEOL JSM-6390 LV, JEOL Ltd., Tokyo, Japan). Before SEM analysis, the composite had been coated with a thin layer of gold.

Synthesis of composite

The GMA-based composite was synthesized via suspension copolymerization in a 500 mL flask equipped with a condenser and mechanical stirrer, under nitrogen and heated in an oil bath. The aqueous phase (225 mL) was heated to 75 °C, followed by the addition of the monomer phase (GMA, 29.2 g), the crosslinker (TMPTMA, 19.5 g), the initiator (AIBN, 0.5 g), and inert components (Cy6, 51.0 g; C₁₄, 12.8 g). The reaction was carried out for 2 h at 75 °C, and 2 h at 80 °C. The product was isolated by decantation, washed, dried, and purified via Soxhlet extraction with ethanol (24 h). Amino-functionalization was performed by treating 7.2 g of the composite with 31.4 g DETA, in toluene (350 mL), stirred at room temperature for 24 h, then heated at 80 °C for 6 h. The resulting amino-functionalized GMA-based composite was filtered, washed, and dried [6].

Sorption of Ag(I) ions from aqueous solution

An aqueous solution of silver(I) ions (0.1 M) was prepared by dissolving $AgNO_3$ in deionized water. Sorption of Ag(I) ions using the amino-functionalized GMA-based composite was performed at room temperature (25 °C), pH 5, for 24 hours, resulting in the amino-functionalized GMA/Ag composite, which was further characterized and used to determine antimicrobial activity.

Agar diffusion method

The microorganisms used in this study were: *Escherichia coli* (ATCC 25922), *Staphylococcus aureus* (ATCC 25923), *Candida albicans* (ATCC 2433), and *Aspergillus niger*.

The nutritious microbiological media were heated to boiling in a water bath to ensure complete dissolution, then sterilized for 25 minutes at 120 °C. After solidification of the media, the microorganisms were directly streaked onto the surface of the agar plates with a sterile inoculating loop, using the zig-zag method. Also, the wells for the GMA/Ag were formed in the agar plates. The GMA/Ag (30 mg) was mixed with 100 µL sterile distilled water, and added to the wells. After 24 hours of incubation at 28°C, the Petri dishes were examined, and the zone of microbial growth inhibition was measured with a millimeter ruler [8, 9].



RESULTS AND DISCUSSION

In Figure 1, the FTIR spectra of the amino-functionalized GMA-based composite before and after silver(I) ions binding are shown. In the spectrum of the analyzed composite before silver sorption, a broad peak is observed in the region around 3500–3300 cm⁻¹, with a maximum at 3365.7 cm⁻¹, which is attributed to –OH groups and N–H stretching vibrations. After silver sorption, the intensity of this peak changes, suggesting that hydroxyl and amino groups likely participated in the binding of silver(I) ions. The region around 2944.4 cm⁻¹ is characteristic of asymmetric and symmetric stretching of –CH₂ and –CH bonds from aliphatic CH₂ and CH₃ groups, while the band at 1465.9 cm⁻¹ corresponds to –CH₂ and –CH bending vibrations. The most prominent peak in the spectrum appears at 1726.7 cm⁻¹ and corresponds to the C=O stretching vibration, characteristic of ester groups. Additionally, peaks corresponding to the vibrations of the epoxy ring are found at 1258.5, 1151.2, and 984.2 cm⁻¹; after sorption, changes in their intensity and slight shifts are observed, which may indicate a disturbance in local symmetry due to coordination with silver ions [10]. After sorption of silver(I) ions, a peak appears at 826.1 cm⁻¹, indicating the formation of an Aq–N complex [11].

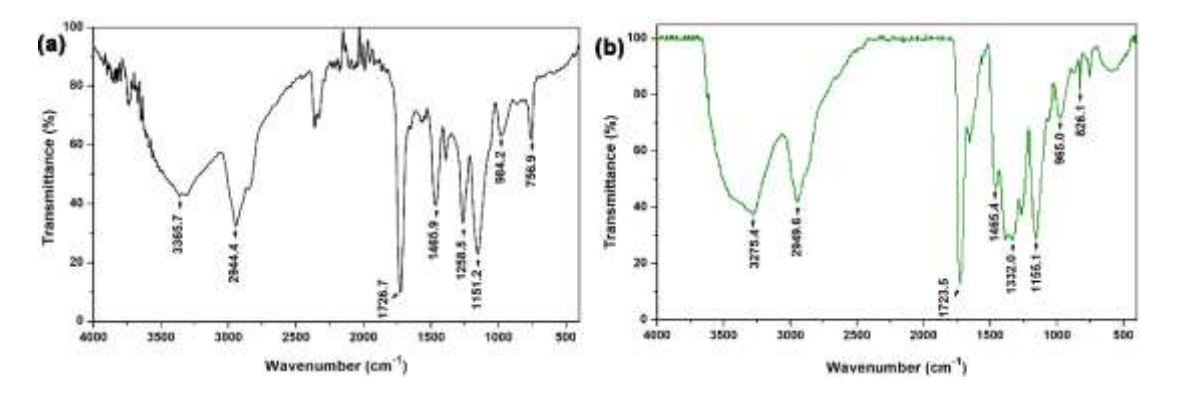


Figure 1. FTIR spectrum of the: (a) amino-functionalized GMA/Ag composite, and (b) after silver(I) ions binding.

In order to obtain morphological information, the surface of the GMA/Ag composite was examined using scanning electron microscopy (SEM) at magnifications of 1 μ m and 100 μ m (Figure 2). SEM analysis revealed that the samples consisted of spherical, opaque particles with a rough surface. The sample exhibited a three-dimensional porous structure with agglomerates of globules, typical for GMA porous composites [6].



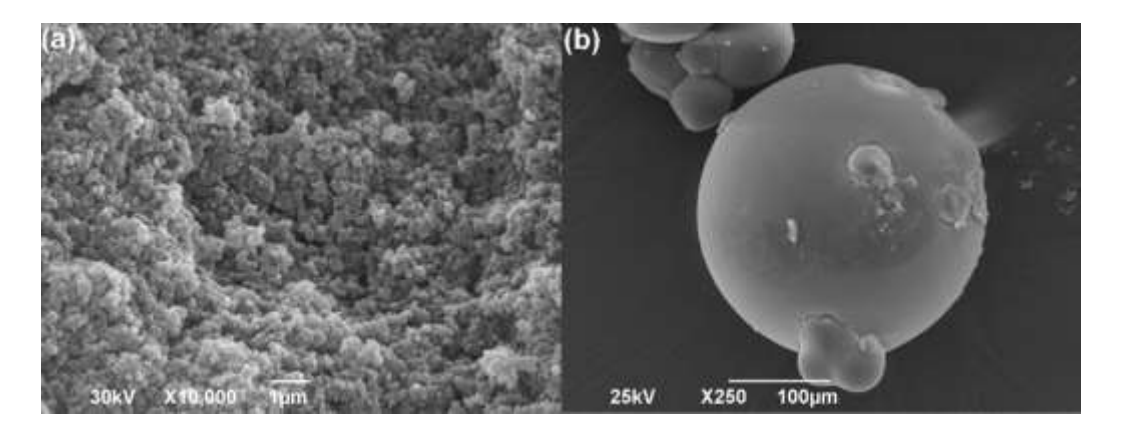


Figure 2. SEM images of GMA/Ag composite at: (a) 1 µm, and (b) 100 µm magnification.

Petri dishes with the test microorganisms used to evaluate the antimicrobial activity of the GMA/Ag composite after Ag(I) ion sorption, as well as control Petri dishes to which only water was added instead of the polymer, are shown in Figure 3. After 24 hours of incubation, the inhibition zones were measured by subtracting the radius of the well (5 mm) from the total radius of the clear inhibition zone (9 mm). The results of the antimicrobial tests demonstrated that the GMA/Ag composite effectively acted against Gram-negative bacteria (such as *E. coli*) and Gram-positive bacteria (*S. aureus*), with the same inhibition zone of 4 mm (Figure 3). The antimicrobial tests against yeast (*C. albicans*) and fungi (*A. niger*) were negative, probably due to the possibility that the silver concentration, or the form used in this study, wasn't adequate to exert a measurable inhibition effect. Therefore, it can be assumed that the analyzed composite is antibacterial because it showed a significant inhibition of bacterial growth.

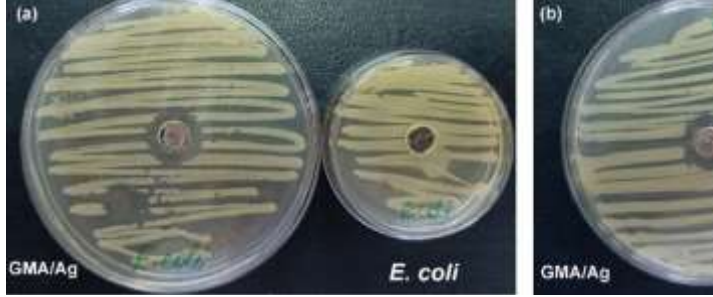




Figure 3. The antimicrobial activity of the GMA/Ag composite against: (a) *E. coli*, and (b) *S. aureus*.

Several studies have examined the antimicrobial activity of glycidyl methacrylate (GMA)-based composites functionalized with silver. Vukoje et al. (2015) demonstrated significant antimicrobial effects of poly(GMA-co-EGDMA) copolymers with immobilized silver nanoparticles against bacteria (*Escherichia coli, Staphylococcus aureus*) and fungi



(Candida albicans). Fan et al. (2011) demonstrated that silver-containing GMA-based dental resins exhibited strong antibacterial activity against *Streptococcus* mutants, while research by Gligorijević et al. (2022) showed that silver-modified polymethyl methacrylate (PMMA) resins effectively inhibited growth of *Staphylococcus aureus* and *Candida albicans*. These findings collectively underscore the antimicrobial potential of silver-functionalized methacrylate composites.

CONCLUSION

In this study, the antimicrobial activity of a novel silver-containing GMA-based composite (GMA/Ag) was evaluated using the agar diffusion method. SEM analysis of GMA/Ag revealed a three-dimensional porous structure, while FTIR spectra confirmed the aminofunctionalization and incorporation of Ag(I) ions in the structure of the crosslinked composite through the formation of Ag–N bonds. Based on the obtained results, it can be concluded that the amino-functionalized GMA-based composite is effective as a sorbent of Ag(I) ions from aqueous solutions, as well as an antibacterial agent. However, the commercial application of this composite would require further studies, analyses, and evaluations to ensure its safe and effective use.

Acknowledgment: This research was financially supported by the Ministry of Science, Technological Development and Innovation of the Republic of Serbia (Contract No. 451-03-136/2025-03/200026). This work is related to the implementation of the United Nations Sustainable Development Goal 6 – Clean water and sanitation.

References

- [1] Yu H, Zhang H, Zhang C, Wang R, Liu S, Du R, Sun W. Advances in treatment technologies for silver-containing wastewater. *Chemical Engineering Journal*. 2024, 496, 153689. https://doi.org/10.1016/j.cej.2024.15368
- [2] Wang Q, Li M, Xi M, Zhao M, Wang X, Chen X, Ding L. Recovery of Ag(I) from wastewater by adsorption: Status and challenges. *Toxics*. 2024, 12, 351. https://doi.org/10.3390/toxics12050351
- [3] Islam MA, Jacob MV, Antunes E. A critical review on silver nanoparticles: From synthesis and applications to its mitigation through low-cost adsorption by biochar. *Journal of Environmental Management*. 2021, 281, 111918. https://doi.org/10.1016/j.jenvman.2020.111918
- [4] Lazim ZM, Salmiati S, Marpongahtun M, Arman NZ, Mohd Haniffah MR, Azman S, Yong EL, Salim MR. Distribution of silver (Ag) and silver nanoparticles (AgNPs) in aquatic environment. *Water.* 2023, 15, 1349. https://doi.org/10.3390/w15071349
- [5] Bektenov N, Baidullayeva A, Chalov T, Jumadilov T, Kanat S. Modified adsorbents aased on glycidyl methacrylate copolymers for the removal of copper and lead ions from wastewater. *Engineered Science*. 2024, 31, 1237 https://dx.doi.org/10.30919/es1237
- [6] Marković B. Synthesis, characterization and application of macroporous nanocomposites of glycidyl methacrylate and magnetite. Thesis, Faculty of Technology and Metallurgy, University of Belgrade, 2019.
- [7] Sofi MA, Sunitha S, Sofi MA, Pasha SK, Choi D. An overview of antimicrobial and



- anticancer potential of silver nanoparticles. *Journal of King Saud University-Science*. 2022, 34, 101791. https://doi.org/10.1016/j.jksus.2021.101791
- [8] Salam MA, Al-Amin MY, Pawar JS, Akhter N, Lucy IB. Conventional methods and future trends in antimicrobial susceptibility testing. *Saudi Journal of Biological Sciences*. 2023, 30, 103582. https://doi.org/10.1016/j.sjbs.2023.103582
- [9] Subramaniam R, Eswaran A, Sivasubramanian G, Gurusamy A. Synthesis and characterization techniques for clay-based polymer nanocomposites and their evaluation of antibacterial, anticancer, and anti-inflammatory activities. *Emergent Materials*. 2023, 6, 261-269. https://doi.org/10.1007/s42247-022-00434-3
- [10] Tadić T, Marković B, Vuković Z, Stefanov P, Maksin D, Nastasović A, Onjia A. Fast gold recovery from aqueous solutions and assessment of antimicrobial activities of novel gold composite. *Metals*. 2023, 13, 1864. https://doi.org/10.3390/met13111864
- [11] Wen H, Raza S, Wang P, Zhu Z, Zhang J, Huang W, Liu C. Robust super hydrophobic cotton fabrics functionalized with Ag and PDMS for effective antibacterial activity and efficient oil–water separation. *Journal of Environmental Chemical Engineering*. 2021, 9, 106083. https://doi.org/10.1016/j.jece.2021.106083
- [12] Vukoje ID, Džunuzović ES., Lončarević DR, Dimitrijević S, Phillip Ahrenkiel S, Nedeljković J M. Synthesis, characterization, and antimicrobial activity of silver nanoparticles on poly(GMA-co-EGDMA) polymer support. *Polymer Composites*, 2015, 38, 1206–1214. https://doi.org/10.1002/pc.23684
- [13] Fan C, Chu L, Rawls HR, Norling BK, Cardenas HL, Whang K. Development of an antimicrobial resin-A pilot study. *Dental Materials*. 2011, 27, 322-328. https://doi.org/10.1016/j.dental.2010.11.008
- [14] Gligorijević N, Mihajlov-Krstev T, Kostić M, Nikolić L, Stanković N, Nikolić V, Dinić A, Igić M, Bernstein N. Antimicrobial Properties of Silver-Modified Denture Base Resins. *Nanomaterials*, 2022, 12, 2453. https://doi.org/10.3390/nano12142453

Izvod

GMA/Ag KOMPOZIT KAO ANTIMIKROBNO SREDSTVO

Sandra Bulatović <u>ID</u>, Natalija Nedić <u>ID</u>, Tamara Tadić <u>ID</u>, Bojana Marković <u>ID</u>, Aleksandra Žerađanin <u>ID</u>, Aleksandra Nastasović <u>ID</u>

Univerzitet u Beogradu, Institut za hemiju, tehnologiju i metalurgiju (IHTM), Institut od nacionalnog značaja za Republiku Srbiju, Beograd, Srbija

Srebro je plemeniti metal koji se koristi u raznim industrijama, tako da može dospeti u životnu sredinu kao nusproizvod industrijskih aktivnosti, što potencijalno može dovesti do zagađenja. Shodno tome, uklanjanje srebra iz otpadnih voda je ključno za poboljšanje kvaliteta životne sredine. Porozni sintetički polimeri (kompoziti), sa svojom visokom specifičnom površinom i jedinstvenim fizičko-hemijskim svojstvima, izazvali su interesovanje kao efikasni sorbenti u očuvanju životne sredine. Kompoziti na bazi glicidil metakrilata (GMA) se široko koriste u različitim primenama kao sorbenti (metala,



organskih jedinjenja itd.), nosači enzima i u biomedicini. Glavni ciljevi ove studije bili su sinteza, karakterizacija i istraživanje antimikrobne aktivnosti novog GMA/Ag kompozita. Za sintezu kompozita korišćeni su GMA kao monomer, i umreživač trimetilolpropan trimetakrilat (TMPTMA), nakon čega je usledila funkcionalizacija dietilentriaminom (DETA). Srebro je ugrađeno u kompozit sorpcijom iz 0.1 M rastvora AgNO₃. na pH 5. i 25°C, tokom 24 sata. Sintetisani kompozit je okarakterisan korišćenjem Furijeovetransformacione infracrvene spektroskopije (FTIR) i Skenirajuće Elektronske Mikroskopije (SEM). Antimikrobna aktivnost GMA/Ag kompozita je procenjena korišćenjem metode difuzije u agar-bunarićima za različite mikroorganizame, ukliučuiući gram-negativnih (Escherichia coli) i gram-pozitivnih predstavnike (Staphylococcus aureus), kvasaca (Candida albicans) i gljiva (Aspergillus niger). Rezultati antimikrobnih testova su pokazali da GMA/Ag kompozit ispoljava dobru antimikrobnu aktivnost protiv analiziranih mikroba i da se potencijalno može koristiti za biomedicinske primene, u prehrambenoj i farmaceutskoj industriji, u tretmanu otpadnih voda itd.

Ključne reči: GMA/Ag kompozit, FTIR, SEM, antimikrobna aktivnost.



Section: ENVIRONMENTAL ENGINEERING

UDK 667.281 : 678.744 : 66.061.3 DOI: 10.46793/NoveITDS16.031M

DISPERSIVE SOLID-PHASE MICROEXTRACTION BASED ON AMINO-FUNCTIONALIZED POLYMER FOR PRECONCENTRATION OF AZO DYE FROM AQUEOUS SAMPLES

Bojana Marković* <u>ID</u>, Tamara Tadić <u>ID</u>, Sandra Bulatović <u>ID</u>, Natalija Nedić <u>ID</u>, Aleksandra Nastasović <u>ID</u>

Institute of Chemistry, Technology and Metallurgy, University of Belgrade, Belgrade, Serbia

Synthetic dyes are extensively used in the food, cosmetic, textile, and pharmaceutical industries, and their release into the environment presents serious health and ecological concerns due to their toxicity and resistance to degradation. Among them, azo dyes represent the most prevalent class and are particularly harmful due to their toxic and persistent nature. They are also linked to serious health issues, affecting organs such as the kidneys, liver, brain, and respiratory system. Therefore, the quantification and removal of azo dyes from different media is essential. In this study, the preconcentration and determination of Congo Red (CR) as a model azo dye in aqueous samples were investigated. For this purpose, dispersive solid-phase microextraction (DSPME) was employed to extract CR from aqueous samples using an amino-functionalized glycidyl methacrylate-based polymer, prior to UV-Vis spectroscopy measurements. Parameters affecting the extraction of CR, adsorption and desorption time, and desorption agent volume, were optimized by the Box-Behnken design (BBD). The optimized methodology involved 10 mL of aqueous CR solution, 50 mg of amino-functionalized polymer, and 500 µL of 0.2 mol/dm3 NaOH as the desorption agent, with sorption and desorption performed at room temperature for 4 and 6 minutes, respectively. The predicted extraction recovery of 76.07 % for CR, obtained from the polynomial model, showed good agreement with the experimental value of 75.50 %. The results confirm that the proposed DSPME procedure is a simple and fast method with strong potential for the determination of azo dyes in aqueous samples.

Keywords: glycidyl methacrylate, diethylene triamine, Congo Red, Box-Behnken design, DSPME

^{*} Author address:Bojana Marković, Institute of Chemistry, Technology and Metallurgy, University of Belgrade, Njegoševa 12, Belgrade, Serbia e-mail address: bojana.markovic@ihtm.bg.ac.rs



INTRODUCTION

Due to their ease of use, broad color palette, and excellent stability, synthetic dyes are widely employed across industries such as textiles, leather, paper, plastics, and foodstuffs. Chemically, they consist of chromophoric compounds that interact physically or chemically with substrates, selectively absorbing specific wavelengths of light to impart color [1]. The advent of synthetic dyes enabled rapid, large-scale textile production with shorter dyeing times and enhanced dye uptake, making dyed fabrics more accessible to a broader consumer base. Beyond fiber dyeing and textile printing, they are also applied in paper and packaging coloration, as well as in the food and beverage industries [2]. Unlike natural dyes, the chemical structures of synthetic dyes can be tailored to yield a vast array of hues. However, their manufacture, use, and disposal pose significant environmental and health challenges [3].

Congo red, CR ($C_{32}N_{6}Na_{2}O_{6}S_{2}$; M_{r} = 696.68 g/mol) is an anionic synthetic dye characterized by a complex aromatic structure [4]. Its multiple aromatic rings and azo linkage (-N=N-) confer resistance to biodegradation and high toxicity, as the azo bond is engineered for chemical stability [5]. CR is extensively used in textile, printing, wool, and silk industries, as well as in histological applications (e.g., amyloidosis diagnosis) and as a pH indicator [6, 7]. Owing to its persistence, CR represents a threat to human health and aquatic ecosystems: it can induce ocular and dermal irritation, gastrointestinal distress, respiratory difficulty, and is known to be carcinogenic, teratogenic, and reproductive toxic [8]. Chronic exposure may damage the liver and circulatory system and has been linked to various cancers, since CR can be metabolized to benzidine, a recognized carcinogen [9]. In aquatic environments, CR impedes light penetration and reduces gas solubility, disrupting photosynthesis and endangering aquatic life [10].

Numerous treatment methods have been developed for textile industry wastewater, which is predominantly contaminated with dyes. These include adsorption [11], membrane filtration [12], coagulation and precipitation [13], oxidation [14], photocatalysis [15], enzymatic degradation [16], and ion exchange [17]. Research is focused on developing cost-effective, locally available, and efficient adsorbents specifically designed for the removal of pollutants like CR and other azo dyes, with dispersive solid-phase microextraction recognized as a highly effective, economical, and environmentally friendly remediation strategy. Consequently, advanced hybrid materials such as aminofunctionalized polymers have garnered considerable attention [18, 19].

Dispersive solid-phase microextraction (DSPME) is a modern sample-preparation technique that integrates sampling, preconcentration, and extraction in a single step, allowing the direct introduction of analytes into analytical instruments. DSPME is characterized by minimal sorbent usage and the ability to extract analytes from very small sample volumes [20]. During the development of DSPME-based methods, numerous factors influencing sample-preparation efficiency must be considered. In this context, multivariate optimization proves highly valuable. Achieving high sensitivity, accuracy, and precision with DSPME requires identifying relevant factors and experimentally controlling their individual and interactive effects. Thus, the application of formal Design of Experiments (DoE) enables a systematic, rapid, and efficient optimization workflow that significantly surpasses traditional one-factor-at-a-time (OFAT)



approaches. The choice of experimental design depends on the research objectives, the number of factors, and available resources [21].

In this work, the applicability of the DSPME method, based on an amino-functionalized glycidyl methacrylate polymer, was systematically investigated for the preconcentration and determination of CR in aqueous media. The method was optimized using the Box-Behnken experimental design to evaluate the combined effects of key operational parameters, including adsorption time, desorption time, and desorption solvent volume, in order to maximize extraction efficiency.

The advantages of the proposed method include the use of an amino-functionalized polymer as the sorbent, which enables effective analyte binding. The method requires only a small amount of sorbent, with short sorption and desorption times, contributing to overall time efficiency. Additionally, the procedure is performed under mild conditions that do not require additional energy input, and the number of experiments was minimized through the application of the DoE methodology.

MATERIALS AND METHODS

Chemicals

All the chemicals used for DSPME were of analytical grade and used as received. Congo red (CR, $C_{32}H_{22}N_6Na_2O_6S_2$), sodium hydroxide (NaOH, p.a. > 98%) were obtained from Sigma Aldrich (Saint Louis, MO, USA). All solutions were prepared with deionized water. A previously synthesized polymer, prepared via suspension polymerization and subsequently amino-functionalized with diethylenetriamine (DETA), was used as the solid phase in dispersive microextraction. The synthesis and amino-functionalization of the polymer (SGE80-deta) have been described in detail elsewhere [22].

Instrumentation

Vortex-assisted dispersive solid phase microextraction was performed employing a Vortex Stirrer (VORX-005-001, V05, Labbox Labware S.L., Spain). Statistical analysis and experimental design were conducted using Minitab (version Minitab 20, Minitab Inc, USA). Quantification of CR was carried out using UV-Vis spectroscopy (NOVEL-102S, COLOLab Experts, Polje ob Sotli, Slovenia) at an absorption wavelength (λmax) of 498 nm.

Box-Behnken design (BBD)

To optimize the extraction of CR from aqueous samples, response surface methodology (RSM) based on the Box–Behnken design (BBD) was applied. The influence of key experimental variables, adsorption time (t_{ads}), desorption time (t_{des}), and desorption solvent volume (V_{des}), was systematically evaluated in order to enhance extraction efficiency prior to UV-Vis spectrophotometric analysis. Therefore, a set of 15 experiments was designed and conducted in a randomized order to prevent systematic errors. Coded factor values were used in the experimental matrix, where minimum, center, and maximum levels were assigned values of -1, 0, and +1, respectively. The values of these variables are presented in Table 1, while the matrix with coded values of the investigated factors is shown in Table 2.



Table 1. Factors affecting DSPME using the amino-functionalized polymer as the sorbent phase

| Variable | -1 | 0 | +1 |
|--|-----|-----|-----|
| Adsorption time (t _{ads}), min | 2 | 4 | 6 |
| Desorption time (t _{des}), min | 2 | 4 | 6 |
| Desorption solvent volume (V_{des}), μL | 500 | 700 | 900 |

Table 2. BBD Matrix with Coded Values

| RunOrder | t _{ads} | t _{des} | V _{des} |
|----------|------------------|------------------|------------------|
| 1 | 0 | 0 | 0 |
| 2 | 0 | +1 | -1 |
| 3 | 0 | +1 | +1 |
| 4 | 0 | 0 | 0 |
| 5 | -1 | -1 | 0 |
| 6 | -1 | 0 | +1 |
| 7 | +1 | 0 | +1 |
| 8 | -1 | +1 | 0 |
| 9 | 0 | -1 | -1 |
| 10 | 0 | -1 | +1 |
| 11 | 0 | 0 | 0 |
| 12 | +1 | -1 | 0 |
| 13 | +1 | +1 | 0 |
| 14 | -1 | 0 | -1 |
| 15 | +1 | 0 | -1 |

Dispersive solid-phase microextraction

The optimized parameters of the experimental procedure involved the use of 10 mL of aqueous CR solution (1 ppm) and 50 mg of amino-functionalized polymer as the sorbent. The sorption process was carried out at unadjusted pH (pH = 5.5) and room temperature for 4 min without any adjustment of the ionic strength, after which the sorbent was separated. For the desorption, 500 μ L of sodium hydroxide solution (0.2 mol/dm³) was added, and the mixture was stirred at room temperature for 6 minutes. Following desorption, the resulting liquid phase was analyzed by UV-Vis spectroscopy at a wavelength of 498 nm to determine the CR concentration.

RESULTS AND DISCUSSION

The BBD was used to define the optimal parameter values of the DSPME method. By conducting a series of 15 experiments in three replicates, three factors, adsorption time (t_{ads}), desorption time (t_{des}), and desorption solvent volume (V_{des}), were varied at three levels. Statistical analysis of the results was performed using Minitab. The system response monitored was the extraction efficiency (ER, %) of the DSPME method, calculated according to Equation 1 [23].



$$ER,\% = \frac{C_{CR,des}V_{CR,des}}{C_{CR,aq}V_{CR,aq}} \times 100 \tag{1}$$

where $C_{CR,des}$ (mg/dm³) and $C_{CR,aq}$ (mg/dm³) denote the concentrations of CR in the desorption solvent and in the aqueous phase, respectively, while $V_{CR,aq}$ (L) and $V_{CR,des}$ (L) represent the volumes of the aqueous solution and the desorption solvent. The BBD matrix with the actual values of the examined factors, along with the

experimentally obtained system response values (ER. %), is presented in Table 3.

Table 3. Experimental design for BBD with actual values of variables and the corresponding system response values

| RunOrder | t _{ads,} min | t _{des} , min | V _{des} , μL | ER, % | ERt, % |
|----------|-----------------------|------------------------|-----------------------|-------|--------|
| 1 | 4 | 4 | 700 | 69.16 | 59.05 |
| 2 | 4 | 6 | 500 | 75.50 | 76.07 |
| 3 | 4 | 6 | 900 | 36.40 | 45.91 |
| 4 | 4 | 4 | 700 | 45.24 | 59.05 |
| 5 | 2 | 2 | 700 | 46.92 | 51.41 |
| 6 | 2 | 4 | 900 | 30.80 | 27.27 |
| 7 | 6 | 4 | 900 | 29.19 | 24.99 |
| 8 | 2 | 6 | 700 | 61.32 | 56.73 |
| 9 | 4 | 2 | 500 | 70.30 | 61.63 |
| 10 | 4 | 2 | 900 | 28.74 | 29.07 |
| 11 | 4 | 4 | 700 | 61.47 | 59.05 |
| 12 | 6 | 2 | 700 | 34.05 | 39.53 |
| 13 | 6 | 6 | 700 | 69.09 | 65.49 |
| 14 | 2 | 4 | 500 | 52.80 | 57.91 |
| 15 | 6 | 4 | 500 | 52.70 | 57.07 |

In order to explain the correlation between the investigated factors and the system response, a second-order polynomial regression model was fitted to the experimental data, resulting in the development of the corresponding regression equation.

ER,
$$\% = -7.2 + 12.2 \, t_{ads} - 7.9 \, t_{des} + 0.223 \, V_{des} - 2.14 \, t_{ads} t_{ads} + 0.70 \, t_{des} t_{des} - 0.000217 \, V_{des} V_{des} + 1.29 \, t_{ads} t_{des} - 0.0009 \, t_{ads} V_{des} + 0.0015 \, t_{des} V_{des}$$

The predicted values of ER, %, calculated using the developed regression equation and marked as ER_t, are presented in Table 3.

Based on these results, the lowest ER of the DSPME method using the amino-functionalized polymer as the solid phase was 28.74%, observed at a desorption solvent volume of 900 μ L, with an adsorption time of 4 minutes and a desorption time of 2 minutes. In contrast, the highest efficiency of 75.50% was achieved with a desorption solvent volume of 500 μ L, an adsorption time of 4 minutes, and a desorption time of 6 minutes. The highest extraction efficiency was achieved using 500 μ L of the desorption solvent, while a notable decrease was observed at higher volumes, such as 900 μ L. This reduction can be attributed to the dilution effect, where the analyte desorbed from the sorbent is dispersed in a larger volume, resulting in lower analyte concentration in the eluent. Consequently, the analytical signal becomes weaker, which negatively affects



the calculated recovery values. Similar observations regarding the dilution effect have been reported in other studies [23, 24]. A longer desorption period affords the analyte sufficient time to be released from the sorbent and transferred into the solvent, whereas shorter intervals often result in partial analyte retention and diminished recovery. Vortex-assisted agitation has been shown to enhance mass transfer between the sorbent and sample phases, thereby improving both adsorption and desorption efficiencies. Consequently, extending the desorption time enhances analyte transfer and improves overall extraction efficiency.

Figures 1, 2, and 3 present a three-dimensional response surface plot (a), which visually illustrates the interdependence of experimental parameters and their combined effect on the response, along with a contour plot (b) that provides a more detailed insight into the influence of individual variables and their interactions on extraction efficiency.

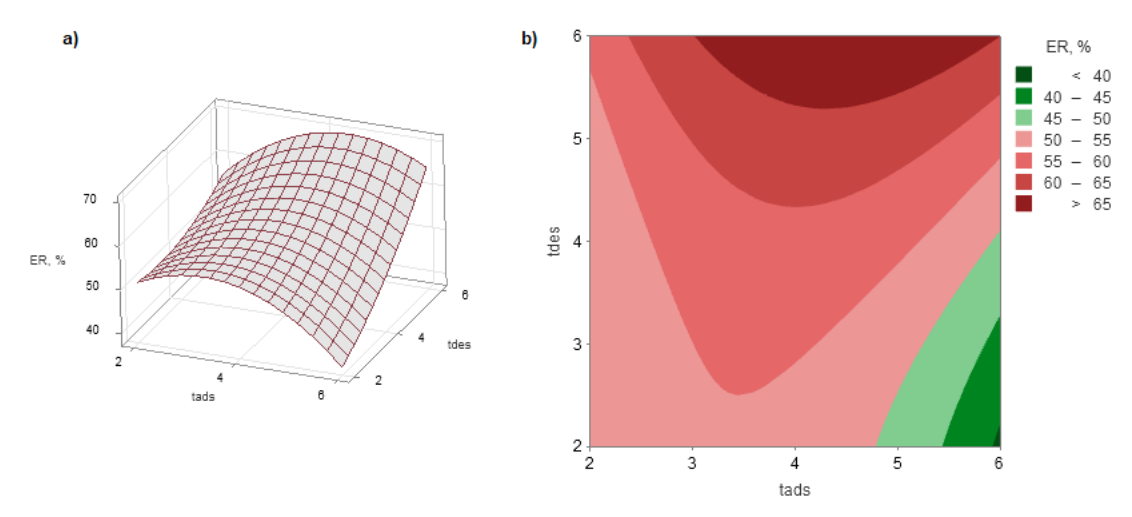


Figure 1. Effect of adsorption and desorption times on DSPME extraction efficiency at constant desorption solvent volume (700 μ I) illustrated by three-dimensional response surface plot (a) and contour plot (b)

In the three-dimensional response surface plot (Figure 1a) and the contour plot (Figure 1b), at a constant desorption-solvent volume of 700 μ L, variations in adsorption time (x-axis) and desorption time (y-axis) are shown to affect the DSPME extraction efficiency (ER, %). At short desorption intervals (2–4 min), recoveries remain moderate (approximately 50–60 %) across all adsorption durations. As the desorption time extends beyond 4 min, a marked increase in efficiency is observed: when adsorption is set to 4 min, extraction yields rise sharply, reaching their maximum at a desorption time of 6 min (> 65 %). Further prolongation of desorption or deviation from the 4 min adsorption interval affords no additional benefit and may even slightly reduce recoveries, indicating that equilibrium has been achieved. These results clearly identify 4 min of adsorption combined with 6 min of desorption as the optimal conditions for maximizing DSPME performance.



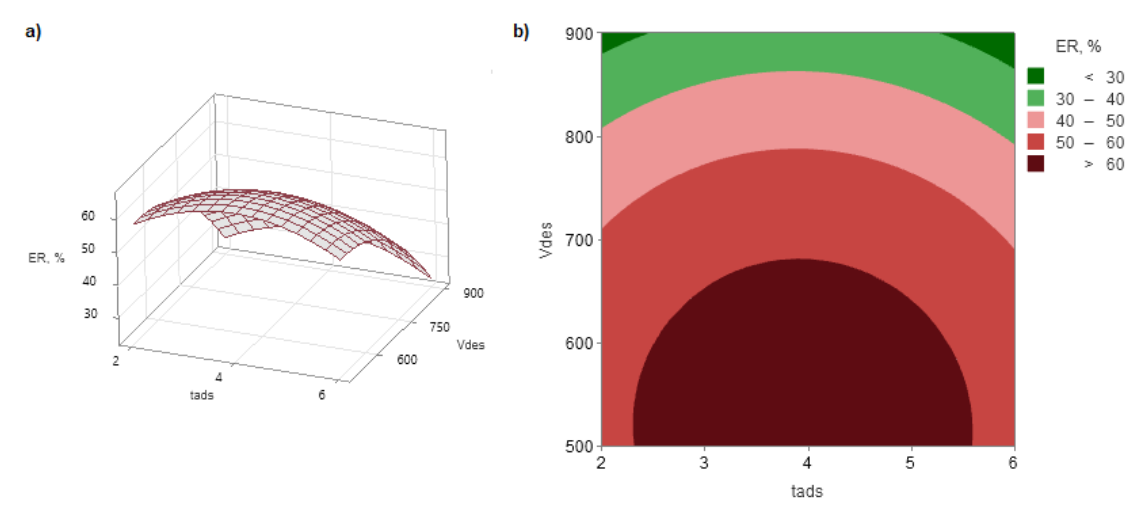


Figure 2. Response surface and contour plots showing the effect of desorption solvent volume and adsorption time on DSPME extraction efficiency at constant desorption time (4 min)

Figure 2 depicts a three-dimensional response surface (a) and contour plots (b) of DSPME extraction efficiency (ER, %) as a function of desorption solvent volume (500–900 μL , y-axis) and adsorption time (2–6 min, x-axis), with desorption time fixed at 4 min. The highest efficiencies (ER > 60 %) are centered precisely at 500 μL and an adsorption time of 4 min, identifying this point as the optimal operating condition. Deviations from 500 μL , either increasing the solvent volume above 500 μL or decreasing it below, result in a steady decline in recovery, passing through the 50–60 % and 40–50 % regions down to less than 40 % at the extremes. Similarly, adsorption times shorter or longer than 4 min yield lower efficiencies. These results confirm that a desorption solvent volume of 500 μL combined with a 4 min adsorption is optimal for achieving maximum DSPME performance.

Figure 3 presents a three-dimensional response surface plot (a) and a contour plot (b) of DSPME extraction efficiency (R, %) as a function of desorption time (2–6 min, x-axis) and desorption solvent volume (500–900 μ L, y-axis), with the adsorption time held constant at 4 min. The darkest region (> 70 %) occurs at a desorption time of 6 min and a solvent volume of approximately 500 μ L, indicating the highest extraction yield. Moving away from this optimal point, either by decreasing the solvent volume below or increasing it above 500 μ L, or by shortening the desorption time below 6 min, leads to a gradual decrease in efficiency, passing through the 60–70 % and 50–60 %, respectively, contours and falling below 40 % at the extreme parameter values. These results clearly confirm that a 6-minute desorption interval combined with a 500 μ L eluent volume represents the optimal conditions for maximizing DSPME performance.



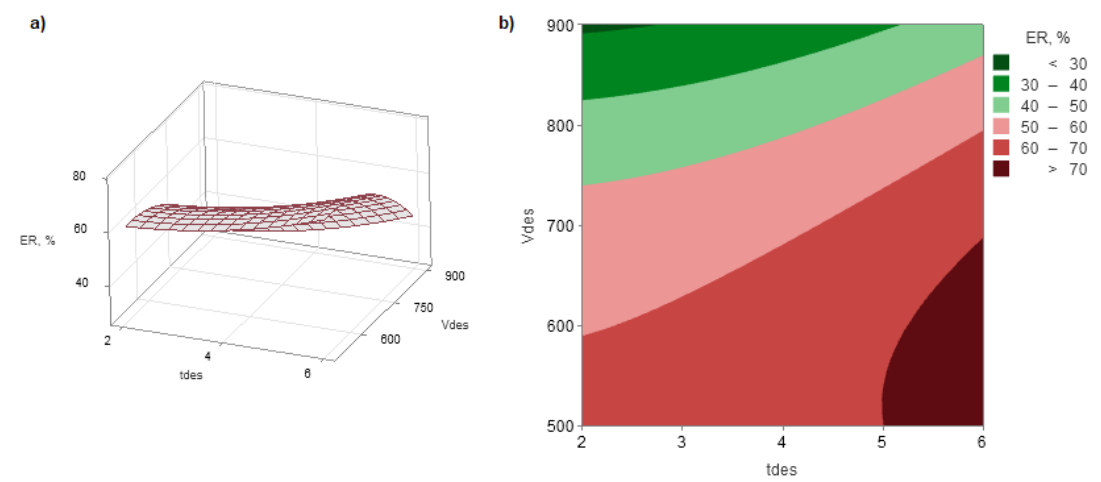


Figure 3. Response surface and contour plots showing the effect of desorption time and solvent volume on DSPME extraction efficiency at constant adsorption time (4 min)

CONCLUSIONS

In the context of modern, industry-driven lifestyles, the textile sector ranks among the fastest-growing industries and plays a pivotal role in a country's economic development. Simultaneously, it invariably exacerbates anthropogenic impacts on the Earth's biosphere by consuming vast quantities of water and generating large volumes of colored wastewater due to the dyes and pigments employed during the dyeing process. CR, an anionic azo dye, poses significant challenges in the dye industry owing to its complex chemical structure. Effective treatment of industrial effluents-often contaminated by the excessive use of CR-remains one of the most pressing and enduring ecological concerns. Therefore, the development of efficient, rapid, and environmentally benign analytical methods for the detection and removal of such pollutants is of paramount importance. In this study, the DSPME procedure utilizing an amino-functionalized glycidyl methacrylate-based polymer was successfully optimized for the selective extraction of CR from aqueous samples. The application of BBD enabled the identification of optimal operational parameters, specifically, 4 minutes of adsorption, 6 minutes of desorption, and 500 µL of NaOH as the desorption agent, yielding a high extraction recovery of over 75%. These results demonstrate that the proposed method is not only cost-effective and straightforward but also highly suitable for the monitoring and treatment of dye-contaminated water in environmental analysis.

Acknowledgment

This research was financially supported by the Ministry of Science, Technological Development and Innovation of the Republic of Serbia, Contract No. 451-03-136/2025-03/200026. This work is related to the implementation of the United Nations Sustainable Development Goal 6 – Clean Water and Sanitation.



References

- [1] Kumar A, Dixit U, Singh K, Prakash Gupta S, Jamal Beg MS. Structure and Properties of Dyes and Pigments. In: *Dyes and Pigments Novel Applications and Waste Treatment*. IntechOpen, 2021. https://doi.org/10.5772/intechopen.97104
- [2] Benkhaya S, M'rabet S, El Harfi A. A review on classifications, recent synthesis and applications of textile dyes. *Inorg Chem Commun.* 2020, 115, 107891. https://doi.org/10.1016/j.inoche.2020.107891
- [3] Alegbe EO, Uthman TO. A review of history, properties, classification, applications and challenges of natural and synthetic dyes. *Heliyon*. 2024, 10(13), e33646. https://doi.org/10.1016/j.heliyon.2024.e33646
- [4] Siddiqui SI, Allehyani ES, Al-Harbi SA, Hasan Z, Abomuti MA, Rajor HK, Oh S. Investigation of Congo Red Toxicity towards Different Living Organisms: A Review. *Processes.* 2023, 11(3), 807. https://doi.org/10.3390/pr11030807
- [5] Rasilingwani TE, Gumbo JR, Masindi V, Foteinis S. Removal of Congo red dye from industrial effluents using metal oxide-clay nanocomposites: Insight into adsorption and precipitation mechanisms. *Water Resources and Industry.* 2024, 31, 100253. https://doi.org/10.1016/j.wri.2024.100253
- [6] Manzoor K, Batool M, Naz F, Nazar MF, Hameed BH, Zafar MN. A comprehensive review on application of plant-based bioadsorbents for Congo red removal. *Biomass Conversion and Biorefinery.* 2022, 14(4), 4511–4537. https://doi.org/10.1007/s13399-022-02741-5
- [7] Ziane S, Bessaha F, Marouf-Khelifa K, Khelifa A. Single and binary adsorption of reactive black 5 and Congo red on modified dolomite: Performance and mechanism. *Journal of Molecular Liquids*. 2018, 249, 1245–1253. https://doi.org/10.1016/j.molliq.2017.11.130
- [8] Sasmal D, Maity J, Kolya H, Tripathy T. Study of Congo red dye removal from its aqueous solution using sulfated acrylamide and N,N-dimethyl acrylamide grafted amylopectin. *Journal of Water Process Engineering*. 2017, 18, 7–19. https://doi.org/10.1016/j.jwpe.2017.05.007
- [9] Miandad R, Kumar R, Barakat MA, Basheer C, Aburiazaiza AS, Nizami AS, Rehan M. Untapped conversion of plastic waste char into carbon-metal LDOs for the adsorption of Congo red. *Journal of Colloid and Interface Science*. 2018, 511, 402–410. https://doi.org/10.1016/j.jcis.2017.10.029
- [10] Ngulube T, Gumbo JR, Masindi V, Maity A. An update on synthetic dyes adsorption onto clay based minerals: A state-of-art review. *Journal of Environmental Management*. 2017, 191, 35–57. https://doi.org/10.1016/j.jenvman.2016.12.031
- [11] Mamane H, Altshuler S, Sterenzon E, Vadivel VK. Decolorization of dyes from textile wastewater using biochar: a review. *Acta Innovations*. 2020, 37, 36–46. https://doi.org/10.32933/actainnovations.37.3
- [12] Ahmad AL, Harris WA, S S, Ooi BS. Removal of dye from wastewater of textile industry using membrane technology. *Jurnal Teknologi*. 2002, 36(1). https://doi.org/10.11113/jt.v36.581
- [13] Dotto, J., Fagundes-Klen, M. R., Veit, M. T., Palácio, S. M., & Bergamasco, R. (2019). Performance of different coagulants in the coagulation/flocculation process of



- textile wastewater. Journal of Cleaner Production, 208, 656–665. https://doi.org/10.1016/j.jclepro.2018.10.112
- [14] Nidheesh PV, Divyapriya G, Titchou FE, Hamdani M. Treatment of textile wastewater by sulfate radical based advanced oxidation processes. *Separation and Purification Technology.* 2022, 293, 121115. https://doi.org/10.1016/j.seppur.2022.121115
- [15] Dihom HR, Al-Shaibani MM, Radin Mohamed RMS, Al-Gheethi AA, Sharma A, Khamidun MHB. Photocatalytic degradation of disperse azo dyes in textile wastewater using green zinc oxide nanoparticles synthesized in plant extract: A critical review. *Journal of Water Process Engineering*. 2022, 47, 102705. https://doi.org/10.1016/j.jwpe.2022.102705
- [16] Liu S, Xu X, Kang Y, Xiao Y, Liu H. Degradation and detoxification of azo dyes with recombinant ligninolytic enzymes from Aspergillus sp. with secretory overexpression in Pichia pastoris. *Royal Society Open Science*. 2020, 7(9). https://doi.org/10.1098/rsos.200688
- [17] Wawrzkiewicz M, Kucharczyk A. Adsorptive removal of direct azo dyes from textile wastewaters using weakly basic anion exchange resin. *International Journal of Molecular Sciences*. 2023, 24(5), 4886. https://doi.org/10.3390/ijms24054886
- [18] Khan WA, Varanusupakul P, Haq HUI, Arain MB, Boczkaj G. Applications of nanosorbents in dispersive solid phase extraction/microextraction approaches for monitoring of synthetic dyes in various types of samples: A review. *Microchemical Journal*. 2025, 208, 112419. https://doi.org/10.1016/j.microc.2024.112419
- [19] Tadić T, Marković B, Radulović J, Lukić J, Suručić Lj, Nastasović A, Onjia A. A Core-Shell Amino-Functionalized Magnetic Molecularly Imprinted Polymer Based on Glycidyl Methacrylate for Dispersive Solid-Phase Microextraction of Aniline. *Sustainability*. 2022, 14(15), 9222. https://doi.org/10.3390/su14159222
- [20] Maranata GJ, Surya NO, Hasanah AN. Optimising factors affecting solid phase extraction performances of molecular imprinted polymer as recent sample preparation technique. *Heliyon*. 2021, 7(1), e05934. https://doi.org/10.1016/j.heliyon.2021.e05934
- [21] Leardi R. Experimental design in chemistry: a tutorial. *Analytica Chimica Acta*. 2009, 652(1-2), 161–172. https://doi.org/10.1016/j.aca.2009.06.015
- [22] Maksin DD, Nastasović AB, Milutinović-Nikolić AD, Suručić LjT, Sandić ZP, Hercigonja RV, Onjia AE. Equilibrium and kinetics study on hexavalent chromium adsorption onto diethylene triamine grafted glycidyl methacrylate based copolymers. *Journal of Hazardous Materials*. 2012, 209-210, 99-110. https://doi.org/10.1016/j.jhazmat.2011.12.079
- [23] Alqarni AM, Mostafa A, Shaaban H, Gomaa MS, Albashrayi D, Hasheeshi B, Bakhashwain N, Aseeri A, Alqarni A, Alamri AA, Alrofaidi MA. Development and optimization of natural deep eutectic solvent-based dispersive liquid—liquid microextraction coupled with UPLC-UV for simultaneous determination of parabens in personal care products: evaluation of the eco-friendliness level of the developed method. *RSC Advances*. 2023, 13(19), 13183–13194. https://doi.org/10.1039/d3ra00769c



DISPERZIVNA MIKROEKSTRAKCIJA NA AMINO-FUNKCIONALIZOVANOM POLIMERU KAO ČVRSTOJ FAZI ZA PREKONCENTRACIJU AZO BOJE IZ VODENIH RASTVORA

Bojana Marković <u>ID</u>, Tamara Tadić <u>ID</u>, Sandra Bulatović <u>ID</u>, Natalija Nedić <u>ID</u>, Aleksandra Nastasović <u>ID</u>

Institut za hemiju, tehnologiju i metalurgiju, Univerzitet u Beogradu, Beograd, Srbija

Sintetičke boje se široko primenjuju u prehrambenoj, kozmetičkoj, tekstilnoj i farmaceutskoj industriji, a njihovo dospevanje u životnu sredinu predstavlja ozbiljan ekološki i zdravstveni problem zbog njihove toksičnosti i hemijske postojanosti. Među njima, azo boje čine najzastupljeniju klasu i naročito su štetne usled svoje toksične i perzistentne prirode. Dodatno, povezane su sa ozbiljnim zdravstvenim problemima, koji mogu zahvatiti bubrege, jetru, mozak i respiratorni sistem. Stoga je kvantifikacija i uklanjanje azo boja iz različitih medijuma od ključne važnosti. U ovom radu ispituje se prekoncentracija i određivanje azo boje Kongo crveno (CR) kao model supstance u vodenim rastvorima. U tu svrhu primenjena je disperzivna mikroekstrakcija na čvrstoj fazi (DSPME) za izdvajanje CR iz vodenih uzoraka pomoću amino-funkcionalizovanog polimera na bazi glicidil-metakrilata, pre merenja na UV-Vis spektrofotometru. Parametri koji utiču na proces ekstrakcije CR, vreme adsorpcije i desorpcije, kao i zapremina agensa za desorpciju, optimizovani su korišćenjem Box-Benken dizajna (BBD). Optimizovani uslovi obuhvatali su 10 mL vodenog rastvora CR, 50 mg aminofunkcionalizovanog polimera i 500 uL rastvora NaOH rastvora (0.2 mol/dm3) kao agensa za desorpciju, pri čemu su adsorpcija i desorpcija sprovedene na sobnoj temperaturi tokom 4. odnosno 6 minuta. Predviđeni prinos ekstrakcije CR izračunat pomoću polinomskog modela iznosio je 76,07 %, što je pokazalo dobru saglasnost sa eksperimentalno dobijenim rezultatom od 75,50 %. Dobijeni rezultati potvrđuju da je predložena DSPME procedura jednostavna i brza metoda sa značajnim potencijalom za određivanje azo boja u vodenim rastvorima.

Ključne reči: glicidil metakrilat, dietilentriamin, Kongo crveno, Box-Behnken dizajn, DSPMF



UDK 667:502.174.1:66.011 DOI: 10.46793/NovelTDS16.042IP

RECYCLING AND REUSE OF ORGANIC SOLVENTS FROM WASTE PAINTS

Jovana Ilić Pajić¹ <u>ID</u>, Jasna Stajić-Trošić¹ <u>ID</u>, Mirko Stijepović² <u>ID</u>, Srdjan Perišić³ <u>ID</u>, Vladimir Stijepović¹ <u>ID</u>, Aleksandar Grujić ^{1,*} <u>ID</u>

- ¹ Institute of Chemistry, Technology and Metallurgy, National Institute of the Republic of Serbia, University of Belgrade, Belgrade, Serbia
 - ² Faculty of Technology and Metallurgy, University of Belgrade, Belgrade, Serbia ³ Innovation Centre of the Faculty of Technology and Metallurgy, University of Belgrade, Belgrade, Serbia

Waste paints and other expired or unused coatings can be recycled before disposal. This is important because it reduces the volume of landfill waste and allows a certain amount of components to be reused. This contributes not only to waste reduction but also to improved environmental sustainability, while significant economic savings are realized.

This paper presents the design of a paint recycling device that works on the principle of distillation. In contrast to classical distillers, which work on the principle of distillation with a heat exchanger condenser, the proposed system consists of a main tank and a distillation column. The advantages of this device are that fractions with similar evaporation temperatures can be separated more easily.

A mathematical model based on thermodynamic and process parameters was developed to predict the behavior of the distillation process for different solvents. Based on the real parameters of the process, such as working pressure, composition, and flow rate of the feed mixture, evaporation temperature, etc., the time, composition, quality, and quantity required for the separation of each component were calculated, which represents the economic justification of this process. Three solvents with different compositions were tested using adjustable parameters of the distillation process, and the results provided insights into the distillation behavior, the characteristics of the recycled mixture, and the quality and yield of the recovered products.

Keywords: Paints, Recycling, Distillation, Mathematical Modeling, Optimization

^{*} Author address: Aleksandar Grujić, Institute of Chemistry, Technology and Metallurgy, National Institute of the Republic of Serbia, University of Belgrade, Njegoševa 12, 11000 Belgrade, Serbia e-mail address: gruja@tmf.bg.ac.rs



INTRODUCTION

Paints and various coatings are used in almost every household as an integral part of regular maintenance. They are also commonly found in everyday applications and across multiple industries, including construction, automotive, shipbuilding, catering, marketing, and others [1,2].

Paints and other organic solvent-based agents that have reached their expiry date, suffered wear and tear, have damaged packaging, or are otherwise no longer usable should be recycled and reused instead of being disposed of directly in landfills or incinerators. These materials can be considered liquid waste containing small amounts (up to maximum of 10%) of non-volatile impurities [3].

Assessing the feasibility of recycling chemical solvents involves calculations based on the type, quantity, and composition of the organic solvent. The results indicate which component can be recovered and how much the volume of solid waste deposited is reduced [2,4].

Waste and unused stocks of paints and other organic solvents pose a significant environmental challenge both locally and globally, as they are classified as hazardous waste [5]. As a result, many waste management organizations are actively working to address this issue. A global trend in recent years has been to encourage consumers to accurately calculate the amount of paint needed for work, thereby minimizing leftover quantities. Effective paint waste disposal is crucial and involves efforts to recycle and minimize the quantity of waste that requires treatment. Additionally, appropriate systems for the disposal of paint waste in landfills should be made available, depending largely on the quantity or volume of waste generated [1].

Paints often contain chemicals such as solvents and heavy metals that can contaminate soil and groundwater, posing risks to both the environment and human health. Recycling unused paint reduces these negative impacts and lowers the costs associated with hazardous waste disposal [4-6].

Several paint recycling associations have been established in Australia, primarily initiated by the paint industry and transporters, covering approximately 95% of all building and decorative paints sold in the country [7]. In addition to ensuring the responsible disposal of paint waste, these organizations are also committed to researching new methods for repurposing or replacing unused paint materials [3]. In the United States, numerous non-profit organizations have been created to represent paint manufacturers in the planning and management of paint recycling programs [8]. Since 2009, one of these organizations has set up 1,765 paint collection points, most of which are located in grocery shops and supermarkets. Their goal is to ensure that as much leftover paint as possible is either recycled or otherwise put to beneficial use [9].

In Canada, the paint and coatings industry operates the world's most extensive post-consumer paint recycling program, with activity in each province. In 2017, 28 million kilograms of used paint were collected and recycled enough to repaint approximately 560,000 average-sized houses [10]. Unused or leftover paint remains an important target of waste management efforts, as it constitutes a significant amount (volume) of household hazardous waste. The associated management costs are high, but there is great potential for waste reduction (volume), refreshment, recycling, and reuse [1,2].



In Serbia, legislation requires all users to store used paints, varnishes, and solvents in appropriately organized facilities that meet fire safety regulations. Several organizations in Serbia are responsible for the packaging, transport, and further treatment of this type of waste. These organizations ensure that such waste is properly stored, transported, and finally disposed of by incineration in accredited facilities abroad. Certain financial resources must be allocated for this service, which largely depends on the quantity (volume) of hazardous waste. If some of the used paints were recycled and reused, the amount of waste sent for incineration and the disposal costs could be significantly reduced [5,11,12].

A semi-batch incineration plant is commonly used for the recycling of paints and organic solvents [3,13]. The design of this plant consists of a conical stainless steel distillation vessel (boiler) equipped with a heating jacket. The solvent is rapidly heated via a double jacket transfer. The setup is based on a chemical solvent recycling device consisting of a main tank with a mixer heated by a jacket and a column with trays used for a more selective separation of the components.

To evaluate the efficiency of solvent recovery, a mathematical model was developed based on simulations of a distiller with a tray column. This model can be used to optimize the separation/purification of organic solvents under environmentally friendly process conditions. The model takes into account all the parameters of the real process, the input data related to the organic solvent being recycled, providing optimized parameters as final information. Recovery rates ranging from 95% to 99.9% can be achieved, depending on the composition of the solvent mixture [2,4,5].

The distillation process

The distillation process is described using a developed mathematical model.

A schematic representation of the paint recycling device is shown in Figure 1. The device consists of a main vessel with a stirrer, heated by hot oil or steam via a jacket, and connected to a column with trays and a condenser. The process operates in a semi-batch mode, where the feed mixture is continuously introduced into the system as long as a constant liquid level is maintained in the vessel. The condensed volatile components are collected in a receiving tank. The advantage of the proposed device compared to a classical distillation unit with a standard heat exchanger (condenser) lies in its ability to achieve a higher purity of the recovered components. Based on the described technological process for the treatment of organic solvents using a specially designed device, a mathematical model was developed to simulate the operation of the unit with various organic solvents [4,5].

The feed mixture is heated under continuous stirring. Separation occurs due to differences in boiling temperatures of the components, with the aid of a distillation column to enhance selectivity. The collected data is used for process simulation and optimisation [2].

The components of the system are labeled in Figure 1 as follows: 1 - solvent collecting tank, 2 - distillation column, 3 - residue collecting tank, P1 - batch pump, V1 - inlet valve, V2 - outlet valve, HE - heat exchanger, LS - level indicator, TI - temperature indicator, S1-S8 – flow indicators for process streams.



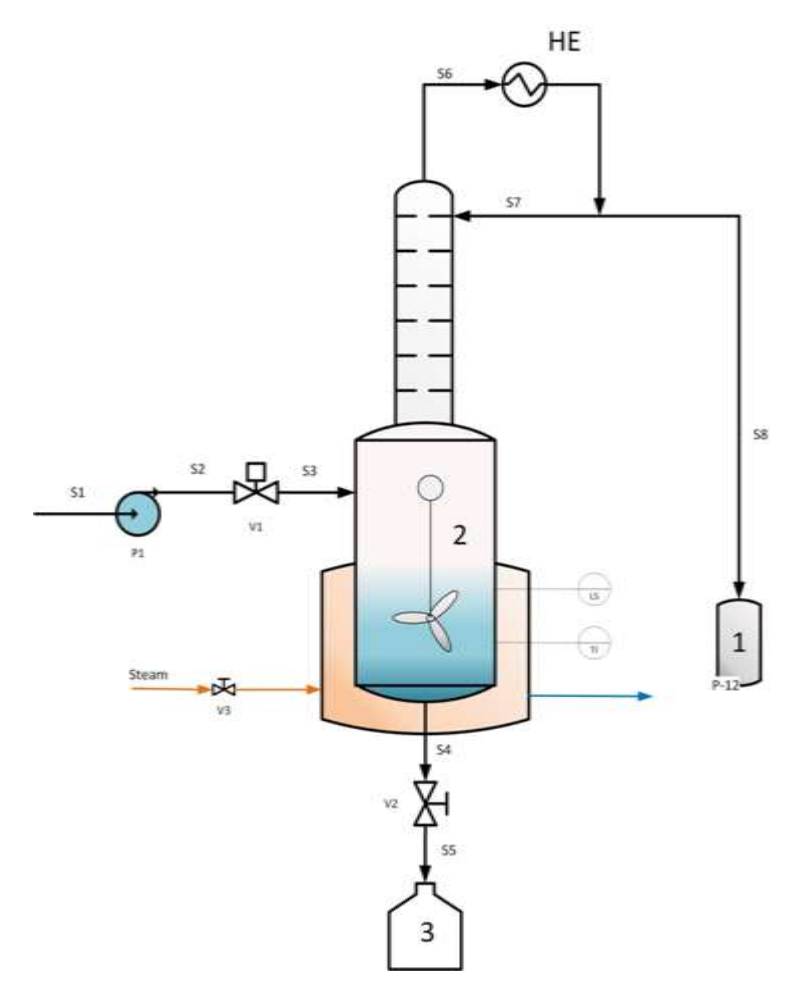


Figure 1. Schematic diagram of the paint recycling system

At the beginning of the process, the distillation apparatus (2) is charged with a recycled solvent-insert mixture (S1). Valve V2 is closed, and the unit is filled by activating pump P1 and opening valve V1. Filling stops once the liquid reaches the LS level sensor. The pump P1 and valve V1 are then deactivated. The operating pressure is set by turning on the vacuum pump. Once the system is fully charged, the distillation begins [12].

The mixer is started, and heating is activated. The temperature of the heating oil should be maintained between 30 and 60 °C above the boiling temperature of the solvent to achieve sufficient driving force for the vaporization. During the distillation process, a recycled mixture is constantly fed in. As the mixture evaporates, it is condensed by a coolant flowing through the condenser. The distillation continues until the temperature of the mixture in the main vessel reaches approximately 10 °C above the boiling point of the pure solvent. The condensed vapor (stream S8) is collected in vessel 1 [12,13].



The distillation process is terminated by closing the valve V1 on the feed line of the solvent S2, by switching off the heater, by switching off the vacuum pump, and the system is allowed to cool to ambient temperature. The valve for the condenser's cooling fluid is also closed.

The non-volatile residue (the sludge) is discharged through valve V2 into the collection container 3 and then packed and sent for disposal by authorized personnel. It should be noted that in real industrial settings, the plant cleaning stage is very important, and begins half an hour after distillation, allowing the residue to cool and preventing unwanted vapor emissions. Before discharging, it is essential to check that atmospheric pressure has been established and the vacuum has been completely released [5,13]. The distiller with mixer is heated by the oil jacket, while the gas phases obtained in the column are routed to the condenser. The volatile components are condensed and collected in the distillate vessel. The recycling solvent mixture is continuously heated and mixed, and the components are separated due to the different evaporation temperatures. The vacuum pump establishes the desired working pressure [13].

The distillation process can be divided into eight separate, consecutive parts:

- 1) Charging the system with inert gas,
- 2) Introducing the mixture for the process of distillation,
- 3) Establishing a vacuum in the system and starting the gas phase cooling system,
- 4) Heating the recycling mixture to the boiling point,
- 5) Distillation process,
- 6) Cooling of the mixture,
- 7) Compression of the system to atmospheric pressure by introducing inert gas,
- 8) Discharging the residue into storage containers [4,12].

All these separate processes are interconnected and form a complete recycling process.

- 1) Charging the system with inert gas. This process is very important to increase the safety of the distillation process, as organic solvents are flammable. Nitrogen is used as an inert gas [4].
- 2) After charging the system with inert gas, the recycling mixture is introduced up to the maximum fill level.
- 3) Decompression of the system and establishment of a cooling system. The operating pressure is built up by switching on the vacuum pump. The operating conditions for the condensation of the vapor phase are established by draining cooling water via the condenser. After building up the vacuum, the cooling system is switched on [13].
- 4) The recycling mixture is heated to a boiling point above the jacket with warm oil. The duration of the process depends on the composition of the batch to be recycled and is determined by the following equations, where all variables are defined in the Nomenclature:



$$M\frac{dh(T,P,x)}{dt} = Q \tag{1}$$

$$Q = UA(\bar{T}_{oil} - T) \tag{2}$$

$$Q = \dot{m}_{oil} \cdot c_{P,oil} \left(T_{oil,inlet} - T_{oil,outlet} \right)$$
(3)

$$h = h(T, P, x) \tag{4}$$

Depending on the composition of the feed mixture, the enthalpy of the batch is determined using the thermodynamic models of Peng-Robinson or the NRTL [2,5].

5) After reaching the boiling temperature, the solvent evaporates and condenses in the condenser and flows off into the collecting tank. A fresh mixture is continuously fed into the vessel, ensuring that the mixture volume is constant. This is achieved by a negative feedback control system (Figure 1) [4].

The distillation process is described by the following system of differential-algebraic equations [2,4]:

$$\frac{dM}{dt} = \dot{m}_i - \dot{m}_o \tag{5}$$

$$\frac{dM_s}{dt} = \dot{m}_i x_u^s \tag{6}$$

$$\frac{dM_r}{dt} = \dot{m}_i x_u^r - \dot{m}_o y_u^r \tag{7}$$

$$\frac{dE}{dt} = \dot{m}_i h_i - \dot{m}_o h_o + Q \tag{8}$$

$$Q = UA(\overline{T}_{oil} - T) \tag{9}$$

$$Q = m_{oil} \cdot c_{P,oil} \left(T_{oil,inlet} - T_{oil,outlet} \right)$$
(10)

$$K_r = K(P, T, x, y) \tag{11}$$

$$h_i = h(P, T, x_i) \tag{12}$$

$$h_o = h(P, T, y_o) \tag{13}$$

$$h = h(P, T, x) \tag{14}$$

$$\rho = \rho(x, P, T) \tag{15}$$

$$E = M \cdot h \tag{16}$$

$$M = \rho(x, P, T) \cdot V \tag{17}$$



The heating oil temperature is maintained at 30-60 °C above the solvent boiling point. During the distillation process, a mixture for recycling is continuously introduced. Distillation continues until the temperature of the mixture in the main vessel reaches a value 10-20 °C above the boiling point of the pure solvent. The distillation process is completed by closing the valve on the feed line for the solvent that is recycled in the distiller, whereupon the heaters and the vacuum pump are switched off [12].

6) The mixture is cooled via the oil jacket system until the ambient temperature is reached. Finally, the valve for the liquid supply to the condenser is closed. The duration of the cooling process depends on the properties of the residue and is determined by the following equations [5,13]:

$$M\frac{dh(T,P,x)}{dt} = -Q \tag{18}$$

$$Q = UA\left(T - \overline{T}_{oil}\right) \tag{19}$$

$$Q = m_{oil} \cdot c_{P,oil} \left(T_{oil,inlet} - T_{oil,outlet} \right)$$
(20)

$$h = h(T, P, x) \tag{21}$$

- 7) The system is compressed to atmospheric pressure by introducing inert gas [4].
- 8) Emptying the residue into the disposal container. The sludge that remains at the bottom of the distiller vessel is emptied into the collection container via a valve and then packaged by the responsible parties and made available for transport. It should be noted that in the real system, the cleaning stage of the plant is very important, which in practice begins half an hour after distillation in order to cool the precipitate and prevent unwanted evaporation. Before starting emptying, it is necessary to check that atmospheric pressure has been established, i.e., that the vacuum in the system has been completely released [4,13].

Based on the described technological process of treating organic solvents, data were obtained for simulation and process optimization. Using appropriate mathematical models, experimental measurements were analyzed and calculations for organic solvent recovery were carried out. Based on the input and output data, an algorithm was developed to optimize the recycling of the individual organic solvent components and simultaneously minimize the volume of the waste sludge. In order to dispose of the waste sludge as economically as possible and to reuse the recycled components, a mathematical model was developed to provide insight into the justification of the recycling process for various organic solvents in advance [2,4,5].



RESULTS AND DISCUSSION

The distillation tests performed on three different solvent mixtures (Solvents 1-3) under reduced pressure (0.5 bar) revealed clear trends in terms of solvent behavior, separation efficiency, and potential for recycling or safe disposal. During the distillation process, the level in vessel 2 is kept constant using two parameters: the control of valve 1 and the temperature control in vessel 2. Despite the differences in composition, the distillation system showed comparable thermal and dynamic profiles, demonstrating the effectiveness of the method used for the recovery of solvents in paint recycling and treatment units. The parameters of the distillation process are listed in Table 1

Table 1: Parameters of the distillation process

| | Distillation process parameters | | | | | |
|--|---------------------------------|------|------|--|--|--|
| | Solvent 1 Solvent 2 Solvent 3 | | | | | |
| Boiling temperature at 0.5 bar, [°C] | 70 | 40.5 | 79.3 | | | |
| Heating fluid operating temperature, [°C] | 115 95.5 124.3 | | | | | |
| Solvent temperature at which the distillation process is interrupted, [°C] | 80 57 89.3 | | | | | |

For all three solvents, a progressive increase in temperature and a corresponding decrease in solvent concentration in vessel 2 were observed as distillation progressed. This is due to the gradual removal of more volatile components and the concentration of suspended solids and higher-boiling fractions.

Solvent 1 was recycled in a distillation system, and the results of the calculations are shown in Table 2. Solvent 1 is a complex mixture with the following composition: 26-48% toluene, 10-23% acetone, 13-26% ethyl acetate, 10-24% methyl acetate, 3-9% methanol, 3-9% THF, 3-11% ethanol, 1-2% cyclohexane, 1-2% propanol, 1-3% butanol and 1-3% butyl acetate with a wide boiling range, which has a steady vapor flow of about 47-55 kg/h after the initial heating phase and stabilizes after about 10 hours. The working temperature increased from 49-70 °C during distillation, with the solvent mass fraction decreasing from 94 to 34%. The suspended solids content gradually increased from 6 to 66%, indicating a concentration effect typical of multi-component distillation systems.



Table 2. The results of the calculation for Solvent 1

| Time | Working | Working | Vapor | Mass | Mass | Amount | Amount | Quantity | Amount |
|-------|-------------|----------|--------|----------|-------------|-----------|--------|-----------|-----------|
| | temperature | pressure | flow | fraction | fraction of | of liquid | of | of liquid | of steam |
| | in the | in the | from | of | suspended | flow in | steam | in the | in the |
| | vessel | vessel | the | solvent | material | the | in the | receiving | receiving |
| | | | vessel | | | vessel | vessel | vessel | vessel |
| [h] | | | [kg/h] | [mass%] | [mass%] | [kg/h] | [kg] | [kg] | [kg] |
| | [°C] | [bar] | | | | | | | |
| 0.00 | 20.00 | 1.01 | 0.00 | 0.94 | 0.06 | 0.00 | 0.31 | 0.00 | 0.00 |
| 1.25 | 49.04 | 0.50 | 51.93 | 0.94 | 0.06 | 124.61 | 0.13 | 2.09 | 0.00 |
| 2.51 | 54.68 | 0.50 | 55.05 | 0.90 | 0.10 | 113.96 | 0.14 | 73.79 | 0.00 |
| 3.76 | 59.08 | 0.50 | 52.28 | 0.86 | 0.14 | 112.32 | 0.15 | 140.89 | 0.00 |
| 5.02 | 62.02 | 0.50 | 50.38 | 0.83 | 0.17 | 110.92 | 0.15 | 205.10 | 0.00 |
| 6.27 | 63.78 | 0.50 | 49.21 | 0.79 | 0.21 | 109.76 | 0.15 | 267.44 | 0.00 |
| 7.53 | 64.78 | 0.50 | 48.51 | 0.76 | 0.24 | 108.77 | 0.15 | 328.66 | 0.00 |
| 8.78 | 65.37 | 0.50 | 48.08 | 0.72 | 0.28 | 107.90 | 0.15 | 389.20 | 0.00 |
| 10.04 | 65.73 | 0.50 | 47.48 | 0.69 | 0.31 | 107.12 | 0.15 | 449.29. | 0.00 |
| 11.29 | 66.00 | 0.50 | 47.54 | 0.65 | 0.35 | 106.40 | 0.15 | 509.06 | 0.00 |
| 12.54 | 66.25 | 0.50 | 47.29 | 0.62 | 0.38 | 105.73. | 0.15 | 568.53 | 0.00 |
| 13.80 | 66.510 | 0.50 | 47.01 | 0.58 | 0.42 | 105.11 | 0.15 | 627.67 | 0.00 |
| 15.05 | 66.82 | 0.50 | 46.68 | 0.55 | 0.45 | 104.53 | 0.15 | 686.42 | 0.00 |
| 16.31 | 67.16 | 0.50 | 46.27 | 0.51 | 0.49 | 104.00 | 0.15 | 744.71 | 0.00 |
| 17.56 | 67.65 | 0.50 | 45.76 | 0.47 | 0.53 | 103.51 | 0.15 | 802.41 | 0.00 |
| 18.82 | 68.20 | 0.50 | 45.14 | 0.44 | 0.56 | 103.07 | 0.15 | 859.41 | 0.00 |
| 20.07 | 68.88 | 0.50 | 44.37 | 0.41 | 0.59 | 102.67 | 0.15 | 915.53 | 0.00 |
| 21.32 | 69.71 | 0.50 | 43.45 | 0.37 | 0.63 | 102.33 | 0.15 | 970.58 | 0.00 |
| 22.58 | 70.70 | 0.50 | 42.33 | 0.34 | 0.66 | 102.03 | 0.15 | 1024.35 | 0.00 |

Solvent 2 was tested in a distiller, and the calculation results are shown in Table 3. Solvent 2 is a mixture with the following composition: 70-80% methyl acetate, 10-13% xylene, 7-10% methanol, 3-5% 2-butoxyethanol. The mixture with a narrower boiling range dominated by methyl acetate, showed higher initial vapor flow peaks due to its lower boiling point (40.5 °C at 0.5 bar). The limited amount of liquid transferred to the receiver can be attributed to azeotropic composition, increased solvent losses due to high volatility, or lower separation performance at lower operating temperatures. Nevertheless, the mass fraction of suspended material increased steadily from 10 % to 57 %, indicating successful separation and partial purification.



Table 3. The results of the calculation for Solvent 2

| Time | Working temperature in the vessel | Working pressure in the vessel | Vapor flow from the vessel | Mass fraction of solvent | Mass fraction of suspended material | Amount of liquid flow in the vessel | Amount of steam in the vessel | Quantity of liquid in the receiving vessel | Amount of steam in the receiving vessel |
|-------|--|---|--|-----------------------------------|--|---|---|--|---|
| [h] | [°C] | [bar] | [kg/h] | [mass%] | [mass%] | [kg/h] | [kg] | [kg] | [kg] |
| 0.00 | 20.00 | 1.01 | 0.00 | 0.90 | 0.10 | 0.00 | 0.31 | 0.000 | 0.31 |
| 1.05 | 30.09 | 0.50 | 1.03 | 0.90 | 0.10 | 131.37 | 0.12 | 103.52 | 0.12 |
| 2.10 | 40.50 | 0.50 | 55.23 | 0.86 | 0.14 | 120.13 | 0.15 | 103.67 | 0.15 |
| 3.15 | 43.00 | 0.50 | 53.00 | 0.81 | 0.19 | 117.74 | 0.15 | 103.85 | 0.15 |
| 4.20 | 46.12 | 0.50 | 49.83 | 0.76 | 0.24 | 115.49 | 0.15 | 104.05 | 0.15 |
| 5.25 | 49.88 | 0.50 | 45.67 | 0.71 | 0.29 | 113.36 | 0.15 | 104.29 | 0.15 |
| 6.30 | 54.34 | 0.50 | 40.61 | 0.67 | 0.33 | 111.41 | 0.15 | 104.58 | 0.15 |
| 7.35 | 59.37 | 0.50 | 34.99 | 0.63 | 0.37 | 109.68 | 0.15 | 104.96 | 0.15 |
| 8.40 | 64.61 | 0.50 | 29.38 | 0.59 | 0.41 | 108.22 | 0.15 | 105.46 | 0.15 |
| 9.46 | 69.53 | 0.50 | 24.39 | 0.57 | 0.43 | 107.04 | 0.15 | 106.13 | 0.15 |
| 10.51 | 73.66 | 0.50 | 20.40 | 0.54 | 0.46 | 106.13 | 0.15 | 107.04 | 0.15 |
| 11.56 | 76.86 | 0.50 | 17.43 | 0.52 | 0.48 | 105.46 | 0.15 | 108.22 | 0.15 |
| 12.61 | 79.23 | 0.50 | 15.27 | 0.50 | 0.50 | 104.96 | 0.15 | 109.68 | 0.15 |
| 13.66 | 80.99 | 0.50 | 13.67 | 0.49 | 0.51 | 104.58 | 0.15 | 111.41 | 0.15 |
| 14.71 | 82.32 | 0.50 | 12.45 | 0.47 | 0.53 | 104.29 | 0.15 | 113.36 | 0.15 |
| 15.76 | 83.38 | 0.50 | 11.47 | 0.46 | 0.54 | 104.05 | 0.15 | 115.49 | 0.15 |
| 16.81 | 84.25 | 0.50 | 10.65 | 0.45 | 0.55 | 103.85 | 0.15 | 117.74 | 0.15 |
| 17.86 | 85.00 | 0.50 | 9.94 | 0.44 | 0.56 | 103.67 | 0.15 | 120.13 | 0.15 |
| 18.91 | 85.67 | 0.50 | 9.29 | 0.43 | 0.57 | 103.52 | 0.15 | 131.37 | 0.15 |

Solvent 3 was tested in a paint recycling device, and the calculation results are shown in Table 4. Solvent 3 is a mixture with the following composition: 70-80 % toluene, 20-30 % ethyl acetate, which requires a higher temperature of the heating oil to reach its boiling range (79.3 °C at 0.5 bar). The vapor flow rate reached about 47 kg/h after 2.5 h. This solvent mixture showed a more gradual and efficient increase in the receiving vessel content (up to 410 kg), indicating good distillation performance and significant solvent recovery potential. The mass fraction of suspended material increased from 10 to 51%, which is consistent with trends observed for other solvents.



Table 4. The results of the calculation for Solvent 3.

| Time | Working temperature | Working pressure | Vapor flow | Mass fraction | Mass fraction of | Amount of liquid | Amount of | Quantity of liquid | Amount of steam |
|-------|---------------------|------------------|---------------|------------------|---------------------|------------------|--------------|--------------------|-----------------|
| | in the vessel | in the | from | of | suspended | flow in | steam | in the | in the |
| | | vessel | the | solvent | material | the | in the | receiving | receiving |
| | | | vessel | | | vessel | vessel | vessel | vessel |
| [h] | [°C] | | [kg/h] | [mass%] | [mass %] | | [kg] | [kg] | [kg] |
| | | [bar] | | | | [kg/h] | 1 01 | . 0. | . 01 |
| 0.00 | 20.00 | 1.01 | 0.00 | 0.90 | 0.10 | 0.00 | 0.31 | 0.00 | 0.00 |
| 0.67 | 22.97 | 0.67 | 0.39 | 0.90 | 0.10 | 126.21 | 0.12 | 0.00 | 0.22 |
| 1.33 | 36.39 | 0.50 | 0.06 | 0.90 | 0.10 | 124.90 | 0.09 | 0.00 | 0.29 |
| 2.00 | 65.10 | 0.50 | 0.51 | 0.90 | 0.10 | 124.71 | 0.13 | 0.09 | 0.36 |
| 2.67 | 80.69 | 0.50 | 47.40 | 0.89 | 0.11 | 110.11 | 0.19 | 14.68 | 0.40 |
| 3.34 | 82.90 | 0.50 | 46.09 | 0.86 | 0.14 | 109.02 | 0.19 | 45.36 | 0.40 |
| 4.00 | 84.30 | 0.50 | 44.75 | 0.83 | 0.17 | 107.92 | 0.19 | 75.61 | 0.40 |
| 4.67 | 85.16 | 0.50 | 43.89 | 0.80 | 0.20 | 107.02 | 0.19 | 105.11 | 0.40 |
| 5.34 | 85.71 | 0.50 | 43.32 | 0.77 | 0.23 | 106.22 | 0.19 | 134.15 | 0.40 |
| 6.00 | 86.10 | 0.50 | 42.92 | 0.75 | 0.25 | 105.50 | 0.19 | 162.89 | 0.40 |
| 6.67 | 86.40 | 0.50 | 42.59 | 0.72 | 0.28 | 104.84 | 0.19 | 191.39 | 0.40 |
| 7.34 | 86.66 | 0.50 | 42.27 | 0.69 | 0.31 | 104.22 | 0.19 | 219.68 | 0.40 |
| 8.00 | 86.93 | 0.50 | 41.95 | 0.66 | 0.34 | 103.64 | 0.19 | 247.75 | 0.40 |
| 8.67 | 87.20 | 0.50 | 41.60 | 0.63 | 0.37 | 103.09 | 0.19 | 275.60 | 0.40 |
| 9.34 | 87.51 | 0.50 | 41.21 | 0.60 | 0.40 | 102.57 | 0.19 | 303.21 | 0.40 |
| 10.01 | 87.85 | 0.50 | 40.77 | 0.58 | 0.42 | 102.09 | 0.19 | 330.53 | 0.40 |
| 10.67 | 88.23 | 0.50 | 40.27 | 0.55 | 0.45 | 101.63 | 0.19 | 357.54 | 0.40 |
| 11.34 | 86.67 | 0.50 | 39.70 | 0.52 | 0.48 | 101.22 | 0.19 | 384.19 | 0.40 |
| 12.01 | 89.17 | 0.50 | 39.06 | 0.49 | 0.51 | 100.83 | 0.19 | 410.43 | 0.40 |

Of the three mixtures studied, Solvent 1 provided the highest recovery of the liquid phase in the receiving vessel, indicating its favorable separation profile despite its complex composition. Its ability to achieve more than 1000 kg of recovered solvent within 22.5 hours emphasizes its recyclability and economic benefit in an industrial environment. The disadvantage lies in its relatively high content of residual suspended solids, which may require post-treatment. Solvent 2 does have a high initial vapor release, possibly due to the formation of an azeotrope or a lower volatilization threshold at the operating pressure. Nevertheless, the lower boiling point offers an energy-saving advantage that reduces heating time and costs. Solvent 3 exhibited the most balanced distillation dynamics, with a constant increase in recovered solvent and a controlled accumulation of suspended solids. Its moderate recovery rate, combined with a stable vapor flow and temperature control, could make it optimal for continuous recycling processes with minimal risk of fouling.

Operation at a reduced pressure of 0.5 bar proved to be effective in all three experiments, as it improved distillation by lowering the boiling points and minimized the risks of thermal degradation. The gradual increase of the solid phase fraction in the residual vessel indicates efficient phase separation, which is crucial for reducing the volume of hazardous waste. The relatively low mass fractions of suspended solids (51–66%) at the end of the process confirm that the majority of volatile organics were successfully removed, contributing to safer handling and reduced environmental impact. Overall, the data obtained demonstrate the suitability of low-pressure distillation for the treatment and reuse of solvent waste from paint recycling processes. Each type of solvent has unique advantages depending on its composition, boiling behavior, and energy requirements, which can be exploited for specific industrial applications.



CONCLUSION

The worldwide problem of pollution of soil, water, and air is considerably aggravated by the improper disposal of paints that are no longer used for various reasons. To protect the environment and to to achieve economic savings on the disposal and incineration of hazardous waste resulting from the use of products from the paint industry, a device for recycling paints and other organic solvents has been developed. The technology for recycling waste mixtures presented in this paper is based on a distillation process. The advantage of this device compared to conventional devices of this type is that it contains a distillation column that enables more efficient distillation of a specific solvent from a mixture of recyclable solvents. In addition to the device, a mathematical model based on technical and technological as well as thermodynamic principles was developed which provides useful information on the distillation process, the recycled mixture, and the quality and quantity of the products obtained, which meet the requirements and needs of users. Further research should focus on the design of larger paint recycling plants, with emphasis on techno-economic analysis, planning, and application.

Acknowledgements

The authors would like to express their gratitude to the Ministry of Science, Technological Development and Innovation of the Republic of Serbia (No. 451-03-136/2025-03/200026) for the support.

Nomenclature

M – mass of mixture in a distiller (kg)

M_s – mass of dry matter in the distiller (kg)

 M_r – mass of solvent r in the distiller (kg)

h – specific enthalpy of the mixture in the distiller (kJ/kg)

h_i – specific enthalpy of the inlet mixture (kJ/kg)

h₀ – specific enthalpy of the outlet mixture (kJ/kg)

Q – heat transferred to the system (kW)

T – temperature in the distiller (°C)

P – pressure in distiller (bar)

x – mass fraction of components in mixture

t - time (h)

U – heat transfer coefficient of heating fluid and mixture in distiller unit (kJ·m⁻²·s⁻¹. °C⁻¹)

A - heat transfer area (m2)

 \overline{T}_{oil} – average temperature of oil (°C)



 \dot{m}_{oil} -mass flow of oil (kg/s)

 $c_{P oil}$ – heat capacity of oil (kJ/kg/°C)

 $T_{oil.inlet}, T_{oil.outlet}$ – inlet and outlet temperature of oil from the thermal jacket

 \dot{m}_i – inlet mass flow of feed in distiller unit (kg/s)

 \dot{m}_{o} – outlet mass flow of feed in the distiller unit (kg/s)

 x_{n}^{r} – mass fraction of solvent r in feed

 $x_{\cdot \cdot}^{s}$ – mass fraction of dry matter in feed

 y_n^r – mass fraction of solvent r in gas phase

 ρ – density of mixture in distiller unit (kg/m³)

V – volume of distiller unit (m³)

E – energy of mixture in distiller unit (kJ)

K_r – equilibrium constant gas-liquid for the solvent r

References

- [1] Surya Nair K, Basavaraju Manu, Adani Azhon, Journal of Environmental Management, 2021, 296, 113105, https://doi.org/10.1016/j.jenyman.2021.113105
- [2] Emmanuel A. Aboagye, John D. Chea, Kirti M. Yenkie, iScience 2021, 24, 103114, https://doi.org/10.1016/j.isci.2021.103114
- [3] Barbara Ruffino, Giuseppe Campo, Siti Shawalliah Idris, Güray Saliho `glu and Mariachiara Zanetti, Resources, 2023, 12, 45, https://doi.org/10.3390/resources12040045
- [4] Laura Pilon, Daniel Day, Harry Maslen, Oliver P. J. Stevens, Nicola Carslaw, David R. Shaw and Helen F. Sneddon, *Green Chemistry*, 2024, 26, 9697, https://doi.org/10.1039/D4GC01962H
- [5] Mafaz Setyawan, J. Jayanudin, Yeyen Maryani, ASEAN Journal for Science and Engineering in Materials, 2025, 4(1), 55-62,

https://ejournal.bumipublikasinusantara.id/index.php/ajsem

Connecticut Paint Stewardship Program, Annual Report July 1, 2017 – June 30, 2018.

[6] Derya Dursun, Fusun Sengul, Waste minimization study in a solvent-based paint manufacturing plant, Resources, Conservation and Recycling 47 (2006) 316-331, https://doi.org/10.1016/i.resconrec.2005.12.004

[7] https://www.paintback.com.au/

[8]https://www.coatingsworld.com/issues/2019-12-01/view breaking-news/paintcarecelebrates-10-years-with-10-paint-recycling-programs/

[9] https://www.paintcare.org/wp-content/uploads/docs/ct-annual-report-2018.pdf [10] https://canpaint.com/paint-care/

[11] Management of Paint and Paint Related Materials, March 2004, Northeastern University Procedure for Management of Paints and Paint Related Materials,



https://www.northeastern.edu/ehs/ehs-programs/hazardous-waste-management/fact-sheets/management-of-paint-and-paint-related-materials/
[12] https://istsurface.com/resources/solvent-distillation-system/
[13]https://www.ofru.com/en/products/solvent-recovery/overview-product-line-asc/solvent-recovery-plant-asc-500-50-kw/

Izvod

RECIKLAŽA I PONOVNA UPOTREBA ORGANSKIH RASTVARAČA IZ OTPADNH BOJA

Jovana Ilić Pajić¹ <u>ID</u>, Jasna Stajić-Trošić¹ <u>ID</u>, Mirko Stijepović² <u>ID</u>, Srdjan Perišić³ <u>ID</u>, Vladimir Stijepović¹ <u>ID</u>, Aleksandar Grujić¹ <u>ID</u>

- ¹ Institut za hemiju, tehnologiju i metalurgiju, Institut od nacionalnog značaja Republike Srbije, Univerzitet u Beogradu, Beograd, Srbija
 - ² Tehnološko-metalurški fakultet, Univerzitet u Beogradu, Beograd, Srbija
 - ³ Inovacioni centar Tehnološko-metalurškog fakulteta, Univerzitet u Beogradu, Beograd, Srbija

Otpadne boje i drugi premazi koji su ostali neiskorišćeni ili kojima je istekao rok trajanja, mogu se reciklirati pre odlaganja. Ovo je važno jer se tako smanjuje zapremina otpada koji se odlaže na deponiju, a i omogućava se ponovna upotreba određene količine recikliranih komponenti. Na ovaj način se doprinosi ne samo smanjenju otpada, već i poboljšanju ekološke održivosti, uz ostvarenje značajnih ekonomskih ušteda. U ovom radu je predstavljen uređaj za reciklažu boja koji radi na principu destilacije. Za razliku od klasičnih destilatora, koji rade na principu destilacije sa kondenzatorom, predloženi sistem se sastoji od glavnog suda sa destilacionom kolonom. Prednost ovog uređaja je što se frakcije sa sličnim temperaturama isparavanja mogu lakše razdvojiti. Razvijen je matematički model zasnovan na termodinamičkim principima i procesnim parametrima, kako bi se predvidelo ponašanje procesa destilacije za različite rastvarače. Na osnovu stvarnih parametara procesa, kao što su radni pritisak, sastav i brzina protoka napojne smeše, temperatura isparavanja itd., proračunavaju se vreme, sastav, kvalitet i količina za svaku od dobijenih komponenti, što predstavlja ekonomsku opravdanost ovog procesa. Tri rastvarača sa različitim sastavima su testirana korišćenjem podesivih parametara procesa destilacije, a rezultati daju uvid u tok procesa destilacije, karakteristike reciklirane smeše, i kvalitet i prinos recikliranih proizvoda.

Ključne reči: boje, reciklaža, destilacija, matematičko modelovanje, optimizacija



Section: TEXTILE ENGINEERING

UDK 677.21.494.674 : 577.15 : 541.183 DOI: 10.46793/NoveITDS16.059T

THE INFLUENCE OF ENZYMATIC PRE-TREATMENT ON THE ADSORPTION OF COTTON-POLYESTER BLENDED FABRIC

Anita Tarbuk* D, Lea Botteri D, Stefana Begović D
Department of Textile Chemistry and Ecology, University of Zagreb Faculty of Textile
Technology, Zagreb, Croatia

Thermophysiological comfort, which is crucial for the overall satisfaction of the wearer, depends largely on effective heat and moisture regulation. Cotton-polyester blends offer a balanced solution due to the hydrophilic and hydrophobic properties of the respective fibers, improving moisture absorption and the ability to dry quickly. However, the conventional alkaline pretreatment with NaOH is ecologically questionable. In this study, an environmentally friendly alternative by enzymatic pretreatment of 50/50 cottonpolyester fabric with pectinase and esterase enzymes was investigated. The effects on water adsorption were evaluated using vertical wicking (AATCC TM 197-2022), and the subsequent adsorption of fluorescent whitening agents (FWAs), Uvitex® BHT and Uvitex® NFW, was analyzed at three concentrations (1%, 2%, and 10% owf). The results showed that both enzymes improved the adsorption properties, with esterase and its combination with pectinase significantly increasing the whiteness of the fabric due to the higher uptake of Uvitex BHT. The optimal whiteness was achieved with 2% Uvitex BHT. while higher concentrations were required for comparable results with Uvitex NFW. The study shows that enzymatic pretreatment is a sustainable method to improve both sorption and optical properties of cotton-polyester fabrics.

Keywords: cotton-polyester blend, pectinase, esterase, FWA, degree of whiteness.

^{*} Author address: Anita Tarbuk, University of Zagreb Faculty of Textile Technology, Prilaz baruna Filipovića 28a, HR-10000 Zagreb, Croatia e-mail address: anita.tarbuk@ttf.unizg.hr



INTRODUCTION

Thermophysiological comfort, which includes heat and moisture regulation, has a major influence on wearer comfort. Adsorption properties maintain thermal balance and dryness, especially under conditions of high physical activity or thermal stress, where the accumulation of sweat can lead to discomfort, skin irritation, or even thermal fatigue. Textiles facilitate moisture transfer from the skin to the environment mainly by two mechanisms: liquid transfer (by wetting and wicking) and vapor transfer (by diffusion and evaporation). The effectiveness of these processes depends on the fiber type (hydrophilic vs. hydrophobic), yarn structure, fabric construction, and surface treatment. Common blends such as cotton-polvester blended fabric, which account for over 15 % of global textile production, combine the best properties of both fibres. Cotton contributes to wearer comfort due to its hydroxyl groups, which improve hydrophilicity, wettability, and antistatic properties, while polyester offers strength and durability as well as easy care, crease resistance, dimensional stability, and quick drying. In order to improve the wearing comfort of garments, especially blends with a higher polyester content, the inherent hydrophobic properties of polyester need to be modified to improve moisture absorption and the adsorption of textile auxiliaries. Various surface modification processes are available for cotton-polyester blended fabrics, usually targeting the polyester fibers in the blend, including plasma treatment, alkaline processing, chitosan functionalization, and enzymatic pre-treatment. Given the environmental concerns associated with chemical treatments, enzymatic pre-treatments are increasingly favoured as an environmentally friendly alternative [1-7].

Enzymes from the hydrolase group are mainly used in the textile industry, e.g., α -amylases in desizing, pectinases in scouring. Various enzymes, such as lipase, esterase, and cutinase, can be used for the pretreatment of polyester materials. Both esterase and lipase perform surface hydrolysis, and the cleavage of the polymer chains leads to an increase in the number of terminal hydroxyl (-OH) and carboxyl (-COOH) groups. Lipases and some esterases are able to hydrolyse the waxes of cotton fibres as well. When used under optimal conditions, esterase and lipase can improve the hydrophilicity of polyester fibers, facilitate further textile finishing processes, and at the same time maintain good mechanical properties. Pectinases are a heterogeneous group of related enzymes that hydrolyse pectin substances of plant origin in scouring and retting processes [6-9].

To achieve a high degree of whiteness, textiles must be treated with fluorescent whitening agents (FWAs). The effect of FWAs is based on fluorescence; molecules absorb ultraviolet light (300-400 nm) and emit it as visible light, usually in the blue range of the spectrum (400-500 nm), which neutralises the yellow tint of the fabric and creates the impression of a high degree of whiteness. Due to the cotton and polyester content in the blend, different FWAs must be used depending on the chemical composition of the fabric. FWAs for cotton fabrics are mainly stilbene derivatives, mostly diaminostilbene derivatives, which differ in the substituents and the number of sulphonate groups. Distyrylbiphenyl derivatives and triazolylstilbene derivatives can also be used for cellulose, but also for blended fabrics with cellulose. In polyester fabrics, FWAs are usually benzoxazole derivatives that have no affinity to cellulose. In addition to the degree of whiteness of the fabric, FWAs also contribute to UV protection [10-13].



Since most of the studies on surface modification of cotton-polyester blended fabrics were aimed at the polyester fibers in the blend, the enzymatic pretreatment of cotton-polyester blended fabrics in this work was aimed at both cotton and polyester, so that two commercially available enzymes – pectinase for the cotton and esterase for the polyester - and their mixture were used. The influence of the enzyme treatment on the adsorption of water and fluorescent whitening agents (FWAs) was determined before and after the enzymatic pretreatment.

MATERIALS AND METHODS

A 50/50 cotton-polyester blend fabric produced by Čateks d.o.o. was used in this research. The fabric was woven in a basket weave (Panama) 2/2, having a mass per unit area of 170 g/m².

The enzymatic pre-treatment of cotton-polyester blended fabric was carried out with two commercially available enzymes – pectinase (Biosol PRO, CHT-Bezema) and esterase (Texazym PES, Inotex), and their mixture. The pretreatment was carried out with 2 % owf (over weight of fabric) of each enzyme (or 1% Beisol PRO + 1% Texazym PES) by the exhaustion method at 60°C for 1 h in the drum of Polycolor Turbomat P4502 (Mathis) at LR 1:10.

Since the influence of enzymatic pre-treatment of cotton-polyester blended fabric on the adsorption of fluorescent whitening agents (FWAs) was investigated, fabrics were treated with two different FWAs for cellulosic fibers and their blends by Huntsman, Uvitex® brand: Uvitex BHT (C.I. Fluorescent Brightener 113) - diamino stilbene disulphonic acid derivative, and Uvitex NFW (C.I. Fluorescent Brightener 351) - distyryl biphenyl derivative. FWAs were used in a wide concentration range: 1, 2, and 10% owf by batch-wise method having LR 1:30 at 80°C for 30 min in stainless-steel bowls (Linitest, Hanau). After treatment, fabrics were air-dried.

Labels and treatments are listed in Table 1.

Table 1. Pre-treatments and Labels

| Label | Treatment |
|-------|--|
| N | Cotton-polyester blend – start fabric |
| T | Fabric pre-treated with commercial lipase Texazym (2% owf) |
| BP | Fabric pre-treated with commercial pectinase Beisol PRO (2% owf) |
| BPT | Fabric pre-treated with commercial lipase and pectinase |
| BHT | Treatment with Uvitex BHT |
| NFW | Treatment with Uvitex NFW |
| conc. | Concentration of FWA - 1, 2, 10% owf |

The changes in water adsorption of the fabric were determined according to AATCC TM 197-2022 *Vertical wicking of textiles*, Option B - length direction. The wicking rate was calculated for the short and long periods according to:

$$W = \frac{d}{t} \tag{1}$$



where: W is wicking rate [mm/s], d is wicking distance [mm], and t is wicking time [s]. The short-period rate was calculated from the distance measured in 2 min, and long-period rate from the distance in 10 min.

The adsorption of fluorescent whitening agent was monitored through spectral characteristics and whiteness of the fabrics. Spectral remission (R [%]) was measured using a remission spectrophotometer Spectraflash SF 300 (Datacolor). The whiteness degree of fabrics (WCIE) according to ISO 105-J02:1997 Textiles – Tests for colour fastness – Part J02: Instrumental assessment of relative whiteness, Tint value (TV), Tint Deviation (TD), and their coloristic meanings according to Griesser [14] were calculated automatically.

RESULTS AND DISCUSSION

The influence of the enzymatic pretreatment of cotton-polyester blended fabrics on the adsorption properties was investigated. For this purpose, the enzymatic pretreatment of cotton-polyester blended fabrics with two commercially available enzymes – pectinase for the cotton and esterase for the polyester - and their mixture was carried out. The adsorption of water and fluorescent whitening agents (FWAs) was determined before and after the enzymatic pretreatment.

The water adsorption of the cotton-polyester blend fabric was determined according to AATCC TM 197-2022. This test method evaluates the vertical wicking rate of fabrics, i.e. the ability of a fabric to transport liquid upwards along its surface due to its capillary forces [3,15]. The distance a liquid travels up a vertically oriented fabric sample over a given time was measured, and the vertical wicking rate was calculated for a short (2 min) and a long (10 min) time using equation (1). The results are summarized in Table 2.

Table 2. Vertical wicking rate of polyester/cotton blend fabric before and after enzyme pretreatment

| Option B | Short perio | od (<i>t</i> = 2 min) | Long period ($t = 10 \text{ min}$) | | |
|----------|---------------|------------------------|--------------------------------------|----------|--|
| Sample | <i>d</i> [mm] | W [mm/s] | <i>d</i> [mm] | W [mm/s] | |
| N | 45.0 | 0.375 | 100.0 | 0.167 | |
| Т | 59.0 | 0.492 | 118.5 | 0.198 | |
| BP | 58.5 | 0.488 | 120.0 | 0.200 | |
| BPT | 55.0 | 0.458 | 121.0 | 0.202 | |

The results of the vertical wicking rate of the cotton-polyester blended fabrics, shown in Table 2, demonstrate the changes in water absorbency after enzymatic pretreatment. It can be seen that the start cotton-polyester blend fabric reaches 45 mm in 2 minutes with a wicking rate of 0.37 mm/s, while this distance is >55 mm after the enzyme pretreatment. Cotton fibers have polar binding sites for water molecules; they can absorb large quantities of liquid and therefore have a high absorption rate. Polyester fibers, on the other hand, have a high crystallinity, so they do not adsorb water, but have better capillary transport of liquid upwards. Blended together, both fibers show their effect,



while the enzyme pretreatment changes this ability. The polyester component hydrolyzed with esterase increases the wicking rate to 0.49 mm/s, and a longer distance has been achieved. This is due to the surface changes on the fibers, which also enable better absorption in the polyester component, as the water binds to the new chemical groups formed during pretreatment. The results of the FWA adsorption confirm these findings.

For the research of FWA adsorption, fabrics were treated with two different FWAs from Huntsman brand Uvitex®: Uvitex BHT, a stilbene derivative with high affinity to cotton (2 sulfonate groups), and Uvitex NFW, a distyrylbiphenyl derivative in three concentrations: 1, 2, and 10 % owf. The spectral remission of cotton-polyester blended fabrics before and after FWA treatment was measured, and the coloristic parameters were automatically calculated. The spectral remission results are shown in Figures 1 and 2, and the whiteness degree (W_{CIE}), the maximum of remission (R_{max}) at a certain wavelength (λ_{max}), Tint value (TV), Tint deviation (TD), and its coloristic meaning are listed in Tables 3-6.

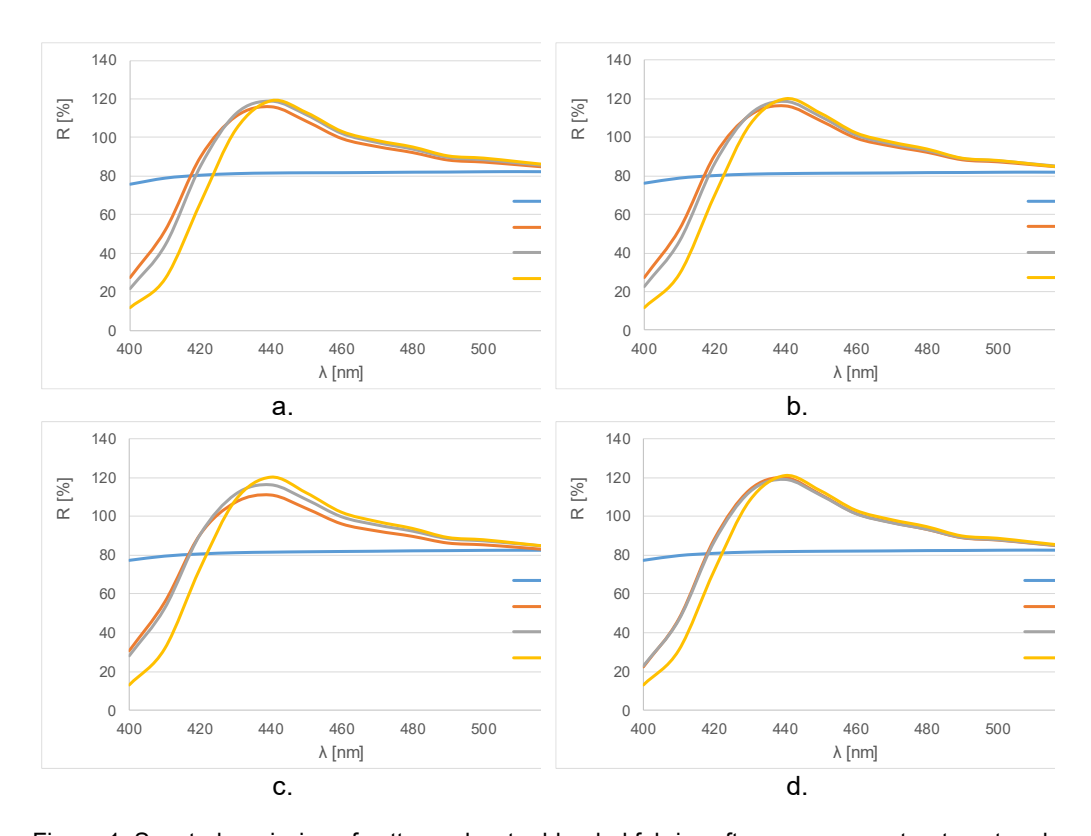


Figure 1. Spectral remission of cotton-polyester blended fabrics after enzyme pre-treatment and FWA treatment with Uvitex BHT



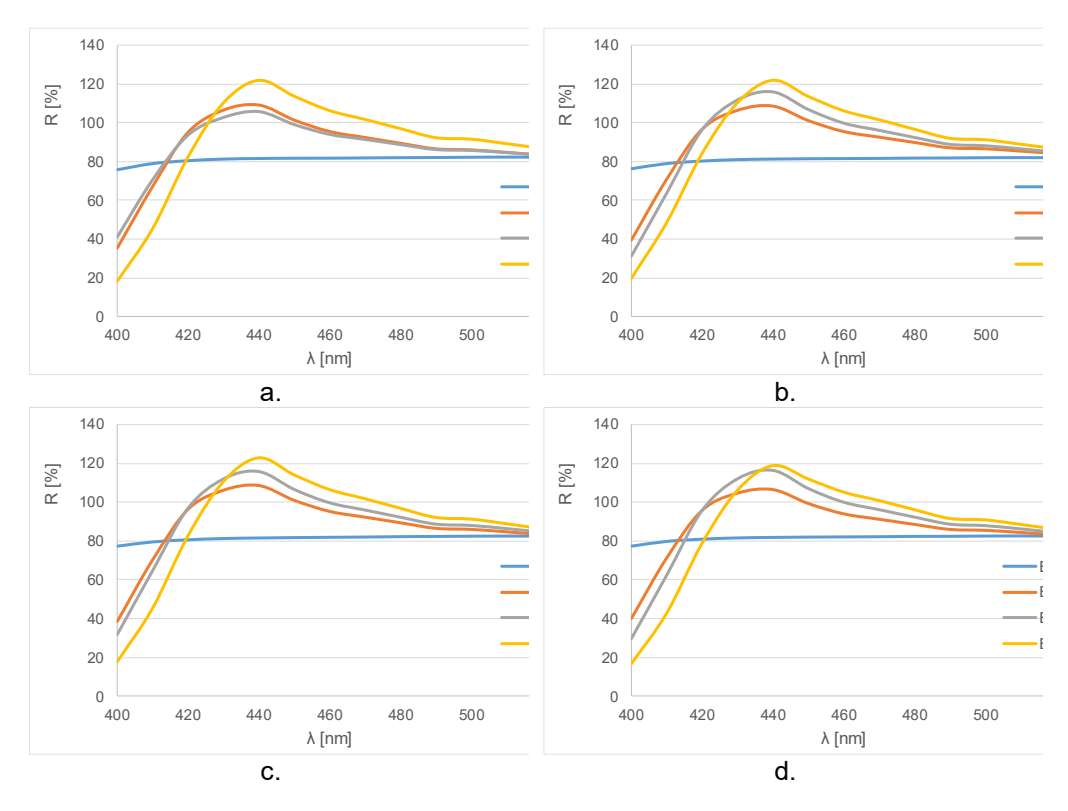


Figure 2. Spectral remission of cotton-polyester blended fabrics after enzyme pre-treatment and FWA treatment with Uvitex NFW

Table 3. Whiteness degree (W_{CIE}) of cotton-polyester blended fabrics before and after FWA treatment, maximum of remission (R_{max}) at a certain wavelength (λ_{max}), Tint value (TV, Tint deviation (TD), and its coloristic meaning

| Fabric | WCIE | R _{max} | λ _{max} [nm] | TV | TD | Coloristic meaning |
|----------|-------|------------------|--------------------------|------|----|------------------------------------|
| N | 78.9 | 84.88 | 700 | -0,6 | R1 | Trace redder than the white scale |
| N_BHT_1 | 136.0 | 115.85 | 440 | -1 | R1 | Trace redder than the white scale |
| N_BHT_2 | 140.3 | 118.61 | 440 | 0.1 | | |
| N_BHT_10 | 133.2 | 119.26 | 440 | 1.2 | G1 | Trace greener than the white scale |
| N_NFW_1 | 123.7 | 105.73 | 440 | -0.8 | R1 | Trace redder than the white scale |
| N_NFW_2 | 128.6 | 108.97 | 440 | -0.9 | R1 | Trace redder than the white scale |
| N_NFW_10 | 142.5 | 121.61 | 440 | 1.2 | G1 | Trace greener than the white scale |



Table 4. Whiteness degree (W_{CIE}) of pretreated cotton-polyester blended fabrics with Texazym PES, and after FWA treatment, maximum of remission (R_{max}) at a certain wavelength (λ_{max}), Tint value (TV, Tint deviation (TD), and its coloristic meaning

| Fabric | WCIE | R _{max} | $\lambda_{\text{max}}[\text{nm}]$ | TV | TD | Coloristic meaning |
|----------|-------|------------------|-----------------------------------|------|----|------------------------------------|
| Т | 78.6 | 84.64 | 700 | -0.6 | R1 | Trace redder than the white scale |
| T_BHT_1 | 136.8 | 113.92 | 440 | -0.7 | R1 | Trace redder than the white scale |
| T_BHT_2 | 139.6 | 116.06 | 440 | -0.4 | | |
| T_BHT_10 | 136.6 | 119.81 | 440 | 0.6 | G1 | Trace greener than the white scale |
| T_NFW_1 | 127.6 | 108.58 | 440 | -1.1 | R1 | Trace redder than the white scale |
| T_NFW_2 | 138.0 | 115.75 | 440 | -0.8 | R1 | Trace redder than the white scale |
| T_NFW_10 | 143.5 | 121.67 | 440 | 1 | G1 | Trace greener than the white scale |

Table 5. Whiteness degree (W_{CIE}) of pretreated cotton-polyester blended fabrics with Beisol PRO, and after FWA treatment, maximum of remission (R_{max}) at a certain wavelength (λ_{max}), Tint value (TV, Tint deviation (TD), and its coloristic meaning

| Fabric | Wcie | R _{max} | λ _{max} [nm] | TV | TD | Coloristic meaning |
|-----------|-------|------------------|-----------------------|------|----|------------------------------------|
| BP | 78.6 | 84.96 | 700 | -0.5 | R1 | Trace redder than the white scale |
| BP_BHT_1 | 131.9 | 110.98 | 440 | -1.1 | R1 | Trace redder than the white scale |
| BP_BHT_2 | 138.6 | 116.23 | 440 | -0.5 | | |
| BP BHT 10 | 137.8 | 120.08 | 440 | 0.4 | | |
| BP NFW 1 | 129.0 | 108.61 | 440 | -0.9 | R1 | Trace redder than the white scale |
| BP NFW 2 | 138.4 | 115.73 | 440 | -0.8 | R1 | Trace redder than the white scale |
| BP_NFW_10 | 144.7 | 122.84 | 440 | 1.2 | G1 | Trace greener than the white scale |

Table 6. Whiteness degree (W_{CIE}) of pretreated cotton-polyester blended fabrics with a mixture of Texazym PES and Beisol PRO, and after FWA treatment, maximum of remission (R_{max}) at a certain wavelength (λ_{max}), Tint value (TV, Tint deviation (TD), and its coloristic meaning

| Fabric | WCIE | R _{max} | λ _{max} [nm] | TV | TD | Coloristic meaning |
|------------|-------|------------------|-----------------------|------|----|---------------------------------------|
| BPT | 79.2 | 85.04 | 700 | -0.6 | R1 | Trace redder than the white scale |
| BPT_BHT_1 | 142.5 | 119.84 | 440 | -0.6 | R1 | Trace redder than the white scale |
| BPT_BHT_2 | 141.1 | 119.28 | 440 | -0.5 | | |
| BPT_BHT_10 | 138.6 | 121.11 | 440 | 0.6 | G1 | Trace greener than the white scale |
| BPT_NFW_1 | 125.0 | 106.51 | 440 | -1.3 | R1 | Trace redder than the white scale |
| BPT_NFW_2 | 139.4 | 116.28 | 440 | -0.8 | R1 | Trace redder than the white scale |
| BPT_NFW_10 | 139.0 | 118.68 | 440 | 1.6 | G2 | Slightly greener than the white scale |



The results shown in Table 3 indicate that the untreated cotton-polyester fabric has a remission at 700 nm and a whiteness of 78.9, and is a trace redder than the white scale. The enzyme pretreatment (Tables 4-6) does not change the whiteness. When both enzymes are applied, the whiteness is slightly higher, 79.2, but the fabric is still a trace redder than the white scale.

Regardless of the chemical composition of the FWA used and its affinity, treatment with the lowest concentration of Uvitex BHT and Uvitex NFW, 1 % owf, results in a significantly higher degree of whiteness ($W_{\text{CIE}}>120$) due to fluorescence emission at 440 nm.

From the spectral remission results shown in Figure 1 and Tables 3-6, it can be seen that the highest degree of whiteness and excellent brightness was achieved at a concentration of 2 % Uvitex BHT. All fabrics, regardless of the pretreatment, achieve the desired degree of whiteness with no appreciable deviation in tint from the white scale. It also shows that a concentration of 1 % is sufficient to achieve excellent whiteness, especially for the cotton-polyester fabric pretreated with both enzymes.

The spectral remission curves (Figure 1) show that the remission at λ_{max} = 440 nm for the fabrics treated with Uvitex BHT increases with the increase in the concentration. At the highest concentration of 10 % owf Uvitex BHT, the remission values are the highest (RN BHT 10 = 119.26 %, RT BHT 10 = 119.81 %, RBP BHT 10 = 120.08 %, RBPT BHT 10 = 121.11 %), but the whiteness is lower. The reason for the lower whiteness is the quenching of the fluorescence phenomenon by the FWA concentration [11]. The peak of the curve for a concentration of 10 % is slightly shifted from 440 nm, and this shift to higher wavelengths is characteristic of quenching. Layering of FWA molecules in high concentration prevents excitation of molecules in all layers, and therefore, there is no fluorescence that directly affects the reduction of whiteness. Additionally, FWA molecules at high concentrations build dimers that do not have the ability to fluoresce. This layering of FWA led to a change in tint: the tint is a trace greener than the white scale. Pretreatment with enzymes, esterase, and/or pectinase, individually or in combination, increases the whiteness of the fabric. The reason for this improved whiteness is the higher adsorption of Uvitex BHT. If both enzymes are used in the pretreatment, a higher number of active groups is available, so that a higher FWA adsorption is achieved, as it is a stilbene derivative with a high affinity to cotton cellulose.

In fabrics treated with Uvitex NFW, the spectral remissions also increase with increasing concentration (Figure 2). In contrast to Uvitex BHT, the degree of whiteness achieved with 1% Uvitex NFW is lower. The reason for this is the lower affinity to cellulose, since Uvitex NFW is a distyrylbiphenyl derivative but also has an affinity to polyester, so that with increasing concentration, the affinity is better and the adsorption is higher. Therefore, the highest remission and the highest degree of whiteness are achieved with 10 % Uvitex NFW. However, the degree of whiteness achieved with 10 % Uvitex NFW shows a green tinting.

Pretreatment with the enzymes increases the adsorption of Uvitex NFW. When the combination of enzymes, esterase and pectinase, was used in the pretreatment, quenching was observed in fabrics. Due to the highest adsorption, Uvitex NFW was layered, and the whiteness is lower, while the fabric itself has the color of FWA. The tint deviation confirms this finding, as the fabric is slightly greener than the white scale.



CONCLUSION

As the conventional alkaline pretreatment with NaOH is ecologically questionable, an environmentally friendly alternative by enzymatic pretreatment of cotton-polyester fabric was investigated. Enzymatic pretreatment with esterase and/or pectinase, individually or in combination, increases the adsorption of cotton-polyester blended fabrics. The wicking effect is faster and the fabrics achieve a higher degree of whiteness after FWA treatment. However, the adsorption of Uvitex BHT and Uvitex NFW is different due to the affinity to cotton. The adsorption of Uvitex BHT is higher, resulting in a higher degree of whiteness of the fabric, especially if it has been pretreated with esterase and its mixture with pectinase. 2% Uvitex BHT is sufficient for the highest degree of whiteness, while a higher concentration is required for Uvitex NFW. The study shows that enzymatic pretreatment is a sustainable method to improve both sorption and optical properties of cotton-polyester fabrics.

Acknowledgment

This work was supported, in part, by the University of Zagreb short-term financial support for the research "Unconventional processes of cotton scouring" TP/2 – 2025.

REFERENCES

- [1] Tegegne W, Haile A. Effect of papain enzyme surface modification on hydrophilic and comfort properties of polyester/cotton blend fabric. *Discover Materials* 2024, 4(2). https://doi.org/10.1007/s43939-023-00071-5
- [2] Tegegne W, Haile A. Improving hydrophilicity and comfort characteristics of polyester/cotton blend fabric through lipase enzyme treatment. *Clean Technologies and Environmental Policy* 2025, 27, 3–16. https://doi.org/10.1007/s10098-024-02756-8
- [3] Tarbuk A, Flinčec Grgac S, Dekanić T. Wetting and wicking of hospital protective textiles. *Advanced Technologies* 2019, 8(2), 5-15. https://doi.org/10.5937/savteh1902005T
- [4] Čorak I, Tarbuk A, Flinčec Grgac S, Dekanić T. Bio-Innovative Modification of Poly(Ethylene Terephthalate) Fabric Using Enzymes and Chitosan. *Polymers* 2024, 16, 2532. https://doi.org/10.3390/polym16172532
- [5] Grancarić AM, Kallay N. Kinetics of polyester fiber alkaline hydrolysis: Effect of temperature and cationic surfactants. *Journal of Applied Polymer Science* 1993, 49, 175–181. https://doi.org/10.1002/app.1993.070490121
- [6] Kumar D, Bhardwaj R, Jassal S, Goyal T, Khullar A, Gupta N. Application of enzymes for an eco-friendly approach to textile processing. *Environmental Science* and Pollution Research 2023, 30, 71838–71848. https://doi.org/10.1007/s11356-021-16764-4
- [7] Čorak I, Pušić T, Tarbuk A. Enzimi za hidrolizu poliestera. *Tekstil* 2019, 68(7-9), 142–51. https://hrcak.srce.hr/251219



- [8] Pušić T, Tarbuk A, Dekanić T. Bio-innovation in cotton fabric scouring acid and neutral pectinases. *Fibres & Textiles of Eastern Europe* 2015, 109, 98–103. https://bibliotekanauki.pl/articles/232192
- [9] Lee SH, Song WS. Effects of treatments with two lipolytic enzymes on cotton/polyester blend fabrics. *Journal of the Korean Society of Clothing and Textiles* 2013, 37(8), 1107–1116. https://doi.org/10.5850/jksct.2013.37.8.1107
- [10] Soljačić I. O optičkim bjelilima, Tekstil 1972, 21(5), 377-398. ISSN 0492-5882
- [11] Grancarić AM, Tarbuk A. Quenching of Fluorescence in World of Whiteness. In *AIC* 2009, Proceedings of the 11th Congress of the International Colour Association, The Colour Society of Australia, Sydney, Australia, 2009, pp. 395-401. CD-ROM, https://aic-color.org/publications-proceedings/
- [12] Botteri L, Dekanić T, Tarbuk A, Đorđević D. The influence of FWA chemical constitution to the whiteness and UV protection of cotton and cotton/polyester blend, *Advanced Technologies* 2021, 10(2), 66-72. https://doi.org/10.5937/savteh2102066B
- [13] Zhou Y, Cox Crews P. Effect of OBAs and repeated launderings on UVR transmission through fabrics, *Textile Chemist and Colorist* 1998, 30(11), 19-24. ISSN 0040-490X
- [14] Griesser R. Assessment of whiteness and tint of fluorescent substrates with good inter-instrument correlation, *Color Research & Application* 1994, 19(6), 446-460. https://doi.org/10.1002/col.5080190605
- [15] Grancarić AM, Tarbuk A, Chibowski E. Slobodna površinska energija tekstila. *Tekstil* 2008, 57(1-2), 28–39. https://hrcak.srce.hr/35482
- [16] Tarbuk A, Flinčec Grgac S, Dekanić T. Wetting and wicking of hospital protective textiles. Advanced Technologies 2019, 8(2), 5-15. https://doi.org/10.5937/savteh1902005T

Izvod

UTICAJ ENZIMSKE PREDOBRADE NA ADSORPCIJU TKANINE OD MEŠAVINE PAMUKA I POLIESTRA

Anita Tarbuk <u>ID</u>, Lea Botteri <u>ID</u>, Stefana Begović <u>ID</u>

Katedra za tekstilnu hemiju i ekologiju, Univerzitet u Zagrebu, Tekstilno-tehnološki fakultet, Zagreb, Hrvatska

U ovom radu je ispitan uticaj enzimske predobrade obrade tkanine od mešavine pamuka i poliestra na adsorpciju fluorescentnih sredstava za izbeljivanje (FWA). U tu svrhu, izvedena je enzimska predobrada tkanine od mešavine pamuka i poliestra (50%/50%) sa dva komercijalno dostupna enzima – pektinazom za pamučnu komponentu i esterazom za poliestarsku komponentu, i njenom smešom. Promene u adsorpciji vode tkanine određene su vertikalnim upijanjem (AATCC TM 197-2022). Za adsorpciju FWA, u zavisnosti od hemijskog sastava tkanine, korišćena su dva različita FWA od Huntsmana, marke Uvitex®: Uvitex BHT, derivat stilbena sa visokim afinitetom prema pamuku (2



sulfonatne grupe) i Uvitex NFW, derivat distirilbifenila. FWA su primenjene u tri koncentracije: 1, 2 i 10%, u odnosu na masu tkanine. Spektralna remisija pre i posle obrade sa FWA merena je pomoću remisionog spektrofotometra Spectraflash SF 300, Datacolor. Stepen beline je izračunat prema ISO 105-J02:1997, a odstupanja nijanse i njihovih kolorističkih parametara određena su prema Griseru. Iako esteraza i pektinaza deluju na različite komponente tkanine, obe doprinose povećanoj adsorpciji mešavine pamuka i poliestra. Što se tiče adsorpcije FWA, postoji razlika između adsorpcije Uvitex BHT i Uvitex NFW. Adsorpcija Uvitex BHT je veća, što rezultira većom belinom tkanine, posebno ako je prethodno obrađena esterazom i njenom mešavinom sa pektinazom. 2% owf Uvitex BHT je dovoljno za najveću belinu, dok je za Uvitex NFW potrebna veća koncentracija.

Ključne reči: mešavina pamuka i poliestra, pektinaza, esteraza, FWA, stepen beline.



UDK 677.074.2.494.674 : 582.687.21 : 547.458.68

DOI: 10.46793/NovelTDS16.070FG

APPLICATION OF IN-SITU HYDROTHERMAL SYNTHESIS FOR THE FUNCTIONALISATION OF COTTON/POLYESTER FABRIC WITH THE INCLUSION COMPLEX OF B-CYCLODEXTRIN AND ESSENTIAL TEA TREE OIL

Sandra Flinčec Grgac* ID, Franka Žuvela Bošnjak ID, Ana Palčić ID, Tanja Krivec University of Zagreb Faculty of Textile Technology, Zagreb, Croatia

Textiles are often used as a medium for the application of active substances through various processes to achieve antimicrobial and wellness properties for medical and cosmetic purposes. The unique structure of β-cyclodextrins, which enables the formation of inclusion complexes, has led to significant commercial applications in areas such as pharmaceuticals, cosmetics, and the textile industry. A key advantage of β-cyclodextrins is their environmental friendliness — they are biodegradable, non-toxic, and do not pollute wastewater systems. This study investigated the formation of inclusion complexes between β-cyclodextrin and tea tree essential oil and their binding to cotton/polyester fabrics by in situ hydrothermal synthesis. Part of the treated fabrics was subjected to a care procedure according to ISO 6330:2012, using the 6330 6N programme and the standard ECE detergent (WFK 88030) to evaluate the durability of the treatment. Changes at the physico-chemical level before and after washing were analysed using FTIR-ATR spectroscopy, while absorption and antimicrobial properties were tested on untreated, treated, and washed treated fabrics, taking into account their intended use in hospital environments. The results indicate effective binding of the βcyclodextrin tea tree oil inclusion complex to the cotton/polyester fabric by in situ hydrothermal synthesis, with the treatment being remarkably durable after laundering. These results emphasise the potential for further research to develop functional, highperformance advanced textiles for use in medical fields.

Keywords: cotton/polyester fabrics, inclusion complexes between β-cyclodextrin and tea tree essential oil, in situ hydrothermal synthesis



^{*} Author address: Sandra Flinčec Grgac, University of Zagreb Faculty of Textile Technology, Prilaz baruna Filipovića 28a, 10000 Zagreb, Croatia e-mail address: sflincec@ttf.unizg.hr

INTRODUCTION

The textile industry is currently undergoing a significant transformation towards sustainability and improved functionality. There is a growing demand for highperformance textile materials that go beyond the basic function of clothing and offer additional benefits to the end user. Functional textiles represent an intersection of textile technology, chemistry, and biotechnology, with a focus on solutions that improve the interaction between textiles and human skin. Of particular interest are cosmetotextiles - textile products with integrated cosmetic effects, such as skin moisturisation, soothing, or antibacterial protection [1, 2]. In this context, essential oils play an important role due to their bioactive properties, although their application is often challenged by their volatility and sensitivity to environmental conditions [3]. Tea tree essential oil (Melaleuca alternifolia) is known for its strong antibacterial, antiviral, and antifungal effects [4,5]. Due to their high volatility and susceptibility to external influences, essential oils require special protection and controlled release methods. One of the most effective approaches is the formation of inclusion complexes with cyclodextrins, especially β-cyclodextrin [6]. This cyclic oligosaccharide has a hydrophilic outer surface and a hydrophobic inner cavity, which makes it an ideal carrier for volatile, hydrophobic molecules such as essential oils. The inclusion complex increases stability, prolongs the bioactive effect, and enables the controlled release of active ingredients. In combination with textile substrates — especially cotton/polvester blends — innovative materials with a wide range of functional properties can be developed. Textiles treated in this way can have antibacterial, deodorising, UV-protective, and anti-inflammatory effects [5].

This study focuses on the application of *in-situ* hydrothermal synthesis as an environmentally friendly method for the functionalisation of textiles [6]. This process involves the direct formation of the β -cyclodextrin/tea tree oil inclusion complex on the textile surface under elevated temperature and pressure. The binding of β - β -cyclodextrin to cotton/polyester fabric, primarily to the cellulose component in the given blend, can be achieved through the application of polycarboxylic acids as crosslinking agents. The most extensively studied is 1,2,3,4-1,2,3,4-butanetetracarboxylic acid (BTCA), which demonstrates durable binding of the β - β -cyclodextrin inclusion complex primarily with cellulose in cotton/polyester blends, mainly due to the reactivity of its functional groups. The process is based on a two–step esterification, where in the first step a cyclic anhydride is formed, followed by a reaction with the hydroxyl groups of cotton and/or cyclodextrin in the second step. In this way, ester bonds are formed, ensuring the durability of the treatment even after multiple washing cycles [7].

Hydrothermal synthesis reduces the need for organic solvents and minimises the environmental impact. At the same time, it ensures high reproducibility of the treatment and permanent functionalisation of the textiles. The use of β -cyclodextrin also supports sustainability, as it is a non-toxic and biodegradable compound [6, 7, 8].

Incorporation into an inclusion complex makes the tea tree oil more stable and resistant to external influences, which prolongs its functional activity [5]. The application of such functional textiles is particularly important in the fields of medicine, sports, and protective textiles. It also enables the development of everyday clothing



with added value for the wearer. Cotton-polyester fabrics have proven to be a suitable substrate due to their balanced ratio between natural and synthetic properties, and the possibility of fixing the inclusion complex to the fibres further expands the application potential [9]. The use of cross-linking agents ensures long-lasting functionality, even after several care cycles. This technology paves the way for the development of textiles that not only protect the skin, but also actively contribute to health and the comfort of the wearer. The combination of *in-situ* synthesis, natural bioactive compounds, and cyclodextrins provides a sustainable basis for a new generation of intelligent textile materials.

MATERIAL AND METHODS

For the research presented in this paper, the following fabrics were used: cotton/polyester (50%/50%) in satin weave with a weft density of 26 threads cm⁻¹, and cotton/polyester (50%/50%) in plain weave with a weft density of 20 threads cm⁻¹. The description of the samples and their designations are provided in Table 1.

Table 1. Specification and labeling of samples

| Table 1. Opcomedicit and labeling of samples | |
|---|------------------|
| Sample | Label |
| Cotton/polyester blend in plain weave, untreated sample | P_PES_P |
| Cotton/polyester blend in plain weave, treated with β-cyclodextrin– | P_PES_P_BCD_TT |
| tea tree essential oil at 70 °C in a bath | |
| Cotton/polyester blend in plain weave, treated with β-cyclodextrin– | P_PES_P_BCD_TT_W |
| tea tree essential oil at 70 °C in a bath, and washed sample after | |
| treatment | |
| Cotton/polyester blend in satin weave, untreated sample | P_PES_A |
| Cotton/polyester blend in satin weave, treated with β-cyclodextrin- | P_PES_A_BCD_TT |
| tea tree essential oil at 70 °C in a bath | |
| Cotton/polyester blend in satin weave, treated with β-cyclodextrin- | P_PES_A_BCD_TT_W |
| tea tree essential oil at 70 °C in a bath, and washed sample after | |
| treatment | |

The inclusion complex of β -cyclodextrin (CycloLab R&D Ltd.) with tea tree essential oil (Sigma Aldrich) was prepared by applying mechanical force using a Retsch MM 400 vibrating mill, with 50% essential oil added in proportion to the mass of β -cyclodextrin. The mechanical-chemical synthesis was carried out at a frequency of 25 Hz for 10 minutes. Subsequently, the β -cyclodextrin-tea tree oil inclusion complex was heated in a microwave oven at a power of 80 W for 3 minutes to promote the reaction and further dry the complex itself [10]. The prepared β -cyclodextrin inclusion complexes with tea tree essential oil were used to functionalise the above substances by an impregnation process with a padding effect of approximately 100%, followed by in situ synthesis in a bath with the following composition:

- > 70 g/L 1,2,3,4-butanetetracarboxylic acid (BTCA) (Sigma Aldrich)
- ➤ 65 g/L sodium hypophosphite monohydrate (SHP) (Sigma Aldrich)
- ➤ 1 g/L Felosan RG-N (nonionic wetting agent) (Bezema)
- > 50% β-cyclodextrin-tea tree essential oil complex relative to the fabric weight



To ensure the binding of the inclusion complexes to the cotton/polyester fabrics, 1,2,3,4-butanetetracarboxylic acid (BTCA) was added to the bath, with sodium hypophosphite monohydrate (SHP) serving as the catalyst.

The impregnated samples, together with the bath, were placed in a Teflon-covered container and kept in a drying oven at 70 °C for 20 hours. The bath pH prior to oven treatment was 3.0, while after the reaction in the oven, the pH decreased to 2.76.

Upon completion of the reaction, the samples were removed and padded using a laboratory padder (Benz, TKF 15/M350 + LFV/2 350R). The samples were then airdried. Thermocondensation of the samples was performed in a laboratory oven (Benz, TKF 15/M350 + LFV/2 350R) at $180 \,^{\circ}C$ for 90 seconds.

A portion of the treated and thermocondensed samples was subjected to washing. Washing was carried out in an industrial washing machine (Wascator, Electrolux) in accordance with ISO 6330:2012 standard, program 6330 6N, using ECE standard detergent without optical brighteners but with phosphates (WFK 88030) at 75 °C for 80 minutes. The washing process was performed to evaluate the durability of the treatment. After washing, the samples were air-dried.

Physico-chemical changes in cotton samples were investigated using Fourier transform infrared spectroscopy in the attenuated total reflectance technique (FTIR-ATR) (Perkin Elmer, Spectrum 100 software). Four scans with a resolution of 4 cm⁻¹ between 4000 cm⁻¹ and 380 cm⁻¹ were performed for each sample, and the spectra obtained were processed using the Spectrum 100 software package, Perkin Elmer. The moisture transfer capability of untreated and treated samples was evaluated according to the AATCC TM 195 - 2017 method. Moisture absorption is an essential property of textile materials, as it significantly influences the thermo-physiological comfort of clothing during wear. In general, cotton fiber is considered a hygroscopic and hydrophilic fiber. The equilibrium moisture content (regain) of cotton is approximately 8.5%, indicating its high moisture absorption capacity. Due to these properties, cotton fiber is less prone to static electricity accumulation, which further contributes to the comfort of garments made from cotton [11]. To evaluate the moisture transfer behavior of both untreated and treated samples, tests were conducted using a Moisture Management Tester (MMT, ATLAS). Untreated and treated fabric samples were cut to dimensions of 6 × 6 cm and conditioned for 24 hours at 21 ± 1 °C and 65 ± 2% relative humidity. During testing, the textile specimen was placed flat between two horizontal, concentric sensors (upper and lower). A precisely defined amount of testing solution—used to monitor changes in electrical conductivity—was dispensed at the center of the specimen, with the face side positioned against the upper sensor. The test solution can move in three directions: Radial spreading on the face side, Vertical penetration through the fabric, and Radial spreading on the back side. Throughout the test, changes in the electrical resistance of the specimen were continuously recorded, and a summary of the measured parameters was used to evaluate the fabric's moisture transfer capability [12]. A single test cycle lasts 2 minutes and provides data on the following parameters: overall moisture management capacity (OMMC), wetting time, wetting speed, maximum wetted radius, absorption rate, and the accumulated one-way transport index [13].

The antimicrobial efficacy of the samples before treatment, after treatment, and following the washing cycle was evaluated in accordance with the AATCC 147 method,



with modifications recommended by experts. The samples were prepared under sterile conditions and subjected to testing. Each sample, in triplicate, was exposed to the action of the bacteria *Staphylococcus aureus* and *Escherichia coli* at concentrations of 10⁸–10⁶ bacteria/mL of nutrient agar (Colony Forming Units, CFU/mL), as well as the fungus *Candida albicans*. The treatment effectiveness was assessed using a qualitative method based on the formation of an inhibition zone, i.e., an area in which the antimicrobial agent from the tested substrate eliminated microorganisms present on the nutrient agar [14]. Achieving inhibition according to this method represents a highly stringent requirement imposed on treated textile materials.

RESULTS AND DISCUSSION

The results obtained from the Fourier Transform Infrared Spectroscopy with Attenuated Total Reflectance (FTIR-ATR) are presented in Figures 1 to 4.

In Figures 1 and 2, the spectral bands of tea tree essential oil and β -cyclodextrin are shown separately, with labeled peaks to facilitate identification of changes in specific wavelength ranges of the treated and untreated samples.

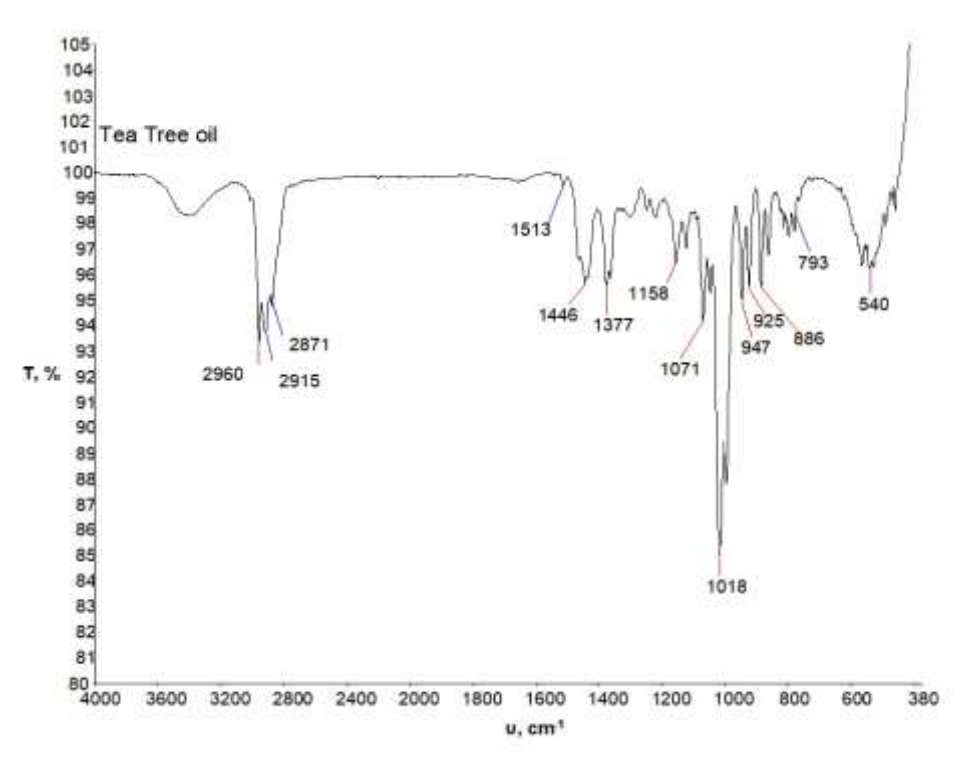


Figure 1. Spectral curve of tea tree essential oil recorded by FTIR-ATR.



The pronounced peaks observed at 2960 cm⁻¹, 2915 cm⁻¹, and 2871 cm⁻¹ correspond to C–H stretching vibrations. The strongly expressed peak at 1018 cm⁻¹ indicates C–C, C–OH, and C–H ring vibrations. The peaks at 886 cm⁻¹ and 793 cm⁻¹ suggest the presence of terpinen-4-ol [15].

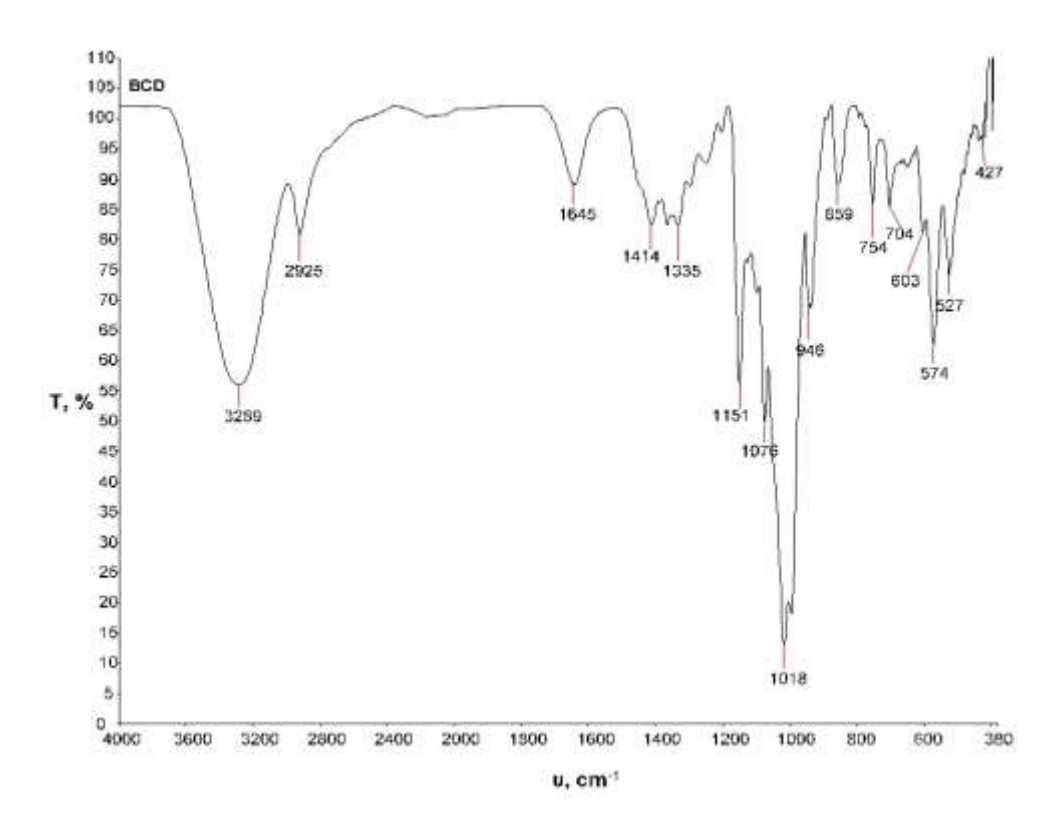


Figure 2. Spectral curve of β-cyclodextrin (BCD) recorded by FTIR-ATR.

The peak at 3289 cm⁻¹ is attributed to the accumulation of water molecules within the hydrophilic cavities of the cyclodextrin molecule. The peak at 2925 cm⁻¹ is associated with C–H and O–H stretching vibrations of cyclodextrin. The peak at 1018 cm⁻¹ corresponds to C–H and C–O–C stretching vibrations, while the peak at 1645 cm⁻¹ arises from O–H stretching of adsorbed water [16].



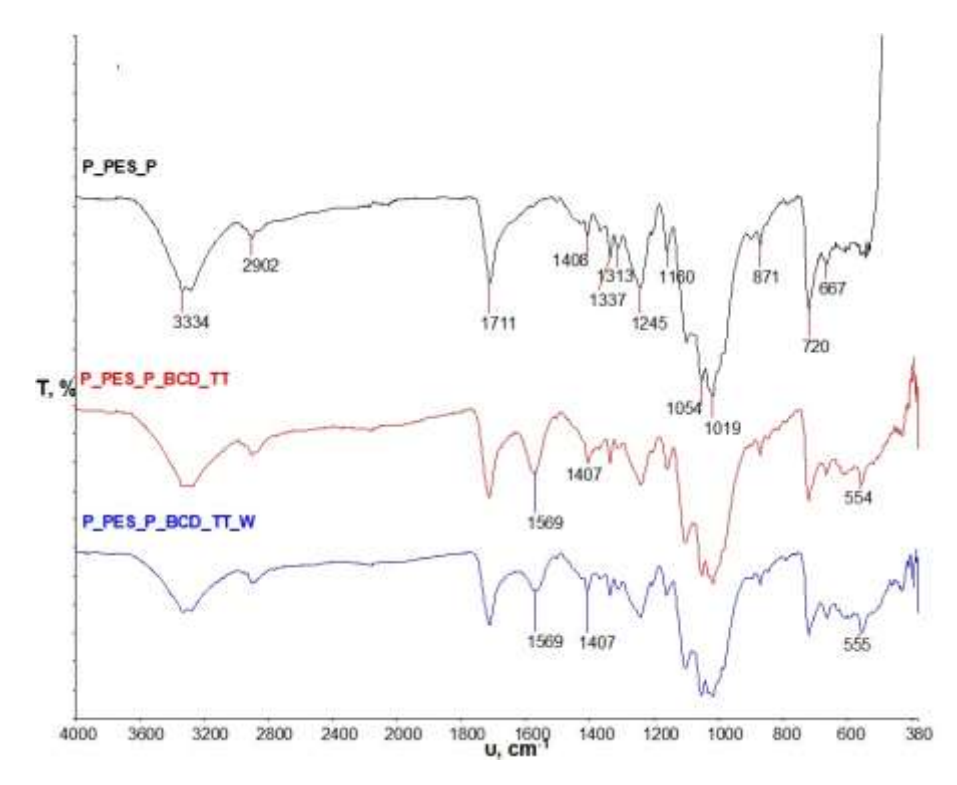


Figure 3. Spectral curves of the untreated (P_PES_P), treated (P_PES_P_BCD_TT), and treated washed sample (P_PES_P_BCD_TT_W) of the cotton/polyester fabric in plain weave.

In all the samples of cotton-polyester blends analysed, both in satin and plain weave, a sharp peak is observed at 1711 cm⁻¹ (Figures 3 and 4), which is caused by vibrations within the ester groups present in the polyester. Furthermore, in the treated samples subjected to FTIR-ATR analysis, a peak appears in the wavenumber range of 1560 -1590 cm⁻¹, indicating the presence of carboxyl groups originating from 1,2,3,4butanetetracarboxylic acid. This acid mediates the cross-linking of the βcyclodextrin/tea tree essential oil inclusion complex with cellulose during in situ synthesis. In addition, distinct peaks at 555 cm⁻¹, 554 cm⁻¹, 558 cm⁻¹, and 557 cm⁻¹ are visible in all treated and washed samples, which can be attributed to bending and out-of-plane vibrations between aromatic rings within C-C bonds as well as C-H bending in the monoterpene structure of γ-terpinene [7, 15]. It is important to note that even after the washing cycle (samples P PES P BCD TT W, Figure 3, and P PES A BCD TT W, Figure 4), the spectral profiles of the treated samples remain unchanged. In particular, the peak at 1509 cm⁻¹ and 1575 cm⁻¹ is clearly distinguishable in the washed samples (P_PES_P_BCD_TT_W, Figure 3, P PES A BCD TT W, Figure 4), which confirms that no structural changes occurred after washing, indicating stable crosslinking.



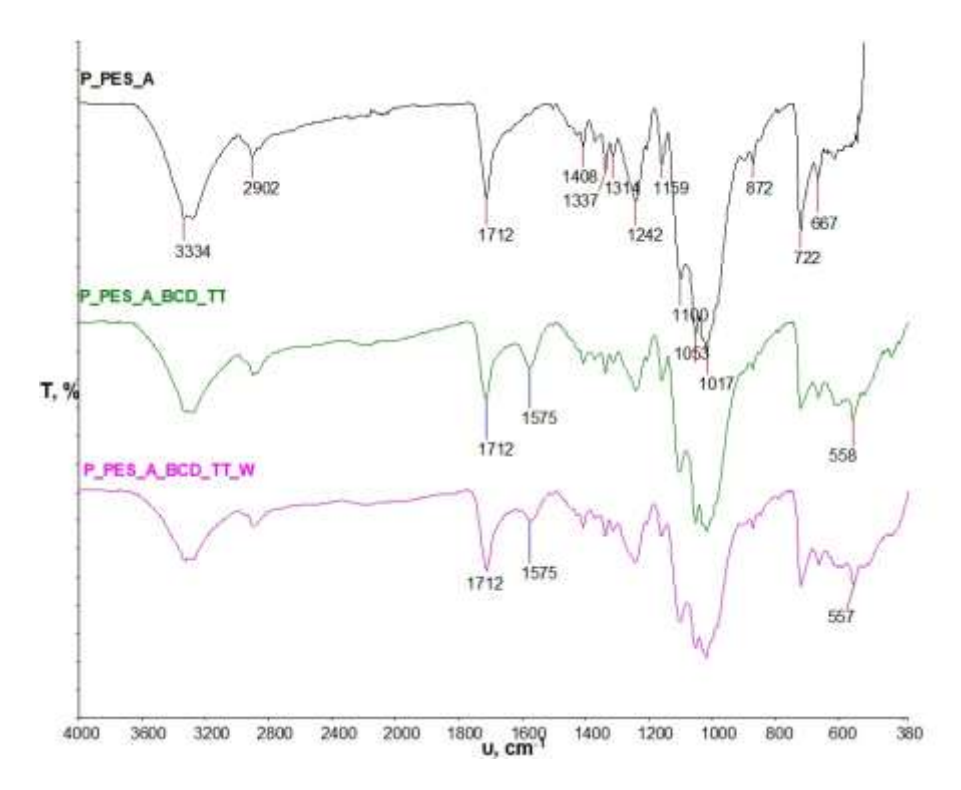


Figure 4. Spectral curves of the untreated (P_PES_A), treated (P_PES_A_BCD_TT), and treated washed sample (P_PES_A_BCD_TT_W) of the cotton/polyester fabric in satin weave.

Table 2 presents the moisture management properties of the samples P PES P. P PES A, P PES P BCD TT, and P PES A BCD TT, measured using a Moisture Management Tester (MMT). The untreated plain weave sample (P PES P) exhibits a longer wetting time on the top surface compared to the same sample in satin weave (P PES A). This can be attributed to the lower number of interlacing points and the smoother surface of the satin weave, which facilitates faster liquid spreading, i.e., surface wicking. Consequently, the wetting time on the bottom surface of the untreated satin weave sample (P PES A) is shorter (2.3713 s) compared to the plain weave sample (P PES P, 5.616 s). The top-surface absorption rate and moisture spreading speed are also higher in the satin weave sample (P PES A), resulting in a larger topsurface wetting radius compared to the plain weave sample (P PES P). Conversely, the bottom-surface absorption rate is slightly higher in the plain weave sample (P PES P). This is likely due to the weave structure: plain weave has more interlacing points, allowing for easier capillary liquid transport, whereas satin weave, with fewer interlacing points, has larger capillary spaces that trap more air. Furthermore, the satin weave fabric sample exhibits a slightly higher Accumulative One-Way Transport Index (%), while its Overall Moisture Management Capacity (OMMC) is slightly lower compared to the plain weave sample. Interestingly, the results presented in Table 2 show that both treated samples (P PES P BCD TT and P PES A BCD TT)



demonstrate identical values across all measured parameters. This suggests a significant effect of the inclusion complexes of β -cyclodextrin and tea tree oil on fabric hydrophilicity and moisture management. Such findings are particularly important considering the potential application of these newly developed samples in hospital environments [7, 17, 18].

Table 2. Moisture management properties of untreated samples in plain weave and satin weave (P_PES_P, P_PES_A) and of the same samples after finishing (P_PES_P_BCD_TT, P_PES_A_BCD_TT)

| | P_PES_P | P_PES_A | P_PES_P_BCD-TT | P_PES_A_BCD-TT |
|---|---------|---------|----------------|----------------|
| Wetting Time – Top Surface (s) | 5.9593 | 2.278 | 2.9328 | 2.9328 |
| Absorption Rate – Top Surface (%/s) | 70.6766 | 83.6562 | 56.0425 | 56.0425 |
| Wetted Radius – Top Surface (mm) | 20 | 30 | 22.5 | 22.5 |
| Spreading Speed – Top Surface (mm/s) | 3.8088 | 7.9669 | 5.4599 | 5.4599 |
| Wetting Time – Bottom Surface (s) | 5.616 | 2.3713 | 3.0422 | 3.0422 |
| Absorption Rate – Bottom Surface (%/s) | 75.2511 | 74.2551 | 58.7217 | 58.7217 |
| Wetted Radius – Bottom Surface (mm) | 20 | 30 | 22.5 | 22.5 |
| Spreading Speed – Bottom Surface (mm/s) | 4.7181 | 7.5601 | 5.416 | 5.416 |
| Accumulative One-Way Transport Index (%) | 95.9004 | 96.34 | 111.7374 | 111.7374 |
| Overall Moisture Management Capacity (OMMC) | 0.5828 | 0.4332 | 0.565 | 0.565 |

Table 3. Antimicrobial efficacy of untreated samples (P_PES_P, P_PES_A), the same samples after finishing (P_PES_P_BCD_TT, P_PES_A_BCD_TT), and after the washing cycle (P_PES_P_BCD_TT_W, P_PES_A_BCD_TT_W).

| Label | S. aureus | Escherichia coli | Candida albicans |
|------------------|-----------|------------------|------------------|
| P_PES_P | - | - | - |
| P_PES_P_BCD_TT | +/- | +/- | + (2 mm) |
| P_PES_P_BCD_TT_W | +/- | +/- | +/- |
| P_PES_A | - | - | - |
| P_PES_A_BCD_TT | +/- | +/- | + (1 mm) |
| P_PES_A_BCD_TT_W | +/- | +/- | +/- |
| | | | |

⁻ No antimicrobial efficacy

The results shown in Table 3 confirm the antimicrobial activity of all treated and washed samples against both Gram-positive and Gram-negative bacteria, as well as



^{+/-} Antimicrobial efficacy visible on the fabric; no presence of bacteria or fungi beneath it, but no inhibition zone developed

⁺ High antimicrobial protection, visible inhibition zone

excellent antifungal activity against Candida albicans. The treated sample P_PES_P_BCD_TT exhibited an inhibition zone of 2 mm, while a slightly smaller zone of 1 mm was observed in the sample P_PES_A_BCD_TT. After the washing cycle, the samples retained their antimicrobial activity against all tested microbial strains.

CONCLUSION

The effectiveness of the binding of the inclusion complex of β -cyclodextrin and tea tree essential oil to polyester cotton fabric in plain and satin weave and the wash durability of the treatment were confirmed by the results of Fourier transform infrared spectroscopy with attenuated total reflectance (FTIR-ATR). Changes in the spectral bands of the treated and washed treated samples were observed, as evidenced by the appearance of new peaks and variations in the intensity of existing peaks compared to the untreated sample.

The results of the moisture management tests show that the treated samples in plain and satin weave (P_PES_P_BCD-TT, P_PES_A_BCD-TT) belong to the category of materials with excellent moisture management properties. They are characterized by rapid wetting, rapid absorption, a large liquid spreading area on both the front and back of the fabric, rapid wicking on the back of the fabric, and an excellent ability to transport liquid in one direction. From these results, it can be concluded that the treated samples have hydrophilic and hygroscopic properties.

The antimicrobial analysis, carried out according to the AATCC 147 standard, showed good antimicrobial efficacy of all treated and washed samples against the Grampositive bacterium S. aureus, the Gram-negative bacterium E. coli, and the fungus C. albicans, without the development of an inhibition zone. However, samples $P_BES_BED_T$ and $P_BES_BED_T$ showed an inhibitory effect against C. albicans, indicating a high antimicrobial protection of the fabrics treated with the β -cyclodextrin-tea tree oil inclusion complex.

All these properties of the treated and laundered polyester—cotton fabrics in plain and satin weave indicate their potential applicability in hospital environments.

Acknowledgement

This work was supported in part by the Croatian Science Foundation under project UIP-2017-05-8780 **H**PROTEX and the short-term support of the University of Zagreb, Faculty of Textile Technology, entitled Functionalization and characterization of textiles and leather to achieve protective properties, TP/7.

References

[1] Flinčec Grgac S, Katović D, Bischof Vukušić S. Wellness: Novi trend i u tekstilnoj industriji. *Tekstil*. 2005;54(1):12–19. DOI nije dostupan, potvrđeno u bazi Tekstil historičnog arhiva gettextbooks.ca+6api.ttf.hr+6CroRIS+6ResearchGate+7tekstil.hist.hr+7api.ttf.hr+7.



- [2] Matijević I, Bischof S, Pušić T; i sur. Kozmetička sredstva na tekstilu: kozmetotekstilije. *Tekstil*. 2016;65(1–2):1–12. https://doi.org/10.5937/savteh2201063R https://doi.org/10.5937/savteh2201063R
- [3] Cerempei A. Aromatherapeutic Textiles. U: Active Ingredients from Aromatic and Medicinal Plants. El-Shemy H, ur. IntechOpen; 2017:88–106. https://doi.org/10.5772/66510.
- [4] Bakkali F, Averbeck S, Averbeck D, Idaomar M. Biological effects of essential oils A review. *Food and Chemical Toxicology*. 2008;46:446–475. https://doi.org/10.1016/j.fct.2007.09.106.
- [5] de Groot AC, Schmidt E. Tea tree oil: contact allergy and chemical composition. *Contact Dermatitis*. 2016;75(3):129–143. https://doi.org/10.1111/cod.12591.
- [6] Tiwari G, Tiwari R, Agrawal P, Bhati L, Kumar M. Cyclodextrins in delivery systems: Applications. *Journal of Pharmacy and Bioallied Sciences*. 2010;2(2):72–79. https://doi.org/10.4103/0975-7406.67010.
- [7] Flinčec Grgac S, Jablan J, Inić S, Malinar R, Kovaček I, Čorak I. The effect of ultrasonic treatment on the binding of the inclusion complex β -cyclodextrin–peppermint oil with cellulose material. Materials. 2022, 15, 470. https://doi.org/10.3390/ma15020470
- [8] Maestá FM, Lis MJ, Firmino HB, Dias da Silva JG, Curto Valle RdCS,
- Borges Valle JA, Scacchetti FAP, Tessaro AL. The Role of β-Cyclodextrin in the Textile Industry—Review. *Molecules*. 2020;25(16):3624.
- https://doi.org/10.3390/molecules25163624 pmc.ncbi.nlm.nih.gov.
- [9] Wang CX, Chen SL. Aromachology and its application in the textile field. *Fibres & Textiles in Eastern Europe*. 2005;13(6):41–44. DOI nije dostupan. Referentno potvrđeno preko Homescience Journal
- en.wikipedia.org+9homesciencejournal.com+9ResearchGate+9.
- [10] Katović D, Bischof-Vukušić S, Flinčec Grgac, S. Aplication of Microwaves in Textile Finishing Processes. *Tekstil : časopis za tekstilnu tehnologiju i konfekciju*. 2005;54;(7):313-325-x.
- [11] Čunko R, Andrassy M. *Vlakna*. Čakovec: Zrinski d.d.; 2005. ISBN 953-155-089-1 gettextbooks.ca+7katalog.kgz.hr+7hrcak.srce.hr+7.
- [12] AATCC TM 195 2017 Test Method for Liquid Moisture Management Properties of Textile Fabrics. 2017. Online; accessed 9. 6. 2025.
- [13] Moisture Management Tester Manual, M290. Testex; 2018. https://www.testextextile.com/product/moisture-management-tester-tf128/ (pristupljeno 9. 6. 2025).
- [14] AATCC 147 2016 Antibacterial Activity Assessment of Textile Materials: Parallel Streak Method. American Association of Textile Chemists and Colorists; 2016. https://microchemlab.com/test/aatcc-147-assessment-textile-materials-parallel-streak-method (accessed 9. 6. 2025).
- [15] Rytwo G, Zakai R, Wicklein B. The Use of ATR-FTIR Spectroscopy for Quantification of Adsorbed Compounds. Journal of Spectroscopy. 2015;2015:1–8. https://doi.org/10.1155/2015/727595
- [16] Flinčec Grgac S, Krešić A, Vrbić A, Čorak I, Tarbuk A, Brnada S, Dekanić T. Investigation of the possibility of binding cationized β-cyclodextrin on cotton fabric. In:



Book of Proceedings of the 10th International Textile, Clothing & Design Conference – Magic World of Textiles. Zagreb, Croatia, 2022, pp. 94–99. ISSN 1847-7275

[17] Tarbuk A, Flinčec Grgac S, Dekanić T: Wetting and Wicking of Hospital Protective Textiles. *Advanced technologies*, 2019;8(2):5-15. doi: 10.5937/savteh1902005T [18] Flinčec Grgac S, Benčević A, Vrbić A, Tarbuk A, Čorak I, Dekanić T. Investigation of moisture management ability of cotton fabric treated with β-cyclodextrin and inclusion complexes β-CD-essential oil.

In: Proceedings of the 8th International Professional and Scientific Conference Occupational Safety and Health. Karlovac, Croatia, 2022, pp. 578–584. ISSN 2975-3139.

https://korana.vuka.hr/fileadmin/user_upload/zrzz/skupovi/8/Book_of_Proceedings.pdf

Izvod

PRIMENA IN-SITU HIDROTERMALNE SINTEZE ZA FUNKCIONALIZACIJU TKANINE PAMUK/POLIESTAR INKLUZIVNIM KOMPLEKSOM BETA-CIKLODEKSTRINA I ETARSKOG ULJA ČAJEVCA

Sandra Flinčec Grgac D, Franka Žuvela Bošnjak D, Ana Palčić D, Tanja Krivec Sveučilište u Zagrebu, Tekstilno-tehnološki fakultet, Zagreb, Hrvatska

Tekstilni materijali se često koriste kao nosači aktivnih supstanci kroz različite postupke radi postizanja antimikrobnih i wellness svojstava za medicinsku i kozmetičku primenu. Jedinstvena struktura β-ciklodekstrina, koja omogućava formiranje inkluzivnih kompleksa, dovela je do značajne komercijalne primene u farmaceutskoj, kozmetičkoj i tekstilnoj industriji. Ključna prednost β-ciklodekstrina je njihova ekološka prihvatljivost biorazgradivi su, netoksični i ne zagađuju sisteme otpadnih voda. U ovom radu ispitivano je formiranje inkluzivnih kompleksa između β-ciklodekstrina i etarskog ulja čajevca, kao i njihovo vezivanje za tkanine pamuk/poliestar metodom in-situ hidrotermalne sinteze. Deo obrađenog materijala podvrgnut je postupku održavanja u skladu sa standardom ISO 6330:2012, koristeći program 6N i standardni ECE deterdžent (WFK 88030), radi procene trajnosti obrade. Promene na fizičko-hemijskom nivou pre i posle pranja analizirane su primenom FTIR-ATR spektroskopije, dok su apsorpciona i antimikrobna svojstva ispitivana na neobrađenom, obrađenom i opranom obrađenom materijalu, uzimajući u obzir njihovu moguću primenu u bolničkom Rezultati pokazuju efikasno vezivanje inkluzivnih kompleksa βokruženiu. ciklodekstrin-etarsko ulje čajevca za tkaninu pamuk/poliestar primenom in-situ hidrotermalne sinteze, pri čemu obrada zadržava visoku trajnost i posle pranja. Dobijeni rezultati naglašavaju potencijal za dalja istraživanja u razvoju funkcionalnih, visoko performansnih naprednih tekstila za medicinsku upotrebu.

Ključne reči: tkanina pamuk/poliestar, inkluzivni kompleksi β-ciklodekstrin–etarsko ulje čajevca, in-situ hidrotermalna sinteza



UDK 677.21.016.24 : 677.027.254.1 DOI: 10.46793/NovelTDS16.082DJ

EFFICIENCY OF COTTON FABRIC DESIZING USING DIFFERENT METHODS

Suzana Đorđević* D, Sandra Stojanović D, Slađana Antić D
Academy of Applied Studies Southern Serbia, Department of Technology and Art
Studies Leskovac, Leskovac, Serbia

Desizing of cotton fabric is a vital step in textile wet processing, directly influencing subsequent treatment and overall fabric performance. This study evaluates the effectiveness of hydrochloric acid, ammonium persulfate, and thermostable amylase asdesizing methods.. The performance of each method was assessed through key parameters: change in fabric mass, water penetration time, water absorption capacity, breaking strength, elongation at break, and air permeability. The results indicate distinct differences in the action mechanisms and effects of the desizing agents. Hydrochloric acid and ammonium persulfate demonstrated rapid sizing material removal, but also caused a noticeable reduction in mechanical properties and air permeability, which is attributed to their oxidative and acidic properties. In contrast, enzymatic desizing using thermostable amylase ensured effective removal of size material while maintaining fabric strength, elongation, and permeability characteristics. These findings support the potential of enzymatic desizing as a more fabric-friendly and sustainable alternative to conventional chemical methods, particularly for plain weave cotton substrates.

Keywords: cotton fabric, desizing, amylase, hydrochloric acid, ammonium persulfate.

INTRODUCTION

Desizing is the process of removing sizing materials (such as starch, CMC, or PVA) applied to cotton yarn (warp) prior to weaving process. This step is essential for improving fabric absorbency and preparing it for subsequent wet processing like scouring, bleaching, dyeing, or printing [1,2].

Common Desizing Methods include [3,4]:

* Author address: Suzana Đorđević, Academy of Applied Studies Southern Serbia, Department of Technology and Art Studies Leskovac Serbia, Partizanska 7, Leskovac, Serbia e-mail address: szn971@yahoo.com



- Enzymatic Desizing Uses amylase enzymes to hydrolyze starch-based sizing agents, making them water-soluble and easy to rinse.
- Acid Desizing Employs dilute acids (usually sulfuric or hydrochloric) to hydrolyze the starch.
- Oxidative Desizing Utilizes oxidizing agents like hydrogen peroxide to break down sizing material.
- Rot Steeping Involves soaking fabric in water at moderate temperatures for extended periods, allowing microorganisms to degrade the starch - a slow and less common method today.

The changes in cotton fabric after desizing are as follows [5,6]:

- 1. Improved Absorbency Starch removal opens up the cotton fibers. It facilitates better penetration of water, dyes, and chemicals, and is essential for even scouring, bleaching, and dyeing.
- 2. Surface Cleanliness Sizing residue (e.g., starch, waxes, PVA) is eliminated. The fabric becomes cleaner and more hydrophilic. There is reduction in spotting, uneven dyeing, or print defects.
- 3. Softer Hand Feel Desizing removes stiff sizing layers. Fabric becomes more flexible and pliable. This is especially noticeable after starch removal.
- 4. Slight Loss in Weight Weight loss (typically 2–5%) is observed due to the removal of size material. This is useful for monitoring desizing efficiency.
- 5. Improved Uniformity in Downstream Processes More consistent results in scouring, bleaching, and dye uptake are observed. This is critical for achieving level dyeing and bright shades.
- 6. Increased Porosity and Capillarity -Capillary action (wicking) is enhanced, which is important for functional finishes. This is especially relevant for technical textiles, sportswear, and medical fabrics.
- 7. Minimal Effect on Mechanical Strength (If properly done) Enzymatic desizing is gentle and preserves fabric tensile strength. Acid or oxidative desizing can cause fiber degradation if misused.
- 8. Change in Surface Chemistry Fabric surface becomes more reactive (by exposing hydroxyl groups on cellulose). This enhances chemical reactivity for bleaching, finishing, and dyeing.

Different desizing processes share the same objective - to break down starch into smaller water-soluble molecules. In the case of so-called synthetic sizing agents, warm water rinsing is generally sufficient for their removal due to their high water solubility. Natural sizing agents are somewhat more economical compared to synthetic ones, but are significantly more difficult to remove [7,8].

Starch removal from greige fabric is an important process because, in subsequent wet finishing treatments, the fabric needs to be easily and thoroughly wetted and dyed. Desizing is characteristic for cotton greige fabrics.

This research investigates various desizing processes for optimization purpose, including conventional chemical methods and eco-friendly enzymatic approaches using amylase as an environmentally sustainable alternative.



MATERIALS AND METHODS

The textile material used was a 100% greige cotton fabric with a starch-sized warp, a plain weave, the linear density of 30 tex for both warp and weft yarns, the thread density of 30 and 20 threads/cm for warp and weft, respectively, and the fabric mass per unit area of 175 g/m².

Recipe (per 100 dm³ of sizing solution) for industrial sizing cotton warp (Karl Mayer Sizing Machine):

- Natural starch (corn): 5 kg.
- Soft water: up to 100 dm³ (for solution preparation).
- Softening agent (Lurol-LA, Goulston Technologies): 0.2 kg.
- Antiseptic (sodium benzoate): 0.05 kg (to prevent fermentation).

Work procedure

The experimental laboratory work consisted of desizing cotton fabric using different methods. The treatments were carried out according to the procedures and formulations given in Table 1. After desizing, the fabric was thoroughly rinsed with warm and cold water, followed by air drying. All tests were conducted without conditioning the samples to standard moisture and temperature.

Table 1. Methods of Desizing of Cotton Fabric

| Method designation (abbreviations) | Formulation for each method |
|------------------------------------|--|
| HCI | Hydrochloric acid 2 g/dm³, Avocet WET-N 1 g/dm³, 1:20, 50 °C, 30 min; neutralize with sodium bicarbonate 1 g/dm³ |
| APS | Ammonium persulfate 3 g/dm³, sodium carbonate 1,5 g/dm³, Avocet WET-OX 1 g/dm³, 1:20, 80 °C, 30 min; mild neutralization with acetic acid 0.5% |
| AMY | Termamyl Ultra 300L, 2 g/dm³, Avocet WET-N 1 g/dm³, pH 7, 1:20, 70 °C, 45 min; remove fabric, rinse thoroughly with warm water |

Testing methods are as follows:

- Degree of desizing (based on mass changes).
- Water penetration absorption (SRPS F.S2.042:1985).
- Water absorption capacity (SRPS F.S2.041:1985).
- Breaking strength and elongation (SRPS EN ISO 13934-1:2015).
- Air permeability (SRPS EN ISO 9237:2010).

RESULTS AND DISCUSSION

Desizing of cotton fabric with warp yarns sized using a natural starch-based sizing agent was carried out using three methods, slightly modified from those commonly used in the industry. Each of these methods utilizes either conventional synthetic chemicals or natural-origin alternatives [7].



The desizing mechanism consists of converting water-insoluble amylose (linear α -1,4-linked glucose) and amylopectin (branched α -1,4 and α -1,6-linked glucose) into water-soluble products such as dextrin, maltose, or glucose.

Hydrochloric acid breaks down starch molecules (a polysaccharide) into smaller, soluble sugars through acid-catalyzed hydrolysis of the glycosidic bonds (α -1,4 and α -1,6 linkages) [9-11]:

$$(C_6H_{10}O_5)_n + nH_2O \xrightarrow{HCI} nC_6H_{12}O_6 \text{ (glucose)}$$
 (1)

The reaction mechanism (1) with this acid is as follows:

- 1. Protonation: The glycosidic oxygen in the starch is protonated by H⁺ from HCl.
- 2. Bond Cleavage: The protonated bond is cleaved, resulting in the formation of smaller dextrins and eventually glucose.
- 3. Solubilization: These products are water-soluble and can be rinsed.

Ammonium persulfate is a strong oxidizing agent. When dissolved in water and heated, it decomposes to form sulfate radicals (SO_4 -) and peroxodisulfate ions (S_2O_8 ²⁻), which attack and break down the polysaccharide (starch) chains.

The key reactions are as follows [12,13]:

1. Decomposition (2,3):

$$(NH_4)_2S_2O_8 \rightarrow 2NH_4^{\dagger} + S_2O_8^{2-}$$
 (2)

$$S_2O_8^2 + H_2O \rightarrow SO_4 + OH + OH$$
 (upon heating or catalysis) (3)

2. Radical Attack: The sulfate radicals (SO₄-) or hydroxyl radicals (OH) attack the C–C bonds and glycosidic linkages in starch molecules, resulting in fragmentation into lower molecular weight compounds like dextrins, aldehydes, and organic acids (4).

$$(C_6H_{10}O_5)_n + \frac{SO_4^-}{OH^-} \rightarrow Shorter dextrins \rightarrow Carboxylic acids + CO_2$$
 (4)

3. Solubilization: These oxidation products are water-soluble and easily removed by rinsing.

Amylases are hydrolase enzymes that cleave the α -1,4-glycosidic bonds in starch. They act specifically on starch, without affecting cellulose (cotton fibers). α -amylase randomly cleaves internal bonds, producing dextrins and maltose, while β -amylase cleaves from non-reducing ends, releasing maltose units [14-16] (5):

$$(C_6H_{10}O_5)n \text{ (starch)} + H_2O \rightarrow \text{dextrins} + \text{maltose} + \text{glucose}$$
 (5)

The step-by-step mechanism is as follows:

1. Enzyme Binding: Amylase binds to the starch layer on the fabric surface.



2. Hydrolysis: It cleaves the α -1,4 bonds, reducing starch into water-soluble fragments (produces dextrins and oligosaccharides) (6).

$$(C_6H_{10}O_5)_n \xrightarrow{\alpha\text{-Amylase}} \text{Dextrins} \rightarrow \text{Maltose}(C_{12}H_{22}O_{11}) \rightarrow \text{Glicose}(C_6H_{12}O_6) \tag{6}$$

3. Desorption: The solubilized sugars (maltose, glucose) are rinsed with water.

The first noticeable effect after various treatments in the desizing process of cotton fabric is the loss of mass due to starch degradation.

Mass loss refers to the reduction in dry weight of the fabric after desizing compared to its initial dry weight. It primarily reflects the removal of the sizing agents (e.g., starch) applied during weaving. However, with certain chemicals, it can also include loss of cellulose - which is undesirable.

Figure 1 presents the results of mass loss of cotton fabric samples depending on the active agent type, i.e., the desizing method employed. Desizing using thermostable amylase (AMY method) demonstrates optimal performance, achieving the highest starch removal efficiency of 7.5%.

The hydrochloric acid method (HCl method) gives relatively high mass loss, but may involve cellulose degradation with sizing material removal. Ammonium persulfate desizing (APS method) has a moderate weight loss, mainly due to starch oxidation, and there is also some fabric degradation. AMY gives the greatest controlled mass loss, effectively targeting starch, while preserving cellulose.

Mass loss is a reliable quantitative marker, but should always be interpreted alongside fabric integrity and performance in further processing.

Monitoring mass loss during desizing helps ensure the removal of sizing agents without damaging the fabric. Enzymatic desizing (AMY method) is the most controlled and sustainable method, while acid or oxidative agents require careful process control to avoid excessive loss.

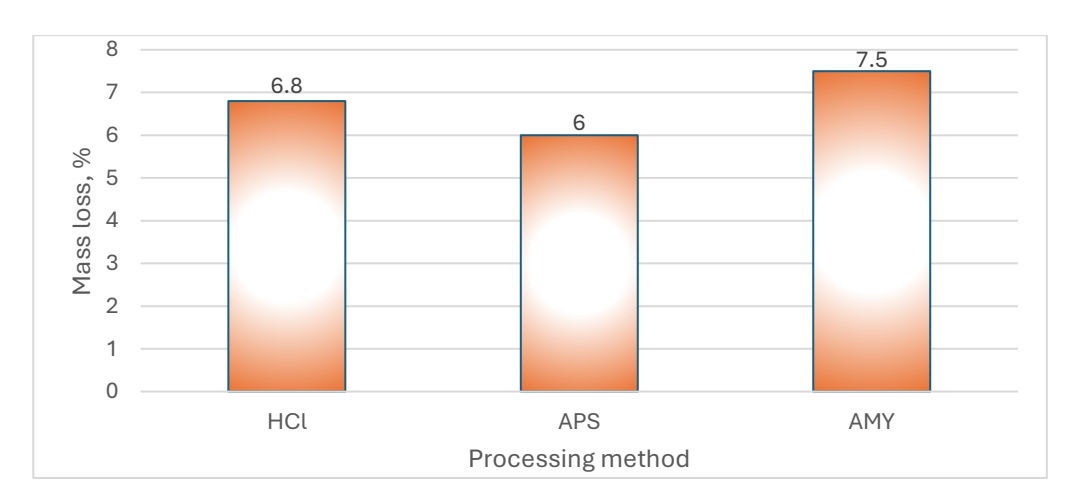


Figure 1. Mass loss of cotton fabric according to the applied desizing method



As a result of the removal of starch-based sizing agents from the fibers, an improvement in sorption properties occurs, along with enhanced surface appearance and hand feel. This is confirmed by fabric properties such as water penetration and absorption. The test results of these properties are presented in Figures 2 and 3.

Moisture absorption (or wetting ability) is a vital indicator of how well cotton fabric absorbs moisture - a property closely linked to desizing efficiency. After desizing cotton fabric using hydrochloric acid, ammonium persulfate, or thermostable amylase, moisture absorption performance reveals the extent of starch (hydrophobic sizing agent) removal and surface energy modification.

All specimens tested in the warp-direction exibited superior performance in this regard, which can be attributed to the higher thread density in the warp direction and consequently greater number of capillary pathways. The moisture absorption performance follows this descending order of desizing methods: AMY > APS > HCl > Greige sample. The AMY method demonstrates approximately ten times greater moisture absorption than the greige sample in both yarn directions.

Rapid moisture absorption after desizing confirms effective starch removal. Thermostable amylase offers the most uniform and safe improvement in moisture absorbency. Monitoring moisture absorption is a quick and practical method to assess desizing efficiency.

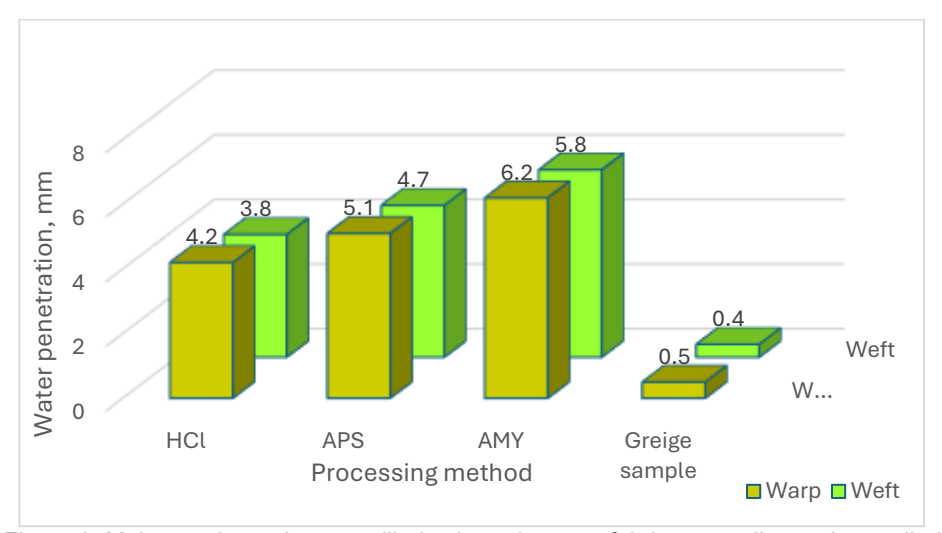


Figure 2. Moisture absorption – capillarity through cotton fabrics according to the applied desizing method

Water absorption is a critical parameter for evaluating the hydrophilicity of cotton fabric after desizing. It reflects how effectively the starch sizing agents have been removed from the fabric surface, allowing the cotton's natural water-absorbing properties to be restored. When desizing is carried out using HCl, APS, or AMY, each method influences water absorption differently, depending on its mechanism and impact on fiber integrity.



It can thus be concluded that all treatments yielded improved values for this parameter compared to the untreated sample. The best result was recorded with the AMY desizing method, which was approximately 4 times higher compared to the greige sample. The next closest result was observed in APY method, which was about 3 times higher in comparison to the greige sample.

The improvement of these sorption characteristics clearly indicates the success of the applied desizing methods, as they achieve a more open fabric structure accessible to the liquid medium. Cotton fibers and the fabric itself have an increased capacity to hold water on the surface and partially within the volumetric layers. This inherently means an enhancement of comfort and hygiene properties during practical use.

Thermostable amylase leads to the highest and most uniform water absorption, ideal for eco-friendly, high-quality processing. HCl can boost water absorption but at the risk of damaging fibers. APS offers a balance but must be optimized to prevent over-oxidation.

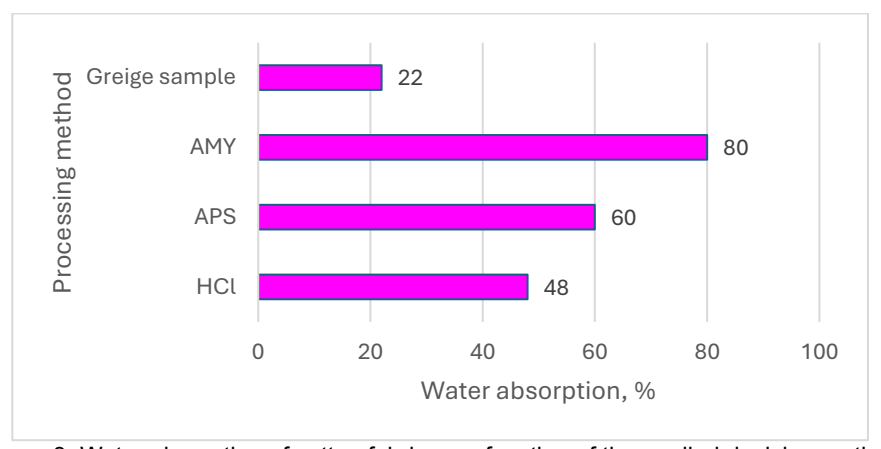


Figure 3. Water absorption of cotton fabric as a function of the applied desizing method

When discussing parameters that define the quality of a textile product, resistance to stress and deformation is particularly important, especially when expressed through breaking strength and elongation.

Breaking strength is a key parameter in evaluating the mechanical integrity of cotton fabric after desizing. When desizing is done using HCI, APS, or AMY, each agent affects the fabric differently – this is reflected in changes to the fabric's breaking strength. Elongation at break measures the extent to which a fabric can stretch before it breaks, and it is a crucial indicator of its flexibility and toughness. In the context of desizing cotton fabric, the choice of desizing agents can significantly impact elongation at break due to their varying effects on fiber integrity.

Figures 4 and 5 show the recorded results of these properties after desizing using different methods. All treatments resulted in lower values of breaking strength and elongation in both warp and weft directions. The greatest decrease in strength was observed with the HCl method, while the smallest decrease was recorded with the AMY method.



In the worst cases, the strength reduction (in the warp direction) amounted to around 19% compared to the value of the greige sample, which should not be a cause for concern. The presence of surfactants during desizing, in addition to improved wettability, contributed to reduced fiber surface damage by protecting the cotton fabric from excessive degradation. On the other hand, it is assumed that the presence of these substances in the desizing solution enables more uniform starch removal, thus allowing more favorable load distribution during tensile testing. The results for elongation at break closely followed the trend of breaking strength, showing a maximum reduction of up to 25%, regardless of the yarn direction. The enzyme Amylase (AMY) caused almost no damage to the fibers, as the results for these mechanical parameters di not significantly deviate from those of the greige sample.

Thermostable amylase is superior for preserving mechanical properties of cotton fabrics. Hydrochloric acid, though effective in removing starch, risks significant fiber damage, while ammonium persulfate offers a balance, but must be carefully controlled.

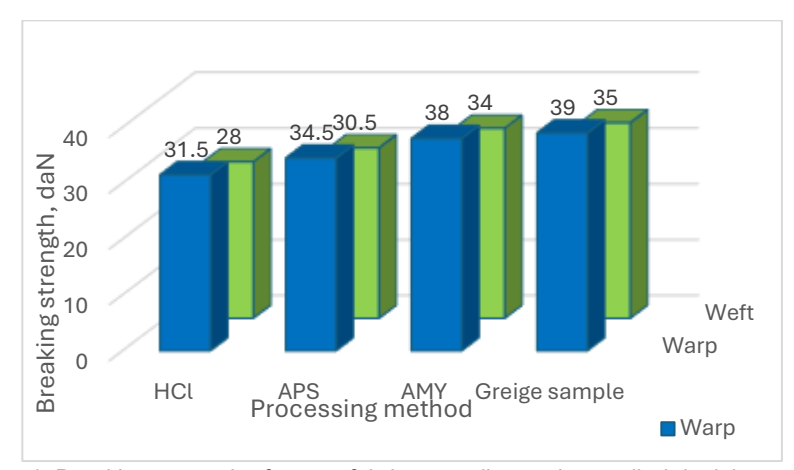


Figure 4. Breaking strength of cotton fabric according to the applied desizing method



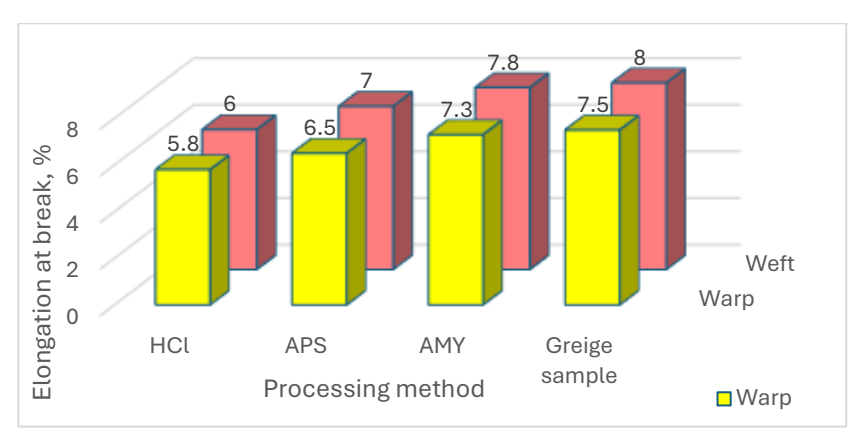


Figure 5. Elongation at break of cotton fabric according to the applied desizing method

Air permeability refers to the ability of air to pass through a fabric and is an important property for assessing breathability, comfort, and structure. During the desizing of the cotton fabric using hydrochloric acid, ammonium persulfate, or thermostable amylase, removal of starch and changes in fiber structure influence air permeability in different ways.

Air permeability of a textile product intended for clothing or other applications is a crucial indicator of the comfort and quality of fabrics. The discrete structure of fibrous constructions determines their porosity, which depends on the degree of compactness, i.e. density.

Figure 6 shows the results of air permeability testing of the fabric according to the desizing method. All treatments showed higher values for this parameter compared to the greige sample. This was expected, as air permeability is a measure of the total volume of free space between fibers, and since the fabric samples became 'freer' from starch after desizing, there was more void space available for air circulation.

The AMY method provided the highest air permeability values (100 cm³/cm²/s, compared to 30 cm³/cm²/s for the greige sample), confirming the assumption that the fabric had been freed from starch, thus opening up pathways for unobstructed ventilation. This is of particular importance, especially if such fabric is intended for clothing production.

Thermostable amylase ensures clean starch removal and preserves weave structure, leading to high and consistent air permeability. Hydrochloric acid may increase permeability but risks structural inconsistency due to cellulose degradation. Ammonium persulfate offers a balanced improvement in permeability with moderate process impact.





Figure 6. Air permeability of cotton fabric according to the applied desizing method

CONCLUSION

In the process of desizing of cotton fabric, starch undergoes hydrolysis and breaks down into lower molecular weight fractions that are water-soluble and can be easily removed from the fibers.

The study demonstrated that all three desizing methods-hydrochloric acid (HCI), ammonium persulfate (APS), and thermostable amylase (AMY)-effectively removed starch from cotton fabric. However, significant differences were observed in terms of fiber integrity, environmental impact, and post-desizing fabric performance. The enzymatic method using thermostable amylase proved to be the most effective and sustainable, achieving the highest desizing efficiency (up to 7.5% weight loss) with minimal damage to fiber structure. This method also resulted in superior improvements in sorption characteristics (water penetration and absorption), tensile strength retention, and air permeability, making it the most suitable for modern eco-friendly textile processing. In contrast, the acid-based method, while effective, caused notable fiber degradation and strength loss. APS showed intermediate performance, offering a balance between effectiveness and fiber preservation.

For sustainable textile processing, thermostable amylase is optimal when starch removal efficiency and fiber integrity are prioritized. APS may serve as a compromise for mixed sizing agents, whereas HCl should be limited to cost-driven applications accepting strength compromises. Future work should explore enzyme immobilization to enhance reusability.



Acknowledgment

This research was supported by the Academy of Applied Studies Southern Serbia, Department of Technology and Art Studies Leskovac.

References

- [1] Karmakar SR. Chemical Technology in the Pre-Treatment Processes of Textiles. Elsevier Science, Amsterdam, 1999.
- [2] Choudhury AKR. *Textile Preparation and Dyeing*. Science Publishers, Enfield, USA, 2006.
- [3] Zhang X, Baek N, Xu J, Yuan J, Fan X. Differences in the desizability of starches and the mechanism of inhibiting desizing. *Textile Research Journal*. 2022, 92(23-24) 4789-4798. https://dx.doi.org/doi:10.1177/00405175221110110
- [4] Sarkodie B, Feng Q, Xu C, Xu Z. Desizability and Biodegradability of Textile Warp Sizing Materials and Their Mechanism: A Review. *Journal of Polymers and the Environment*. 2023, 31, 3317–3337. https://doi.org/10.1007/s10924-023-02801-5
- [5] Ul-Haq N, Nasir H. Cleaner production technologies in desizing of cotton fabric. The Journal of the Textile Institute, 2011, 103(3) 304–310. https://doi.org/10.1080/00405000.2011.570045
- [6] Singh S, Hooda S. Effect of pretreatment on physical properties of cotton fabric. *International Journal of Ecology and Environmental Sciences*. 2021. 3, 472-476.
- [7] Var C, Palamutcu S. Sustainable Approaches in Textile-Sizing Process. In: Sustainable Manufacturing Practices in the Textiles and Fashion Sector. Springer Nature Switzerland, 2024, 55-74. https://doi.org/10.1007/978-3-031-51362-6 3
- [8] Jeffrey DF, John FR. Modification of starch granules by hydrolysis with hydrochloric acid in various alcohols, and the formation of new kinds of limit dextrins. *Carbohydrate Research*. 1992, 227, 163-170, https://doi.org/10.1016/0008-6215(92)85068-B
- [9] Yuya N, Isao K, Masaru G, Yoshiko N, Naoyoshi I. The Formation of Resistant Starch during Acid Hydrolysis of High-amylose Corn Starch. *Journal of Applied Glycoscience*. 2013, 60, 2, 123-130. https://doi.org/10.5458/jag.jag.JAG-2012 008
- [10] Yu H, Fang Q, Cao Y, Liu Z. Effect of HCl on starch structure and properties of starch-based wood adhesives. *BioResources*. 2016, 11(1) 1721-1728.
- [11] Xuerong F, Qiang W, Li C, Ping W. Hydrolysis of modified starches with amylases used for textile desizing. *Journal of Biotechnology*. 2008, 136, S384-S385. https://doi.org/10.1016/j.jbiotec.2008.07.885
- [12] Inventor KA, Inventor GR. Liquid oxidative desizing agent and process for oxidative deszing. United States Patent, Patent Number: 4,478,737, 1984.
- [13] https://products.evonik.com/assets/78/48/Evonik_Persulfates_Technical_Inform ation Brochure EN Asset 2237848.pdf. Accessed Jun 2023.
- [14] Grujić D, Savić A, Papuga S, Miloševic M, Kolar M, Milanovic PM, Milanovic JZ. Optimization of enzymatic desizing and scouring of cotton fabric by response



- surface methodology. *Cellulose Chemistry and Technology*. 2023, 57(1-2) 167-184. https://doi.org/10.35812/CelluloseChemTechnol.2023.57.17
- [15] Landage SM. 3 Biotechnological approaches in desizing of textile materials, In The Textile Institute Book Series, Applications of Biotechnology for Sustainable Textile Production. Editor(s): O.L. Shanmugasundaram, Woodhead Publishing, 2022, 47-73. https://doi.org/10.1016/B978-0-323-85651-5.00012-8
- [16] Rehman A, Saeed A, Asad W, Khan I, Hayat A, Rehman MU, Shah TA, Sitotaw B, Dawoud TM, Bourhia M. Eco-friendly textile desizing with indigenously produced amylase from *Bacillus cereus* AS2. *Scientific Reports*. 2023, 13, 11991, 1-12. https://doi.org/10.1038/s41598-023-38956-3

Izvod

EFIKASNOST ODSKROBLJAVANJA PAMUČNE TKANINE PRIMENOM RAZLIČITIH POSTUPAKA

Suzana Đorđević <u>ID</u>, Sandra Stojanović <u>ID</u>, Slađana Antić <u>ID</u>
Akademija strukovnih studija Južna Srbija, Odsek za tehnološko-umetničke studije
Leskovac, Srbija

Odskrobljavanje pamučnih tkanina predstavlja ključnu fazu u procesu mokre obrade tekstila, koja direktno utiče na kasnije obrade i ukupne performanse tkanine. Ovo istraživanie istražuje efikasnost tri metode odskrobljavanja, koje za aktivne agense imaju: hlorovodoničnu kiselinu, amonijum-persulfat i termostabilnu amilazu. Efikasnost svake metode ocenien ie na osnovu sledećih parametara; promena mase tkanine. penetracija vode, kapacitet apsorpcije vode, čvrstoća na kidanje, izduženje pri kidanju i propustljivost vazduha. Rezultati daju jasne razlike u mehanizmima delovanja i efektima primenljivih sredstava za odskrobljavanja. Hlorovodonična kiselina i amonijum-persulfat su pokazali brzo uklanjanje sredstva za skrobljenje, ali su takođe izazvali primetno smanjenje mehaničkih svojstava i propustljivosti vazduha, što se pripisuje njihovom oksidacionom i kiselom dejstvu. Nasuprot tome, enzimsko odskrobljavanja upotrebom termostabilne amilaze omogućilo je efikasno uklanjanje sredstva za skrobljenje uz očuvanje čvrstoće, elastičnosti i propustljivosti tkanine. Ovi nalazi ukazuju na potencijal enzimskog odskrobljavanja kao prikladnije i ekološki prihvatljivije alternative u odnosu na konvencionalne hemijske metode, naročito za supstrat koji čini pamučna tkanina u platno prepletaju.

Ključne reči: pamučna tkanina, odskrobljavanje, amilaza, hlorovodonična kiselina, amonijum-persulfat.



UDK 677.023.75.21 : 678-13 DOI: 10.46793/NoveITDS16.094DJ

SIZING OF COTTON YARN WITH A COPOLYMER OF ACRYLAMIDE AND ACRYLIC ACID

Suzana Đorđević^{1,*} <u>ID</u>, Anita Tarbuk² <u>ID</u>, Nikola Stojanović³ <u>ID</u>, Tihana Dekanić² <u>ID</u>, Dragan Đorđević⁴ ID

¹Academy of Applied Studies Southern Serbia, Department of Technology and Art Studies Leskovac, Leskovac, Serbia

²University of Zagreb, Faculty of Textile Technology, Zagreb, Croatia

³Higher School of Communications, Belgrade, Serbia

⁴University of Niš, Faculty of Technology, Leskovac, Serbia

The aim of this study is the development of a new sizing agent for cotton warp yarn based on a copolymer of acrylamide and acrylic acid. Traditional sizing agents for warp yarns have the following limitations: environmental concerns, cost and resource intensity, recycling and recovery issues, performance limitations, health and safety risks. The research focuses on the application of different concentrations of the copolymer as a sizing agent for cotton varn, as well as the sizing process itself. It was found that a decrease in solution concentration causes a drop in viscosity, while an increase in temperature reduces the viscosity of the copolymer solution. The activation energy of flow (7.9-20.7 kJ/mol) for sizing was also monitored for different copolymer concentrations. Higher concentrations of copolymer sizing agents, as well as certain viscosities, allow for greater add-on percentages on cotton yarn (4-12%). The deposited copolymer causes shrinkage (from 0.4 to 1.5%) and changes in yarn fineness (from 2 to 12%), while the breaking strength increases after sizing (up to 19%) as well as elongation at break (up to 22%). The efficiency of sizing the cotton warp using the acrylamide-acrylic copolymer depends on the rheology of the sizing solution. The use of acrylamide and acrylic acid copolymers as a sizing agent for cotton yarns offers several advantages over traditional sizing agents: improved film-forming and adhesion, enhanced yarn strength and abrasion resistance, excellent water solubility and ease of removal, environmentally friendly, thermal and chemical stability, consistent quality and performance.

Keywords: copolymer, rheology, sizing, cotton yarn.

^{*} Author address: Suzana Đorđević, Academy of Applied Studies Southern Serbia, Department of Technology and Art Studies Leskovac Serbia, Partizanska 7, Leskovac, Serbia e-mail address: szn971@yahoo.com



INTRODUCTION

The use of high-speed looms alone does not guarantee the success of a weaving mill, which is measured by the quality of the woven fabrics and the weaving costs. Based on economic indicators, it has been proven that the significance of downtime is directly related to productivity. Therefore, the efficiency of high-performance weaving systems depends on the possibility of reducing downtime. This can be indirectly achieved by improving the quality of warp preparation for weaving, where the sizing phase plays a key role [1-3].

Warp sizing involves applying a protective adhesive coating (sizing agent) to warp yarns (the lengthwise yarns in a fabric) before weaving. This improves their strength, abrasion resistance, and reduces breakage during weaving [4].

The quality of sized warps, considering the dynamic stresses on the warp threads during weaving, must keep pace with the quality and speed of high-productivity looms. The complexity of the sizing process is reflected in numerous parameters related to the properties of the sizing paste, the characteristics of the yarns used, and the features of the sizing machine, which always represents a significant field of research aimed at obtaining the highest quality sized warps [5–7].

The efficiency of sizing directly depends on the adhesion between the applied sizing agent and the warp yarn or the ability to form a film. All of this is determined by the rheological properties of the sizing paste, the physicochemical properties of the yarn, as well as the technological parameters of the sizing machine. Additionally, there is always an essential requirement that the sizing agent can be easily removed from the greige fabric after weaving [8–10].

Synthetic polymers or copolymers are often used as sizing agents or thickener agents due to their properties: water solubility, film-forming ability, viscosity control, and adhesive properties [11].

For example, the advantages of a copolymer of acrylamide and acrylic acid would be as follows [12-14]:

- Water Solubility: These copolymers are highly water-soluble, making preparation and application straightforward. They can be easily removed from the yarn after weaving, facilitating desizing and reducing environmental impact.
- <u>Abrasion Resistance</u>: Yarns sized with acrylamide-acrylic acid copolymers exhibit excellent abrasion resistance, which is crucial for minimizing yarn breakage during weaving.
- Adaptability: The properties of acrylate-based sizing agents can be tailored by adjusting the polymer composition, molecular weight, and solution conditions, allowing customization for different yarn types and weaving requirements.

This study aims to correlate the results obtained from measuring the rheological characteristics of the copolymer solutions with those of the sized yarn, in order to achieve a more economical and efficient application of the new polymer preparation in the sizing process of cotton yarn. By optimizing the rheology of the acrylamide-acrylic acid copolymer, manufacturers can balance viscosity, film strength, and application



characteristics to improve cotton warp sizing efficiency. A copolymer with moderate viscosity, good shear-thinning behavior, and elastic yet tough film-forming properties is likely to perform best.

MATERIAL AND METHODS

In the experiment, a single-thread yarn (100% cotton) with a fineness of 28 tex was used as the substrate, while the chemicals included a previously prepared solution of a copolymer of acrylamide and acrylic acid.

This copolymer, with a molar mass of 113,000 g/mol, was a ready-made agent, previously prepared for various purposes.

Rheological measurements of the polymer sizing agent were carried out using a rotational viscometer Visco Basic Plus (Fungilab S.A. Spain).

Based on preliminary research, this copolymer solution behaves like a Newtonian fluid; the viscosity remains constant and does not depend on the rate or intensity of mixing, i.e. the rate of deformation.

The activation energy (Ea) is usually extracted from the Arrhenius equation using temperature-dependent viscosity data [15]:

$$\eta = A \cdot e^{Ea/RT} \tag{1}$$

Where:

η - dynamic viscosity (Pa·s).

Ea - activation energy (J/mol).

R - gas constant (8.314 J/mol·K).

T - absolute temperature (K).

A - pre-exponential factor.

Plotting $ln(\eta)$ vs. 1/T gives a straight line with slope Ea/R, from which Ea is calculated. Pure copolymer of acrylamide and acrylic acid, at various concentrations, served as the polymer sizing agent. The concentrations of the sizing agent ranged from 2 to 8%. Sizing of the cotton yarns was performed by padding (bath ratio 1:10) at room

temperature (22 °C), followed by drying, also at room temperature. Size Pick-up (%) is the percentage increase in weight of a yarn after applying a sizing agent, relative to its original dry weight [16]:

Size Pick-up (%) =
$$\frac{\text{Dry weight after sizing-Dry weight before sizing}}{\text{Dry weight before sizing}} \times 100$$
 (2)

The following parameters were tested: viscosity (SRPS ISO 6388), size pick-up, yarn shrinkage (ISO 18066), yarn fineness (SRPS EN ISO 2060), breaking strength, and elongation (SRPS EN ISO 13934-1).

RESULTS AND DISCUSSION

The rheology (flow behavior) of acrylamide-acrylic acid copolymer solutions significantly affects their performance as sizing agents for cotton warp yarns. Key rheological



parameters such as viscosity are influenced by both the concentration of the polymer solution and temperature. Lower polymer concentration and higher temperatures both reduce the viscosity of the sizing solution. This change in viscosity directly impacts the ability of the sizing agent to penetrate and coat the cotton yarns effectively.

Changes in the rheological parameters of the copolymer sizing agent with varying concentration and temperature of the copolymer solution are shown in Figure 1.

According to the results, it is noticeable that the viscosity decreases with a reduction in the concentration of the polymer sizing agents. The influence of the polymer solution temperature on viscosity is also evident, changing according to the Arrhenius equation. As expected, the viscosity of the polymer solution decreases with increasing temperature at the same concentration.

Viscosity values up to a concentration of 4% differ only slightly. For concentrations of 5% and higher, viscosity increases significantly and decreases more steeply with rising temperature. At a concentration of about 5 copolymer, the following occurs. Enough polymer chains are present to form a dense, partially crosslinked network, leading to increased intertwining and potential hydrogen bonding between acrylamide (-CONH₂) and acrylic acid (-COOH) units. Furthermore, the denser network structure resists molecular motion, increasing the energy barrier (activation energy) required for processes such as diffusion, swelling, or reaction. In contrast, below 5% copolymer concentration, the network is too loose or dilute, with fewer interactions between chains. Molecular mobility is higher, so the activation energy is lower. Above 5% copolymer concentration, the system may become too compact or saturated, reducing further structural development. Additional polymer chains may not significantly increase interactions, or may even create phase separation or saturation of the gel, reducing the energy requirements for movement. On the other hand, acrylic acid increases hydrophilicity, while acrylamide provides flexibility and the potential for hydrogen bonding. At 5% copolymer concentration, the equilibrium of these components likely results in maximum resistance to swelling, requiring more energy to activate diffusion or reaction processes (e.g., ion transport, hydrogel deswelling). When it comes to electrostatic and hydrogen bonding, acrylic acid provides carboxyl groups that can ionize, while acrylamide provides polar amide groups. At a copolymer concentration of 5%, the system can reach a maximum interaction density (e.g., hydrogen bonding, ion pairing), increasing viscosity or diffusion barriers, which again increases the activation energy. Also, in many copolymer-based systems, there is a critical concentration at which the system transitions from a sol to a gel or exhibits maximum resistance to external influences (e.g., diffusion, reaction). This gelatinization threshold often corresponds to the maximum activation energy, as the system is most physically constrained at that point.

The viscosity of acrylamide and acrylic acid copolymer solutions decreases as the solution temperature increases. This inverse relationship is a typical behavior for polymer solutions, including poly(acrylic acid-co-acrylamide), and is attributed to increased thermal motion of polymer chains at higher temperatures, which reduces intermolecular interactions and facilitates easier flow. Additionally, the complex ionic and nonionic hydrophilic groups in these copolymers mean that temperature effects can also influence molecular conformation and aggregation, further impacting viscosity [14].



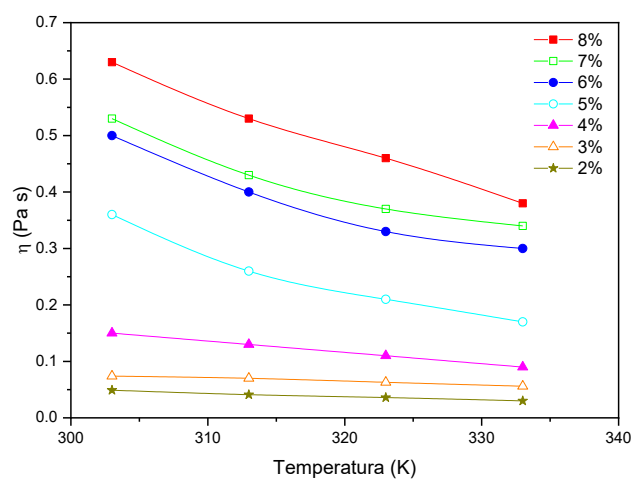


Figure 1. Dependence of the viscosity of the polymer sizing agent on temperature

Figure 2 shows the plot of $Ln(\eta)$ versus 1/T. Based on the curves, the activation energy of flow of the copolymer solution and the pre-exponential factor were determined. The coefficient of determination for the curves ranges from 0.970 to 0.995.

The activation energy of flow reflects how sensitive a fluid's viscosity is to changes in temperature. Ea for aqueous solutions of poly(acrylamide-co-acrylic acid) reflects how sensitive the viscosity is to temperature changes. It is a key rheological parameter, especially important for various industrial applications, but also for sizing varn [17, 18].

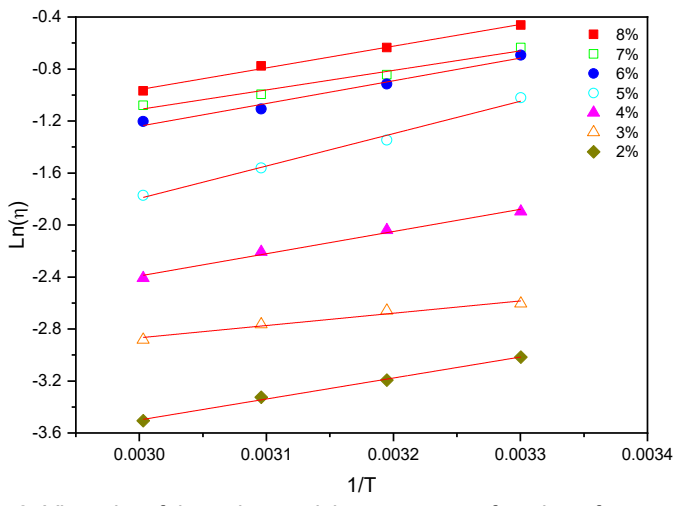


Figure 2. Viscosity of the polymer sizing agent as a function of temperature



According to Table 1, the activation energy has the highest value at a concentration of 5%, amounting to 20.72 kJ/mol, while the lowest value (7.86 kJ/mol) was recorded at a concentration of 3%.

Higher temperatures reduce the activation energy barrier for polymer chain movement, resulting in lower viscosity and easier flow.

Activation energy values for acrylamide-acrylic acid copolymer flow depend on the copolymer composition, molecular weight, and solution conditions (such as pH and ionic strength), but the general trend is that increasing temperature lowers the effective energy barrier for flow.

The copolymer's ionic nature (due to acrylic acid units) means that temperature effects may be more pronounced compared to non-ionic polymers, as increased thermal energy can help overcome electrostatic interactions that hinder chain mobility [18].

The activation energy for the sizing process decreases with lower polymer concentration, indicating that less energy is required for the sizing agent to interact with the yarn at lower concentrations. However, this may also reduce the effectiveness of the size layer.

Table 1. Kinetic parameters of polymeric sizing agent at different concentrations

| Concentration of sizing agent (%) | Activation energy (kJ/mol) | Pre-exponential factor (×10 ⁻⁶ kJ/mol) |
|-----------------------------------|----------------------------|---|
| 8 | 13.89 | 2.55 |
| 7 | 12.49 | 3.62 |
| 6 | 14.53 | 1.53 |
| 5 | 20.72 | 0.09 |
| 4 | 14.22 | 0.54 |
| 3 | 7.86 | 3.34 |
| 2 | 13.43 | 0.24 |

Table 2 presents the values of parameters indicating the effect of treatment with the polymer sizing agent: mass change, length change, and fineness change.

The copolymer's rheology affects how well it spreads and adheres to cotton. Optimal viscosity ensures sufficient hydrogen bonding between the -OH groups of cotton and the -COOH/-CONH₂ groups of PAM-co-PAA, as well as uniform coverage without excessive add-on. The groups in the copolymer are very polar and capable of forming multiple hydrogen bonds, while the hydroxyl groups are hydrophilic and readily form hydrogen bonds. The interaction between PAM-co-PAA and cellulose yarn (usually cotton) in yarn sizing involves a mix of physical adsorption, hydrogen bonding, and potentially ionic interactions, but not covalent bonds under standard conditions. Furthermore, electrostatic interactions are possible if PAA is ionized (–COO⁻) and reacts with cationic impurities or additives on the yarn. There are also van der Waals forces due to non-specific physical adsorption, as well as mechanical anchoring, when the copolymer physically entangles itself in the microfibrils/surface pores of the fibers.

Higher viscosity (from higher polymer concentration) allows for greater deposition of the sizing agent on the yarn (Size Pick-up), improving the bonding between the polymer and cotton fibers. This enhances the protective film formed on the yarn surface, leading to



better abrasion resistance and reduced yarn hairiness during weaving. As temperature increases, the viscosity of the polymer solution decreases, which can affect the uniformity and amount of size pick-up on the yarn. Optimal temperature and concentration conditions must be maintained to ensure efficient sizing.

The numerical values of the fineness (%) of yarn - a measure of the yarn's mass per unit length (tex) - increase after sizing, as the yarn absorbs the sizing material. This apparent change is due to an increase in weight and sometimes a slight swelling effect. The increase is proportional to size pick-up, since the size film adds mass to the yarn. Higher copolymer concentrations result in heavier coatings, thus increasing the yarn's linear density. This change affects weaving performance and must be controlled to prevent issues like stiffness or poor fabric handle.

When yarn is treated with a sizing solution that includes 2% to 8% copolymer of acrylamide and acrylic acid, its length can slightly decrease because of moisture absorption, tension relaxation, shrinkage from drying, or film formation on the surface. As the copolymer concentration increases, the yarn tends to shrink more. This is because higher copolymer levels form a thicker film that tightens the yarn, causing a slight reduction in length during drying. Additionally, the ionic nature of acrylic acid leads to increased moisture absorption, which contributes to temporary swelling followed by shrinkage.

Table 2. The influence of sizing on the change of certain yarn properties

| rable z. The initialities of cizing of the change of contain fair properties | | | | |
|--|--------------|-----------------------|-------------------------|--|
| Concentration of | Size Pick-up | Change in yarn length | Change in yarn fineness | |
| sizing agent (%) | (%) | (shrinkage) (%) | (deterioration) (%) | |
| 8 | 12 | 1.5 | 12 | |
| 7 | 11 | 1.2 | 10 | |
| 6 | 9 | 1.2 | 8 | |
| 5 | 8 | 0.9 | 6 | |
| 4 | 7 | 0.8 | 4 | |
| 3 | 6 | 0.5 | 3 | |
| 2 | 4 | 0.4 | 2 | |

Table 3 presents the values of the mechanical properties of cotton yarn after sizing with the new sizing agent, a copolymer of acrylamide and acrylic acid. Generally, the treatments of the yarn with copolymer sizing agents at higher concentrations, and thus higher viscosities, result in increased breaking strength. Exceptions are largely influenced by the kinetic flexibility of the macromolecules, i.e., the distribution of polymer macromolecules along the fibers on the surface and inside the yarn. With a decrease in the viscosity of the polymer sizing agents, the ability to bind to the yarn fibers also decreases, and at concentrations of 4% or lower, the treatments cannot meet the required standards for these parameters.

In essence, sizing cotton yarn with a copolymer of acrylamide and acrylic acid improves its breaking strength and elongation due to the film-forming and lubricating properties of the polymer. The increase is generally proportional to the concentration of the copolymer up to an optimal point (around 7%), beyond which gains may plateau or slightly decline due to excess stiffness or brittleness.

Breaking strength increases due to fiber bonding and reduced hairiness, which leads to better force distribution. At the same time, elongation improves because of smoother



fiber interaction and the flexibility provided by the copolymer. However, if the concentration of the sizing agent is further increased (>8%), it could result in a decrease in yield or even slight declines if the yarn becomes too stiff or brittle.

Table 3. Breaking strength and elongation of sized yarn

| Concentration of sizing agent (%) | Breaking Strength (N) | Elongation (%) |
|-----------------------------------|-----------------------|----------------|
| - | 4.7 | 11.0 |
| 8 | 5.4 | 13.5 |
| 7 | 5.6 | 12.0 |
| 6 | 5.4 | 12.8 |
| 5 | 5.2 | 12.3 |
| 4 | 5.1 | 12.0 |
| 3 | 5.0 | 12.0 |
| 2 | 4.9 | 11.8 |

A precisely defined viscosity of the solution, along with a precisely defined activation energy of flow, is necessary so that during the impregnation of the yarn-that is, practically during the polymer flow-adequate stresses (tangential, normal) develop as a function of the shear rate. This ultimately leads to the most favorable arrangement and distribution of the polymer sizing agent molecules inside and on the surface of the yarn, as well as binding to the fiber surface.

The viscosity of the polymer sizing agent at a concentration of 7% and an activation energy of 12.49 kJ/mol results in the most favorable sizing outcomes, i.e., it will ensure the most suitable add-on of the sizing agent, breaking strength, and elongation.

CONCLUSION

In production conditions, inappropriate add-ons of sizing material are very often applied for warp sizing, with these amounts determined based on empirical indicators. Insufficient add-on of sizing material on the warp leads to an increased number of warp yarn breaks due to its inadequate strength and higher hairiness. Conversely, if excessive amounts of sizing material are applied to the warp, the stiffness of the yarn increases, which is unfavorable for the weaving process and results in unnecessary consumption of sizing agents.

By careful selection of the procedure, i.e., the active agent, as well as optimal selection of the temperature-time regime based on rheological indicators, it is possible to achieve an appropriate bath composition and treatment method aimed at obtaining uniform sizing and subsequent desizing.

The efficiency of cotton warp sizing using acrylamide-acrylic acid copolymer agents is highly dependent on the rheological properties of the sizing solution. Proper adjustment of concentration and temperature optimizes viscosity, which in turn enhances penetration, bonding, and the protective qualities of the size layer. These factors collectively lead to improved weaving performance and easier removal of the sizing agent in subsequent processing steps.

The positive environmental aspects of using this copolymer in starching cotton yarn are as follows: water solubility and low volatility, potential for biodegradation, and application in environmental protection technologies (wastewater treatment, soil moisture retention



in agriculture, or in slow-release fertilizers or agrochemical carriers). Environmental concerns regarding the use of copolymers include: the toxicity of the monomer acrylamide, persistence, or potential microplastics. To mitigate environmental concerns, researchers are exploring: bio-based monomers (e.g., itaconic acid instead of acrylic acid), blending with biodegradable polymers such as starch, cellulose, or chitosan, and there are also green synthesis methods.

References

- [1] Anmen A, Alemayehu A. Effects of Loom Speed, Insertion Air Pressure, and Yarn Type on Fabric Air Permeability: Case Study on Air Jet Loom. *Journal of Engineering*. 2024, 2660559. https://doi.org/10.1155/2024/2660559
- [2] Xiao Y, Zhang H, Yuan C. Gao N, Meng Z, Peng K. The Design of an Intelligent High-Speed Loom Industry Interconnection Remote Monitoring System. *Wireless Personal Communications*. 2020, 113, 2167-2187. https://doi.org/10.1007/s11277-020-07317-y
- [3] Wang K, Wang J, Gao W. Enhancing warp sizing effect and quality: a comprehensive review of the squeezing process and future research. *Textile Research Journal.* 2024, 94, 2296-2315. https://doi:10.1177/00405175241235400
- [4] Pan X, Qin D, Song K, Dong A. Environmental friendly warp yarn coating from feather wastes with enhanced toughness and tenacity via thiol-ene click chemistry grafting modification. *Bioresources and Bioprocessing*. 2025, 12, 10. https://doi.org/10.1186/s40643-025-00838-z
- [5] Wang K, Pan X, Guo M, Wang J, Gao W. Effect of pre-squeezing force in a single-sizing-roll triple-roll-type sizing machine on size pick-up and quality indexes of sized yarns. *Textile Research Journal*. 2024, 95, 1092-1107. https://doi:10.1177/00405175241286235
- [6] Wu H, Shen Y, Yao Y, Zhang B. Size formulations for cotton yarn weaving at lower relative humidity. *Textile Research Journal*. 2020, 91, 168-174. https://doi:10.1177/0040517520934880
- [7] Zhu B, Cao X, Liu J, Gao W. Effects of different drying methods on physicochemical and sizing properties of granular cold water swelling starch. *Textile Research Journal.* 2018, 89, 762-770. https://doi:10.1177/0040517518755786
- [8] Jian L. Effect of sizing agent on interfacial properties of carbon fiber-reinforced PMMA composite. Composites and Advanced Materials. 2021, 30, 1-6. https://doi:10.1177/2633366X20978657
- [9] Chen J, Li S, Ma X, Liu H, Ge H. Synthesis of polymeric emulsifier and its application in epoxy emulsion-type sizing agent for carbon fiber. *Journal of Composite Materials*. 2015, 50, 3395-3404. https://doi:10.1177/0021998315620712
- [10] Liu J, Ge H, Chen J, Liu H. Preparation of Epoxy Sizing Agent for Carbon Fiber by Phase Inversion Emulsification. *Polymers and Polymer Composites*. 2012, 20, 63-68. https://doi:10.1177/0967391112020001-212



- [11] Djordjevic S, Kovacevic S, Djordjevic D, Konstantinovic S. Sizing process of cotton yarn by size from a copolymer of methacrylic acid and hydrolyzed potato starch. *Textile Research Journal*. 2018, 89, 3457-3465. https://doi:10.1177/0040517518813628
- [12] Ailing Z, Youheng Z, Song W, Sanxi L, Tingting G. Electrochemical copolymerization of acrylic acid and acrylamide on the carbon fiber surface. *High Performance Polymers*. 2016, 29, 386-395. https://doi:10.1177/0954008316645390
- [13] Rafikov AS, Ibodulloyev BSU, Yasinskaya NN, Khakimova MS. Graft copolymers of collagen and acrylic monomers-Reagents for sizing of cotton yarn. *Polymer Engineering* & *Science*. 2024, 64, 2018-2034. https://doi:10.1002/pen.26668
- [14] Riahinezhad M, McManus N, Penlidis A. Shear Viscosity of Poly (Acrylamide/Acrylic Acid) Solutions. *Macromolecular Symposia*. 2016, 360, 179-184. https://doi.org/10.1002/masy.201500092
- [15] Jie Zheng, Zhuang Mao Png, Shi Hoe Ng, Guo Xiong Tham, Enyi Ye, Shermin S. Goh, Xian Jun Loh, Zibiao Li. Vitrimers: Current research trends and their emerging applications, *Materials Today*, 2021, 51, 586-625. https://doi.org/10.1016/j.mattod.2021.07.003.
- [16] Wang K, Pan X, Guo M, Wang J, Gao W. Effect of pre-squeezing force in a single-sizing-roll triple-roll-type sizing machine on size pick-up and quality indexes of sized yarns. *Textile Research Journal*. 2024, 95, 1092-1107. https://doi:10.1177/00405175241286235
- [17] Vega-Hernández MA, Munguia-Quintero MF, Rosas-Aburto A, Alcaraz-Cienfuegos J, Valdivia-Lopez MA, Hernandez-Luna MG, Vivaldo-Lima E. Effect of teak wood lignocellulose pretreatment on the performance of cellulose-graft-(net-poly(acrylamide-co-acrylic acid)) for water absorption and dye removal. International Journal of Biological Macromolecules. 2024, 274, 133482. https://doi.org/10.1016/j.ijbiomac.2024.133482.
- [18] Ashraf IM, El-Zahhar AA. Studies on the photoelectric properties of crosslinked-poly(acrylamide co-acrylic acid) for photo detector applications. *Results in Physics*. 2018, 11, 842-846. https://doi.org/10.1016/j.rinp.2018.10.048.



SKROBLJENJE PAMUČNE PREĐE KOPOLIMEROM OD AKRIL AMIDA I AKRILNE KISELINE

Suzana Đorđević¹ <u>ID</u>, Anita Tarbuk² <u>ID</u>, Nikola Stojanović³ <u>ID</u>, Tihana Dekanić² <u>ID</u>, Dragan Đorđević⁴ ID

¹Akademija strukovnih studija Južna Srbija, Odsek za tehnološko-umetničke studije Leskovac, Srbija

²Univerzitet u Zagrebu, Tekstilno-tehnološki fakultet, Zagreb, Hrvatska 3Visoka škola za komunikacije, Beograd 4Univerzitet u Nišu, Tehnološki fakultet, Leskovac, Srbija

Cilj ovog rada je formiranje novog sredstva za skrobljenje pamučne osnove od kopolimera akrilamida i akrilne kiseline. Tradicionalna sredstva za skrobljenje osnove imaju sledeća ograničenja: ekološke problemi, troškovi i intenzitet korišćenja resursa, probleme sa reciklažom i ponovnom upotrebom, ograničenja u performansama, zdravstveni i bezbednosni rizici. Istraživanje se bavi primenom različitih koncentracija kopolimera, kao agensa za skrobljenje pamučne pređe, kao i samim procesom skroblienia. Utvrđeno je da smanjenie koncentracije rastvora uslovljava pad viskoziteta dok sa rastom temperature opada viskozitet rastvora kopolimera. Praćena je i energija aktivacije tečenja sredstva (7,9-20,7 kJ/mol) za skrobljenje za različite koncentracije kopolimera. Veća koncentracija kopolimernih sredstava za skrobljenje kao i određeni viskozitet dozvoljavaju više nanosa na pamučnoj pređi (4-12%). Određene vrednosti viskoziteta, odnosno energije aktivacije tečenja, uzrokuju odgovarajuće ponašanje polimernih molekula u rastvoru a onda veću ili manju sposobnost vezivanja za pamučnu pređu. Deponovani kopolimer uzrokuje skupljanje (od 0,4 do 1,5%) i promenu finoće pređe (od 2 do 12%), dok jačina na kidanje raste posle skrobljenja (maksimalno za 19%) kao i izduženje do kidanja (maksimalno za 22%). Efikasnost skrobljenja pamučne osnove upotrebom akrilamid-akrilnog kopolimera zavisi od reologije rastvora za skrobljenje. Upotreba kopolimera akrilamida i akrilne kiseline kao sredstva za skrobljenje pamučne pređe pruža više prednosti u odnosu na tradicionalna sredstva za skrobljenje: poboljšano formiranje filma i adhezije, povećana čvrstoća pređe i otpornost na habanje, odlična rastvorljivost u vodi i lako uklanjanje, ekološka prihvatljivost, termička i hemijska stabilnost, kao i konzistentan kvalitet i performanse.

Ključne reči: kopolimer, reologija, skrobljenje, pamučna pređa.



UDK 677.494.674.075 : 677.027.411 DOI: 10.46793/NovelTDS16.105K

COLOURABILITY AND FASTNESS OF COLOURED POLYESTER KNITTED FABRIC AFTER PRETREATMENT

Marija Kodrić^{1,*} <u>ID</u>, Shahidul Islam² <u>ID</u>, Zorica Eraković³ <u>ID</u>, Predrag Tasić⁴ <u>ID</u>, Dragan Đorđević³ <u>ID</u>

¹Innovation Center, University of Nis, Niš, Serbia ²Department of Textile Engineering, BGMEA University of Fashion and Technology (BUFT), Dhaka, Bangladesh ³University of Niš, Faculty of Technology in Leskovac, Leskovac, Serbia

*University of Nis, Faculty of Technology in Leskovac, Leskovac, S 4V.I. Vunil d.o.o. Leskovac. Serbia

The effects of pretreatment on the dyeing efficiency of polyester knitted fabric using a yellow disperse dye were investigated in this study. The raw fabric was pretreated with an alkaline solution (calcium hydroxide) and pure higher alcohols (1-pentanol and 1octanol), while dyeing was carried out in the presence of an environmentally friendly carrier (caffeine). The results showed that pretreatment improved dye uptake during the dveing process. Significant weight loss was observed after treatment with 1-octanol (8.2%), resulting in the greatest fabric swelling (thickness increase). Shrinkage was uniform across all samples, averaging around 3%. The tensile strength of the pretreated fabric was slightly reduced, particularly in the sample treated with alkali. The CIELab colour system parameters showed more intense colouring in all samples; for example, the sample modified with 1-octanol exhibited the darkest shade. The sample pretreated with 1-octanol was the darkest, as confirmed by the highest difference in lightness (ΔL = -18.23). In addition, its high chroma (C = 32.47) and hue angle (H = 86.23) contribute to a pronounced yellow colouration with good brilliance. These CIELab parameters, along with the subjective evaluation of colour levelness, confirm the significant colouration and the effectiveness of this modification in achieving intense and uniform dyeing. Caffeine proved to be an effective, non-toxic carrier, enabling better dyeing results than procedures without a carrier or those using a conventional carrier. The colour fastness of the pretreated polyester knitted fabrics to light, washing, rubbing, seawater, and water drops was found to be satisfactory and acceptable.

Keywords: polyester, pretreatment, dyeing, CIELab, colour fastness.

* Author address: Marija Kodrić, Innovation Center, University of Nis, University Square 2, Niš, Serbia

e-mail address: izida50@gmail.com



INTRODUCTION

Polyester (PES) is one of the most widely used synthetic polymers in the textile industry, thanks to its high mechanical strength, durability, affordable cost, and excellent performance in everyday use. Its chemical structure is based on repeating units of terephthalic acid and ethylene glycol, resulting in fibers with high crystallinity and good resistance to abrasion, wrinkling, and photoaging. Polyester fibers are also characterized by low moisture absorption, making them suitable for use in outdoor clothing, sports equipment, technical textiles, and furniture [1,2].

However, the very low moisture absorption, as well as the hydrophobic nature and smooth surface of the fibers, present a challenge when dyeing, as they reduce the affinity for dyes. Disperse dyes, which are the most commonly used for dyeing PES materials, require specific conditions for successful fixation in the fibers. Therefore, dyeing polyester is significantly more demanding compared to natural fibers such as cotton or wool [3,4].

There is a continuous effort to improve the performance properties of existing PES fibers through physical and chemical modifications. Today, polyester fibers with sufficient hydrophilicity and enhanced dyeability are being developed. The wetting and absorption of liquids, including dyes, are fundamentally important in many industrial processes, influencing both the conventional and functional properties of fibrous materials [5].

Alkaline hydrolysis of polyester fabrics is one of the possible methods for modifying polyester in order to enhance its comfort and wearability. Fabrics treated with alkali exhibit improved aesthetic appearance and drape, a softer handle (touch), and greater comfort, with properties similar to silk. In addition to these primary effects, treated materials show reduced pilling tendency, increased resistance to soiling, and improved hydrophilicity. At the same time, alkaline treatment effectively removes oligomers by breaking them down into water-soluble molecules [6,7].

Standard dyeing procedures for polyester require the application of high operating temperatures (above 120 °C) and specific auxiliary agents, carriers, which enhance the dye's penetration into the fibers. Unfortunately, many of these carriers harm the environment due to their toxicity and long-term biodegradability. Therefore, current research is focused on developing alternative technological approaches that would enable high-quality dyeing at lower temperatures, while reducing the use of harmful chemicals [8.9].

Chemical surface modification of polyester fibers through alkaline hydrolysis using a calcium hydroxide (Ca(OH)₂) solution in the presence of 1-pentanol and 1-octanol represents a promising method for increasing hydrophilicity and creating microporous structures on the fiber surface. These changes enable better diffusion of dispersed dyes, which can contribute to improved dyeing performance.

The dyeing process was carried out using an environmentally friendly carrier, caffeine, at a temperature of 95 °C for 60 minutes, in an Original Hanau Linitest (Hanau, Germany) apparatus. This study aims to investigate the effect of chemical surface modification of PES knit fabric and the use of caffeine as a natural carrier on the physical properties of the fabric and the quality of dyeing with disperse dyes. This research contributes to the



development of sustainable and environmentally friendly technologies in the textile industry, with the potential to reduce negative environmental impacts.

MATERIALS AND METHODS

In this experiment, 100% polyester knit fabric (PET - polyethylene terephthalate) with a surface mass of 135 g/m² was used. The pretreatment of the PES knit was carried out through three procedures. The first procedure involved chemical modification in a calcium hydroxide solution (40 g/dm³) in water at 40 °C, with a bath ratio of 1:60, for 60 minutes. This was followed by rinsing with distilled water, neutralization with formic acid (2 g/dm³), washing with Sarabid DLO, a non-ionic surfactant based on a combination of specific oxyethylates (2 g/dm³, 20 minutes at 60 °C), a second rinse, and drying at room temperature.

The second and third procedures were performed using pure alcohols: 1-pentanol and 1-octanol, under the same conditions (40 °C, 1:60, 60 minutes), followed by drying, nonionic surfactant washing, rinsing, and drying. The abbreviated labels for these procedures are: $Ca(OH)_2-H_2O$, 1-pentanol, and 1-octanol.

The knit fabric was then dyed with the disperse dye C.I. Disperse Yellow 54 in the presence of a natural carrier — caffeine (1% relative to the weight of the fabric) at a temperature of 95 °C for 60 minutes, in an Original Hanau Linitest (Hanau, Germany) apparatus.

The physical and mechanical properties of the samples were evaluated by measuring weight loss, thickness, shrinkage, and bursting strength. Dyeing performance was assessed using CIELab parameters.

The change in mass (Δ m, %) of textile samples was expressed as a percentage relative to the mass of the control (unmodified) sample and was calculated based on the difference in mass before and after treatment:

$$\Delta m = \frac{m_0 - m_1}{m_0} \cdot 100 \tag{1}$$

where m_1 is the mass of the sample after treatment (g), and m_0 is the mass of the unmodified sample (g).

Thickness was measured using a device called a thickness gauge. The apparatus consists of two parallel metal plates, between which the material is placed. The pressure of the upper plate on the tested product depends on the type of textile material. If not specified by the standard, a pressure of 50 cN/cm² is applied for all textile materials. The thickness of the knitted fabric was measured in accordance with the SRPS EN ISO 5084:2013 standard. Five measurements were carried out, and the mean value was calculated.

Dimensional stability was determined in line with SRPS EN ISO 5077:2010. According to the new procedure, the standards SRPS EN ISO 3759:2012 and SRPS EN ISO 6330:2022 are used together. On the test sample, markings were made in three places in both length and width, and the mean value of the three results was calculated.



Bursting strength of the knit fabric was measured according to SRPS F.S2.022:2017. This standard determines the resistance of textiles to rupture under the pressure of a steel ball and applies to all textile products regardless of composition, structure, or shape. Bursting strength is expressed as the maximum force (daN) causing the fabric to rupture. Five measurements were carried out, and the mean value was calculated.

Colour fastness to light was determined according to SRPS EN ISO 105-B02:2015. Testing was carried out on a Xenotest "Hanau" apparatus, Germany, No. 507 S-2253, using blue wool reference fabrics (ratings 1–8) supplied by SDC Enterprises Limited, United Kingdom. A total of three samples were tested. The exposure time to light was 72 hours. A xenon arc lamp simulating sunlight was used. After exposure, the light-exposed and covered parts of the samples, as well as the reference blue wool fabrics, were compared. Evaluation was performed using the grey scale, with values calculated from spectrophotometric remission measurements on a Spectraflash 300, Datacolor instrument under D65, A, and F8B2 illumination, 8° geometry.

Colour fastness to rubbing was tested in accordance with SRPS EN ISO 12947-4:2008. The samples were rubbed with dry and wet white fabric for 1,000 cycles, using the specified load according to the standard. Three tests were carried out. The change in appearance and colour transfer were assessed using the grey scale, with values obtained from spectrophotometric remission measurements under the same instrument and illumination conditions as above.

Colour fastness to washing was tested according to SRPS EN ISO 105-C06:2016. Testing was conducted on a Linitest apparatus, in a water bath heated to 40 ± 2 °C. One sample was tested, prepared as a sandwich with adjacent fabrics sized 10×5 cm, and three ratings were given, sewn together with white accompanying fabrics — cotton on one side and wool on the other. Detergent type 2705 SDC Sodium Perborate Tetrahydrate was used at a concentration of 5 g/dm^3 , with a liquor ratio of 50:1. Samples were placed in hermetically sealed metal containers and subjected to 30 minutes of mechanical agitation, then rinsed and dried. Evaluation of colour transfer was made using the grey scale based on spectrophotometric remission measurements (Spectraflash 300, Datacolor, D65/A/F8B2 illumination, 8° geometry).

Colour fastness to seawater was determined according to SRPS EN ISO 105-E02:2013. One sample was tested, prepared as a sandwich with adjacent fabrics sized 10 × 5 cm, and three ratings were given. The sample was immersed in a sodium chloride solution of defined concentration for the duration specified in the standard, then dried. Grey scale evaluation was performed based on spectrophotometric measurements as described above.

Colour fastness to water was assessed according to SRPS EN ISO 105-E01:2014. One sample was tested, prepared as a sandwich with adjacent fabrics sized 10 × 5 cm, and three ratings were given. The assessment of colour fastness to water, based on resistance to fading and colour transfer in contact with water and other textiles. Evaluation was performed using the spectrophotometric remission data as above.

Colour fastness to water spotting was evaluated according to SRPS EN ISO 105-E16:2013. One sample was tested, prepared as a sandwich with adjacent fabrics sized 10 × 5 cm, and three ratings were given, possibly two. Water droplets were applied to the fabric surface for the exposure period specified in the standard. After drying, the



colour change was evaluated using the grey scale, calculated from spectrophotometric remission measurements on the same instrument and illumination conditions.

RESULTS AND DISCUSSION

Table 1 presents the results of testing changes in weight loss, thickness, shrinkage, and bursting strength of the PES knit fabric after prior chemical treatment. The first noticeable effect of polyester modification was the weight loss (ranging from 3.8% to 8.2%, depending on the pretreatment), caused by changes in the surface morphology of the PES fibers due to the action of various chemicals. In the case of the alcohol 1-octanol solution, the weight loss was more pronounced compared to other solutions, which may be attributed to the specific action of higher alcohols involved in polyester hydrolysis and their potential influence on the degradation of the fiber surface layer.

The applied modification led to a significant reduction in fabric thickness, resulting from mass loss due to delamination and peeling of the fiber surface layer. The thickness of the knit fabric showed a direct correlation with weight changes, indicating the impact of chemical treatment on the structural characteristics of the textile. A slight change in thickness was observed due to modification, with the sample treated with $Ca(OH)_2-H_2O$ showing a mild decrease in thickness compared to the untreated sample. In contrast, the samples modified with 1-pentanol and 1-octanol showed a slight increase in thickness. Weight loss indicates the removal of material from the fiber surfaces, but this removal loosens the structure, increases porosity, and allows the fibers to swell and relax, leading to increased thickness. These variations suggest localized structural changes in the fibers occurring during chemical treatment. The most pronounced increase in thickness was recorded in the samples treated with pure alcohols, with all values of this parameter being higher compared to the unmodified sample.

Although more significant changes might have been expected, they were mitigated by the shrinkage of the material that occurred during the warm treatments in a relaxed state (at 40 °C), which contributed to compensating for potentially more drastic variations in thickness.

Table 1. Selected physical properties of PES knitted fabric after pretreatment

| Drotrootmont Codo | Weight | Thickness | Shrinka | age (%) | Bursting | |
|---------------------------------------|----------|-----------|-----------|---------|----------------|--|
| Pretreatment Code | Loss (%) | (mm) | Warp Weft | | Strength (daN) | |
| - | - | 0.95 | - | - | 58 | |
| Ca(OH) ₂ -H ₂ O | 5.0 | 0.91 | 3 | 3 | 53 | |
| 1-Pentanol | 3.8 | 0.98 | 3 | 3.5 | 55 | |
| 1-Oktanol | 8.2 | 1.02 | 3 | 3.5 | 55 | |

Dimensional stability of textile materials is a key requirement, with the goal of minimizing shrinkage during and after processing. Although it is almost inevitable for the material to undergo dimensional changes, such changes must be as small and consistent as possible. Yarn tension during production has a significant influence on subsequent relaxation and, consequently, on dimensional changes.

Dimensional stability is a crucial property of textiles, with the aim of minimizing size alterations. In this case, material shrinkage is the result of fiber relaxation, knit structure,



and the thermodynamic instability of PES fibers during wet and thermal treatment. The greatest shrinkage (3.5%) was recorded with solvent treatments, while the alkaline treatment caused the least (3%). All applied treatments reduced the bursting strength of the PES knit fabric, with the most significant reduction observed after alkaline treatment and the smallest after treatment with alcohols.

The results of CIELab parameters quantify the dyeing outcomes of PES knit fabric following different pretreatments and a single dyeing method — dyeing with the ecocarrier caffeine, at a temperature of 95 °C for 60 minutes. In addition to quantitative results, it is important to emphasize that qualitative, subjective evaluation (e.g., regarding dye levelness or uniformity) significantly contributes to the overall impression of the effectiveness of new solutions and dyeing procedures for polyester. All dyed samples exhibited uniform colouration with acceptable levelness, as confirmed by subjective assessment.

Table 2 presents the CIELab parameters for PES knitted fabrics dyed with disperse yellow dye, following prior modification with different agents (calcium hydroxide, 1-pentanol, and 1-octanol), along with data for the uncoloured reference sample. The lightness component (L^*) is lower in all dyed samples compared to the undyed sample, indicating a darker appearance after dyeing.

Differences are also evident in the colour coordinates (a^* and b^*), as well as in hue angle (H) and chroma (C^*). The a^* values for the samples modified with calcium hydroxide and 1-octanol are significantly lower than those of the sample modified with 1-pentanol, while their b^* values are much higher, resulting in a more intense yellow hue. These variations in hue (H) are also the most pronounced, likely due to the influence of caffeine as an eco-carrier on the dye uptake and shade development in the PES knit, both with and without ultrasound assistance.

Table 2. CIELab system parameters for yellow dyed PES knitted fabric

| Table 2. Ole Lab system parameters for year and the label | | | | | | |
|---|-------------------------------|--------------------------|-------------|------------|--------|--|
| Undyed PES knit fabric | | | | | | |
| Light sources | L* | a* | b* | C* | Н | |
| D65 | 94.10 | -1.06 | 5.57 | 5.67 | 100.75 | |
| Α | 94.36 | 0.37 | 5.54 | 5.56 | 86.17 | |
| FB2 | 94.31 | -0.79 | 6.24 | 6.29 | 97.22 | |
| Modifie | ed with Ca(OH) ₂ - | H ₂ O and dye | d with DY54 | + caffeine | | |
| Light sources | Ĺ | a | b | С | Н | |
| D65 | 78.67 | 6.72 | 37.10 | 37.71 | 79.74 | |
| Α | 81.47 | 12.00 | 40.01 | 41.78 | 73.30 | |
| FB2 | 80.69 | 4.12 | 41.57 | 41.78 | 84.33 | |
| Modif | ied with 1-penta | nol and dyed | with DY54 | + caffeine | | |
| Light sources | Ĺ | a | b | С | Н | |
| D65 | 77.56 | 22.20 | 6.10 | 23.02 | 15.36 | |
| Α | 80.55 | 21.33 | 12.31 | 24.63 | 29.98 | |
| FB2 | 79.37 | 16.14 | 8.33 | 18.16 | 27.30 | |
| Modi | fied with 1-octar | nol and dyed | with DY54 + | caffeine | | |
| Light sources | L | a | b | С | Н | |
| D65 | 75.87 | 2.13 | 32.40 | 32.47 | 86.23 | |
| Α | 77.95 | 7.42 | 34.06 | 34.86 | 77.71 | |
| FB2 | 77.40 | 0.99 | 36.24 | 36.25 | 88.43 | |
| | | | | | | |



Among the samples, the one modified with 1-octanol exhibited the lowest lightness (L^* = 75.87 under D65 illumination), confirming it as the darkest. The colour coordinates (a^* = 2.13, b^* = 32.40), combined with a hue angle (H = 86.23) and chroma (C^* = 32.47), confirm a strong yellow tone with high brilliance and good saturation, indicating a significant distance from the neutral grey axis.

Table 3 quantitatively presents the colour differences between the uncoloured PES knit reference sample and the dyed samples modified with different agents and dyed using disperse yellow dye. These differences, expressed as delta values (Δ), were measured under various illumination conditions. The uncoloured, unmodified sample was used as the reference point for comparison with all dyed and modified variants.

As expected, all dyed samples show elevated total colour difference (ΔE) values, regardless of the modification method. The sample modified with calcium hydroxide and dyed with the eco-carrier caffeine displays the highest ΔE value, while the sample modified with 1-pentanol shows the lowest.

The lightness difference (ΔL) is negative in all cases, indicating that all dyed samples are darker than the uncoloured reference. Under D65 illumination, ΔL values range from -15.43 to -18.23 for the respective treatments: calcium hydroxide, 1-pentanol, and 1-octanol.

The chroma (ΔC) and hue (ΔH) values provide additional insight into the tone and brilliance of the dyed samples. A positive ΔC reflects increased saturation, while ΔH describes tonal shifts between dyeing processes. The positive Δa values across all samples suggest an increased presence of red tones, whereas the positive Δb values confirm enhanced yellow tones and a reduction in blue hues.

Table 3. Colour differences of PES knit fabric (uncoloured/vellow-dved sample)

| | Table 3. Colour differences of PES knit tabric (uncoloured/yellow-dyed sample) | | | | | | |
|---|--|---------------|-------------|------------|-------|-------|--|
| Modified with Ca(OH)₂-H₂O and dyed with DY54 + caffeine | | | | | | | |
| Light sources | ∆E | ΔL | ⊿a | ∆b | ∆C | ∆H | |
| D65 | 35.95 | -15.43 | 7.78 | 31.53 | 32.04 | 5.30 | |
| Α | 38.60 | -12.89 | 11.63 | 34.47 | 36.22 | 3.40 | |
| F02 | 38.18 | -13.62 | 4.91 | 35.33 | 35.49 | 3.57 | |
| Modified with 1-pentanol and dyed with DY54 + caffeine | | | | | | | |
| Light sources | ∆E | ΔL | ⊿a | ∆b | ∆C | ∆H | |
| D65 | 28.55 | -16.54 | 23.26 | 0.53 | 17.35 | 15.50 | |
| Α | 26.00 | -13.81 | 20.96 | 6.77 | 19.07 | 11.02 | |
| F02 | 22.68 | -14.94 | 16.93 | 2.09 | 11.87 | 12.25 | |
| | Modified with | 1-octanol and | d dyed with | DY54 + caf | feine | | |
| Light sources | ∆E | ΔL | ∆a | ∆b | ∆C | ∆H | |
| D65 | 32.59 | -18.23 | 3.19 | 26.83 | 26.80 | 3.43 | |
| Α | 33.65 | -16.41 | 7.05 | 28.52 | 29.30 | 2.15 | |
| F02 | 34.48 | -16.91 | 1.78 | 30.00 | 29.96 | 2.36 | |

The colour fastness of PES knit fabric was tested on all modified samples that underwent an identical dyeing procedure using the eco-carrier caffeine at 95 °C for 60 minutes. Light fastness refers to the resistance of the dyed textile to the effects of daylight. Evaluation was conducted according to the relevant standard by comparing the degree of fading



(colour loss) between the tested textile and a standard, using a rating scale from 1 (very poor fastness) to 5 (very good fastness).

The best light fastness result for the yellow dye (Table 4) was achieved by the sample modified with 1-octanol, which received the maximum rating of 5. Slightly lower ratings of 4–5 were observed for the PES knit samples modified with $Ca(OH)_2-H_2O$ and 1-pentanol, indicating very good but slightly less consistent resistance to light exposure. In addition to light fastness, abrasion fastness was also evaluated for all dyed PES knit samples. This property indicates the resistance of the textile surface to mechanical wear during use, which is particularly important for clothing and technical textiles. The assessment was carried out using a standardised method, and the results are presented using a grading scale, where higher values indicate better abrasion resistance.

As shown in Table 4, the sample modified with 1-octanol again demonstrated the best performance, achieving a rating of 4, which suggests good resistance to wear. The samples modified with $Ca(OH)_2$ – H_2O and 1-pentanol showed slightly lower abrasion fastness ratings of 3–4, indicating moderate to good resistance to mechanical stress. These results suggest that the type of modification agent can influence not only the colour properties but also the durability of the dyed fabric.

Table 4. Light fastness and abrasion fastness results of yellow-dyed PES knit fabric

| Procedure designation | Light fastness | Abrasion fastness |
|---------------------------------------|----------------|-------------------|
| Ca(OH) ₂ -H ₂ O | 4-5 | 3-4 |
| 1-Pentanol | 4-5 | 3-4 |
| 1-Octanol | 5 | 4 |

Colour fastness to washing was tested according to the prescribed standard by monitoring the transfer of colour from the dyed test specimen to adjacent white fabrics. Evaluation was carried out using the appropriate grey scales, such as the AATCC Gray Scale for Staining.

As shown in Table 5, all modified PES samples exhibited very good washing fastness, with ratings ranging from 4–5 to 5. The colour transfer to white polyester fabric consistently achieved the highest rating (5), while slightly lower or equal values were observed for white cotton fabric, indicating better fastness to polyester. These high ratings confirm the durability of the dyeing process for both tested colours.

Table 5. Colour fastness results of yellow-dyed PES knit fabric to washing (40 °C)

| Procedure designation | Colour change of the test specimen | Colour transfer to white polyester fabric | Colour transfer to white cotton fabric |
|---------------------------------------|---------------------------------------|---|--|
| Ca(OH) ₂ -H ₂ O | 4-5 | 5 | 4-5 |
| 1-Pentanol | 4-5 | 5 | 4-5 |
| 1-Octanol | 4-5 | 5 | 5 |

Colour fastness to seawater refers to the resistance of textile dyes to the effects of salty seawater. To assess changes in colouration, a grey scale is used, along with a grey scale for evaluating colour transfer to white fabrics (both white polyester and white cotton). In the context of colour transfer to white fabric, a rating of 5 means no staining



occurred (i.e., no colour transfer), while a rating of 1 indicates significant staining and noticeable colour transfer.

The highest seawater fastness was observed in the samples modified with calcium hydroxide and 1-octanol, as shown in Table 6. Although there are differences between the samples, the ratings are generally close, mostly differing by half a point to one point. Colour transfer to white cotton fabric received better ratings compared to the transfer to white polyester fabric.

Table 6. Results of the colour fastness of yellow-dyed PES knitted fabric to seawater

| Procedure designation | Change in colour of the sample | Colour transfer to white polyester fabric | Colour transfer to white cotton fabric |
|---------------------------------------|--------------------------------|---|--|
| Ca(OH) ₂ -H ₂ O | 4-5 | 5 | 4-5 |
| 1-Pentanol | 4 | 4 | 4-5 |
| 1-Octanol | 4-5 | 5 | 4-5 |

Colour fastness to water refers to the resistance of a textile's colouration to the effects of water exposure. Testing was conducted according to the standard procedure, following a similar method used for assessing colour fastness to seawater.

For the modified samples, colour fastness values ranged from 4 to 5. The best results (Table 7) were predominantly observed in the sample modified with 1-octanol, followed by the sample modified with $Ca(OH)_2-H_2O$, and lastly by the one modified with 1-pentanol.

Table 7. Results of the colour fastness of yellow-dyed PES knit to water

| Procedure | Change in colour of | Colour transfer to | Colour transfer to |
|---------------------------------------|---------------------|--------------------|---------------------|
| designation | the test solution | white fabric | white cotton fabric |
| Ca(OH) ₂ -H ₂ O | 5 | 4-5 | 4-5 |
| 1-Pentanol | 4 | 4-5 | 4 |
| 1-Octanol | 4-5 | 5 | 5 |

Testing of colour fastness to water droplets was conducted according to the relevant standard, with evaluation performed after drying at room temperature. The colour change was assessed using a gray scale. This test measures the resistance of the textile's colouration to the impact of water droplets and is rated on a scale from 1 (significant change) to 5 (no visible change).

The obtained results (Table 8) show that the highest fastness to water droplets was recorded for the samples modified with Ca(OH)₂–H₂O and 1-octanol, followed by the sample modified with 1-pentanol, which received slightly lower ratings (4–5).

Table 8. Results of the Colour Fastness of Yellow-Dyed PES Knitted Fabric to Water Droplets

| Procedure designation | Colour change 2 minutes after wetting | Colour change after drying the specimen |
|---------------------------------------|---------------------------------------|--|
| Ca(OH) ₂ -H ₂ O | 2-3 | 4-5 |
| 1-Pentanol | 2 | 4 |
| 1-Octanol | 2-3 | 5 |



CONCLUSION

The results of this study showed that the chemical modification of PES knitted fabric using calcium hydroxide solution, as well as aliphatic alcohols (1-pentanol and 1-octanol), in combination with the environmentally friendly carrier caffeine, significantly affected the efficiency of the dyeing process with disperse dyes.

The best dyeing performance was achieved on the sample treated with $Ca(OH)_2$ and dyed with the addition of caffeine, as confirmed by the high values of total colour difference ($\Delta E = 38.60$), colour saturation (C = 41.78), and pronounced hue (b = 41.57). This combination provided uniform colouration, good light fastness, and minimal dimensional changes in the material. The samples treated with alcohols showed more pronounced physical changes, particularly in thickness and mass loss, indicating a greater degree of surface modification. The use of caffeine as a natural carrier proved to be an effective and sustainable alternative to conventional toxic auxiliaries, allowing a reduction in dyeing temperature without compromising dyeing quality. In addition, the modified samples demonstrated satisfactory colour fastness properties, including resistance to washing, light, seawater, abrasion, and water droplets, which are essential for practical textile applications.

This study confirms that the combination of chemical modification and environmentally friendly additives can achieve satisfactory results in dyeing synthetic materials while preserving the environment and reducing energy consumption. Further research is recommended to evaluate the stability of these procedures under industrial conditions and to explore their application to various types of synthetic textiles.

Acknowledgment

The authors would like to thank the Ministry of Science, Technological Development and Innovation of the Republic of Serbia, Program for financing scientific research No. 451-03-136/2025-03/200371, 451-03-137/2025-03/200133, 451-03-136/2025-03/200133.

References

- [1] Smelik A. Polyester: A cultural history. *Fashion Practice*. 2023, 15, 279-299. https://doi.org/10.1080/17569370.2023.2196158
- [2] Barot AA, Panchal TM, Patel A, Patel CM. Polyester the workhorse of polymers: A review from synthesis to recycling. *Archives of Applied Science Research*. 2019, 11, 1-19.
- [3] Riaz S, Jabbar A, Siddiqui H, Salman M, Sarwar A. A sustainable process for cotton and polyester/cotton blend dyeing with nucleophilic disperse dyes through chemical modification. *Cellulose*. 2024, 31, 3981-3992. https://doi.org/10.1007/s10570-024-05820-0
- [4] Ketema A, Worku A. Review on intermolecular forces between dyes used for polyester dyeing and polyester fiber. *Journal of Chemistry*. 2020, 2020, 6628404. https://doi.org/10.1155/2020/6628404



[5] Nagy NM. Selecting textile fibers to match the design & final product functional use to meet the challenges of the local & global market. *International Design Journal*. 2021, 11, 265-278.

https://doi.org/10.21608/idj.2021.162524

[6] Mamdouh F, Hassabo AG, Othman H. Improving the performance properties of polyester fabrics through treatments with natural polymers. *Journal of Textiles, Coloration and Polymer Science*. 2025, 22, 219-231.

https://doi.org/10.21608/itcps.2024.291557.1373

- [7] Sarno A, Olafsen K, Kubowicz S, Karimov F, Sait ST, Sørensen L, Booth AM. Accelerated hydrolysis method for producing partially degraded polyester microplastic fiber reference materials. *Environmental Science & Technology Letters*. 2020, *8*, 250-255. https://doi.org/10.1021/acs.estlett.0c01002
- [8] Carrion-Fite FJ, Radei, S. Development auxiliaries for dyeing polyester with disperse dyes at low temperatures. *Materials Science and Engineering*. 2017, 254, 082006.

https://doi.org/10.1088/1757-899X/254/8/082006

[9] Babaei M, Jalilian M, Shahbaz K. Chemical recycling of Polyethylene terephthalate: A mini-review. *Journal of Environmental Chemical Engineering*. 2024, 12, 112507. https://doi.org/10.1016/j.jece.2024.112507

Izvod

BOJIVOST I POSTOJASNOST OBOJENJA POLIESTARSKE PLETENINE POSLE PRETHODNE PRIPREME

Marija Kodrić¹ <u>ID</u>, Shahidul Islam² <u>ID</u>, Zorica Eraković³ <u>ID</u>, Predrag Tasić⁴ <u>ID</u>, Dragan Đorđević³ ID

¹ Inovacioni centar Univerziteta u Nišu, Niš, Srbija

² Katedra za tekstilni inženjering, BGMEA Univerzitet mode i tehnologije (BUFT), Daka, Bangladeš

³ Univerzitet u Nišu, Tehnološki fakultet u Leskovcu, Leskovac, Srbija
⁴ V.I. Vunil d.o.o, Leskovac, Srbija

U ovom radu je istražen uticaj prethodne pripreme poliestarske pletenine na efikasnost bojenja žutom disperznom bojom. Priprema sirove pletenine je urađena rastvorom alkalije (kalcijum-hidroksid), i čistim višim alkoholima (1-pentanol i 1-oktanol), dok je bojenje izvedeno u prisustvu ekološki pogodnog kerijera (kofein). Rezultati pokazuju da je prethodna priprema dovela do poboljšanja prijema boje tokom bojenja. Kao rezultat prethodne pripreme, značajan gubitak mase zabeležen je kod obrade sa 1-oktanolom (8,2%), što je dovelo do najvećeg bubrenja tkanine (povećanje debljine). Skupljanje je bilo ujednačeno kod svih uzoraka, u proseku oko 3%. Otpornost na pucanje prethodno obrađene pletenine je nešto slabija, posebno kod obrade alkalijom. Vrednosti parametara CIELab sistema pokazuju intenzivnije nijanse obojenja kod svih uzoraka, npr. uzorak posle modifikacije sa 1-oktanolom je najtamnije obojen. Uzorak prethodno



tretiran 1-oktanolom je najtamniji, što potvrđuje najveća zabeležena razlika u svetlini ($\Delta L = -18,23$). Pored toga, njegova visoka zasićenost boje (C = 32,47) i vrednost nijanse (H = 86,23) doprinose izraženoj žutoj boji sa visokom briljantnošću. Ovi CIELab parametri, zajedno sa subjektivnom procenom ujednačenosti boje, potvrđuju značajno bojenje i efikasnost ove modifikacije u postizanju intenzivnog i ujednačenog bojenja. Kofein se pokazao kao efikasan, netoksičan nosač, omogućavajući bolje rezultate bojenja nego postupci bez nosača ili oni sa konvencionalnim nosačem. Postojanost boje prethodno tretiranih poliesterskih pletenih tkanina na svetlost, pranje, trljanje, morsku vodu i kapi vode ocenjena je kao zadovoljavajuća i prihvatljiva.

Ključne reči: poliestar, prethodna priprema, bojenje, CIELab, postojanost boje.



UDK 667.281 : 544.7 : 628.316.12 DOI: 10.46793/NovelTDS16.117I

MECHANISTIC INSIGHTS INTO THE CHEMISORPTION OF INDUSTRIAL DYES ON TI₃C₂ MXENE SURFACE FOR WASTE WATER TREATMENT APPLICATION: A THEORETICAL APPROACH

Shahidul Islam¹ D, Md. Rahamatolla² D, Marija Kodric³ D, Sanjay Belowar¹,* Department of Textile Engineering, BGMEA University of Fashion and Technology (BUFT), Dhaka 1230, Bangladesh

2Department of Natural Sciences, BGMEA University of Fashion and Technology (BUFT), Dhaka 1230, Bangladesh

3Innovation Center, University of Niš, Niš, Serbia

The discharge of azo dyes from industrial effluents poses serious environmental and health risks due to their persistence and resistance to biodegradation. Hydroxyl-functionalized ${\rm Ti_3C_2(OH)_2}$ MXenes have emerged as promising adsorbents due to their large surface area, hydrophilicity, and versatile surface chemistry. In this study, we employed Monte Carlo and molecular dynamics simulations to investigate the adsorption behavior of four industrial dyes—Congo Red (CR), Methylene Blue (MB), Direct Black 1 (DBk), and Direct Blue 38 (DBu)—on ${\rm Ti_3C_2(OH)_2}$ MXene surfaces.

Monte Carlo adsorption locator results showed that CR exhibited the most favorable static adsorption energy (-182.346 kcal/mol), followed by DBu (-46.576 kcal/mol), DBk (-23.994 kcal/mol), and MB (-16.35 kcal/mol). Notably, the deformation energy of CR was -151.353 kcal/mol, indicating strong chemisorption due to significant molecular reorganization. Molecular dynamics simulations in aqueous media further validated these trends, with DBu showing the highest dynamic adsorption energy (-1676.365 kcal/mol), followed by DBk (-1348.604 kcal/mol), CR (-1157.238 kcal/mol), and MB (-895.651 kcal/mol). The binding energies reflected a similar order, confirming that strong π - π stacking, hydrogen bonding, and surface-induced reorientation were dominant interaction mechanisms.

These findings provide molecular-level insight into the structure–function relationship governing dye–MXene adsorption and highlight $Ti_3C_2(OH)_2$ MXene as an effective material for selective and sustainable dye removal in wastewater treatment.

Keywords: Azo dyes, Ti₃C₂ MXene, Adsorption energy, Chemisorption, Molecular dynamics, Wastewater remediation.

* Author address: Sanjay Belowar, Department of Natural Sciences, BGMEA University of Fashion and Technology (BUFT), Dhaka 1230, Bangladesh e-mail address: sanjay.belowar@buft.edu.bd



INTRODUCTION

The rampant discharge of synthetic dyes from textile and allied industries poses a serious environmental threat due to their toxicity, persistence, and non-biodegradability. Among various pollutants, azo dyes represent a major class of contaminants that severely degrade water quality and disrupt aquatic ecosystems [1]. The direct discharge of untreated or inadequately treated dye-laden effluents into water bodies leads to reduced light penetration, altered photosynthetic activity, and exerts significant toxicity on aquatic organisms and human health. As traditional wastewater treatment methods often fall short in removing these complex organic molecules effectively, the search for advanced adsorbent materials has become imperative [2].

Adsorption has been widely recognized as one of the most effective techniques for dye removal due to its simplicity, low operational cost, and ability to target a wide range of pollutants without generating secondary waste [3]. However, the success of this method largely depends on the nature of the adsorbent material. Traditional adsorbents such as activated carbon, clays, and zeolites, while effective to some extent, often face limitations such as low selectivity, poor regeneration capability, and high production costs. These shortcomings have spurred the search for next-generation adsorbent materials with superior performance characteristics [4,5].

Recently, MXenes, a family of two-dimensional transition metal carbides and nitrides, have attracted immense attention as novel nanomaterials for environmental remediation applications. Owing to their exceptional surface area, hydrophilic nature, layered structure, and tunable surface chemistry, MXenes exhibit strong potential for the adsorption and removal of various pollutants, including dyes, from aqueous environments [6]. Particularly, Ti_3C_2 -based MXenes, functionalized with surface hydroxyl, oxygen, or fluorine groups, offer reactive sites capable of engaging in strong electrostatic, hydrogen bonding, and π - π interactions with organic pollutants. Their lamellar structure and exposed functional groups make them promising candidates for the selective and high-capacity adsorption of dye molecules [7,8].

Despite encouraging experimental findings, a fundamental understanding of the molecular-level interactions between MXenes and complex dye molecules remains limited. To bridge this knowledge gap, computational modeling techniques provide an invaluable tool. By simulating the adsorption process under controlled conditions, computational methods can offer detailed insights into adsorption energies, binding configurations, charge distributions, and the influence of molecular structure on adsorption efficiency [9,10].

In this study, we conduct a theoretical investigation of the interaction mechanisms between $T_{i3}C_2OH)_2$ MXene and four representative industrial azo dyes: Congo Red (CR), Methylene Blue (MB), Direct Black 1 (DBk), and Direct Blue 38 (DBu). These dyes were selected based on their widespread industrial usage and varying structural, electronic, and functional characteristics. By using Monte Carlo-based adsorption locator simulations and molecular dynamics (MD) modeling, we analyze key parameters such as adsorption energy, deformation energy, and binding configurations to evaluate the strength and spontaneity of dye adsorption on the MXene surface. Additionally, solvent



effects are considered through the inclusion of water molecules in the simulation box to mimic realistic aqueous conditions.

The results not only provide comparative insights into the adsorption potential of various dye molecules but also reveal the role of functional groups, molecular geometry, and electronic structure in determining adsorption efficiency. This study contributes to the rational design and optimization of MXene-based materials for sustainable wastewater treatment technologies.

COMPUTATIONAL METHOD

To investigate the adsorption behavior of industrial azo dyes on the $Ti_3C_2(OH)_2$ MXene surface, a series of computational simulations was performed using BIOVIA Materials Studio (Versions 7.0 and 8.0) [11]. The crystal structure of Ti_3C_2 MXene (100 surface orientation) was obtained from the Materials Project database and processed using the Materials Studio interface. Similarly, molecular structures of the selected dyes—Congo Red, Methylene Blue, Direct Blue 38, and Direct Black 1—were downloaded from the Materials Explorer database and geometry-optimized using the Universal Force Field (UFF) [12,13]. The structures of MXene (Fig. 1) and the four industrial dyes are shown in Fig. 2. Initial geometry optimization was conducted to minimize the total energy of each system and ensure a stable configuration. During this process, atomic positions were iteratively adjusted until the system reached a local minimum on the potential energy surface. Following successful optimization, a simulation box was constructed containing the MXene (100) slab, individual dye molecules, and water molecules to mimic aqueous environmental conditions [14].

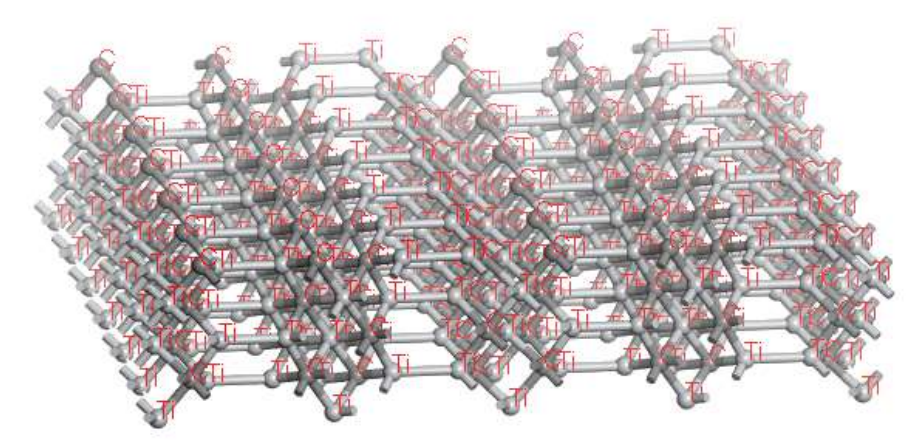


Figure 1. 3D structure of Ti3C2-based MXene



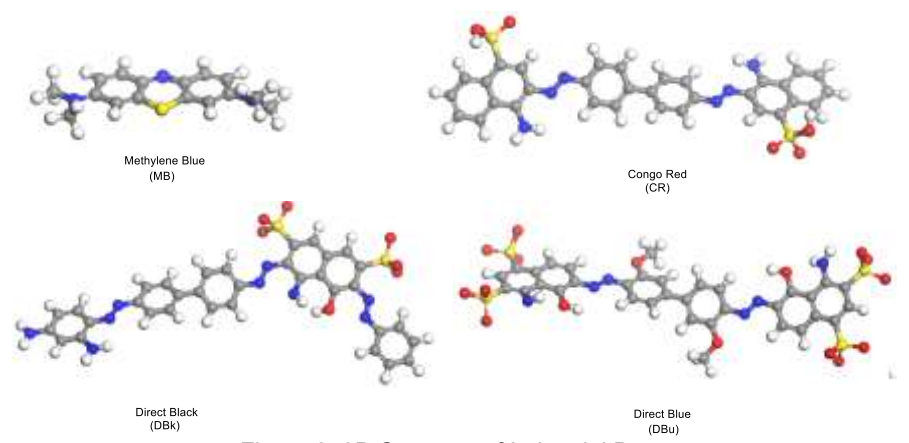


Figure 2. 3D Structure of Industrial Dyes

Monte Carlo adsorption locator simulations

To investigate the adsorption characteristics of the selected azo dves on the Ti₃C₂(OH)₂ MXene surface, Monte Carlo-based adsorption locator simulations were employed using the Adsorption Locator module in BIOVIA Materials Studio. This module systematically searches for energetically favorable configurations by sampling various orientations and positions of dye molecules relative to the MXene surface. Each dye—Congo Red, Methylene Blue, Direct Blue 38, and Direct Black 1—was modeled in the presence of the MXene (100) crystal surface, and their interaction configurations were evaluated under periodic boundary conditions. The Universal Force Field (UFF) was applied to optimize each structure, ensuring that both the adsorbent and adsorbate reached a minimum energy configuration. Key energetic parameters were calculated, including total system energy, adsorption energy (E_{ads}), rigid adsorption energy, and deformation energy, as well as the adsorption energy per molecule (dEads/dNi). These values provided quantitative insights into the strength and spontaneity of dye adsorption. The simulation results revealed the most stable binding configurations for each dye molecule and allowed for a comparative analysis of their affinities towards the MXene surface. This computational approach served as a critical foundation for understanding the adsorption mechanism and guiding subsequent molecular dynamics studies.

Molecular dynamics simulations

To further validate the adsorption behavior and assess the dynamic stability of dye–MXene complexes in aqueous environments, molecular dynamics (MD) simulations were performed using the Forcite module in BIOVIA Materials Studio (Version 8.0). The simulations were carried out under an NPT ensemble at 298 K and 1 atm pressure to mimic standard ambient conditions. Each system included a geometry-optimized $Ti_3C_2(OH)_2$ MXene (100) slab, a selected dye molecule (Congo Red, Methylene Blue, Direct Blue 38, or Direct Black 1), and water molecules within a periodic simulation box measuring 18.0 Å × 30.23 Å × 25.08 Å.



A time step of 1.0 femtosecond (fs) was used, and each system was simulated for 300 picoseconds (ps) to allow sufficient equilibration and conformational sampling. Berendsen thermostat and barostat were employed to regulate temperature and pressure, respectively. Long-range electrostatic interactions were computed using the Ewald summation method with an accuracy of 1 × 10⁻⁵ kcal mol⁻¹, while van der Waals interactions were treated with the same level of precision. Qeq charge equilibration was utilized to compute partial atomic charges dynamically throughout the simulation [15,16]. The main objective of these MD simulations was to evaluate the adsorption energy, binding energy, and radial distribution functions (RDFs) of the dye molecules relative to the MXene surface [9]. These metrics provided quantitative and structural insights into the degree of physical versus chemical adsorption. RDF analysis, in particular, was used to estimate the most probable separation distances between dye atoms and MXene surface atoms, calculated using the following equation (1):

$$g_{xy}(\mathbf{r}) = \frac{\rho_y(r)}{\rho_y} \tag{1}$$

Where:

- ρ_y (r)= local density of atoms of species Y at distance r from species X
- ρ_y = average density of species Y over the entire volume

RESULTS AND DISCUSSION

Adsorption locator studies

The adsorption behavior of the four industrial azo dyes—Methylene Blue, Congo Red, Direct Black 1, and Direct Blue 38—on the $Ti_3C_2(OH)_2$ MXene surface was investigated using the Adsorption Locator module in Materials Studio. The simulation identified the most energetically favorable dye orientations and adsorption sites on the MXene (100) surface using c vvbg a Monte Carlo algorithm. For each dye, the most stable configuration was selected and visualized (Fig. 3-6), and the corresponding adsorption energy parameters were recorded (Table 1). The total energy, adsorption energy (Eads), rigid adsorption energy, and deformation energy were calculated for each dye-MXene system, offering valuable insights into the strength and nature of interactions.





Figure 3. Total energy Monte Carlo adsorption Locator Simulations of Methylene Blue (MB)

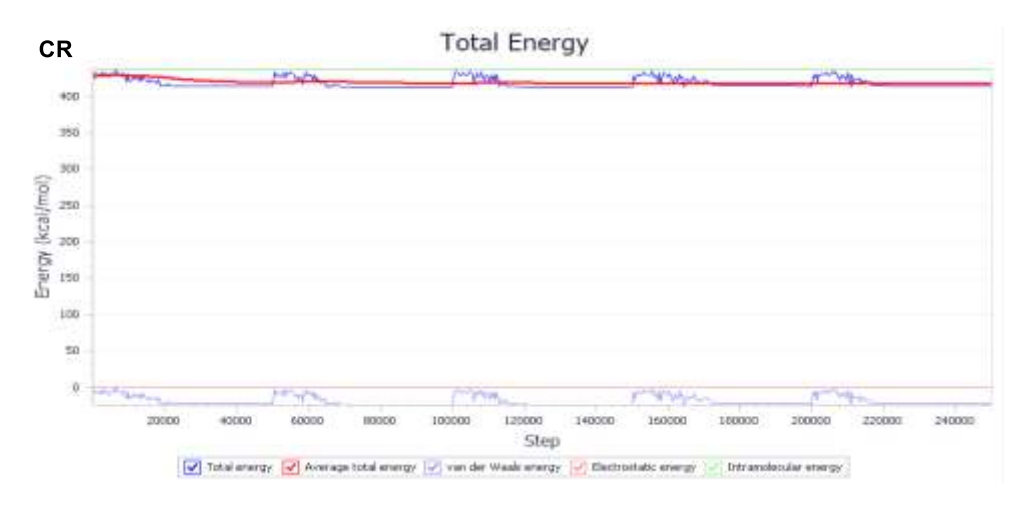


Figure 4. Total energy Monte Carlo adsorption Locator Simulations of Congo Red (CR)



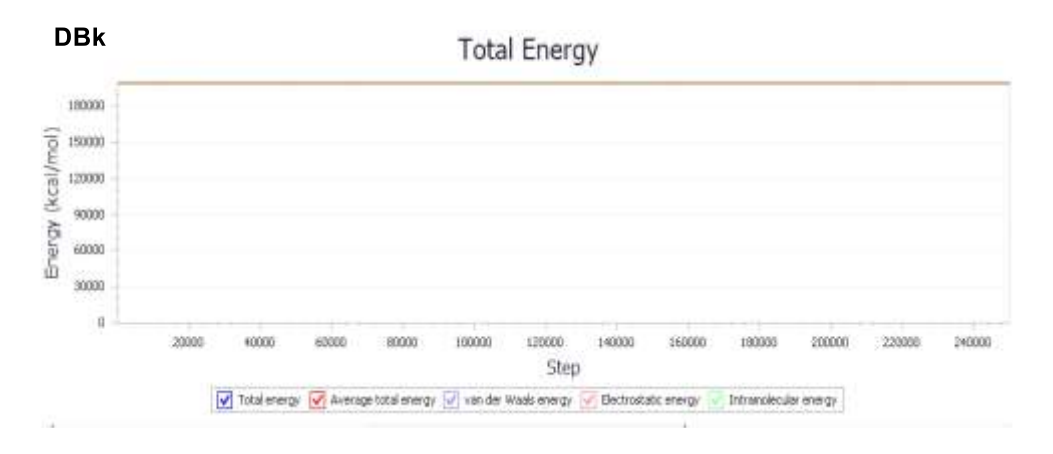


Figure 5. Total energy Monte Carlo adsorption Locator Simulations of Direct Black (DBk)

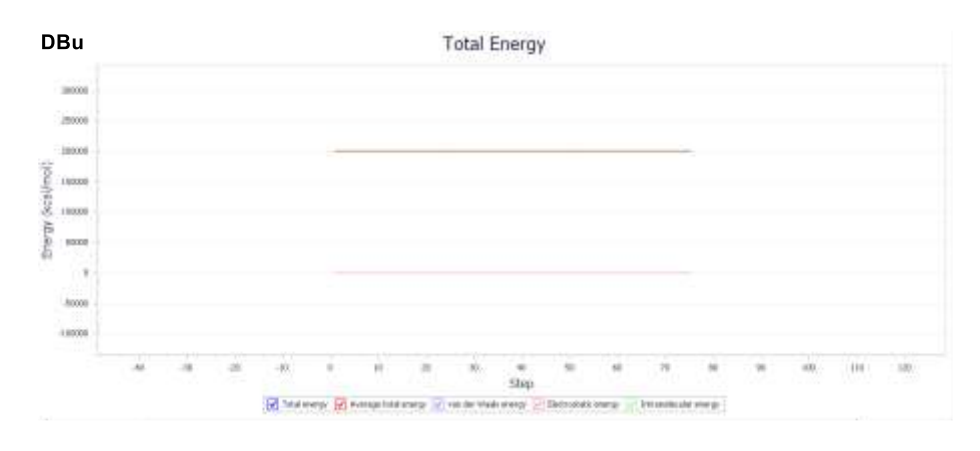


Figure 6. Total energy Monte Carlo adsorption Locator Simulations of Direct Blue (DBu)

Table 1. Adsorption Energy Parameters of Azo Dyes on ${\rm Ti_3C_2}({\rm OH})_2$ MXene Surface from Monte Carlo Adsorption Locator Simulations

| Structure | Total energy | Adsorption energy | Rigid adsorption energy | Deformation energy | dE _{ad} /dN _i |
|-----------|-----------------|-------------------|-------------------------------|--------------------|-----------------------------------|
| MB | 34.2 | -16.35 | -16.578 | 0.230 | -16.348 |
| CR | 254.138 | -22.346 | -30.993 | -23.353 | -22.346 |
| DBk | 266.066 | -23.994 | -33.014 | -23.993 | -23.993 |
| DBu | 477.271 | -46.576 | -33.839 | -46.578 | -46.576 |



Methylene Blue (MB)

The adsorption of Methylene Blue (MB) on $Ti_3C_2(OH)_2$ MXene, as illustrated in Figure 3 and Table 1, revealed the weakest interaction among the four studied dyes, with an adsorption energy of -16.35 kcal/mol. MB is a relatively small, planar cationic dye containing a thiazine ring system and minimal polar functional groups. Its limited π -conjugation and lack of strongly electron-donating or withdrawing groups reduce its ability to interact strongly with the MXene surface. The deformation energy for MB is the lowest (only +0.230 kcal/mol), indicating negligible structural rearrangement upon adsorption, which is characteristic of physisorption. This weak van der Waals forces and possible limited hydrogen bonding explain its low affinity toward $Ti_3C_2(OH)_2$, confirming that MB primarily relies on surface contact rather than strong chemical interaction mechanisms.

Congo Red (CR)

Congo Red (CR) exhibited the most favorable adsorption parameters among all dyes, with a highly negative adsorption energy of -182.346 kcal/mol, as shown in Figure 4 and Table 1. CR contains two azo groups linking aromatic systems, along with two sulfonic acid groups (–SO $_3$ H), which greatly enhance its hydrophilicity and ability to form hydrogen bonds. Additionally, its large, delocalized π -system promotes strong $\pi-\pi$ stacking with the planar MXene layers. The deformation energy (–151.353 kcal/mol) is notably high, indicating significant molecular rearrangement and reorientation to optimize interaction with the surface—strong evidence of chemisorption. The combined effect of π -conjugation, polar functionalities, and structural flexibility allows CR to anchor tightly to the hydroxylated MXene, making it the most effective dye in this adsorption study.

Direct Black 1 (DBk)

Direct Black 1 (DBk) demonstrated intermediate adsorption strength on $Ti_3C_2(OH)_2$ MXene, with an adsorption energy of -23.994 kcal/mol, as shown in Figure 5. DBk contains azo linkages and sulfonic acid groups like CR, but with a more compact and sterically hindered molecular framework. While it does possess multiple aromatic rings, the spatial arrangement of its functional groups may restrict optimal orientation and surface contact, thus reducing overall interaction strength. The deformation energy (-23.993 kcal/mol) is relatively moderate, indicating a partial chemisorptive character, though less intense than that of CR. This suggests that DBk interacts with the MXene surface via a combination of electrostatic interactions, hydrogen bonding, and limited $\pi-\pi$ stacking, but the overall binding is weaker due to molecular bulk and orientation constraints.

Direct Blue 38 (DBu)

Direct Blue 38 (DBu), as presented in Figure 6, displayed the second strongest interaction with the MXene surface, following CR, with an adsorption energy of -46.576 kcal/mol. DBu is a large dye molecule containing multiple aromatic rings, sulfonic acid groups, and azo linkages. These structural features enable strong $\pi-\pi$ interactions and hydrogen bonding with the hydroxyl-terminated MXene. Interestingly, its deformation energy (-46.578 kcal/mol) is close to the adsorption energy, indicating that DBu



undergoes moderate molecular adjustment to achieve a favorable adsorption geometry—evidence of a significant chemisorption component. The enhanced adsorption compared to DBk is attributed to better conjugation and more favorable spatial alignment of functional groups. Thus, DBu exhibits a stable interaction profile, supported by both molecular size and functional diversity.

Molecular Dynamics Simulation Studies

To gain deeper insight into the adsorption mechanisms of the selected azo dyes on the $Ti_3C_2(OH)_2$ MXene surface under dynamic, aqueous conditions, molecular dynamics (MD) simulations were conducted using the Forcite module in BIOVIA Materials Studio (Version 8.0). Each simulation system consisted of a $Ti_3C_2(OH)_2$ (100) crystal slab, the dye molecule, and water molecules (solvent), all confined within a periodic simulation box measuring 18.0 Å × 30.23 Å × 25.08 Å shown in figure 7. Before the MD run, all components—including the dye molecules (Congo Red, Methylene Blue, Direct Black 1, and Direct Blue 38)—were geometry-optimized using the Universal Force Field (UFF) to ensure energy minimization and structural stability.

To complement the static adsorption analysis, molecular dynamics (MD) simulations were employed to evaluate the stability, spontaneity, and nature of dye adsorption on the ${\rm Ti_3C_2(OH)_2}$ MXene surface under realistic aqueous conditions. These simulations provide dynamic insights into the interaction mechanisms by considering thermal fluctuations, solvent effects, and molecular motion over time. By analyzing adsorption and binding energies alongside radial distribution functions (RDF), this section elucidates the extent of physical versus chemical adsorption for each dye and validates the comparative adsorption trends observed in the Monte Carlo simulations.



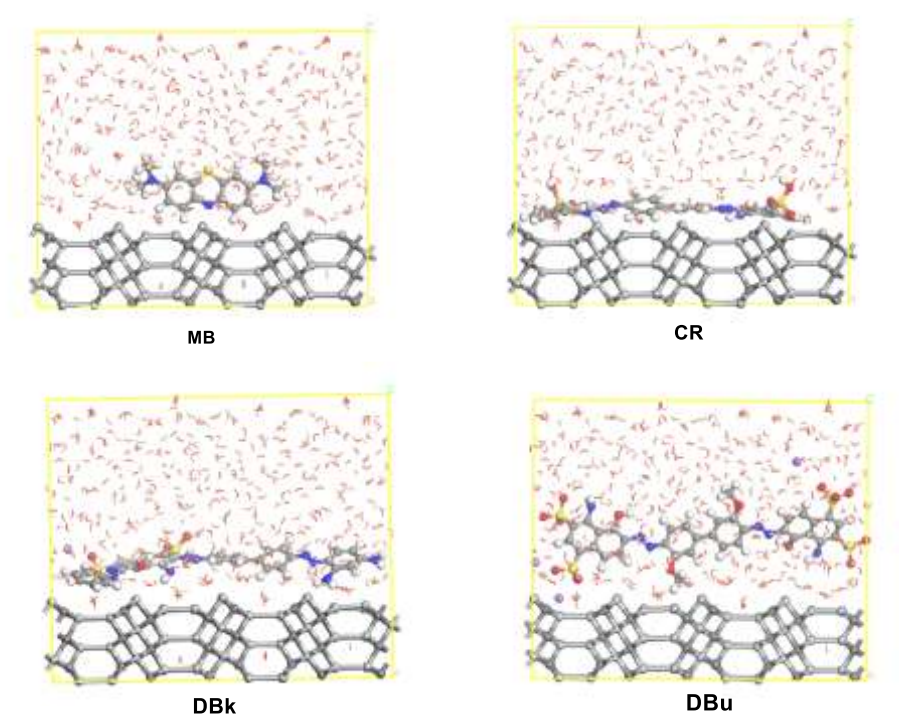


Figure 7. Molecular dynamic simulation of Methylene Blue (MB)-MXene-water, Congo Red (CR)-MXene-water, Direct Black 1 (DBk) MXene-water, and Direct Blue 38 (DBu)-MXene-water.

Methylene Blue (MB)

The MD simulation results (Table 2 and Fig. 8) indicate that Methylene Blue (MB) shows the weakest adsorption interaction with the $Ti_3C_2(OH)_2$ MXene surface, with an adsorption energy of -895.651 kcal/mol. This relatively lower binding energy reflects a limited interaction potential, which aligns with MB's molecular structure. MB is a planar, cationic dye containing a thiazine ring but lacks extensive π -conjugation and polar anchoring groups like sulfonates. The radial distribution function (RDF) curve in Figure 8 suggests that MB molecules maintain a slightly larger distance from the MXene surface, with less pronounced peaks, indicating weak electrostatic or van der Waals forces. The planar geometry aids in some surface contact, but the absence of strong hydrogen-bond donors/acceptors and minimal deformation upon adsorption confirms that the dye undergoes primarily physisorption. Thus, MB's interaction is governed mostly by weak non-covalent forces with limited chemisorptive character.



Table 2. Adsorption and Binding Energies of Azo Dyes on $Ti_3C_2(OH)_2$ MXene Surface from Molecular Dynamics Simulations

| Obs | E sol+water | E _{dye} | E total | Eads | Ebind |
|-----|-------------|------------------|------------|-----------|----------|
| MB | -26930.875 | -50.564 | -27877.09 | -895.651 | 895.651 |
| CR | -26930.875 | -283.582 | -28371.625 | -1157.238 | 1157.238 |
| DBk | -26930.875 | -297.351 | -28576.79 | -1348.604 | 1348.604 |
| DBu | -26930.875 | -500.469 | -29107.669 | -1676.365 | 1676.365 |

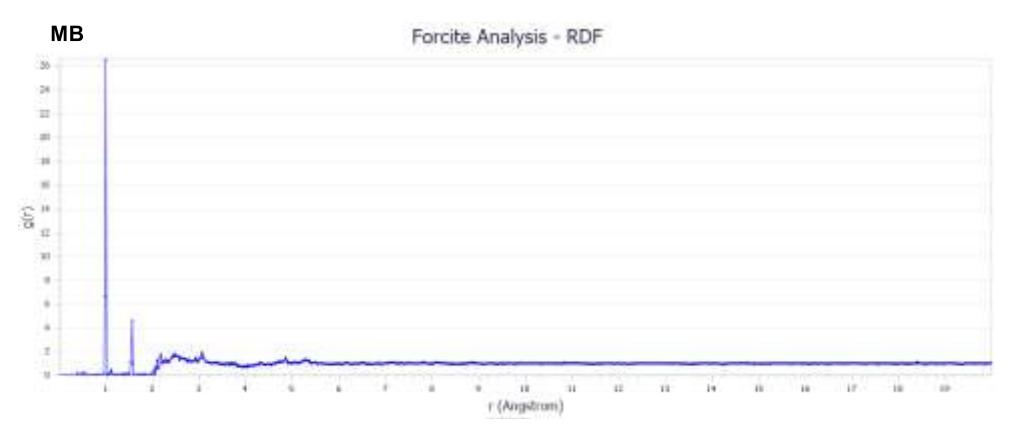


Figure 8. Radial distribution function of Methylene Blue (MB)

Congo Red (CR)

According to the data in Table 2 and Figure 9, Congo Red (CR) demonstrates a significantly stronger interaction with the MXene surface, with an adsorption energy of - 1157.238 kcal/mol. CR contains extended $\pi\text{-systems},$ azo linkages, and sulfonic acid groups (–SO $_3$ H), which facilitate both $\pi-\pi$ stacking and strong hydrogen bonding with the –OH-terminated MXene. The RDF profile in Fig. 9 exhibits sharp and high peaks within 2.5–3.5 Å, indicating a close and structured interaction between the dye and the surface, consistent with chemisorption. The large negative deformation energy reported in previous sections also suggests substantial molecular reorganization during binding. This indicates that CR reorients itself dynamically in solution to maximize electrostatic and hydrogen bonding interactions. Its high binding energy and favorable RDF pattern reinforce that CR exhibits strong and stable adsorption, with both structural and electronic features contributing to its robust chemisorption.



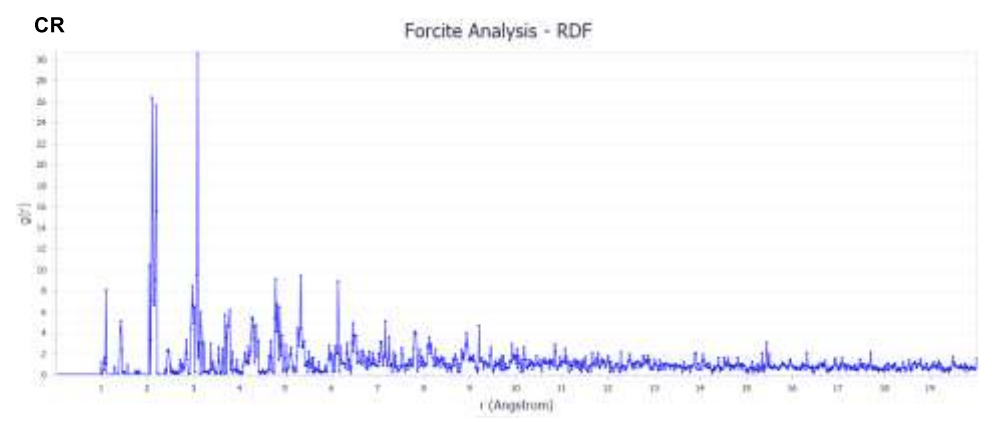


Figure 9. Radial distribution function of Congo Red (CR)

Direct Black 1 (DBk)

Direct Black 1 (DBk) exhibits an adsorption energy of -1348.604 kcal/mol (Table 2), placing it between CR and DBu in adsorption strength. From a chemical perspective, DBk features multiple aromatic rings, azo groups, and sulfonic acid functionalities, which collectively contribute to moderate-to-strong $\pi-\pi$ and hydrogen bonding interactions with the Mxene surface. The RDF profile in Figure 10 reveals a pronounced peak around 3.0 Å, indicating that DBk maintains a fairly close and consistent orientation relative to the surface, supporting chemisorption. However, compared to CR, DBk's more sterically hindered and bulkier structure likely limits its adsorption efficiency due to less favorable spatial alignment. Nonetheless, the strong binding energy suggests that DBk still undergoes effective chemisorption, albeit with slightly lower flexibility or reorientation capability than CR.

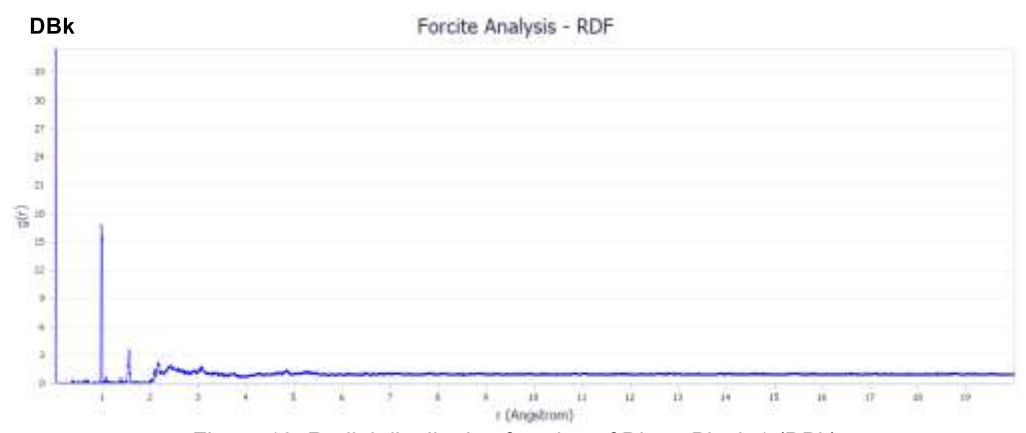


Figure 10. Radial distribution function of Direct Black 1 (DBk)



Direct Blue 38 (DBu)

Among all studied dyes, Direct Blue 38 (DBu) demonstrates the highest adsorption energy of –1676.365 kcal/mol (Table 2), clearly indicating the most favorable interaction with the $Ti_3C_2(OH)_2$ surface. Chemically, DBu possesses multiple conjugated aromatic systems, sulfonic acid groups, and azo linkages, providing abundant sites for π – π stacking, hydrogen bonding, and electrostatic interactions. Figure 11 shows an RDF curve with highly pronounced peaks in the 2.5–3.5 Å region, confirming very strong and close-range interactions—hallmarks of dominant chemisorption. The dye's planar segments likely align well with the MXene layers, maximizing surface contact and interaction energy. Moreover, the large negative deformation energy observed earlier reinforces that DBu undergoes significant reconfiguration to adopt a stable adsorbed state. Overall, DBu exhibits the most thermodynamically favorable and chemically intensive interaction, making it the best-performing dye in terms of spontaneous, stable adsorption on the MXene surface.

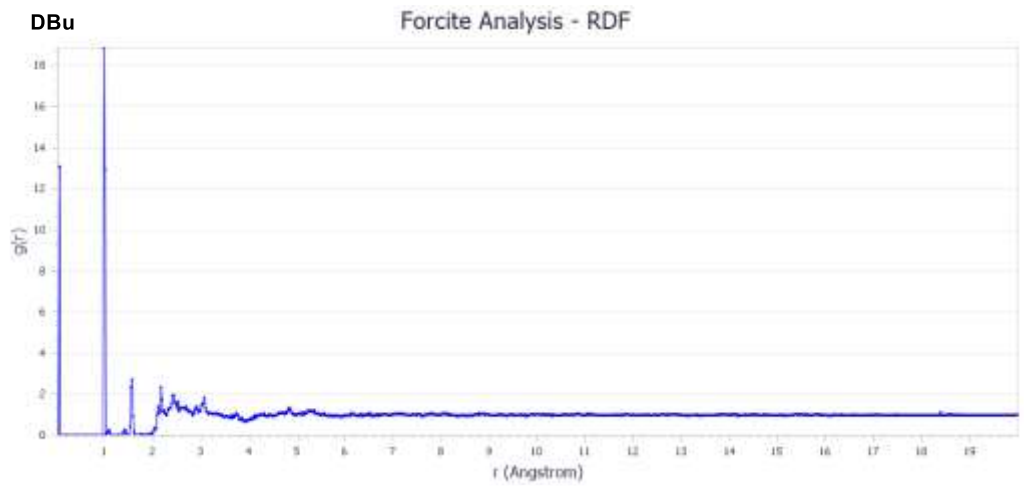


Figure 11. Radial distribution function of Direct Blue 38 (DBu)

CONCLUSION

This study offers a molecular-level perspective on the chemisorption behavior of four widely used industrial azo dyes—Congo Red, Methylene Blue, Direct Black 1, and Direct Blue 38—on hydroxyl-functionalized Ti $_3$ C $_2$ MXene surfaces. By employing a dual computational strategy of Monte Carlo adsorption locator simulations and molecular dynamics under aqueous conditions, we unveil that dye–MXene interactions are governed by a synergy of π – π stacking, hydrogen bonding, and surface-induced molecular reorganization. Among the dyes, Congo Red and Direct Blue 38 consistently demonstrated the most favorable energetics, not only in static conditions but also under dynamic environments, suggesting their adsorption is both spontaneous and structurally



adaptive—a hallmark of strong chemisorption. Notably, the deformation energy analyses provided insight into the extent of structural adjustments dyes undergo, revealing the importance of molecular flexibility and functional group orientation in determining adsorption strength.

These findings extend beyond comparative adsorption metrics, offering mechanistic insights that highlight the role of dye architecture—such as planarity, electron-donating groups, and steric hindrance—in influencing dye–MXene affinity. The significant binding energy profiles suggest that ${\rm Ti_3C_2(OH)_2}$ MXene is not merely a passive adsorbent but an active participant in the dye capture process. Future directions should aim at correlating these theoretical predictions with experimental adsorption isotherms and kinetics, as well as exploring surface functionalization strategies to further tune selectivity and efficiency. This work thus establishes a foundational framework for the rational design of MXene-based adsorbents in advanced wastewater treatment technologies.

References

- [1] Kusumlata AB, Kumar A, Gautam S. Sustainable solutions: reviewing the future of textile dye contaminant removal with emerging biological treatments. Limnological Review. 2024, 24, 126-149. https://doi.org/10.3390/limnolrev24020007
- [2] Aragaw TA. A review on biodegradation of textile dye wastewater: Challenges due to wastewater characteristics and the potential of alkaliphiles. Journal of Hazardous Materials Advances. 2024, 16, 100493. https://doi.org/10.1016/j.hazadv.2024.100493
- [3] Satyam S, Patra S. Innovations and challenges in adsorption-based wastewater remediation: a comprehensive review. Heliyon. 2024, 10, e29573. https://doi.org/10.1016/j.heliyon.2024.e29573
- [4] Whaieb AH, Jasim FT, Abdulrahman AA, Gheni SA, Fattah IMR, Karakullukcu NT. Tailoring zeolites for enhanced post-combustion CO2 capture: A critical review. Current Research in Green and Sustainable Chemistry. 2025, 10, 100451. https://doi.org/10.1016/j.crgsc.2025.100451
- [5] Gkika DA, Tolkou AK, Katsoyiannis IA, Kyzas GZ. The adsorption-desorption-regeneration pathway to a circular economy: the role of waste-derived adsorbents on chromium removal. Separation and Purification Technology. 2025, , 132996. https://doi.org/10.1016/j.seppur.2025.132996
- [6] Yu S, Tang H, Zhang D, Wang S, Qiu M, Song G, Wang X. MXenes as emerging nanomaterials in water purification and environmental remediation. Science of the Total Environment. 2022, 811, 152280. https://doi.org/10.1016/j.scitotenv.2021.152280
- [7] Amani AM, Abbasi M, Najdian A, Mohamadpour F, Kasaee SR, Kamyab H, Mosleh-Shirazi S. MXene-based materials for enhanced water quality: Advances in remediation strategies. Ecotoxicology and Environmental Safety. 2025, 291, 18. https://doi.org/10.1016/j.ecoenv.2025.18
- [8] Gao Y, Cao Y, Gu Y, Zhuo H, Zhuang G, Deng S, Wang JG. Functionalization Ti3C2 MXene by the adsorption or substitution of single metal atom. Applied Surface Science. 2019, 465, 911-918. https://doi.org/10.1016/j.apsusc.2018.09.254



- [9] Salahshoori I, Wang Q, Nobre MA, Mohammadi AH, Dawi EA, Khonakdar HA. Molecular simulation-based insights into dye pollutant adsorption: a perspective review. Advances in Colloid and Interface Science. 2024, 333, 103281. https://doi.org/10.1016/j.cis.2024.103281
- [10] Mullani S, Kim C, Lokhande V, Ji T. MXene structural and surface modifications for enhanced Li-ion diffusion in lithium-ion capacitors: A critical mini review of recent advances. Chemical Engineering Journal. 2025, 510, 161565. https://doi.org/10.1016/i.cei.2025.161565
- [11] Narayanaswamy V, Alaabed S, Obaidat IM. Molecular simulation of adsorption of methylene blue and rhodamine B on graphene and graphene oxide for water purification. Materials Today: Proceedings. 2020, 28, 1078-1083. https://doi.org/10.1016/i.matpr.2020.01.086
- [12] Mahdavi M, Rahmani F, Nouranian S. Molecular simulation of pH-dependent diffusion, loading, and release of doxorubicin in graphene and graphene oxide drug delivery systems. Journal of Materials Chemistry B. 2016, 4, 7441-7451. https://doi.org/10.1039/C6TB00746E
- [13] Terban MW, Billinge SJ. Structural analysis of molecular materials using the pair distribution function. Chemical Reviews. 2021, 122, 1208-1272. https://doi.org/10.1021/acs.chemrev.1c00237
- [14] Zheng J, Frisch MJ. Efficient geometry minimization and transition structure optimization using interpolated potential energy surfaces and iteratively updated hessians. Journal of chemical theory and computation. 20, 13, 6424-6432. https://doi.org/10.1021/acs.jctc.7b00719
- [15] Salahshoori, I., Wang, Q., Nobre, M. A., Mohammadi, A. H., Dawi, E. A., & Khonakdar, H. A. (2024). Molecular simulation-based insights into dye pollutant adsorption: A perspective review. *Advances in Colloid and Interface Science*, 333, 103281. https://doi.org/10.1016/j.cis.2024.103281
- [16] Khnifira, M., Boumya, W., Atarki, J., Sadiq, M., Achak, M., Bouich, A., Barka, N., & Abdennouri, M. (2024). Experimental, DFT and MD simulation combined studies for the competitive adsorption of anionic and cationic dyes on activated carbon in an aqueous medium. *Journal of Molecular Structure*, 1310, 138247. https://doi.org/10.1016/j.molstruc.2024.138247



MEHANIZMI HEMISORPCIJE INDUSTRIJSKIH BOJA NA POVRŠINI TI₃C₂ MXENE ZA PRIMENU U PREČIŠĆAVANJU OTPADNIH VODA: TEORIJSKI PRISTUP

Shahidul Islam¹ <u>ID</u>, Md. Rahamatolla² <u>ID</u>, Marija Kodric³ <u>ID</u>, Sanjay Belowar¹ <u>ID</u>

¹ Katedra za tekstilni inženjering, BGMEA Univerzitet mode i tehnologije (BUFT), Daka 1230, Bangladeš

² Katedra za prirodne nauke, BGMEA Univerzitet mode i tehnologije (BUFT), Daka 1230, Bangladeš

³ Inovacioni centar Univerziteta u Nišu, Niš, Srbija

Ispuštanje azo boja iz industrijskih otpadnih voda predstavlja ozbiljan ekološki i zdravstveni rizik zbog njihove postojanosti i otpornosti na biorazgradnju. MXeni funkcionalizovani hidroksilnim grupama ${\rm Ti_3C_2(OH)_2}$ pojavili su se kao obećavajući adsorbensi zahvaljujući velikoj specifičnoj površini, hidrofilnosti i raznovrsnoj površinskoj hemiji. U ovoj studiji primenjene su Monte Karlo i simulacije molekulske dinamike za ispitivanje adsorpcionog ponašanja četiri industrijske boje — Kongo crvena (CR), Metilen plava (MB), Direktna crna 1 (DBk) i Direktna plava 38 (DBu) — na površinama MXena ${\rm Ti_3C_2(OH)_2}$.

Rezultati Monte Karlo lociranja adsorpcije pokazali su da CR ima najpovoljniju statičku energiju adsorpcije (-182,346 kcal/mol), zatim slede DBu (-46,576 kcal/mol), DBk (-23,994 kcal/mol) i MB (-16,35 kcal/mol). Posebno je značajno da je energija deformacije CR iznosila -151,353 kcal/mol, što ukazuje na jaku hemisorpciju usled značajne molekulske reorganizacije. Simulacije molekulske dinamike u vodenom medijumu dodatno su potvrdile ove trendove, pri čemu je DBu pokazala najveću dinamičku energiju adsorpcije (-1676,365 kcal/mol), zatim DBk (-1348,604 kcal/mol), CR (-1157,238 kcal/mol) i MB (-895,651 kcal/mol). Energije vezivanja pratile su sličan redosled, potvrđujući da su π - π interakcije, vodonične veze i površinski indukovana reorijentacija dominantni mehanizmi interakcije.

Ova saznanja pružaju uvid na molekulskom nivou u odnos između strukture i funkcije koji upravlja adsorpcijom boja na MXenima i ističu Ti₃C₂(OH)₂ MXen kao efikasan materijal za selektivno i održivo uklanjanje boja iz otpadnih voda.

Ključne reči: Azo boje, Ti₃C₂ MXen, Energija adsorpcije, Hemisorpcija, Molekulska dinamika, Prečišćavanje otpadnih voda.



UDK 677.072 : 677.027.423.1 DOI: 10.46793/NoveITDS16.133JP

DYEING KINETICS OF MULTI-COMPONENT TEXTILE YARN WITH BASIC DYE

Jelena Jovićević Pavković* D, Dragan Djordjević D University of Niš, Faculty of Technology, Serbia

Kinetic analysis of the dyeing process of multi-component textile yarn with a basic dye was performed in this article. The yarn consists of multiple components, specifically three different fibers, with the highest proportion being modal, followed by cotton, and the least being polyamide. Dyeing of the yarn was carried out using a discontinuous method, with the appropriate initial dye concentration and different dyeing times. The aim is to elucidate the dynamic events during the adsorption of dye molecules onto the fibers and their diffusion into the interior. Two kinetic reaction models (Pseudo-first-order and Avrami) and one kinetic diffusion model (Weber-Morris) were used to test the experimental data from the dyeing process. Dyeing multi-component yarn yields satisfactory results, with even coloration of the yarn. The degree of dye exhaustion and the amount of dye on the fibers increase with time, while the initial dye concentration in the solution decreases as the dyeing process progresses. In the linear simulation of the kinetic dyeing parameters, the Avrami reaction model proves to be efficient, while the Weber-Morris model is found to be a very favorable diffusion equation.

Keywords: yarn, basic dye, dyeing, kinetic models.

INTRODUCTION

Textile products made from fiber blends are often found in the market, and they can be either dyed or undyed. The dyeing of fabrics, knits, or yarns made from fiber blends can be performed at various stages of their production. For instance, two or more different fibers can be separately dyed and then mixed to achieve a two-tone or multicolored effect in the final product. In many cases, dyeing blends is done in the form of fabric or

* Author address: Jelena Jovicevic, University of Nis, Faculty of Technology in Leskovac, Bulevar oslobođenja 124, 16000 Leskovac, Serbia e-mail address: jejchin@gmail.com



knits. Dyeing fibers in their loose state is cheaper, but dyeing fabrics or knits is safer and more convenient, especially if these products need to be stored and dyed according to fashion market demands [1].

Dyeing textile materials in the form of fibers, yarns, or fabrics containing different components can be executed in the following ways [2]:

- Dyeing all components in the same shade.
- Dyeing only one component.
- Dyeing all components in different shades.

In practice, the most common scenario is the dyeing of two-component blends, and the most interesting form is dyeing each component with the appropriate dye in a single bath. In this case, dyeing each type of fiber is much better controlled than when both fibers are dyed with the same dye simultaneously. An example of an "ideal" blend for dyeing is a blend of viscose and acetate rayon. Direct dyes, if selected correctly, do not have much affinity for the acetate cellulose rayon, while disperse dyes, which successfully dye acetate cellulose rayon, practically do not dye viscose rayon [3].

Dyeing blends can be carried out using the following methods [4]:

- In a single bath, by dyeing all components in the same bath with one or more suitable dyes.
- In two or more baths, by dyeing each component in a separate bath with the appropriate dye.

Dyeing with basic dyes operates by forming ionic bonds with the fibers, similar to the process of dyeing with acid dyes. Basic dyes are also known as cationic dyes because their structure allows them to dissociate in an aqueous solution, giving a colored cation [5].

This paper presents a comprehensive set of research activities related to the kinetic analysis of the dyeing process of multi-component yarn with a basic (cationic) dye. By analyzing the rate and mechanism of dyeing, this research contributes to the understanding of the sorption process of the basic dye on yarn composed of three different fibers. The goal is to successfully perform the dyeing of multi-component yarn in a single bath and clarify the interactions between dye and fibers.

MATERIALS AND METHODS

In the experimental part of the study, a multi-component yarn was used, consisting of 2.0% Polyamide, 38.0% Cotton, and 60.0% Modacrylic (Figure 1).

Some of the key characteristics of the yarn that should be highlighted include the following: the average fineness is 31.6 tex, the average twist count is 200 twists per meter, the average shrinkage value is 2.6%, and the average thickness is $290 \mu m$.





Figure 1. Appearance of the multi-component yarn before and after dyeing

For dyeing, a basic (cationic) dye, Basic Green 4 (Astrazon Green M) from Huntsman, Switzerland, was used. The structure of this dye is shown in Figure 2.

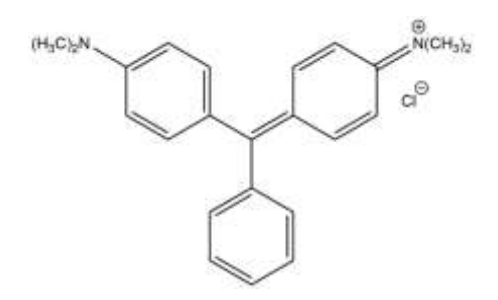


Figure 2. Structure of the green basic dye used

To verify the kinetic parameters of the dyeing process, a batch (discontinuous) process was employed. A fiber sample weighing 0.5 g was dyed in a bath with a constant volume of 0.05 dm 3 . The dyeing temperature was maintained at a constant temperature of 98 $^{\circ}$ C, while the dyeing time varied from 10 to 60 minutes, and the dye concentration was kept constant at 100 mg/dm 3 . In addition to the dye, sodium chloride at 20 g/dm 3 and acetic acid at 1 g/dm 3 were used as additives in all cases.

To determine the dye concentration in the solution using a calibration curve, absorbance was measured with the Varian Cary 100 UV-VIS Spectrophotometer (measurements were taken at the absorption maximum, 590 nm).

The kinetics of the adsorption of the basic green dye on the yarn were analyzed using the following reaction kinetic models: *Pseudo-first-order* and *Avrami*.

The kinetic data described by the *Pseudo-first-order* model represent the first known equation that describes the rate of sorption based on the adsorption capacity [6]:

$$\log(q_e - q_t) = \log(q_e) - \frac{k_1}{2,303}t\tag{1}$$

Where *qe* and *qt* are the adsorption capacities at equilibrium (*e*) and after some time (*t*), respectively (mg/g), and k1 is the rate constant of the pseudo-first-order sorption (1/min).



The *Avrami* model defines certain kinetic parameters, such as possible changes in the sorption rate as a function of initial concentration and sorption time, as well as determining the kinetic order of the fraction [7].

$$q_t = q_e \cdot \{1 - \exp[-(K_A \cdot t)]^{n_A}\} \tag{2}$$

where qt - is the adsorption capacity at time t (mg/g), K_A - is the adjusted kinetic constant $(1/\min)^{nAV}$, n_A - is the constant related to the sorption mechanism.

In the research, the Weber-Morris kinetic diffusion model was used.

The *Weber-Morris* model, also known as the intra-particle diffusion model, is described by the following equation [7]:

$$q_t = k_{WM} \cdot t^{0.5} \tag{3}$$

Where: k_{WM} - is the intra-particle diffusion rate constant (mg/g·min^{-0.5}); t - is the contact time (min)

RESULTS AND DISCUSSION

Information about dyeing kinetics is crucial for determining the optimal operating conditions for a full batch process. The kinetics of sorption can be represented graphically as the uptake-exhaustion of dye over time, and this dependency is known as the kinetic isotherm. The kinetics depend on material factors such as the adsorbent (fibers) and adsorbate (dye), as well as experimental factors like temperature or pH. The results confirm that higher temperatures accelerate the diffusion of dye molecules into the fiber structure, leading to a faster attainment of apparent equilibrium. However, the final adsorption capacity decreases with increasing temperature, which is consistent with the exothermic nature of the adsorption process and the weaker interactions between the dye and the fiber at elevated thermal energy [3, 4].

The diagram in Figure 3 illustrates the dependence of the amount of basic dye in the dye bath and the amount of dye on the yarn over the dyeing time. It can be observed that, as expected, the dye concentration in the bath decreases during the dyeing process in all cases, while longer dyeing times result in a slightly higher amount of adsorbed dye per unit mass of yarn. The adsorption process continues until equilibrium is reached between the dye concentration in the solution and the dye concentration on the fiber. Since dye molecules tend to form aggregates in the aqueous solution, mechanical agitation breaks apart the dye aggregates in the solution and reduces the particle size of the dye in dispersion, which is the first condition for better sorption on fibers.



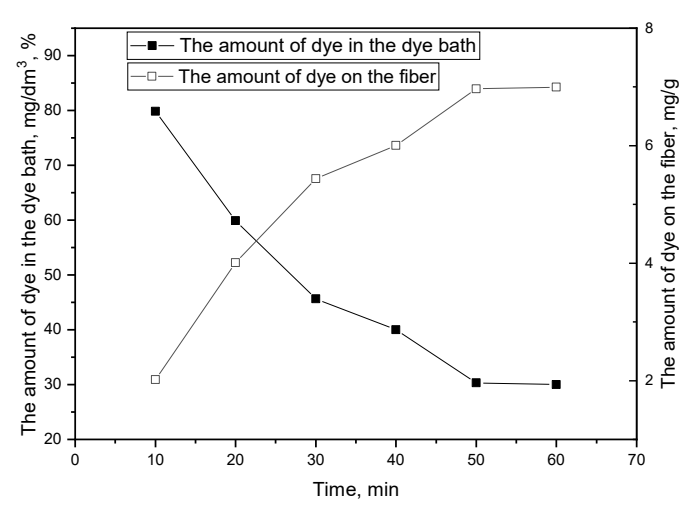


Figure 3. Change in the amount of dye in the dye bath and the amount of dye on the yarn during dyeing

In a similar study, the dyeing of polyamide composite fabric with a cationic dye was conducted, where the success was attributed to the electrostatic interaction between the dye cations and the negatively charged surface of the fabric treated with nanoclay. On the other hand, van der Waals forces can also serve as a means of bonding between the polymer chains and dye cations. The results indicated that the optimal conditions for dyeing polyamide fabric were as follows: pH 7 and a dyeing temperature of 85 °C. The impact of dyeing time (5, 10, 15, 20, 30, and 60 min) on the exhaustion level revealed a significant increase in the dye exhaustion percentage onto the polyamide fabric during dyeing. Under optimal conditions, polyamide fiber achieved an exhaustion of 97%, which was attributed to the swelling and expansion of the nanoclay, facilitating the penetration and distribution of dye molecules within the fabric [8].

Figures 4 and 5 present diagrams for the dye sorption kinetics on fibers, including experimental data points and linear kinetic reaction models: *Pseudo-first-order*, and *Avrami*, for an initial concentration of basic green dye of 100 mg/dm³. According to the fitting curves that match the experimental data points, the *Avrami* equation appeared to be better suited for describing the kinetics of basic green dye sorption (Figure 5), with the fitted curve of this kinetic equation closely following the experimental points. In contrast, based on the curve in Figure 4, the *Pseudo-first-order* model noticeably lags behind and makes a smaller contribution to explaining the sorption kinetics.



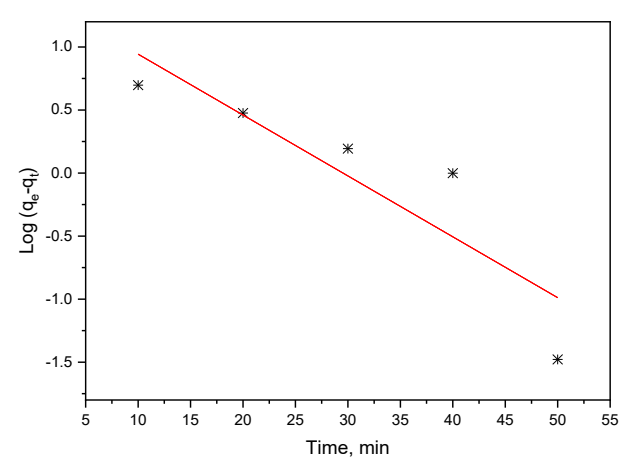


Figure 4. Sorption kinetics of basic green dye according to the *Pseudo-first-Order* kinetic reaction model

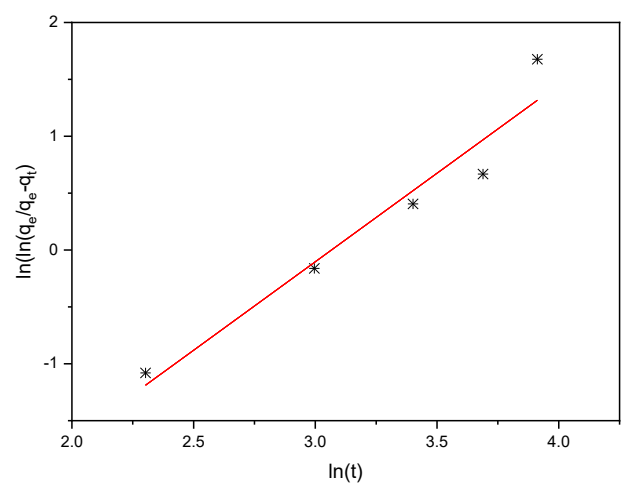


Figure 5. Sorption kinetics of basic green dye according to the kinetic reaction model Avrami

To understand the mechanism that controls the entire sorption kinetics, preference is given to kinetic diffusion models or mechanistic (theoretical) models. From a diffusion perspective, to interpret experimental data, it is necessary to identify the steps involved in sorption, described by external mass transfer, diffusion through the boundary layer, and diffusion within particles [8].

Figure 6 shows a dyeing rate diagram with experimental points and the curve of the *Weber-Morris* kinetic diffusion model for an initial concentration of basic dye of 100 mg/dm³. Based on the appearance of the fitting curve, this model describes the dyeing kinetics very well. Considering that the fitting line passes through the coordinate origin,



it can be concluded that diffusion within particles is the dominant phase controlling the rate of sorption. Therefore, diffusion through the film or boundary layer is negligible, while diffusion within particles is practically the only rate-controlling step for dyeing a multi-component yarn with basic green dye.

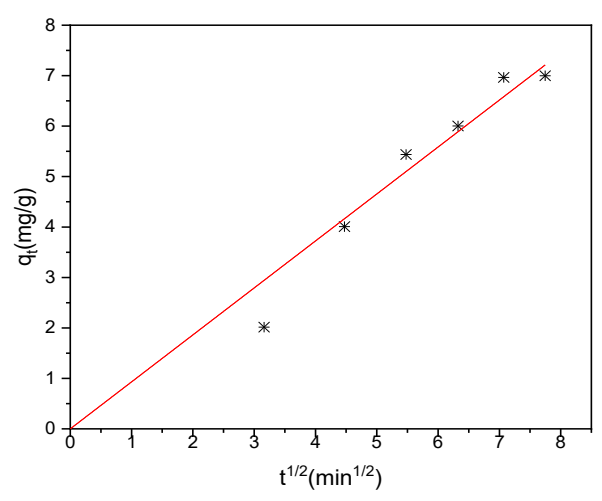


Figure 6. Sorption kinetics of basic green dye according to the diffusion model Weber-Morris

Similar kinetic studies are presented in a research paper dealing with the kinetics of adsorption and the thermodynamics of dyeing a copolyester fabric with a basic dye at 80, 90, and 100 °C. The results showed that the *Pseudo-second-order* model proved to be the most favorable and could be used to effectively explain the adsorption kinetics and predict the rate coefficient (k_2) at different temperatures. It was found that the adsorption equilibrium data were in accordance with the *Langmuir* isotherm with high correlation, while the thermodynamic parameters revealed that the dye adsorption on the fabric was a spontaneous, endothermic, and chemisorption process [6].

Table 1 provides numerous values of parameters for kinetic reaction models and the diffusion model for the sorption of a basic dye on yarn. Based on the highest coefficient of determination, the dominance of the *Weber-Morris* kinetic model is confirmed. This model is very suitable and useful since its curve fits the experimental points excellently. Very high statistical parameters of suitability (validity) (R^2 =0.993) obtained from the *Weber-Morris* model for diffusion and sorption of a basic dye on a multi-component yarn indicate that diffusion within particles is the rate-controlling step for dyeing.

The *Pseudo-first-order* kinetic model proved to be the weakest of the models used (R^2 =0.795), meaning that the sorption rate cannot be described solely based on the adsorption capacity, and the change in the sorption rate does not depend solely on the initial concentration and reaction time.

The *Avrami* equation was used to verify specific changes in kinetic parameters during dyeing. This model has a high coefficient of determination, R^2 =0.940. The data suggest



that the dyeing process is limited to surface reaction, and the diffusion of dye molecules is fast $(n_A > 1)$. Since it is an exponential equation, n_A as a fractional number is associated with possible changes in the sorption mechanism during dyeing. This model assumes that the distribution of dye molecules on the fiber surface is homogeneous and that sorption occurs at a constant growth rate, as the values of n_A are greater than 1. Therefore, the sorption mechanism is accompanied by multiple kinetic fractions that change during the contact of the dye with different fibers.

Table 1. Numerous values of parameters for kinetic reaction models and diffusion model with statistical parameters.

| | Analytical expression | | |
|--------------------|---|--|-----------------------|
| Kinetic model | | Parameters | Values |
| Pseudo-first-order | $\log(q_e - q_t) = \log(q_e) - \frac{k_1}{2,303}t$ | <i>k</i> ₁ (min⁻¹) <i>R</i> ² | 0.11 0.795 |
| Avrami | $q_t = q_e \cdot \{1 - exp[-(K_A \cdot t)]^{n_A}\}$ | $K_A \left(\text{min}^{-1} \right)^{-n_{AV}}$ n_A R^2 | 0.05 1.55 0.940 |
| Weber-Morris | $q_t = k_{WM} \cdot t^{0.5}$ | <i>kwм</i> (mg⋅g⋅min ⁻ ^{0.5}) <i>R</i> ² | 0.93 0.993 |

CONCLUSION

Based on the research results, it can be concluded that yarn composed from various types of fibers can be effectively dyed with basic green dye at the boiling temperature in a single bath. The aim is to successfully complete the dyeing process in a single bath to avoid the costs associated with dyeing in multiple baths, considering that each component is dyed separately.

During the dyeing of the yarn, the amount of adsorbed dye and the degree of dye exhaustion continuously increase over time, while the initial concentration of dye in the solution decreases.

The Avrami model exhibited the best agreement with to the experimental data, as it most efficiently describes the complex kinetics of dye adsorption in multicomponent textile yarn, where the process occurs through several simultaneous mechanisms, including rapid surface adsorption and slower intra-fiber diffusion. In comparison, the pseudo-first-order model is overly simplified and cannot capture this complexity. Among the kinetic diffusion models, the Weber–Morris equation is the most favorable for linearly simulating the kinetics of fiber dyeing in multicomponent yarn. According to the Avrami and Weber–Morris models, the distribution of dye molecules on the fiber surface is homogeneous, sorption proceeds at a constant growth rate, and the overall sorption mechanism is governed by intra-particle diffusion.

The results of this study suggest the feasibility of a different approach to the simultaneous dyeing of yarn made from a mixture of fibers in a single bath, therefore enabling greater exhaustion, cost savings, and reduced waste dye after the dyeing process.



Acknowledgment

This research was supported by the Ministry of Science, Technological Development and Innovation of the Republic of Serbia (The record number: 451-03-137/2025-03/200133).

References

- [1] Yousuf, M., Khatri, A., Hussain, T., Kim, S.H. Eco-friendly dyeing of cotton fabric with reactive dyes using ultrasound: Kinetics, mechanism and optimization. *Ultrasonics Sonochemistry* **48** (2018): 411-417. https://doi.org/10.1016/j.ultsonch.2018.06.016
- [2] Abdelrahman, E.A., Mohamed, H.M., Fathy, M. Enhanced dye removal and adsorption kinetics of cationic dyes onto activated carbons from agricultural wastes. *Journal of Environmental Chemical Engineering* **9**, 1 (2021): 104662. https://doi.org/10.1016/j.jece.2020.104662
- [3] Bechtold, T. and T. Pham: Textile Chemistry. Berlin, Boston, De Gruyter (2019) p.85. https://doi.org/10.1515/9783110528826
- [4] Mahapatra, N.N.: Textile Dyeing. India (2018) p.299.
- [5] Saroj, S., J. Singh and N.M. Rose: Fundamentals of Textile Dyeing. (2022) p.176.
- [6] Wang, J., X. Li, Z. Cai and L. Gu: Absorption Kinetics and Thermodynamics of Cationic Dyeing on Easily Dyeable Copolyester Modified by 2-Methyl-1,3-Propanediol, Fiber. *Polym.* 16, 11 (2015) 2384-2390. https://doi.org/10.1007/s12221-015-5157-6
- [7] Benjelloun, M., Y. Miyah, G.A. Evrendilek, F. Zerrouq and S. Lairini: Recent Advances in Adsorption Kinetic Models: Their Application to Dye Types, Arab. *J. Chem.* **14**, 4 (2021) 103031. https://doi.org/10.1016/j.arabjc.2021.103031
- [8] El-Gabry, L.K., M.F. Nasr and A.A.A. El-Kheir: A new economical technique for dyeing polyamide fibre/nanoclay composite with basic dye, *Res. J. Text. Apparel.* **25**, 1 (2021) 47-63. https://doi.org/10.1108/RJTA-04-2020-0032
- [9] Ovejero, R.G., J.R. Sánchez, J.B. Ovejero, J. Valldeperas and M.J. Lis: Kinetic and Diffusional Approach to the Dyeing Behavior of the Polyester PTT. *Text. Res. J.77*, 10 (2007) 804-809. https://doi.org/10.1177/0040517507077861



KINETIKA BOJENJA VIŠEKOMPONENTNE TEKSTILNE PREĐE BAZNOM BOJOM

Jelena Jovićević Pavković <u>ID</u>, Dragan Djordjević <u>ID</u> Универзитет у Нишу, Технолошки факултет, Лесковац, Србија

U ovom radu izvršena je kinetička analiza procesa bojenja višekomponentne tekstilne pređe baznom bojom. Pređa se sastoji od više komponenti, konkretno od tri različita vlakna, pri čemu je najzastupljeniji modal, zatim pamuk, a najmanje poliamid. Bojenje pređe izvedeno je diskontinuiranom metodom, pri odgovarajućoj početnoj koncentraciji boje i različitim vremenima bojenja. Cilj je razjašnjenje dinamičkih dešavanja tokom adsorpcije molekula boje na vlakna i njihove difuzije u unutrašnjost. Za ispitivanje eksperimentalnih podataka dobijenih tokom procesa bojenja korišćena su dva kinetička reakciona modela (pseudo-prvog reda i Avrami) i jedan kinetički model difuzije (Veber-Moris). Bojenje višekomponentne pređe daje zadovoljavajuće rezultate, sa ujednačenim nijansiranjem pređe. Stepen iskorišćenja boje i količina boje na vlaknima rastu tokom vremena, dok početna koncentracija boje u rastvoru opada kako proces bojenja napreduje. U linearnoj simulaciji parametara kinetike bojenja, Avramijev reakcioni model se pokazao kao efikasan, dok se Veber-Morisov model istakao kao veoma pogodna difuziona jednačina.

Ključne reči: pređa, bazna boja, bojenje, kinetički modeli.



DOI: 10.46793/NovelTDS16.143JP

DECOLORIZATION OF AQUEOUS SOLUTION OF TEXTILE DYE USING VOLCANIC ASH-BASED ADSORBENT

Jelena Jovićević Pavković* D, Dragan Đorđević D University of Niš, Faculty of Technology, Leskovac, Serbia

This study investigates the potential application of modified volcanic ash as an adsorbent for the removal of textile direct dye from wastewater. The aim of the research was to optimize the decolorization process of model solutions using volcanic ash previously modified through physical and chemical treatments. Various process parameters were examined, including the pH value, initial dye concentration, contact time, temperature, and adsorbent dosage. The highest adsorption efficiency was achieved at a pH value of 3, while maximum dye removal efficiency was reached after 60 minutes of treatment. The maximum adsorption capacity was 7 mg/g, and the dye removal rate exceeded 82%, positioning the modified volcanic ash as a competitive adsorbent. In conclusion, modified volcanic ash represents a low-cost and effective material for the decolorization of aqueous solutions of textile direct dyes, with potential application under industrial conditions for the treatment of colored wastewater from the textile industry.

Keywords: volcanic ash, adsorption, decolorization, textile direct dye, wastewater.

INTRODUCTION

The modern textile industry is facing serious environmental challenges, among which the problem of water pollution due to the discharge of colored effluent stands out [1,2]. During the dyeing process of textile materials, especially natural fibers such as cotton, a large number of synthetic dyes are used, which are characterized by high chemical stability and complex molecular structure [3].

Textile direct dyes are a type of synthetic dye that is directly applied to cellulosic fibers, such as cotton, flax, etc. They are water-soluble and bind to the fibers mainly through * Author address: Jelena Jovicevic, University of Nis, Faculty of Technology in Leskovac, Bulevar oslobođenja 124, 16000 Leskovac, Serbia

e-mail address: jejchin@gmail.com



hydrogen bonds and van der Waals forces. The main characteristics of textile direct dyes are: good solubility in water, which allows for a simple dyeing process; a simple dyeing procedure, usually carried out in neutral or slightly alkaline conditions; an affordable price and ease of application make them suitable for use in small productions and for home dyeing; lower fastness to light and washing compared to reactive or sulfur dyes, which makes them less suitable for textiles that are frequently washed; a wide range of colors, which enables diverse application in decoration and less demanding textile products [4]. The main ecological problems of direct dyes in waters are: low degradability - these dyes are often of complex structure (e.g. based on azo or anthraquinone cores), which makes them difficult to biodegrade; they decompose very slowly in nature; coloration of water – even in small concentrations (e.g. <1 ppm), direct dyes cause strong coloration of watercourses, which affects light penetration and disturbs photosynthesis in aquatic ecosystems; toxicity and mutagenicity - some azo derivatives formed by dye degradation can be toxic, carcinogenic, or mutagenic to aquatic organisms and humans; accumulation in living organisms - direct dyes can adsorb onto sediments and enter the food chain, accumulating in fish and other aquatic organisms [7].

Methods of removing direct dyes from wastewater: physico-chemical processes – adsorption (e.g., activated carbon), coagulation/flocculation, membrane technologies (e.g., nanofiltration); biological processes – aerobic and anaerobic bioreactors, microorganisms modified for dye degradation; advanced oxidation processes – ozonation, Fenton reaction ($Fe^{2^+} + H_2O_2$), UV/H_2O_2 or UV/O_3 systems [8].

The use of direct dyes without adequate wastewater treatment represents a serious threat to the environment. The introduction of more environmentally friendly dyes (e.g., reactive dyes with better fixation) and efficient wastewater treatment systems is crucial for the sustainable development of the textile industry.

Volcanic ash as an adsorbent is increasingly being investigated as an environmentally friendly and economically acceptable material for the removal of various pollutants from water, including dyes from textile wastewater, heavy metals, and organic compounds. As a natural mineral waste material, it is always an interesting subject of research in the field of adsorption, primarily because of its heterogeneous mineral structure, porosity, and the possibility of chemical modification to increase its adsorption capacity [5,6]. Although volcanic ash is not soluble in water, its physical and chemical properties allow it to act as a natural adsorbent in various purification and environmental protection applications. The mode of application, in this sense, is that the ash is mixed with wastewater or used in filter systems, and it can be activated with acid or base for greater efficiency [9].

Advantages of using volcanic ash are [10]:

- Environmentally friendly (natural material).
- Economical compared to synthetic adsorbents.
- High efficiency for removal of cationic dyes and metals.

This paper investigates the potential of chemically modified volcanic ash as an adsorbent for the removal of textile direct dye from model wastewater. The aim of the research is to, through systematic experimental analysis, examine the influence of key parameters – solution pH value, contact time between adsorbent and adsorbate, as well as initial dye concentration – on adsorption efficiency, along with determining kinetic and equilibrium characteristics of the process. Based on the obtained results, the potential



application of this system in textile effluent treatment was assessed, thereby contributing to the development of environmentally acceptable, technically feasible, and economically sustainable solutions in the field of water protection.

MATERIALS AND METHODS

For the modification and application in the process of decolorization of model dyed waters, waste volcanic ash collected from the foothills of the active volcano Etna, Italy, was used. Models for wastewater, after dyeing, were prepared using the direct dye designated as C.I. Direct Green 26. The commercial name is Solophenyl Green BLE, from the company Huntsman, Germany. The molecular formula of the dye is $C_{50}H_{33}N_{12}Na_5O_{18}S_4$ (Fig. 1), with a molar mass of 1,333.08 g/mol. The dye fastness ratings are 6 for light, 4 for perspiration, and 4 for washing, according to the relevant ISO standards.

Figure 1. Structural formula of the direct green dye C.I. Direct Green 26

Preparation of the active agent from volcanic ash was carried out as follows: Collected waste volcanic ash (precursor) was washed in hot distilled water (60 °C, 30 min), then dried and treated with 5% sulfuric acid for 48 hours (bath ratio 1:100) at room temperature (18–20 °C), with occasional stirring. The resulting product was rinsed with distilled water until a neutral pH of 7 was reached. After drying (100 °C), the obtained active agent was manually ground. The material prepared in this way was used in experiments for the adsorption of direct green dye from aqueous solution.

In a reaction vessel (200 cm³), the adsorbent (active agent – volcanic ash) was suspended in a solution of direct green dye (adsorbate). The vessel was placed on a shaker with orbital motion (125 min $^{-1}$) at 20 °C and kept for a defined time. The amount of active agent was always 2 g, while the green dye solution was maintained at a constant volume of 50 cm³ with concentrations of 10, 20, 30, 40, 50, and 60 mg·dm $^{-3}$. The treatment time, with continuous shaking, was 5, 10, 15, 30, 40, 50, and 60 minutes. All experiments were performed at a solution pH of 3, adjusted using a diluted aqueous solution of $\rm H_2SO_4$.



It was determined that the equilibrium adsorption time of the dye on the active agent was achieved after 60 minutes, after which no significant change in adsorption was observed. After the adsorption process was completed, the absorbance of the solution was measured using a spectrophotometer, Varian Cary 100 UV-Vis Spectrophotometer (at 680 nm). The obtained values were used to construct a calibration curve: absorbance vs. dye concentration, from which the unknown dye concentrations during and after adsorption were calculated.

The efficiency of dye removal, or the degree of dye exhaustion from the solution, was defined by the expression [7]:

Degree of exhaustion =
$$\frac{(C_O - C_e) \cdot V}{W}$$
 (1)

Where: C_O and C are the initial and final dye concentrations in the solution (mg/dm³), w – mass of adsorbent (g), and V – volume of solution for adsorption (dm³), respectively. The amount of dye (adsorbate) adsorbed per unit mass of adsorbent was determined by the expression [7]:

$$q_e = \frac{(C_0 - C_e) \cdot V}{W} \tag{2}$$

Where: C_O - is the initial adsorbate concentration (mg/dm³), C_e - is the equilibrium adsorbate concentration after adsorption (mg/dm³), w - is the mass of the adsorbent (g), and V - is the volume of the adsorption solution (dm³), q_e – adsorption capacity at equilibrium (mg/g or mmol/g).

RESULTS AND DISCUSSION

To describe the process of adsorption of the direct dye onto the volcanic ash adsorbent, it is important to emphasize that direct dyes in aqueous solution exhibit a pronounced anionic character. In order to achieve effective adsorption, it is necessary to reduce or eliminate the negative charge on the surface of the adsorbent, thereby enhancing its ability to bind anionic dye molecules. In the dyeing solution, the dye can be present in various forms—such as individual molecules, micelles, aggregates, or solid particles—with smaller forms, like molecules and micelles, being much more easily adsorbed onto the surface of the active agent.

During the preparation process of the adsorbent, a mass loss of 15–25% was recorded after washing the raw ash, while the yield of the active agent after chemical modification with acid was 60–70%.

The analysis of the pH effect showed that the maximum efficiency of dye removal was achieved at a pH value of 3. Under these conditions, protonation of the acidic sites on the adsorbent occurs, making its surface positively charged and allowing strong electrostatic binding with the anionic sulfo-groups of the dye. In neutral and alkaline media, deprotonation of these sites takes place along with an increased presence of OH⁻ ions, which reduces the number of available active sites and significantly decreases the adsorption efficiency. These results are in agreement with earlier studies on similar materials, which confirm the key role of pH in adsorption processes [13,14].



The analysis of the effect of contact time (Figures 2–4) showed that the dye was adsorbed more rapidly in the later stage of the experiment, especially after 30 minutes, until reaching equilibrium concentration after 60 minutes. The efficiency of adsorption depends on several factors, including solution temperature, pH value, degree of mechanical stirring, and the diffusion rate of the dye molecules. For example, an increase in temperature can accelerate diffusion but may simultaneously reduce the final degree of exhaustion due to weaker binding. In the initial phase of the process, the mass transfer rate is limited by the thickness of the boundary layer around the adsorbent particles, while increasing the stirring speed reduces this resistance and accelerates dye transfer. Once a critical speed is reached, further increases in stirring no longer have a significant impact, as the process then becomes limited by the rate of diffusion of dye molecules into the internal pores of the adsorbent.

Figure 2 shows the dependence of the amount of adsorbed dye (q_t) on contact time using 2 g of adsorbent at a temperature of 20 °C. As expected, the amount of bound dye increases with prolonged contact time.

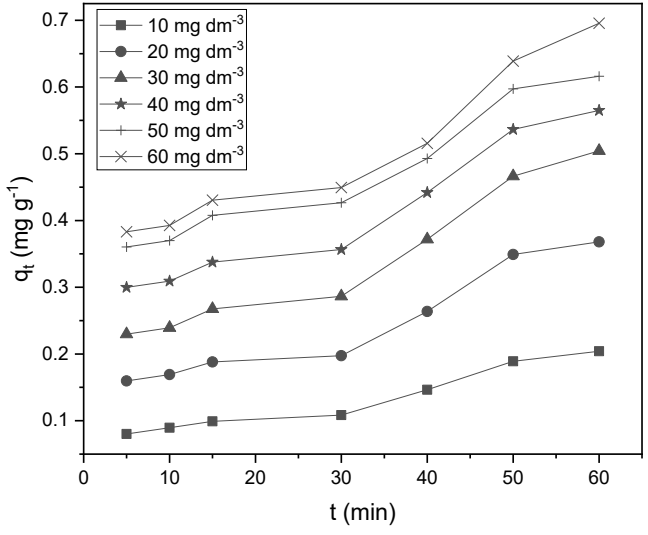


Figure 2. Change in the amount of direct green dye during adsorption

Figure 3 shows the degree of dye exhaustion, which increases over time and is particularly pronounced for solutions with lower initial dye concentrations. After 30 minutes, a sharp rise in exhaustion is evident, which is explained by the onset of dye absorption into the interior of the particles after accumulation on the surface of the volcanic ash-based adsorbent.



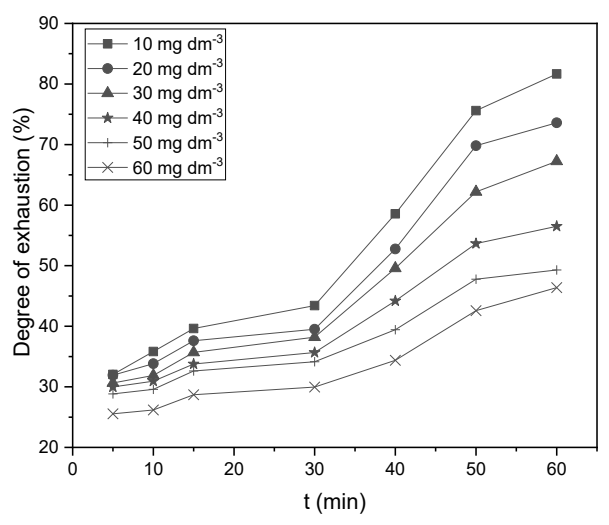


Figure 3. Change in the degree of exhaustion of direct green dye during adsorption

Figure 4 shows the change in the initial dye concentration (C_0) in the solution over time, where a clear, continuous, and monotonic decrease in dye concentration is observed during adsorption, indicating effective and uniform dye removal.

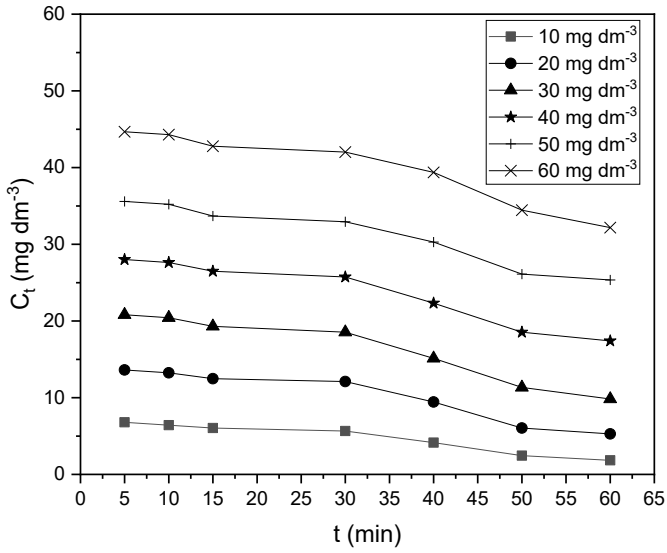


Figure 4. Change in the initial concentration of direct green dye during adsorption



The investigation of the effect of the initial dye concentration (Figures 5 and 6) was carried out in the concentration range from 10 to 60 mg/dm³. According to the results, with an increase in the initial dye concentration, the relative degree of exhaustion decreases in all cases, while the absolute amount of dye adsorbed per unit mass of adsorbent (q_t) increases and reaches a maximum at 60 minutes. The initial dye concentration in the solution represents an important driving force that enables overcoming the mass transfer resistance between the aqueous and solid phases. Although the initial dye concentration does not significantly affect the time required to reach equilibrium, it substantially determines the mass transfer rate, as a higher concentration gradient ensures a more intense transport of molecules toward the adsorbent surface.

It is important to emphasize that at first glance, dye exhaustion appears highest at lower initial concentrations, which is an apparent effect. More detailed calculations show that the actual amount of dye adsorbed, expressed in mg/g, is greatest at the highest initial concentrations, while q_t values are the lowest for solutions with the smallest C_θ .

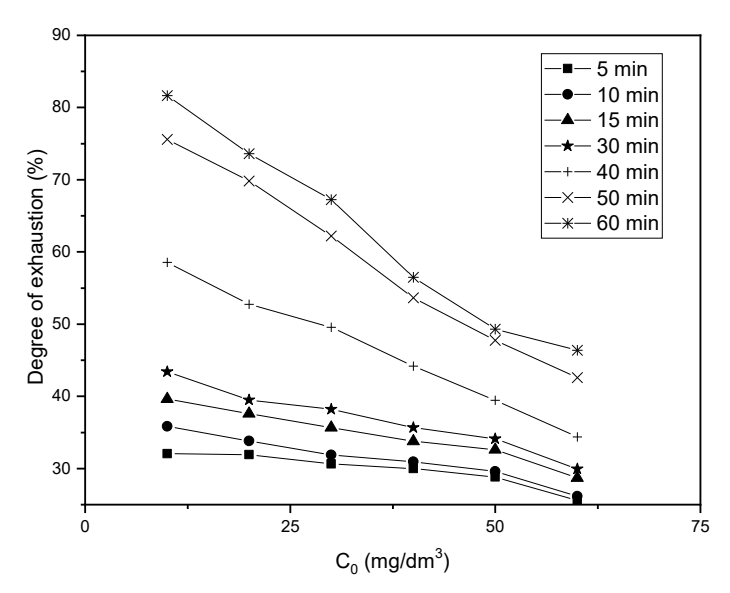


Figure 5. Degree of removal of direct green dye during adsorption as a function of initial dye concentration



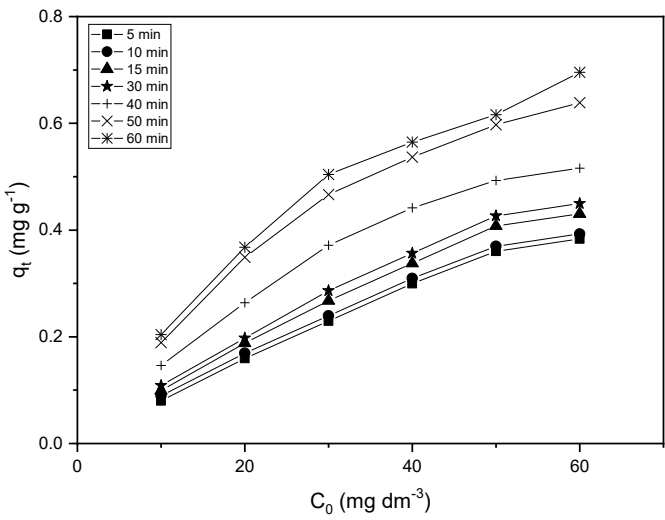


Figure 6. Amount of adsorbed direct green dye during adsorption as a function of initial dye concentration

In general, the results indicate that the adsorption mechanism involves multiple stages: initial diffusion of molecules through the solution, transfer across the boundary layer, adsorption on the surface of the adsorbent, and penetration into the internal pores. The key contribution to dye removal comes from physicochemical interactions, including ionic bonds, hydrogen bonds, and Van der Waals forces. When the obtained data are compared with literature results for other natural and synthetic adsorbents [11], the modified volcanic ash demonstrates competitive performance, with an adsorption capacity of 7 mg/g and a dye removal efficiency exceeding 82% under optimal conditions. These results confirm that natural waste materials, with appropriate chemical modification, can provide sustainable and economically viable solutions for wastewater treatment, contributing to environmental protection and the implementation of circular economy principles.

CONCLUSION

The study on the application of modified volcanic ash as an adsorbent for the removal of the direct dye C.I. Direct Green 26 from aqueous solutions showed that this natural waste material, after chemical modification, can be effectively used for the treatment of textile industry wastewater. The experimental results clearly demonstrated that the adsorption process is significantly influenced by pH value, contact time, and initial dye concentration.

The maximum adsorption capacity was 7 mg/g, while the dye removal efficiency exceeded 82%, placing modified volcanic ash among competitive adsorbents compared to more expensive commercial materials. Analysis of the process mechanism indicates a complex multi-phase course, involving surface adsorption and internal diffusion, with



dominant roles played by physicochemical interactions, including ionic bonds and electrostatic forces.

These findings confirm that modified volcanic ash represents a sustainable, cost-effective, and environmentally friendly solution for dye removal from wastewater, with the additional benefit of incorporating the recycling of a natural waste material. Further research should focus on investigating the regenerative potential of the adsorbent, process scaling, and testing under real industrial conditions to confirm its applicability in large-scale wastewater treatment systems.

Acknowledgment

The authors express their gratitude to the Academy of Technical and Art Applied Studies Belgrade for the support provided, which contributed to the realization of this research.

References

- [1] Robinson T., McMullan G., Marchant R., Nigam P. Remediation of dyes in textile effluent: a critical review on current treatment technologies with a proposed alternative. Bioresource Technology. 2001, 77(3), 247–255. https://doi.org/10.1016/S0960-8524(00)00080-8
- [2] Crini G. Non-conventional low-cost adsorbents for dye removal: a review. Bioresource Technology. 2006, 97(9), 1061–1085. https://doi.org/10.1016/j.biortech.2005.05.001
- [3] Forgacs E., Cserháti T., Oros G. Removal of synthetic dyes from wastewaters: a review. Environment International. 2004, 30(7), 953–971. https://doi.org/10.1016/j.envint.2004.02.001
- [4] Yıldız, M., & Başaran, B. (2024). Sustainable cationic cotton with keratin hydrolysate. Fibers and Polymers, 25, 403–411. https://doi.org/10.1007/s12221-024-00626-0
- [5] Allen S. J., Koumanova B. Decolourisation of water/wastewater using adsorption. Journal of the University of Chemical Technology and Metallurgy. 2005, 40(3), 175–192. https://dl.uctm.edu/journal/node/j2005-3.html
- [6] Gupta V. K., Suhas. Application of low-cost adsorbents for dye removal: a review. Journal of Environmental Management. 2009, 90(8), 2313–2342. https://doi.org/10.1016/j.jenvman.2008.11.017
- [7] R. Saadi, Z. Saadi, R. Fazaeli, N. E. Fard, Monolayer and multilayer adsorption isotherm models for sorption from aqueous media, Korean J. Chem. Eng., 32(5), 787-799 (2015).
- [8] Yaseen, D. A., & Scholz, M. (2019). Textile dye wastewater characteristics and constituents of synthetic effluents: a critical review. *International Journal of Environmental Science and Technology*, 16(2), 1193–1226. https://doi.org/10.1007/s13762-018-2130-z
- [9] Crini, G., & Lichtfouse, E. (2019). Advantages and disadvantages of techniques used for wastewater treatment. *Environmental Chemistry Letters*, 17(1), 145–155. https://doi.org/10.1007/s10311-018-0785-9



- [10] Shikuku, V. O., Tome, S., Hermann, D. T., & Tompsett, G. A. (2022). Rapid adsorption of cationic methylene blue dye onto volcanic ash—metakaolin based geopolymers. *Silicon*, 14, 9349–9359. https://doi.org/10.1007/s12633-021-01637-9
- [11] Prajaputra, V., Abidin, Z., & Widiatmaka. (2019). Methylene Blue Removal Using Developed Material From Volcanic Ash Soils. *International Journal of Scientific & Technology Research*, 8(7), 706–710.
- [12] Etana, R., Angassa, K., & Getu, T. (2025). Dye removal from textile wastewater using scoria-based vertical subsurface flow constructed wetland system. *Scientific Reports*, 15, Article 949.
- [13] Lim, S., Kim, J. H., Park, H., Kwak, C., Yang, J., Kim, J., Ryu, S. Y., & Lee, J. (2021). Role of electrostatic interactions in the adsorption of dye molecules by Ti₃C₂-MXenes. *RSC Advances*, 11(12), 7060–7070. https://doi.org/10.1039/D0RA10876F
- [14] Vojnović, B., Cetina, M., Franjković, P., & Sutlović, A. (2022). Influence of Initial pH Value on the Adsorption of Reactive Black 5 Dye on Powdered Activated Carbon: Kinetics, Mechanisms, and Thermodynamics. *Molecules*, 27(4), 1349. https://doi.org/10.3390/molecules27041349

Izvod

DEKOLORIZACIJA VODENOG RASTVORA TEKSTILNE BOJE POMOĆU ADSORBENTA NA BAZI VULKANSKOG PEPELA

Jelena Jovićević Pavković D, Dragan Đorđević D Univerzitet u Nišu, Tehnološki fakultet, Leskovac, Srbija

Ovaj rad istražuje mogućnosti primene modifikovanog vulkanskog pepela kao adsorbenta za uklanjanje tekstilne direktne boje iz otpadnih voda. Cilj istraživanja bio je optimizacija procesa dekolorizacije modelnih voda korišćenjem vulkanskog pepela prethodno modifikovanog fizičkim i hemijskim tretmanima. Razmatrane su različite varijante parametara, uključujući pH vrednost, početnu koncentraciju boje, vreme kontakta, temperaturu i količinu adsorbenta. Najefikasniji stepen adsorpcije postignut je pri pH vrednosti od 3, dok se maksimalna efikasnost u uklanjanju boje postiže nakon 60 minuta tretmana. Maksimalni kapacitet adsorpcije iznosio je 7 mg/g, dok je stepen uklanjanja boje premašio 82%, što modifikovani vulkanski pepeo svrstava među konkurentne adsorbente. U zaključku, modifikovani vulkanski pepeo predstavlja jeftin i efikasan materijal za dekolorizaciju vodenih rastvora tekstilne direktne boje, sa potencijalnom primenom u industrijskim uslovima za obradu obojenih otpadnih voda tekstilne industrije.

Ključne reči: vulkanski pepeo, adsorpcija, dekolorizacija, tekstilna direktna boja, otpadna voda.



UDK 687.254.8 : 677.074.16 : 677.1/.5 DOI: 10.46793/NovelTDS16.153T

DOI: 10.46793/NOVELLDS 16.1531

COMPRESSIBLE PROPERTIES OF MEN'S SOCKS MADE FROM DIFFERENT FIBERS IN PLAIN JERSEY

Predrag Tasić^{1,*} D, Dušan Trajković² D, Nenad Ćirković² D, Jelka Geršak³ D

1V.I. "Vunil", d.o.o., Leskovac, Serbia

2University of Nis, Faculty of Technology in Leskovac, Serbia

3University of Maribor, Faculty of Mechanical Engineering, Slovenia

This paper examines the most important compressible properties of socks made from different fibers in a plain jersey. These properties indirectly affect the parameters of thermo-physiological comfort of socks during wear. Three yarns were used in the sock composition; the first, a dominant yarn made from six different fibers, makes up 77%. The other two yarns are made from nylon and wrapped elastic threads, accounting for 23%. The most compressible sock is made from cotton yarn, with the modal yarn sock model being very close in performance. The highest linearity of compression, compression energy, and compression resistance are found in socks made from bamboo and modal yarns, with viscose yarn socks not falling far behind. Bamboo yarn socks exhibit weaker elastic recovery compared to socks made from cotton-compact yarn, which have better elastic characteristics. Out of the six combinations of raw material compositions for socks and the examination of several compression properties, sock models in plain jersey can be selected for specific purposes, such as medical, home, or outdoor use.

Keywords: men's socks, plain jersey, fibers, compressibility.

INTRODUCTION

Compressibility is a property of a material that describes its ability to change volume under the influence of pressure. In physics and engineering, compressibility is quantitatively expressed as the relative change in the material's volume per unit change in pressure [1].

Understanding the compressibility of materials is crucial for accurately modeling and predicting their behavior under different pressure conditions, which is essential in the design and analysis of engineering systems [2].

* Author address: Predrag Tasić, V.I. "Vunil", d.o.o., Viljema Pušmana 19, 16000, Leskovac, Serbia e-mail address: tasic.predrag1970@gmail.com



The compressibility of textiles refers to the ability of textile materials to reduce their volume under the influence of external pressure and return to their original state once the pressure is removed. Compressibility depends on several factors that determine how the textile will behave under pressure: the type of fibers, the weave or knit structure, material density, thickness, treatments and finishes, elasticity, and others [3, 4].

The compressibility of socks refers to the ability of the material from which the socks are made to compress or adjust under pressure. This property is crucial for the functionality of certain types of socks, particularly compression socks, which play a medical and preventive role [5].

Socks made from elastic fibers, such as spandex, elastane, and nylon, have a greater compression capability. The combination of these materials allows for even expansion and return to their original shape, which is crucial for the proper application of pressure. Thinner socks generally have lower compressibility and provide lighter pressure. Thicker materials offer stronger compression but may be less comfortable to wear over longer periods [6].

Quality socks have high resistance to permanent deformation, meaning they return to their original shape and retain their properties over time. Medical socks have high compressibility and precisely defined pressure levels to provide a therapeutic effect. Sports socks focus on muscle support and reducing fatigue, with slightly lower compressibility. Fashion socks usually have a lower degree of compressibility as they are primarily aesthetic [7].

This paper explores the most important compressible properties of men's socks in plain jersey made from different yarns to determine which raw material composition of socks is best suited to providing adequate comfort during wear.

MATERIALS AND METHODS

For the research and production of men's short socks, yarns made from fibers such as bamboo, modal, viscose, cotton, cotton-compact, and a cotton/PES blend, 60/40%, (77% dominant yarn) from the company Bimtex (Serbia), polyamide yarn (22% participation), and rubber thread (1% participation) from the company Dunav Grocka (Serbia) were used. Based on the given knitting parameters, all socks were knitted at the local company Nikoplet in Leskovac. The socks were made in plain jersey in size 11 (42-43).

The examination of sock characteristics was conducted according to the relevant standards and methods:

- Thickness, according to the EN ISO 5084 standard.
- Surface mass, according to the EN 12127 standard.
- Volumetric mass was calculated based on the research paper [8].
- Porosity was calculated based on the research paper [9].
- The compressibility properties of knitted fabrics under low loads were tested on the KES-FB system (Kato Technical Co. Ltd., Japan). The testing conditions for the compressive characteristics of the knitted fabrics involved lateral compression of a 2 cm² surface tube at a speed of 50 s·mm⁻¹ within a compression range of 0.5 cN·cm⁻² to 50 cN·cm⁻² [12, 13].



Table 1 presents the results of the structural parameters of size 11 socks in plain jersey. The thickness of the socks depends on the type of dominant yarn used. Since the socks are made from yarns with similar properties, significant differences in knitting thickness arise due to differences in the raw material composition. For socks in plain jersey, cotton and modal socks, as the dominant yarn, have the greatest thickness.

The surface mass of the socks varies depending on the type of dominant yarn in the structure. Socks knitted from bamboo-dominant yarn have the highest numerical value for surface mass. This parameter combines essential structural parameters and is an important economic factor [10].

The volumetric mass of the sock best reflects and defines the structural parameters of the sock, as it represents the mass of the knit of a certain volume, which is directly related to the thickness, type of knit, and surface mass of the knitted fabric. Volumetric mass generally follows the surface mass and is the highest in cases where the surface mass is also the highest [10].

Compactness - porosity of the knitted fabric represents the fill of the empty space between the loops or the empty space within the loop itself. Good porosity is a result of the structure of knitted products, as the yarn in the loops is arranged in a way that allows a large amount of air to be present between the loops [11]. Generally, socks made from cotton-dominant yarn have the highest percentage of porosity. Porosity depends on thickness, with thinner socks usually having lower porosity and vice versa.

Table 1. Key parameters of men's socks with different raw material compositions in plain jersey

| Raw Material Composition of | | Thickness | | Volumetric Mass | Porosity | |
|------------------------------|--------------|-----------|----------------------|-----------------|----------|--|
| Soc | ks | (mm) | (g⋅m ⁻²) | (g·cm⁻³) | (%) | |
| Bamboo (BB), | 30 tex | | | | | |
| PA 6.6, | 4.4/13×2 tex | 0.918 | 282.9 | 0.3082 | 79.7 | |
| Wrapped Rubber Ya | arn, 100 tex | | | | | |
| Modal (MD), | 30 tex | | | | | |
| PA 6.6, | | 0.928 | 279.1 | 0.3007 | 80.2 | |
| Wrapped Rubber Ya | , | | | | | |
| Viscose (CV), | | | | | | |
| PA 6.6, | 4.4/13×2 tex | 0.911 | 281.4 | 0.3089 | 79.7 | |
| Wrapped Rubber Ya | , | | | | | |
| Cotton (CO), | 30 tex | | | | | |
| PA 6.6, | | 0.949 | 274.9 | 0.3003 | 80.6 | |
| Wrapped Rubber Ya | | | | | | |
| Cotton-compact (CC | ,, | | | | | |
| PA 6.6, | | 0.892 | 275.6 | 0.3202 | 79.3 | |
| Wrapped Rubber Yarn, 100 tex | | | | | | |
| Cotton/Polyester (Co | ,, | | | | | |
| PA 6.6, | | 0.893 | 267.4 | 0.2995 | 79.8 | |
| Wrapped Rubber Ya | arn, 100 tex | | | | | |

The relationship between thickness and compressive load is expressed by the following equation [14]:

$$h = \frac{k}{\sqrt[3]{F_k}} \tag{1}$$

where:

h – thickness of the knitted fabric (mm), k – proportionality constant,

F_k – compressive or surface force per unit area (cN).



The compressibility of knitted fabrics is calculated using the formula [14]:

$$C = \frac{h_0 - h_m}{h_0} \cdot 100 \tag{2}$$

where:

ho - knitted fabric thickness under compressive load of 0.49 cN·cm⁻² (mm),

h_m – knitted fabric thickness under compressive load of 49.035 cN·cm⁻² (mm).

The deformation work, Wc, represents the energy required for the compressive deformation of the knitted structure and is calculated using the formula [11]:

$$c = \int_{h_m}^{h_0} F_k \Delta h \tag{3}$$

where:

Wc – deformation or compressive work per unit area of 1 cm² of the sample (cN⋅cm),

 F_k – compressive force per unit area (cN),

 Δh – change in the thickness of the knitted structure (mm),

h₀ – thickness under compressive load of 0.49 cN·cm⁻² (mm),

h_m - thickness under compressive load of 49.035 cN·cm⁻² (mm).

3The linearity of the curve, LC, of compressive load and deformation F_k is calculated using the formula [15,16]:

$$LC = \frac{Wc}{Woc}$$
 (4)

where:

WOC - deformation work in the case of linear deformation (cN·cm),

WC (J·m⁻²) - compression energy.

The relaxation ability, RC, expresses the ratio between reversible and deformation energy under compressive load, and is calculated using the formula [15,16]:

$$RC = \frac{wc'}{wc} 100 \tag{5}$$

where:

RC – relaxation ability (%),

WC' – recoverable or reversible energy per unit area (cN·cm).

RESULTS AND DISCUSSION

The results presented in Table 2 provide various values of important compressibility parameters for socks made from different fiber compositions in plain jersey. The softest (most compressible) sock is made from cotton-dominant yarn, very close to the model of socks made from modal-dominant yarn (according to the results for parameter C). The parameter C (%), on the other hand, represents the percentage comparison of the initial thickness measurement with the measurement at maximum applied force; a higher value indicates greater compressibility (softness).

The socks made from bamboo and modal-dominant yarn exhibit the highest linearity of compression, compression energy, and resistance to compression. For the LC parameter, values closer to one indicate firmer (stiffer) compressibility, while lower values provide higher stretchability in the initial stage of stress, which enhances comfort



during wear. A higher value of the WC parameter corresponds to greater compressibility, meaning the textile product becomes softer and more comfortable. It should be noted that the resistance to compression, RC, represents the percentage of recovery or return to the original thickness once the compressive force is removed; a higher value indicates greater recovery from compression, or in other words, assesses the sponge-like behavior of the knit. The greater the stretchability of the knit, the better the quality in terms of the tactile feel of the knit, meaning a higher RC value results in greater comfort during wear, as well as a fuller and smoother sensation of the textile product.

Greater work or compression energy means a lower ability for elastic recovery of the socks. The highest work or compression energy of the "softest" cotton knit (C=41.78%) indicates that it exhibited the least ability for elastic recovery (RC=42.62%). In contrast, ithe lowest compressibility was observed in socks made from cotton-compact dominant yarn (C=35.16%), which is partly compensated by the highest elastic recovery (RC=47.36%).

When examining the sock models made from cotton and cotton-compact, it is noticeable that due to the lower fuzziness of the yarn in the cotton-compact sock model, the outer layers of the knit are poorer in fibers, which contributed to its lower compressibility. Specifically, compared to traditional cotton spinning, the production of cotton-compact yarn involves an additional phase in which protruding fibers are drawn into the yarn body with the help of air, resulting in a more compact structure of the cotton yarn, which is less fuzzy compared to the yarn produced through traditional spinning.

Plain jersey, regardless of the type of fibers in the dominant yarn, has a low LC value (Table 2), indicating a less linear compression characteristic of these socks. This implies that, due to the appropriate construction of the knit and the absence of surface fibers, the fibers in the inner layer of the knit tend to slide under the influence of compressive forces, which contributes to a reduction in the relative compressibility of the knit.

The elasticity of the fibers did not significantly affect the compression capability of the socks. Specifically, the less elastic fibers of the cotton-dominant yarn generally exhibit the highest compressibility in socks. The thickness of the socks under different pressures varies according to the raw material composition of the dominant yarn. The greatest thickness is found in socks made from cotton-dominant yarn at both pressure levels.

Table 2. Compression properties results of men's socks in plain iersev

| Dominant yarn | C (%) | LC | WC (J·m⁻²) | RC (%) | Knitted fabric thickness (×10 ⁻³ m) | Knitted fabric thickness (×10 ⁻³ m) |
|------------------|----------|------|---------------|-----------|---|--|
| BB | 36.15 | 0.52 | 0.59 | 47.77 | 1.30 | 0.83 |
| MD | 40.29 | 0.46 | 0.61 | 40.81 | 1.39 | 0.83 |
| CV | 36.72 | 0.40 | 0.46 | 45.00 | 1.28 | 0.81 |
| CO | 41.78 | 0.39 | 0.56 | 42.62 | 1.46 | 0.85 |
| COc | 35.16 | 0.36 | 0.39 | 47.36 | 1.28 | 0.83 |
| CO/PES | 38.17 | 0.35 | 0.43 | 42.85 | 1.31 | 0.81 |

The surface properties of the yarn could also be involved or have an impact as a potential factor in the compression of the knitted fabric, although there is no absolute certainty.



Fibers protruding from the surface of the socks, along with a larger amount of air, form practically two outer layers that are quite susceptible to compression. In other words, it can be expected that the knitted fabric with more pronounced fuzziness on the surface will be softer, i.e., it will exhibit greater compressibility, which is confirmed in the case of the cotton-dominant yarn sock model. This establishes a direct link between the fuzziness of the yarn and the softness (compressibility) of the socks used in the models. The compression curves, derived from recorded changes in the thickness of the knitted fabrics during loading and unloading, shown in Figures 1-3, provide a more detailed insight into the phenomenon of lateral compression. These curves show a nonlinear relationship between the change in knitted fabric thickness and the increase in compressive load, except in the initial phase of the compression cycle. In this part, at lower load values, the thickness of the knitted fabric changes linearly with the load, corresponding to elastic deformation. With further increase in compressive load, the compressibility of the socks decreases, which can be explained by their structure. The third phase of compression, in which there is minimal change in knitted fabric thickness with an increase in compressive load, involves the lateral compression of the fibers themselves. It has been determined that the parts of each region, as well as the slopes of the linear regions, vary depending on the knitted construction and the varn structure of the socks.

Although the facilitated sliding and shifting of fibers during compression contribute to the compressibility of the material, which is important for the feeling of softness and comfort, it should be noted that these processes are partially irreversible. The hysteresis that occurs in knitted fabrics indicates the presence of permanent deformation during the compression of socks (Figures 1–3). Since the ability of the material to elastically recover is inversely proportional to the area of the hysteresis loop, a smaller hysteresis area indicates better elastic recovery of the socks.

The differences in the slope of the compression curves of the tested sock models confirm the assumptions about the impact of surface geometry and the fiber composition of the knitted fabrics. Although the results of compression tests at low loads indicated differences in the behavior of socks made from different dominant yarns, it was found that the surface properties of different yarns significantly affect the compression properties of socks, including both their compression capability and the material's elastic recovery ability.

In comparison of sock models in plain jersey with different fiber compositions (Figures 1–3), a similarity in the appearance of the compression and decompression curves can be observed. For example, in socks made from BB yarn as the dominant material, the thickness during compression varies from 1.4 mm, while during decompression, it decreases to 1.1 mm. In contrast, socks made from COc yarn have a thickness range from 1.25 mm to 1.05 mm. A greater difference between the starting and final points of the hysteresis loop results in a larger loop area. Since the elastic recovery ability of the knitted fabric is inversely proportional to the area of the hysteresis loop, socks made from BB yarn exhibit weaker elastic recovery compared to socks made from COc yarn, which show better elastic characteristics.



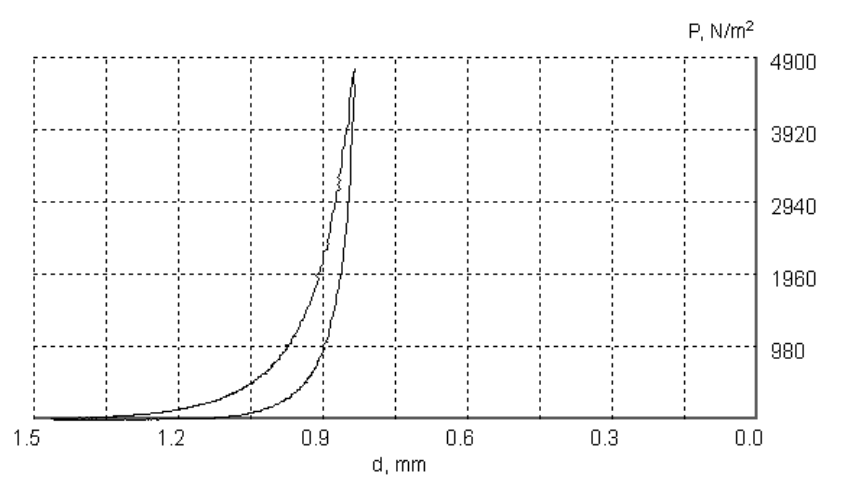


Figure 1. Pressure/Thickness diagram for bamboo men's socks

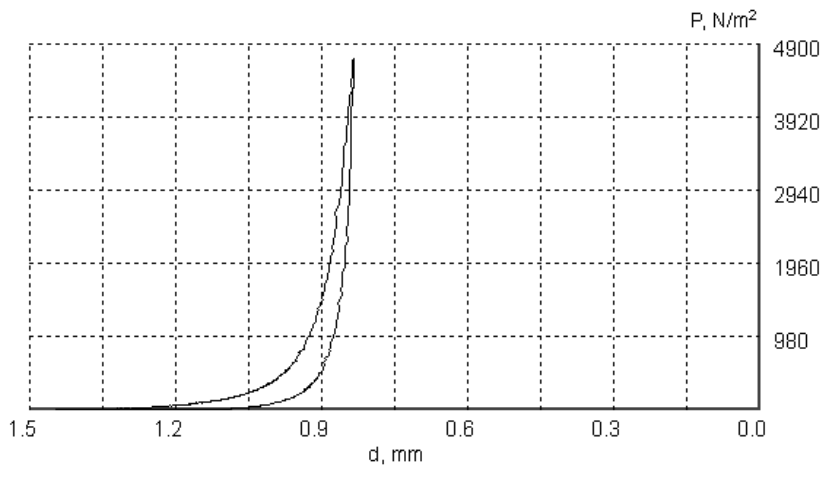


Figure 2. Pressure/Thickness diagram for cotton-compact men's socks



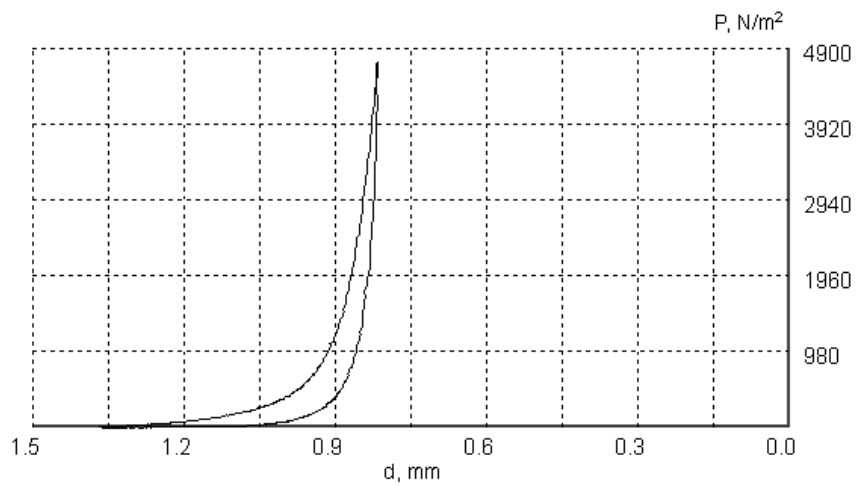


Figure 3. Pressure/Thickness diagram for CO/PES men's socks

CONCLUSION

This paper discusses the most important compressible properties of men's socks knitted in plain jersey, made from six different fibers in three yarns used .

The sensation a textile material leaves in contact with the skin can vary depending on various parameters, such as the physiological state of the body, climatic conditions, moisture content in the material, the surface area, or the intensity of the contact between the material and the skin. Testing the compressive behavior of the material under low loads provides an opportunity to assess functionality, feel, etc., in relation to comfort.

The most compressible sock is made from yarn with a cotton dominance, while the sock made from modal-dominant yarn is very similar in this property. Socks made from bamboo and modal-dominant yarns exhibit the greatest linearity of compression, as well as the highest energy and resistance to compression. Greater compression energy indicates a reduced ability for elastic recovery of the socks. The "softest" cotton socks have the weakest ability to return to their original shape. In contrast, socks made from cotton-compact dominant yarn, although the least compressible, compensate for this with the highest elastic recovery ability.

Based on six different combinations of fiber compositions and the analysis of several compressive properties, the most suitable material combination for plain-jersey socks was chosen, in accordance with their specific purpose: for recreation, medical needs, home use, or for outdoor wear.

Acknowledgement:

Project BG16RFPR002-1.014-0005-Competence Centre "Smart Mechatronic, Eco and Energy-Saving Systems and Technologies", Technical University-Gabrovo, Bulgaria.



The project was financed by the Ministry of Science, Technological Development and Innovation of the Republic of Serbia (ev.No. 451-03-137/2025-03/ 200133)

References

- [1] Çengel YA, Boles MA, Kanoglu M. *Thermodynamics, An Engineering Approach*. McGraw-Hill, United Kindom, 2023.
- [2] White F. Fluid Mechanics. McGraw Hill, United Kindom, 2015.
- [3] Nawab Y. *Textile Engineering: An Introduction*. De Gruyter Textbook, Germany, 2016. https://doi.org/10.1515/9783110413267
- [4] Muthu SS. *Textiles and Clothing Sustainability*. Springer Singapore, 2017. https://doi.org/10.1007/978-981-10-2131-2,
- [5] Roshan S. *Textiles for Sportswear*. Woodhead Publishing, United Kingdom, 2015. https://doi.org/10.1016/C2013-0-16491-4
- [6] Pan N, Sun G. Functional Textiles for Improved Performance, Protection and Health. Woodhead Publishing Series in Textiles, United Kingdom, 2011.
- [7] Vink P. Comfort and Design, Principles and Good Practice, CRC Press, Boca Raton, 2004. https://doi.org/10.1201/9781420038132
- [8] Elmogahzy Y. Engineering Textiles: Integrating the Design and Manufacture of Textile Products. Woodhead Publishing, United Kingdom, 2019.
- [9] Khalila A, Eldeeb M, Těšinova P, Fouda A. Theoretical Porosity of Elastic Single Jersey Knitted Fabric Based on 3D Geometrical Model of Stitch Overlapping, Journal of Natural Fibers. 2023, 20, 1, 2181274. https://doi.org/10.1080/15440478.2023.2181274.
- [10] Trajković DS, Tasić PS, Stepanović JM, Šarac TI, Radmanovac NM. Physiological Characteristics of the Socks Made from Bamboo and Conventional Fibers. Advanced technologies. 2014, 3(1) 59-65. https://doi.org/10.5937/savteh1401059T
- [11] Asanovic KA, Kostic MM, Mihailovic TV, Cerovic DD. *Compression and strength behaviour of viscose/polypropylene nonwoven fabrics*. Indian Journal of Fibre & Textile Research. 2019, 44, 329-337.
- [12] Stankovic SB, Bizjak M. Effect of Yarn Folding on Comfort Properties of Hemp Knitted Fabrics. Clothing and Textiles Research Journal. 2014, 32(3) 202-214. https://doi.org/10.1177/0887302X14537114
- [13] Geršak J. *Objektivno vrednovanje plošnih tekstilija i odjeće*. Sveučilište u Zagrebu, Tekstilno-tehnološki fakultet, Zagreb, 2014.
- [14] Stojanović S, Geršak J, Trajković D. *Compression properties of knitted fabrics printed by sublimation transfer printing technique*. Advanced technologies. 2021, 10(1) 46-53. https://doi.org/10.5937/savteh2101046S
- [15] Murthyguru, *Novel Approach To Study Compression Properties In Textiles*. Autex Research Journal. 2005, 5(4) 176-193. https://doi.org/10.1515/aut-2005-050401
- [16] Gurumurthy B.R. *Prediction of Fabric Compressive Properties Using Artificial Neural Networks*. Autex Research Journal. 2007, 7, 1, 19-31. https://doi.org/10.1515/aut-2007-070103



KOMPRESIBILNA SVOJSTVA MUŠKIH ČARAPA OD RAZLIČITIH VLAKANA U GLAT PREPLETAJU

Predrag Tasić¹ <u>ID</u>, Dušan Trajković² <u>ID</u>, Nenad Ćirković² <u>ID</u>, Jelka Geršak³ <u>ID</u>

¹ V.I."Vunil", d.o.o., Leskovac, Srbija

² Univerzitet u Nišu, Tehnološki fakultet, Leskovac, Srbija

³ Univerzitet u Mariboru. Mašinski fakultet. Slovenija

U ovom radu razmatraju se najvažnija kompresibilna svojstva čarapa od različitih vlakana u glat prepletaju. Ova svojstva, posredno utiču na parametre termo-fiziološke udobnosti čarapa tokom nošenja. Korišćene su tri pređe u sastavu čarapa, prva, dominantna pređa izrađena od šest različitih vlakana čini 77%. Ostale dve pređe su od poliamida i obmotane gumene niti sa učešćem od 23%. Najkompresibilnija čarapa je izrađena od pamučne pređe, vrlo blizu je i model čarapa od modalne pređe. Najveću linearnost kompresije, energiju kompresije i otpornost na kompresiju imaju modeli čarapa od bambus i modalne pređe, ne zaostaje puno ni viskozna pređa. Čarape od bambus pređe pokazuju slabiji elastični oporavak u poređenju sa čarapama od pamukkompakt pređe, koje imaju bolje elastične karakteristike. Od šest kombinacija sirovinskog sastava za čarape i provere više kompresijskih svojstava, mogu se odabrati modeli čarapa u glat prepletaju za odgovarajuću namenu, na primer za medicinsku, kućnu ili izvan kućnu namenu.

Ključne reči: čarapa, glat prepletaj, vlakna, kompresibilnost.



UDK 687.254.8 : 677.545 : 677.02 DOI: 10.46793/NovelTDS16.163T

THERMAL, PHYSIOLOGICAL, AND THERMOGRAPHIC ANALYSIS OF MEN'S BAMBOO SOCKS IN A RIGHT-LEFT KNIT STRUCTURE

Predrag Tasić^{1,*} D, Dusan Trajković² D, Jovan Stepanović² D, Jelka Geršak³ D

1V.I. "Vunil", d.o.o., Leskovac, Serbia

2University of Nis, Faculty of Technology in Leskovac, Serbia

3University of Maribor, Faculty of Mechanical Engineering, Slovenia

The study utilizes the results of thermal and physiological methods, as well as thermographic imaging, to obtain information about the condition of bamboo socks on the foot. Bamboo socks in a right-left knit (plain knit) exhibit satisfactory physical properties, including thickness, bulk density, and porosity. The hydrophilic properties of bamboo socks are highly pronounced, as these fibers strongly absorb moisture and also have good air permeability. Thermal properties, according to the Thermo Lab II and Thermal Manikin methods, reveal that bamboo socks leave a cool sensation on the skin and have lower thermal resistance but higher thermal conductivity, making them recommended for wear on warmer days. According to the results of infrared radiation measurements, i.e., by comparing the measured temperature values on different parts of the foot, it is concluded that bamboo socks are more suitable for wearing during higher temperatures in closed footwear.

Keywords: thermo-physiology, thermography, men's socks, bamboo fibers, plain knit fabrics.

e-mail address: tasic.predrag1970@gmail.com



^{*} Author address: Predrag Tasić, V.I. "Vunil", d.o.o., Viljema Pušmana 19, 16000, Leskovac, Serbia

INTRODUCTION

When the human body is in motion, air movement occurs within the microclimate of the garment, both between layers of textile material and around the body. The volume of air spaces dynamically moves due to compression and decompression, caused by different body parts in relation to the clothing. When one part presses on the garment, the air spontaneously moves to another part of the microclimatic interspace, transferring heat via conduction from the body to the layers of clothing and exiting through an opening to the surrounding environment [1-3].

The foot, like the entire human body, is homeothermic, meaning it is capable of maintaining its internal temperature within certain physiological limits, regardless of the surrounding temperature. Foot thermoregulation is the process by which excess heat is lost, with thermoreceptors in the skin of the foot playing a vital role in these mechanisms. Several such mechanisms exist in the foot, such as blood flow, sweating, and metabolic heat production [4].

Internal body heat increases during physical activity, and as a result, the skin shows an increase in blood flow, sweating, and temperature, which are the main mechanisms for dissipating the heat produced. Since the feet remain covered by socks and shoes during physical activity, they are subjected to an increase in temperature. Different heat transfer mechanisms observed in the skin include conduction, convection, evaporation, and radiation. Socks can affect all of these mechanisms, especially if made from high-quality fibers, enabling better heat conduction from the feet to the socks, shoes, and surrounding environment through direct contact [5,6].

Bamboo socks are becoming an increasingly popular choice due to their exceptional characteristics and advantages compared to traditional cotton or synthetic socks. These socks are known for their hygroscopic properties, meaning their ability to absorb moisture efficiently. Bamboo fibers can absorb up to 60% more moisture than cotton, making these socks ideal for people with sweaty feet. Although they absorb moisture well, bamboo socks allow for quick evaporation of that moisture, keeping the feet dry and reducing the risk of unpleasant odors or infections. Thanks to the natural antimicrobial properties of bamboo, absorbed moisture does not promote bacterial growth, which further helps in reducing odors. Even after intense activities, the socks remain dry and comfortable to wear.

In the examination of thermal properties of clothing, infrared thermography can be used to determine heat losses from parts of the body to the surrounding environment. This technique has a very significant application in studying heat losses caused by vertical airflow through the microclimate between clothing and body parts, as well as in analyzing temperature changes on the textile surface when it comes into contact with the body part [7,8].

Thermography is a technique that uses a thermal camera to capture and analyze temperature differences on various surfaces that emit radiation. The camera detects the infrared radiation emitted by an object (body) and converts it into thermal images.

This research analyzes the results of thermal, physiological, and thermographic methods after testing bamboo socks, in order to obtain information about the thermophysiological state and comfort of wearing these socks.



MATERIALS AND METHODS

The study used short men's socks made from three yarns: bamboo (dominant yarn), PA 6.6 filament yarn, and rubber-wrapped yarn. The sock, made in size M, has a foot length of 28 cm, a sock leg length without the welt of 16 cm, and a welt width of 4 cm. These sock dimensions correspond to a shoe size of 42-43. The sock, made in size L, has a foot length of 29 cm, a sock leg length without the welt of 17 cm, and a welt width of 4 cm. These sock dimensions correspond to a shoe size of 43-44.

The examination of the sock characteristics was performed according to the appropriate standards and methods:

- Thickness, according to standard EN ISO 5084.
- Horizontal and vertical density, according to standard DIN 53883.
- Loop length, according to standard EN 14970.
- Surface mass, according to standard EN 12127.
- Total loop density is the product of the horizontal and vertical density of the knitted fabrics.
- Bulk density of the knitted fabric represents the ratio of the mass per unit area to the thickness of the knitted fabric [9].
- Porosity of the knitted fabric defined as the total amount of air in the knitted fabric (between and within the yarns) [9].
- Relative humidity, according to standard SRPS EN ISO 139:2007.
- Water retention capacity, according to standard DIN 53814:1974-10.
- Water vapor permeability, according to standard ASTM E-96/E96 M-16.
- Air Permeability, according to standard SRPS EN ISO 9237:2010.
- Warm/Cool sensation, the measuring instrument Thermo Lab KES-F7 was used
- Thermal conductivity coefficient, the measuring instrument Thermo Lab KES-F7 was used.
- Coefficient of heat retention capacity, the measuring instrument Thermo Lab KES-F7 was used.
- Thermal Resistance, the measuring instrument Thermo lab KES-F7 was used.
- Thermal Resistance Thermal Manikin, according to standard ISO 15831:2004.
- For thermographic measurements, the FLIR ThermoCAM™ P65
 thermographic system was used. It is a mobile system that utilizes the longwave infrared spectral range (LWIR), with wavelengths from 7.5 to 13 μm. The
 lenses project the object's image onto a microbolometer with resolutions of
 640×480, 384×288, and 320×240 pixels. The electrical signal from the detector
 (microbolometer) is then processed in the camera system's internal electronics
 [10-12].

Table 1 provides data on the raw material composition and important parameters of the yarns from which the sock is made. According to the various values in this table, the dominant yarn is single-ply with a high twist number, and there is also a polyamide two-ply multifilament yarn, with a much lower twist number. The rubber thread is the coarsest



and present in the smallest amount in the sock composition, only 1%, and is used for making the sock at the beginning, the so-called welt of the sock. This rubber thread is flat and without twist. The linear density of yarns of the yarn with the appropriate degree of twist of the fibers around the yarn body affects the properties of the manufactured socks, such as: texture, wear, pilling, absorption properties, and others [13].

Table 1. Raw material composition and key properties of the yarn

| Sock raw material composition | Nominal linear density of yarns | Nominal yarn twist number | |
|-------------------------------|---------------------------------|---------------------------|--|
| (%) | (tex) | (m ⁻¹) | |
| Bamboo, 77% | 31 | 772 Z | |
| Polyamide, 22% | 4.4/13×2 | 90 S | |
| Rubber-wrapped yarn, 1% | 100 | | |

RESULTS AND DISCUSSION

Table 2 presents the results of the most important physical properties of bamboo socks. There is no significant difference in parameters when it comes to sock sizes. Size M (42-43) socks have lower thickness and porosity, but higher surface mass and bulk density compared to size L. The thickness of the sock (0.918 mm and 0.925 mm) depends on the type of base yarn as well as the knit structure itself, and it affects permeability, comfort, deformability, etc. The surface mass of the sock (283 g/m² and 268.5 g/m²) is an important technological parameter and largely depends on its horizontal and vertical density. In addition, this parameter integrates all the important parameters of the knit structure and is an important economic factor because it significantly influences the cost 1141.

The bulk density of the sock knitted fabric (0.308 g/cm³ and 0.290 g/cm³) best reflects and defines the structural parameters of the socks, as it represents the mass of the knitted fabric of a specific volume, which is directly related to the thickness, type of stitch, and surface mass of the knitted fabric.

Compactness - porosity of knitted fabrics represents the filling of the empty space between loops or the empty space within the loop itself. Good porosity is a consequence of the very structure of knitted products. During movement, i.e., wearing the sock, the interstices in the sock change their shape, leading to the displacement of air and accelerated air exchange, resulting in a pleasant sensation. The porosity of the knitted fabric (79.70 % and 80.9 %) indicates the volumetric proportion of voids in the knitted fabrics.

Table 2. Significant parameters of bamboo socks size

| | ock 7 ze | Γhickness, (mm) | Surface mass (g/m²) | Bulk density, (g/cm³) | Porosity, (%) |
|----|-------------|--------------------|------------------------|--------------------------|------------------|
| 42 | -43 | 0.918 | 283 | 0.308 | 79.7 |
| 43 | -44 | 0.925 | 268.5 | 0.290 | 80.9 |



Table 3 presents the results of key physiological parameters for bamboo socks in a plain jersey. The size L sock has slightly higher numerical values for these examined parameters compared to the size M sock.

The relative humidity of socks depends on the raw material composition, the type of stitch design, and other structural indicators. It is known that bamboo, as a chemical fiber, significantly absorbs and retains moisture (9.42% and 9.70%), followed by natural fibers, and finally synthetic fibers.

The water retention capacity is relatively high for bamboo socks (50.6% and 50.9%), which is due to a greater ability to absorb moisture, and it is also known that these fibers have a higher relative humidity than all other fibers.

Water vapor permeability, according to the results from Table 3 (3437 g/m²/24h and 3605 g/m²/24h), reveals that this sorption characteristic is pronounced in bamboo socks with a plain jersey. Considering that hydrophilic bamboo fibers, in addition to allowing vapor to pass through, also absorb water vapor, swelling occurs, which reduces the size of the air-filled spaces between the fibers, thereby slowing down the diffusion process. Water vapor permeability is a crucial property of knitted fabrics, especially for clothing worn in working conditions (sweating) or socks that are enclosed in footwear.

Air permeability and water vapor permeability are fundamental hygienic and thermal insulation properties of textile materials. Since knitted fabrics have a porous structure, they possess good hygienic and thermal insulation properties. According to the results in Table 3, air permeability (56.1 m³/m²/min. and 61.2 m³/m²/min.) is pronounced and correlated with water vapor permeability. Generally, a material with higher air permeability also has higher water vapor permeability.

Table 3 Physiological parameters of bamboo socks

| Table 6.1 Hydrological parameters of barries section | | | | | | | |
|--|--------------|--------------------------|--------------------------|--|--|--|--|
| Sock | Relative | Water Retention Capacity | Water Vapor Permeability | Air Permeability | | | |
| size | Humidity (%) | (%) | (g/m²/24h) | (m ³ /m ² /min.) | | | |
| 42-43 | 9.42 | 50.6 | 3437 | 56.1 | | | |
| 43-44 | 9.70 | 50.9 | 3605 | 61.2 | | | |

Tables 4 and 5 contain the results of the thermal properties of bamboo socks according to the Thermo Lab method and the Thermal Manikin. The size M sock has a higher numerical value for the warm-cool sensation, the thermal conductivity coefficient is identical, while it has lower numerical values for the coefficient of heat retention capacity and thermal resistance compared to size L.

The first characteristic, the warm-cool sensation, indicates a cooler feeling with a higher numerical value and a warmer feeling with a lower value; in other words, a higher value signifies a textile with faster heat loss, creating a cooling effect. The value for the warm-cool sensation parameter is relatively higher (0.115 W/cm² and 0,111 W/cm²) and significantly depends on the raw material composition. Bamboo socks leave a cool sensation on the skin, making them recommended for use on warmer days, specifically in spring and summer. Additionally, the warm-cool sensation parameter is quite dependent on the moisture content in the fibers (especially important for bamboo fiber



yarn), where an increase in relative humidity also leads to an increase in the warm-cool sensation parameter.

Thermal conductivity is a crucial parameter for the insulation capability of a material, and the measurement is based on the transfer of heat from the warmer to the cooler area, following the principles of heat conduction. As the thermal conductivity coefficient increases (0.065 W/mK for both sock sizes), the thermal resistance of the socks decreases, while the ability for thermal conductivity increases. This parameter typically depends on the raw material composition of the socks and the stitch design. Therefore, socks with a plain jersey have lower thermal resistance and higher thermal conductivity, making them recommended for use on warmer days.

The thermal resistance parameter - Thermo Lab II of socks (0.0815 m²/KW and 0.0824 m²/KW) depends on the stitch design and the raw material composition. Practically, the sock allows a greater or lesser flow of heat into the environment, which is expressed by the thermal resistance constant. Essentially, thermal resistance represents the thermal insulation of the material and is highest in a state of rest because, in that case, the air beneath the sock also remains still [15].

Single-cylinder knitting (plain jersey) implies a structure that has a larger contact surface and a more uniform number of contact points compared to other knits (e.g., double-cylinder knitting). This ensures a greater contact area with the skin, thereby resulting in weaker heat dissipation.

Table 4 presents the results of the thermal resistance testing of bamboo fiber socks in a plain jersey (Thermal Manikin). A slightly lower thermal resistance (0.01796 m²/KW and 0.01806 m²/KW) was observed in this specific case for bamboo socks. This value refers to the thermal resistance of the socks on the Thermal Manikin when the socks are in a stretched, slightly extended state, similar to when they are being worn.

It should be noted that surface and volumetric mass are inversely proportional, while porosity is directly proportional to the thermal resistance of socks in a tense state. Additionally, a higher number of binding points per unit area of the socks, where the mutual contact of fibers in the yarn is intensified, accelerates heat conduction.

Table 4. Thermal properties of bamboo socks – Thermo Lab II

| Sock size | Warm-Cool Sensation CW/cm²) Thermal conductivity coefficient (W/mK) | | Coefficient of heat retention capacity (%) | Thermal resistance (m²/KW) |
|--------------|---|-------|--|----------------------------------|
| 42-43 | 0.115 | 0.065 | 22.03 | 0.0815 |
| 43-44 | 0.111 | 0.065 | 22.88 | 0.0824 |



Table 5. Thermal properties of bamboo socks – Thermal Manikin

| Sock size | The appearance of the sock stitch design | Appearance of the knitted socks | Thermal resistance (m²/KW) |
|--------------|--|---------------------------------|----------------------------|
| 42-43 | | | 0.01796 |

To highlight the heat losses from a garment, thermography was utilized, allowing temperature comparisons over a large surface through a visible image. The result of the thermographic measurement is a thermogram that, using a specific color code, provides a visual representation of the temperature distribution across the surface. The temperature distribution indirectly provides information about the condition of the surface itself, but also reflects the internal state of the observed object.

In the thermographic images of the surface of men's socks (M size) on the feet, maximum and minimum temperature areas can be observed, as shown in Figs. 1 - 3.

In Figure 1, a thermogram of feet in socks before walking is presented (climate chamber, 60 minutes, 20 °C, relative air humidity 50%, air circulation 0.5 m/s). On the right side of the thermogram, a temperature scale is shown, ranging from 27 to 31 °C. The darkest blue color indicates a temperature of 27 °C, while the yellow-orange transitioning into red represents the highest temperature on this thermogram, 31 °C.

Before walking, the dorsal region of the foot in socks has the highest temperature (31 °C), the arch of the foot or plantar area is around 29 °C. The coolest part of the foot in socks is near the toes, with an average temperature of about 28 °C. Generally, the temperature of the right foot with a sock is slightly higher (by 1-2 °C) than that of the left foot before walking, which is associated with the physical condition of the feet (circulation status, etc.).

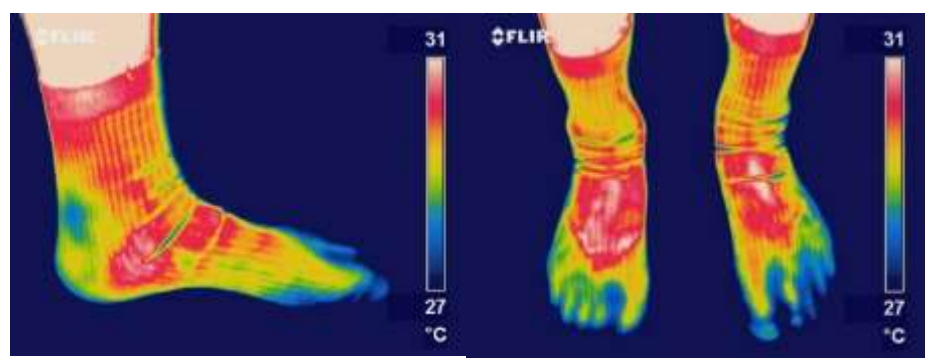


Figure 1. Thermograms of the lateral and dorsal (upper) surface of the feet in socks before walking



The purpose of thermography for shoes with feet and socks relates to footwear ergonomics, injury prevention, medical applications, sock selection, and more. In footwear ergonomics, analyzing heat distribution within the shoes is essential to determine comfort and design adequacy, as well as to assess ventilation and thermoregulation. Additionally, this technique allows for evaluating how different layers (socks, footwear, insoles) affect the thermal balance of the feet.

In Figure 2, a thermogram of shoes with feet and socks after walking is shown. As expected, the dorsal part of the foot inside the shoe is the warmest (around 29 °C), while the edges, i.e., the shoe area near the toes, are the coolest (around 24 °C). No significant differences were found between the temperatures of the left and right shoe.

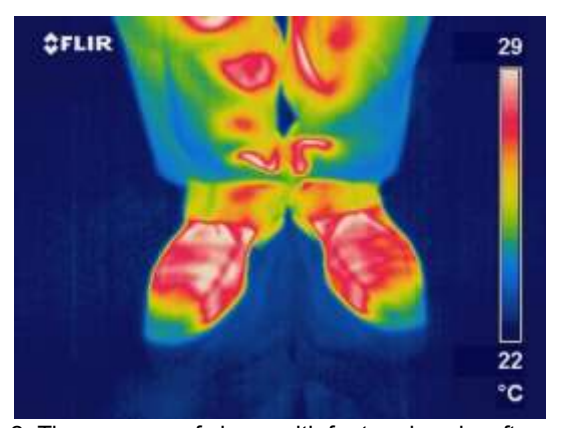


Figure 2. Thermogram of shoes with feet and socks after walking

Foot thermography with socks assesses how different types of socks affect heat distribution, thermoregulation, and overall foot health. It analyzes the socks' ability to maintain a uniform temperature across the foot or identify areas where heat accumulates or excessive cooling occurs. For instance, the analysis of socks used in extreme conditions (cold or hot environments) is particularly important, helping in the selection of socks that reduce the risk of overheating or sweating during intense activities.

The feet with socks, after walking, have a higher temperature than before walking, as expected. The dorsal part of both feet is the warmest, 31-32 °C, while the edges are somewhat cooler, 26-27 °C, as shown in Figure 3. There are no significant differences between the left and right feet in socks.



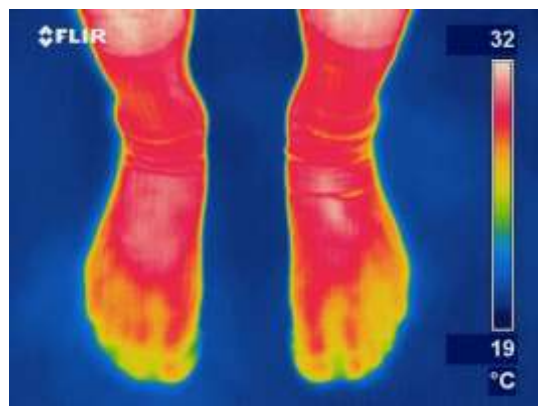


Figure 3. Thermogram of feet with socks after walking

The manufacturing and design of socks (with different knitting structures, thickness, and airspace ratio) should be organized in such a way that they reduce high plantar pressure in specific zones, which has a significant impact on controlling the temperature and humidity of the foot skin. This beneficial effect greatly improves metabolism and blood flow, and consequently, foot comfort. Additionally, when the raw material composition allows the sock to absorb heat from the feet, better thermoregulation is promoted, leading to improved physiological comfort [16,17].

It is evident that a bamboo sock cools the foot, providing a cooling effect, as part of the heat is absorbed by the bamboo fiber and transferred to the surrounding environment. According to the values from the thermo-physiological and thermographic measurements, feet in bamboo fiber socks fully meet the conditions for physiological comfort, as the skin temperature of the feet needed to prevent a feeling of cold is typically around 28–30 °C. Below these temperatures, the feet begin to cool down, and if the temperature drops below 25 °C, the risk of frostbite and other consequences, such as circulatory disorders and physiological discomfort, significantly increases.

CONCLUSIONS

The thermo-physiological comfort of socks during wear depends on numerous factors related to the structure of the yarn and the knitted fabric itself. Socks made from bamboo are particularly interesting because bamboo yarn provides lower porosity of the socks, lower bending stiffness, and allows for easy compression of the knitted loops, thereby reducing the thickness of the material.

Based on the results of these tests, insights are gained into thermal insulation, for example, how much the socks retain or lose heat, or whether the textile material provides sufficient breathability to dissipate excess heat, as well as to what extent the socks manage moisture, especially in the case of sweaty feet. Bamboo socks are more suitable for wear during higher temperatures or in summer when wearing closed footwear. The reason is the well-known cooling effect on the skin that bamboo fiber leaves, as well as its excellent moisture (sweat) absorption from the surface of the foot, which quickly evaporates due to the high ambient temperature.



Thermographic imaging of the feet with socks reveals how well the socks retain or lose heat, whether the textile material provides sufficient breathability to release excess heat, and to what extent the socks manage moisture, especially for sweaty feet. In the end, leather shoes combined with bamboo socks on the feet are physiologically comfortable, providing a natural combination of insulation, breathability, and durability under the specific conditions of this study.

Acknowledgement:

Project BG16RFPR002-1.014-0005-Competence Centre "Smart Mechatronic, Eco and Energy-Saving Systems and Technologies ", Technical University-Gabrovo, Bulgaria. The project was financed by the Ministry of Science, Technological Development and Innovation of the Republic of Serbia (ev.No. 451-03-137/2025-03/ 200133)

References

- [1] Samolov AD, Simić DM, Fidanovski BZ, Obradović VM, Tomić LjD, Knežević DM. Improvement of VIS and IR camouflage properties by impregnating cotton fabric with PVB/IF-WS2. *Defence Technology*. 2021, 17, 6, 2050-2056. https://dx.doi.org/10.1016/j.dt.2020.10.008
- [2] Čubrić IS, Rosić D, Petrov A. Improvement of Thermophysiological Comfort of Athletes Based on Thermographic Evaluation of Sportswear Material. Advanced technologies. 2022, 11,2, 55-61. https://dx.doi.org/10.5937/savteh2202055S
- [3] Usamentiaga R, Venegas P, Guerediaga J, Vega L, Molleda J, Bulnes F. Infrared Thermography for Temperature Measurement and Non-Destructive Testing. *Sensors*. 2014, 14, 7, 12305–12348. https://doi.org/10.3390/s140712305
- [4] Van Amber RR., Wilson CA, Laing RM, Lowe BJ, Niven BE. Thermal and moisture transfer properties of sock fabrics differing in fiber type, yarn, and fabric structure. *Textile Research Journal*. 2015, 85, 12, 1269–1280. https://doi.org/10.1177/0040517514561926
- [5] Irzmanska E, Dutkiewicz JK, Irzmanski R. New approach to assessing comfort of use of protective footwear with a textile liner and its impact on foot physiology. *Textile Research Journal*. 2014, 84, 7, 728–738. https://doi.org/10.1177/0040517513507362
- [6] Bertaux E, Derler S, Rossi RM, Zeng X, Koehl L, Ventenat V. Textile, Physiological, and Sensorial Parameters in Sock Comfort. *Textile Research Journal*. 2010, 80, 17, 1803-1810. https://doi.org/10.1177/0040517510369409
- [7] Ziaei M, Ghane M, Hasani H, Saboonchi A. Investigation into the Effect of Fabric Structure on Surface Temperature Distribution in Weft-Knitted Fabrics Using Thermal Imaging Technique. *Thermal Science*. 2020, 24, 3B, 1991-1998. https://doi.org/10.2298/TSCI180811290Z
- [8] Pakdel E, Naebe M, Sun L, Wang X. Advanced Functional Fibrous Materials for Enhanced Thermoregulating Performance. *ACS Applied Materials & Interfaces*. 2019, 11, 13039–13057. https://doi.org/10.1021/acsami.8b19067



- [9] Tasić P, Trajković D, Geršak J. Influence of structural and constructional parameters of knitted fabrics on the thermal properties of men's socks. *Hem. Ind.* 2023, 77(3) 181-190. https://doi.org/10.2298/HEMIND220724004T
- [10] FLIR Systems, Inc., *User's manual*, FLIR Tools/Tools+, Wilsonville, USA, 2014.
- [11] Banerjee D, Chattopadhyay SK, Tuli S. Infrared thermography in material research A review of textile applications. *Indian Journal of Fibre & Textile Research*. 2013, 38, 427-437.
- [12] Rubežiene V, Padleckiene I, Varnaite-Žuravliova S, Baltušnikaite J. Reduction of Thermal Signature Using Fabrics with Conductive Additives. *Materials Science*. 2013, 19, 4, 409-414. https://doi.org/10.5755/j01.ms.19.4.1730
- [13] Maqsood M, Seide G. Development of biobased socks from sustainable polymer and statistical modeling of their thermo-physiological properties. *Journal of Cleaner Production*. 2018, 197, 170-177. https://doi.org/10.1016/j.jclepro.2018.06.191
- [14] Trajković DS, Tasić PS, Stepanović JM, Šarac TI, Radmanovac NM. Physiological Characteristics of the Socks Made from Bamboo and Conventional Fibers. *Advanced technologies*. 2014, 3, 1, 59-65. https://doi.org/10.5937/savteh1401059T
- [15] Stančić M, Grujić D, Novaković D, Kašiković N, Ružičić B, Geršak J. Dependence of warm or cold feeling and heat retention ability of knitwear from digital print parameters. *Journal of Graphic Engineering and Design*. 2014, 5(1) 25-36. https://doi.org/10.24867/JGED-2014-1-025
- [16] Dan R, Fan XR, Chen DS, Wang Q. Numerical simulation of the relationship between pressure and displacement for the top part of men's socks. *Textile Research Journal*. 2011, 81, 2, 128–136. https://doi.org/10.1177/0040517510377830
- [17] Arezes PM, Neves MM, Teixeira SF, Leao CP, Cunha JL. Testing thermal comfort of trekking boots: An objective and subjective evaluation. *Applied Ergonomics*. 2013, 44, 557-565. https://doi.org/10.1016/j.apergo.2012.11.007

Izvod

TOPLOTNA, FIZIOLOŠKA I TERMOGRAFSKA ANALIZA MUŠKE ČARAPE OD BAMBUSA U DESNO-LEVOM PREPLETAJU

Predrag Tasić¹ ID, Dusan Trajković² ID, Jovan Stepanović² ID, Jelka Geršak³ ID

1 V.I. "Vunil", d.o.o., Leskovac, Srbija

2 Univerzitet u Nišu, Tehnološki fakultet, Leskovac, Srbija

3 Univerzitet u Mariboru, Mašinski fakultet, Slovenija

Istraživanje koristi rezultate toplitnih i fizioloških metoda, kao i termtermografskih snimanja radi dobijanja informacija o stanju čarapa od bambusa na stopalu. Čarape od bambusa u desno-levom prepletaju imaju zadovoljavajuća fizička svojstva, debljinu, zapreminsku gustinu i poroznost. Hidrofilna svojstva čarapa od bambusa su jako



izražena, ova vlakna jako upijaju vlagu a imaju i dobra svojstva propustljivosti vazduha. Toplotna svojstva prema metodi Thermo Lab II i Thermal Manikin, otkrivaju da čarape od bambusa ostavljaju hladan osećaj na koži, kao i da imaju manju toplotnu otpornost a veću toplotnu provodljivost, pa se preporučuje za nošenje u toplijim danima. Prema rezultatima merenja infracrvenog zračenja, tj. upoređujući izmerene vrednosti temperature na različitim delovima stopala, zaključuje se da su čarape od bambusa pogodnije za nošenje tokom viših temperatura u zatvorenoj obući.

Ključne reči: termo-fiziologija, termografija, muška čarapa, bambus vlakna, desno-leva pletenina.



UDK 677.075.027.5 : 677.016.6 DOI: 10.46793/NovelTDS16.175S

ANALYSIS OF SURFACE PROPERTY CHANGES ON THE REVERSE SIDE OF KNITTED FABRICS AFTER PRINTING

Sandra Stojanović^{1,*} ID, Dušan Trajković² ID, Suzana Đorđević¹ ID, Slađana Antić¹ ID, Tanja Nikolić¹ ID, Svetomir Golubović¹ ID

Academy of Applied Studies Southern Serbia, Department of Technology and Art Studies Leskovac, Leskovac, Serbia

Faculty of Technology, University of Niš, Leskovac, Serbia

The surface properties of textile materials play a key role in their appearance, tactile perception, and wearing comfort, with the reverse side of knitted fabrics being critical due to their direct connection with the wearer's skin. This paper aimed to investigate the effect of sublimation printing on the surface properties of the reverse side of interlock knitted fabrics intended for activewear. Two types of knitted fabrics were printed using the sublimation printing technique in the CMYK colour model. Surface properties were evaluated using the KES-FB4 instrument, analysing the

Surface properties were evaluated using the KES-FB4 instrument, analysing the surface friction coefficient (MIU), mean deviation of the friction coefficient (MMD), and geometrical roughness (SMD). The results indicated that the knitted fabric structure and yarn fineness significantly affected the resistance of knitted fabrics to changes induced by sublimation printing. Knitted fabric 2KF exhibited higher SMD values and lower MIU values compared to 1KF. Greater stability of surface parameters after printing was observed in knitted fabric 1KF, which is attributed to its higher thickness and more homogeneous structure. For printed samples 1KF, SMD values in the course direction ranged from 2.430 μ m to 3.661 μ m, while for 2KF samples they ranged from 5.212 μ m to 6.965 μ m. A strong linear correlation was established between SMD and knitted fabric weight (R² = 0.8615), indicating that SMD values increased proportionally with knitted fabric weight. Although sublimation printing was applied to the fabric's face side, the high temperature and pressure also affected the reverse side.

Keywords: Knitted fabrics, surface properties, printing process.

^{*} Author address: Sandra Stojanović, Academy of Applied Studies Southern Serbia, Department of Technology and Art Studies Leskovac, Vilema Pusmana 17, 16000 Leskovac, Serbia e-mail address: sandra.k770@gmail.com



INTRODUCTION

Knitted fabrics are particularly well-suited for the production of clothing, especially for sportswear, due to their porous structure, high elasticity, and ability to conform to body contours [1]. A wide range of physical and functional properties of knitted fabrics is achieved through the use of different fibres and yarns in their production, as well as through various machine settings [2].

Both the visual and tactile perception of textile materials largely depend on their surface characteristics, making these properties highly relevant for evaluating comfort and the aesthetic value of clothing. In the case of knitted fabrics, these characteristics are even more pronounced because of their structure.

The surface of knitted fabrics is not smooth; it varies in roughness depending on yarn and characteristics (irregularity, hairiness, friction, surface roughness, shape, diameter, density, spinning technology, and fibre composition) and structure of the fabric itself (type, density, thickness) [3–7].

Previous studies have demonstrated that the surface properties of knitted fabrics greatly affect the subjective perception of comfort. For instance, studies comparing the technical face and reverse side of rib knits (1×1 and half-Milano) revealed that the reverse side was perceived as softer and more flexible due to its unbalanced structure, which can be an important factor when selecting materials for garments that come into direct contact with the skin [8].

The importance of the surface roughness (SMD) parameter in assessing surface texture has been confirmed in studies showing that non-contact measurement methods can yield reliable results, closely correlated with the KES-F evaluating system [9].

In recent years, sublimation printing has increasingly been used because of advantages such as environmental sustainability, rich colour, and high color fastness. However, it has been shown that the process can induce changes in the structure and physical properties of knitted fabrics, particularly those made from cotton (Co) and cotton/polyester blends (Co/PES), where alterations in weight, surface roughness, and even compressional properties have been observed. Although changes in polyester (PES) knitted fabrics appear to be less pronounced, they are still present, especially in surface properties such as surface friction (MIU), mean deviation of friction (MMD), and surface roughness (SMD), which directly influence tactile sensation and overall comfort [10, 11].

A particular challenge lies in preserving the stability of surface characteristics on the reverse side of knitted fabrics after the printing process, as this side is in direct contact with the wearer's skin, especially in sportswear. Unfavourable changes in surface attributes – such as increased roughness or reduced softness – can significantly affect subjective comfort and athletes' performance. Therefore, this paper aimed to experimentally assess the impact of sublimation printing on the surface properties of the reverse side of interlock knitted fabrics intended for sportswear, with particular emphasis on parameters that directly affect tactile comfort.

MATERIALS AND METHODS

The surface properties of the knitted fabrics — surface friction (MIU), mean deviation of



the friction coefficient (MMD), and surface roughness (SMD) were measured using the KES-FB4 AUTO instrument (Figure 1a), part of the Kawabata Evaluation System (Kato Tech Co., Ltd., Kyoto, Japan). This system provides detailed information about the tactile characteristics of textile materials.

During measurement, the textile material was fixed between two clamps and moved across a metal plate over a distance of 20 mm at a constant speed of 0.1 cm·s⁻¹. A preload of 19.62 cN (equivalent to 20 gf·cm⁻¹) was applied. Surface friction was recorded using a U-shaped sensor made of 10 steel wires, each 0.5 mm in diameter. This sensor was designed to mimic a human fingertip. This sensor applied a constant normal force of 49.035 cN to the fabric surface.

Another U-shaped sensor (Figure 1b), consisting of a single wire 0.5 mm in diameter, was used to measure surface roughness by applying a force of 9.807 cN to the textile material.

The MIU parameter represents the ratio of the frictional force to the applied normal force, the MMD indicates variations in friction as the sensor moves over the surface, while the SMD reflects irregularities in the surface structure as deviations from an ideally smooth surface [12]. Three measurements were performed for each sample, and the mean values are reported in this paper.



Figure 1. a) KES-FB4 AUTO instrument; b) Sensor for measuring geometric roughness

Structural properties of the tested knitted fabrics are presented in Table 1.

Table 1. Structural properties of the tested unprinted knitted fabrics

| | | Raw material | Yarn | Density | | | Thickness | Wight |
|--------|-----------|-----------------|----------------------------|--|--|---|-----------|-----------|
| Sample | Pattern | | linear density Tt (tex) | Horizontal D _h (cm ⁻¹) | Vertical D _v (cm ⁻¹) | Total D _t (cm ⁻²) | h (mm) | m (g·m⁻²) |
| 1KF-W | Interlock | PES | 7.40 | 16.3 | 10.5 | 171.2 | 0.38 | 122.4 |
| 2KF-W | Interlock | PES | 7.04 3.60 | 16.5 | 11.8 | 194.7 | 0.28 | 134.9 |



The printing process was carried out using an EPSON L1800 piezo-electric ink-jet printer, at a resolution of 7760 \times 1440 dpi , with Canapa Ventus Master 100 transfer paper of 100 g·m-² and Sublisplash dye sublimation inks Splashjet-Super-Sub-6C. For ink fixation, a Digital High-Pressure Heat Press SHP-15/20/24LP2MS was used. The curing process was conducted at 185°C for 120 seconds.

Knitted fabrics were printed in the CMYK colour model, using four separate dyes: cyan, magenta, yellow, and key, i.e., black. Each printed sample was labelled based on the applied colour (C for cyan, M for magenta, Y for yellow, and K for black, while unprinted knitted fabrics were labelled with the code W (white).

Before testing, all knitted fabric samples were conditioned under standard atmospheric conditions according to ISO 139:2005 [13].

Structural properties were evaluated according to the following standards:

- Density of the knitted fabric: EN 14971 [14]
- Weight of the knitted fabric: ISO 3801 [15]
- Thickness of the knitted fabric: ISO 5084 [16].

RESULTS AND DISCUSSION

In order to gain deeper insight into how sublimation printing affects the surface properties of knitted fabrics intended for sportswear, the parameters MIU, MMD, and SMD were measured on the reverse side of knitted fabrics.

Figure 2 presents the MIU results for the tested knitted fabrics, measured on the reverse side.

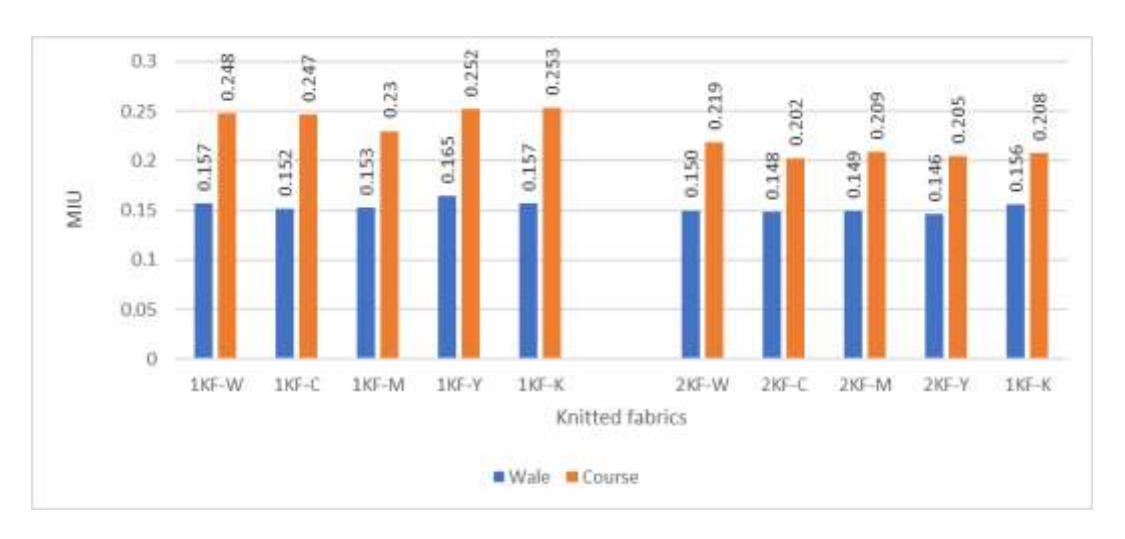


Figure 2. MIU results of knitted fabrics, measured on the reverse side



For the unprinted samples, MIU values were slightly higher for sample 1KF-W (wale: 0.157, course: 0.248) compared to sample 2KF-W (wale: 0.150, course: 0.219). These differences indicate higher surface friction in the 1KF sample, which can be attributed to its greater thickness and rougher surface structure.

In the 1KF sample series, a decrease in MIU values in the wale direction was observed after the sublimation printing process, except for sample 1KF-K, which showed no change. The decrease in MIU values in the wale direction ranged from 2.55% (1KF-M) to 3.18% (1KF-C), while an increase of 5.1% was observed for sample 1KF-Y, compared to the unprinted sample. In the course direction, a decrease in MIU values was observed for samples 1KF-C and 1KF-M, while increases of 1.61% and 2.02% were observed for samples 1KF-Y and 1KF-K, respectively.

Within the 2KF sample group, MIU values in the wale direction slightly decreased after printing, except for sample 2KF-K, which showed an increase of 4%. In the course direction, all 2KF samples exhibited a decrease in MIU values after printing, ranging from 4.57% (2KF-M) to 7.76% (2KF-C).

In general, the printed 2KF samples showed a decrease in MIU values. As this knitted fabric was produced using two types of yarns of different fineness (including one filament yarn), the applied heat contributed to "ordering" of the surface, reducing roughness. On the other hand, the variations in MIU values observed in the 1KF samples may be attributed to the structural characteristics — being made from one yarn, these knitted fabrics lack internal heterogeneity, which may lead to localized changes.

The obtained MIU values for all printed knitted fabrics ranged from 0.15 to 0.25, which is in the characteristic range of this parameter (0.15 to 0.30) [12]. This indicates that sublimation printing did not adversely affect the surface friction.

The results of MMD for the tested knitted fabrics, measured on the reverse side, are presented in Figure 3.

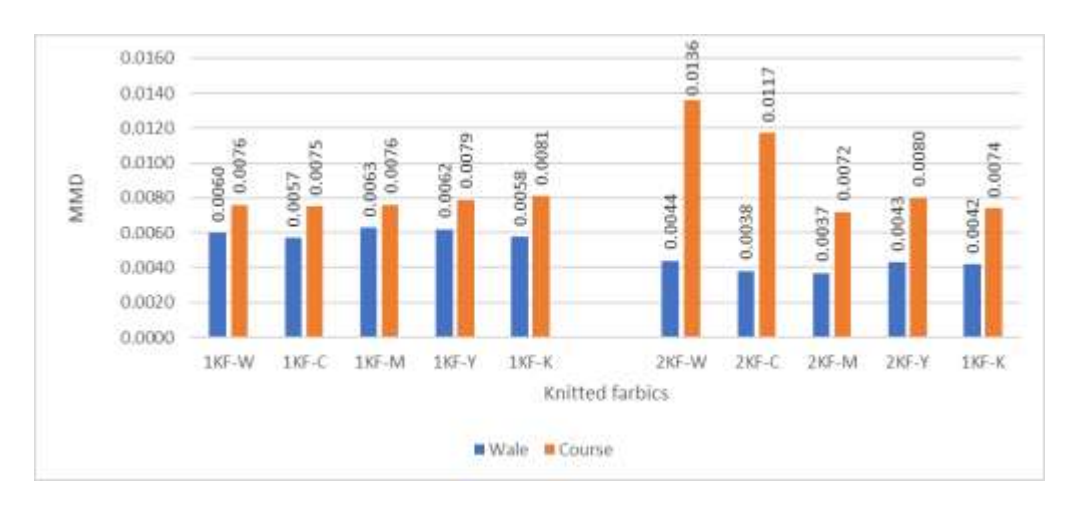


Figure 3. MMD results of knitted fabrics, measured on the reverse side



In comparison to the 1KF samples (1KF-W wale: 0.0060), MMD values were generally lower for the 2KF samples in the wale direction (2KF-W wale: 0.0044). After printing, slight changes in MMD values were observed in 1KF.

A decrease of 6.58% was observed for sample 1KF-K, while an increase of 5% was noted for sample 1KF-M compared to the unprinted sample in the wale direction. In the course direction, minor changes were detected.

For the 2KF knitted fabrics, MMD values in the course direction were significantly higher than in the wale direction, and a substantial decrease in these values was observed after printing in the course direction, ranging from 13.97% (2KF-C) to 47.06% (2KF-M).

The 1KF knitted fabric showed more stable MMD values after the printing process, while more pronounced changes were recorded in the 2KF sample group, especially in the course direction. The higher density and structural complexity of 2KF make it more susceptible to deformation and changes in the microstructure distribution during printing. This leads to reduced friction variation and a more uniform surface (lower MMD).

Figure 4 presents the results of SMD for the tested knitted fabrics, measured on the reverse side

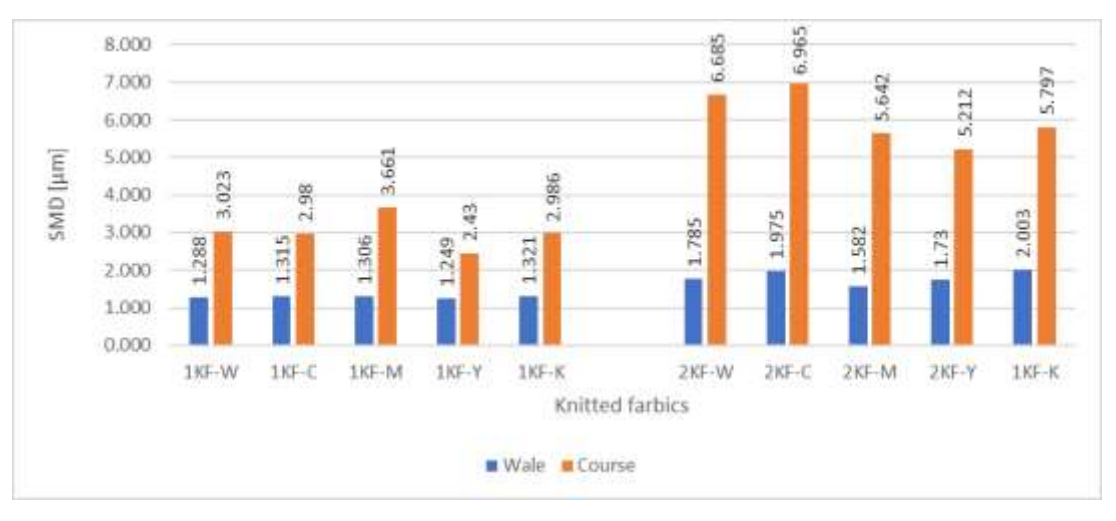


Figure 4. SMD results of knitted fabrics, measured on the reverse side

SMD values for the 1KF fabrics increased in the wale direction after printing, ranging from 1.40% to 2.56% compared to the unprinted sample, with the exception of sample 1KF-M, where a slight increase in SMD values was recorded. In the course direction, an increase was observed for all 1KF samples, with the largest being 21.10% (sample 1KF-M), while sample 1KF-C was the exception, showing a decrease of 1.42%.

In the 2KF samples, minor changes of SMD values in the wale direction were recorded, with the highest increase of 12.21% for sample 2KF-K. Additionally, in the course direction, SMD values decreased after printing in all samples except for 2KF-M, which showed an increase of 4.19%.



Although the 2KF fabric is thinner, its higher density and more complex structure contributeto a greater perception of roughness. The applied heat and pressure during the printing process contributed to alterations in the structures of knitted fabrics. Regarding changes in the structure on the reverse side of knitted fabrics 2KF, it is possible that the yarns were "impressed" under the influence of the press, which reduced the roughness in the course direction. In the 1KF sample group, with a less dense and thicker structure, only minor changes were observed in comparison to the unprinted sample.

In addition, based on the analysis of the results shown in Figures 2, 3, and 4, it can be concluded that the printing process had a smaller effect on the change of the surface properties of 1KF knitted fabrics.

Figures 5 and 6 show the linear dependence of MIU on the surface mass and thickness of printed knitted fabrics, respectively.

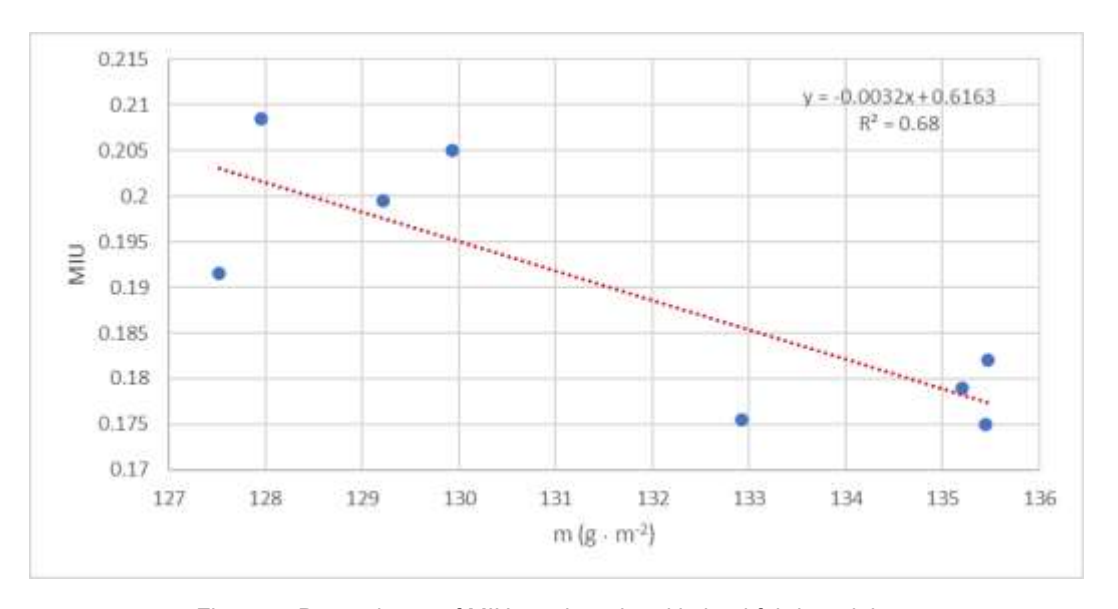


Figure 5. Dependence of MIU on the printed knitted fabric weight



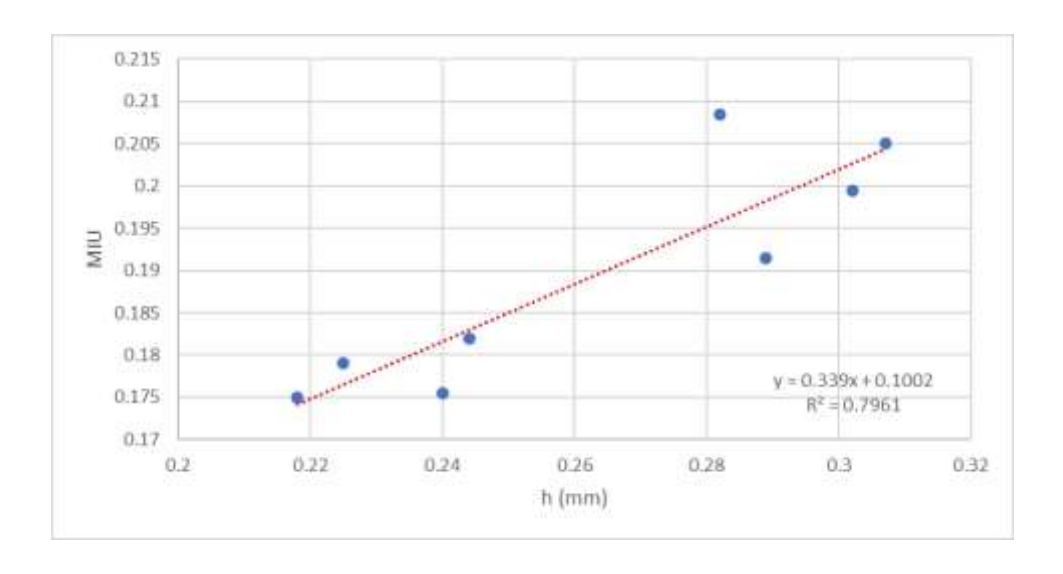


Figure 6. Dependence of MIU on the thickness of printed knitted fabrics

A strong linear correlation was observed between MIU and the weight of printed knitted fabrics, as confirmed by a high Pearson correlation coefficient (R = 0.9275; R² = 0.8600). In contrast, the linear correlation between MIU and the thickness of knitted fabrics was slightly lower (R = 0.8911; R² = 0.7961).

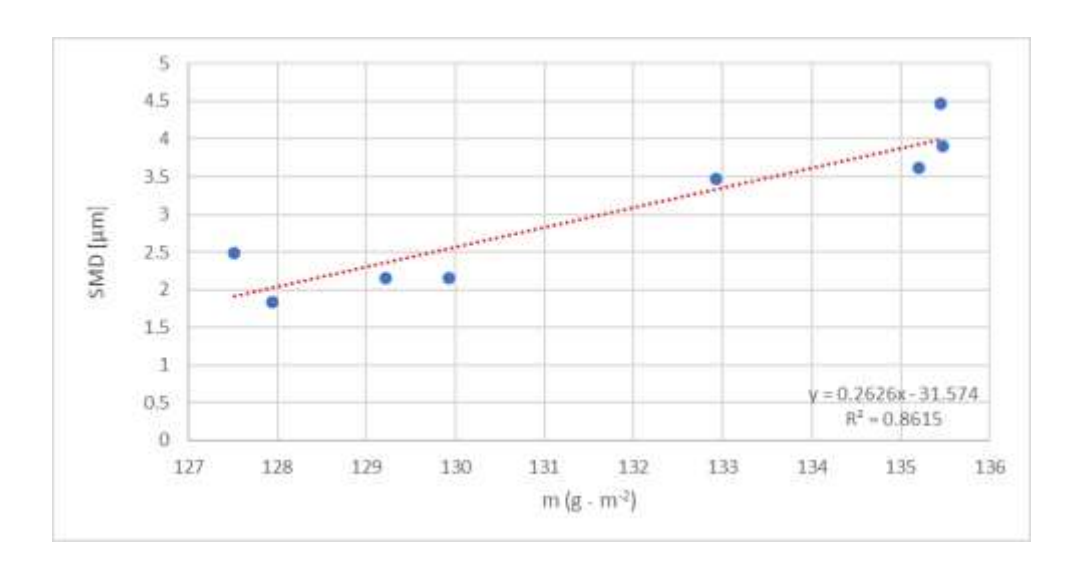


Figure 7. Dependence of SMD on the printed knitted fabric's weight



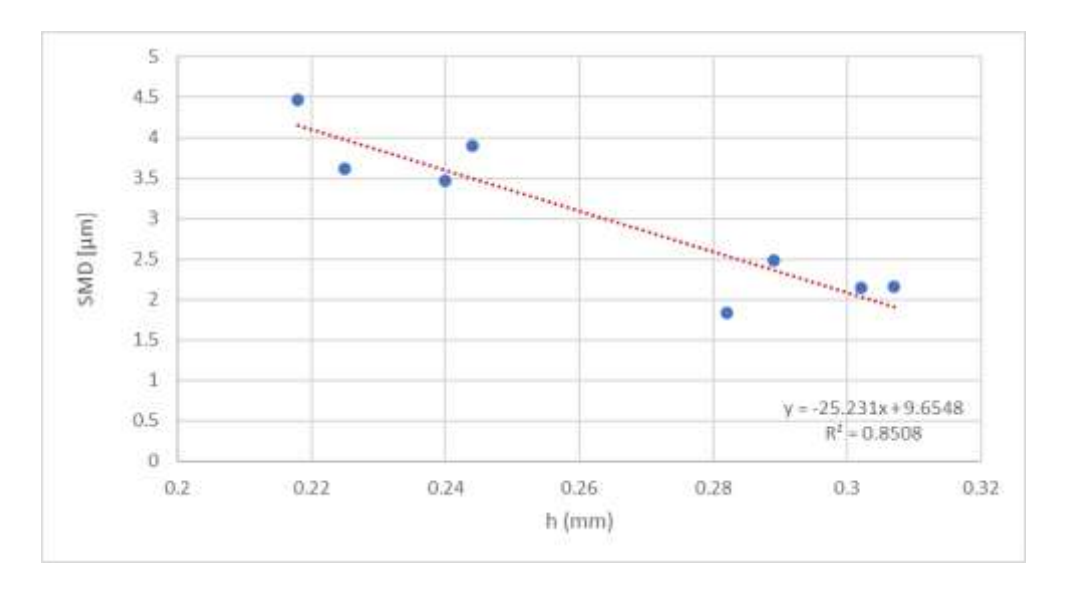


Figure 8. Dependence of SMD on the printed knitted fabric's thickness

Based on the results presented in Figure 7, a strong linear correlation was found between the SMD and the weight of printed knitted fabrics, with a Pearson correlation coefficient of R = 0.9282 (R² = 0.8615). Similarly, the correlation between SMD and (printed) knitted fabric thickness was also high, with R = 0.9224 (R² = 0.8508), as shown in Figure 8.

The results showing the dependence of the MMD parameter on the thickness and weight of printed knitted fabrics are not presented due to the weak linear dependence.

CONCLUSION

This paper examined the influence of sublimation printing on the surface properties of the reverse side of knitted fabrics made from PES yarns of different fineness. Two knitted fabric types were tested: 1KF, produced from a single yarn, and 2KF, made from a combination of two yarns.

The experimental results confirmed that sublimation printing affected the surface characteristics of knitted fabrics on the reverse side, despite being applied to the face side. The degree of change is closely related to the thickness and weight of the fabrics. The 2KF knitted fabric, which has a thinner and denser structure, exhibited sensitivity to the printing process, as indicated by decreased MIU (in both directions) and increased SMD values in the course direction. The 1KF knitted fabrics, on the other hand, showed more resistance to structural alterations following printing due to their higher thickness and uniform structure (made from a single yarn).



Acknowledgement

Project BG16RFPR002-1.014-0005-Competence Centre "Smart Mechatronic, Eco and Energy-Saving Systems and Technologies", Technical University-Gabrovo, Bulgaria. The project was financed by the Ministry of Science, Technological Development and Innovation of the Republic of Serbia (ev.No. 451-03-137/2025-03/ 200133)

References

- [1] Ajayi JO, & Elder HM. Fabric Friction, Handle, and Compression. *The Journal of The Textile Institute*. 1997, *88*(3), 232–241. https://doi.org/10.1080/00405009708658547
- [2] Ramkumar SS, Wood DJ, Fox K, & Harlock SC. Developing a Polymeric Human Finger Sensor to Study the Frictional Properties of Textiles: Part II: Experimental Results. *Textile Research Journal*. 2003, 73(7), 606-610. doi:10.1177/004051750307300708
- [3] Ramkumar SS, Leaf GAV, & Harlock SC. A Study of the Frictional Properties of 1×1 Rib-knitted Cotton Fabrics. *The Journal of The Textile Institute*. 2000, 91(3), 374–382. https://doi.org/10.1080/00405000008659514
- [4] Maatoug N, Sahnoun M, & Sakli F. Statistical analysis of surface roughness parameters for weft knitted fabrics measured by the textile surface tester (TST). *Journal of Engineered Fibers and Fabrics*. 2012, 7, 104–112. DOI:10.1177/155892501200700407
- [5] Akgun M, Becerir B, & Alpay HR. Investigation of the relation between surface roughness and friction properties of polyester fabrics after abrasion. *The Journal* of *The Textile Institute*. 2018, 109, 322–337. DOI:10.1080/00405000.2017.1344117
- [6] Akgun, M. Assessment of the surface roughness of cotton fabrics through different yarn and fabric structural properties. Fibers and Polymers. 2014, 15, 405–413. https://doi.org/10.1007/s12221-014-0405-7
- [7] Balci Kilic G, & Okur A. Effect of yarn characteristics on surface properties of knitted fabrics. *Textile Research Journal*. 2018. 004051751879733. doi:10.1177/0040517518797337
- [8] Asfand N, & Daukantienė V. A study of the physical properties and bending stiffness of antistatic and antibacterial knitted fabrics. *Textile Research Journal*. 2022, 92(7-8), 1321-1332. DOI: 10.1177/00405175211055070
- [9] Semmani D, Hasani H, Behtaj S, et al. Surface roughness measurement of weft knitted fabrics using image processing. *Fibres & Textiles in Eastern Europe.* 2011, 19, 55–59. Available online: http://fibtex.lodz.pl/article523.html
- [10] Stojanović S, Geršak J, Trajkovic D, & Cirkovic N. Influence of sublimation transfer



- printing on alterations in the structural and physical properties of knitted fabrics. *Coloration Technology*, 2021, *137*(2) 108-122. https://doi.Org/10.1 11 1/cote.1250
- [11] Stojanović S, Geršak J, & Trajkovic D. Compression properties of knitted fabrics printed by sublimation transfer printing technique. *Advanced technologies*. 2021, 10(1) 05-12. DOI 10.5937/savteh2101046S
- [12] Geršak J. Objektivno vrednovanje plošnih tekstilija i odeće, Zagreb: Sveučilište u Zagrebu, Tekstilno-tehnološki fakultet. 2014. ISBN 978-953-7105-42-6.
- [13] ISO 139:2005. Textiles Standard atmospheres for conditioning and testing.
- [14] EN 14971:2006. Textiles Knitted fabrics Determination of number of stitches per unit length and unit area.
- [15] ISO 3801:1997. Textiles—Woven fabrics Determination of mass per unit length and mass per unit area.
- [16] ISO 5084:1996. Textiles—Determination of thickness of textiles and textile products.

Izvod

ANALIZA PROMENA POVRŠINSKIH SVOJSTAVA NA NALIČJU PLETENINA NAKON ŠTAMPANJA

Sandra Stojanović¹ <u>ID</u>, Dušan Trajković² <u>ID</u>, Suzana Đorđević¹ <u>ID</u>, Slađana Antić¹ <u>ID</u>, Tanja Nikolić¹ <u>ID</u>, Svetomir Golubović¹ <u>ID</u>

¹Akademija strukovnih studija Južna Srbija, Odsek visoka tehnološko umetnička škola Leskovac, Leskovac, Srbija

²Tehnološki fakultetu u Leskovcu, Univerzitet u Nišu, Leskovac, Srbija

Površinska svojstva tekstilnih materijala imaju ključnu ulogu u njihovom vizuelnom izgledu, taktilnom osećaju i udobnosti pri nošenju, pri čemu je naličje pletenih tekstilnih materijala od posebnog značaja zbog neposrednog kontakta sa kožom korisnika. Ovaj rad ima za cilj da ispita uticaj sublimacione štampe na površinska svojstva naličja interlok pletenina namenjenih za sportsku odeću. Dve vrste pletenina štampane su tehnikom sublimacije u CMYK kolor modelu.

Površinska svojstva ocenjivana su pomoću KES-FB4 uređaja, analizom koeficijenta površinskog trenja (MIU), prosečnom vrednošću apsolutnog odstupanja koeficijenta trenja (MMD) i geometrijske hrapavosti (SMD). Rezultati su pokazali da struktura pletenine i finoća pređe značajno utiču na otpornost materijala na promene izazvane procesom sublimacione štampe. Pletenina označena kao 2KF imala je višu vrednost SMD i nižu vrednost MIU u poređenju sa pleteninom 1KF. Veća stabilnost površinskih parametara nakon štampe uočena je kod pletenine 1KF, što se pripisuje njenoj većoj debljini i homogenijoj strukturi. Kod štampanih uzoraka 1KF, vrednosti SMD u pravcu osnove kretale su se od 2.430 μ m do 3.661 μ m, dok su kod 2KF uzoraka iznosile od 5.212 μ m do 6.965 μ m. Ustanovljena je snažna linearna korelacija između SMD vrednosti i površinske mase pletenine (R² = 0.8615), što ukazuje da se vrednosti SMD



proporcionalno povećavaju sa površinskom masom materijala. Iako je sublimaciona štampa primenjena na lice materijala, visoka temperatura i pritisak delovali su i na naličje.

Ključne reči: Pletenine, površinska svojstva, proces štamapanja.



THE INFLUENCE OF RELATIVE AIR HUMIDITY ON THE ELECTRICAL RESISTIVITY OF WOVEN FABRICS INTENDED FOR OUTERWEAR

Slađana Antić^{*} <u>ID</u>, Suzana Đorđević <u>ID</u>, Sandra Stojanović <u>ID</u>, Tanja Nikolić <u>ID</u>, Svetomir Golubović <u>ID</u>

Academy of Applied Studies Southern Serbia, Department of Technology and Art Studies Leskovac, Leskovac, Serbia

The electrical resistance of woven fabrics is strongly influenced by the moisture content of the tested sample, which is largely determined by the relative humidity of the environment. Water molecules can become partially ionized, and the resulting water ions near the textile material help neutralize surface charges. Additionally, depending on their fibre composition, fabrics absorb varying amounts of moisture from the environment, which increases their electrical conductivity. This paper presents the results of the volume electrical resistivity testing of three fabrics with different fibre compositions intended for the production of women's blazers (F1 - 100% PES, F2 -96.1% PES and 3.9% Elastane, F3 - 100% Silk). In blazers, certain pattern pieces require reinforcement with a fusible interlining, which created the need for two-laver samples. Tests were conducted for fusible interlining (I - 71.2% and 28.8% PES) and fabrics fixed to it frontally (F1I, F2I, and F3I). The electrical resistivity of samples was measured in both warp and weft directions, in an environmental chamber with humidity ranging from 40% to 65%, in 5% increments. At 40% humidity, the lowest electrical resistivity was recorded in F3, while the highest was in F2. At 65% humidity, F1 showed the lowest resistivity and F2 the highest. The silk fabric (F3) lost its initial advantage over the PES fabric, which may be explained by its structural characteristics. It can be concluded that lowering the relative humidity of the environment by 25% significantly increases the electrical resistivity of the textile materials by several times.

Keywords: woven fabric, raw material, electrical resistance.

^{*} Author address: Slađana Antić, Academy of Applied Studies Southern Serbia, Department of Technology and Art Studies Leskovac Serbia, Partizanska 7, Leskovac, Serbia e-mail address: sladjaantic61@gmail.com



INTRODUCTION

Clothing covers the human body, and beyond its functional role, it should enhance the body's shape, conceal imperfections, and provide a pleasant and comfortable wearing experience. The synthesis of appearance, functionality, and comfort is crucial from both physiological and health perspectives. Skin sensory comfort is influenced by the woven fabrics, where desirable properties include softness and smoothness, while undesirable and potentially harmful features include stiffness, roughness, allergic reactions, and clinging to the skin [1]. Garments clinging to the body are an especially unpleasant phenomenon caused by the accumulation of static electricity within the textile material. The effect is particularly pronounced in synthetic fibres; therefore, numerous authors have attempted to evaluate the quality of clothing fabrics through their electrophysical properties, one of which is volume electrical resistivity [2-5].

MATERIALS

The experimental material included three apparel fabrics with different fibre compositions: polyester (PES), a polyester/elastane (PES/EL) blend, silk, and fusible interlinings made from a cotton/ polyester (Co/PES) blend. The structural characteristics of the selected base fabrics before thermal fixation (labelled F1, F2, and F3) are presented in Table 1.

Table 1. Structural characteristics of base fabrics

| Tested characteristic | | Unit of | | Test results | |
|-----------------------|-------|------------------|-------------|----------------------|----------------|
| | | measurement | F1 | F2 | F3 |
| Fibre compositio | n | (%) | 100% PES | 96,1% PES 3.9% EL | 100% Silk |
| Weave type | | | Plain weave | Plain weave | Weft rib weave |
| Effective fabric w | /idth | (cm) | 150 | 148 | 140 |
| Fabric thickness | | (mm) | 0.450 | 0.580 | 0.680 |
| Surface mass | | (g/m²) | 179 | 264 | 226 |
| Fabric density | warp | (threads/cm) | 22.5 | 45 | 10 |
| | weft | (threads/cm) | 21 | 31 | 6.5 |
| Yarn fineness | warp | (tex) | 41.5 | 36 | 56 |
| | weft | (tex) | 41 | 33 | weft 1 - 96.4 |
| | | ` , | | | weft 2 - 448.4 |
| Yarn insertion | Warp | (%) | 10 | 21 | 7.75 |
| | weft | ([%]) | 10 | 17.1 | 3.61 |
| Shrinkage | Warp | (`%´) | -0.8 | -0.6 | -0.39 |
| J | weft | (̂%) | -0.5 | -0.5 | +0.15 |

The structural characteristic of the selected fusible interlining is presented in Table 2.



Table 2. The structural characteristic of the selected fusible interlining

| Tested characteristic | Uı | nit of measurement | Test results | |
|------------------------|------|--------------------|--------------|--|
| | | | I | |
| Fibre composition | | (%) | 71.2% Co | |
| • | | ` , | 28.8% PES | |
| Weave type | | | Plain weave | |
| Effective fabric width | | (cm) | 90 | |
| Fabric thickness | | (mm) | 0.435 | |
| Surface mass | | (g/m²) | 99 | |
| Fabric density | warp | (threads/cm) | 16 | |
| • | weft | (threads/cm) | 9 | |
| Yarn fineness | warp | (tex) | 40 | |
| | weft | (tex) | 39 | |
| Yarn insertion | warp | (%) | 2.6 | |
| | weft | (%) | 5.8 | |
| Shrinkage | warp | (['] %) | 0 | |
| | weft | (%) | 0 | |

By applying thermal bonding of the frontal side (face side) of base fabrics with the fusible interlining, a so-called "double-layer textile material" is obtained. The properties of these composite materials are presented in Table 3 [6].

Table 3. Investigated properties of the double-layer textile material

| Tested characteristic | Unit of measurement | | Test results | | |
|-----------------------|---------------------|-------|--------------|-------|--|
| | | F1I | F2I | F3I | |
| Layer thickness | (mm) | 0.754 | 0.899 | 0.889 | |
| Fabric mass per layer | (g/m²) | 273 | 360 | 319 | |

All tested samples were conditioned for 24 hours under standard atmospheric conditions at a temperature of 20 ± 2 °C and relative humidity (RH) of 65 ± 2 %.

METHODS

To determine the volume electrical resistivity (Rx, $G\Omega$) of the selected materials, a measuring device developed at the Department of Textile Engineering, Faculty of Technology and Metallurgy, University of Belgrade, was used [7, 8]. Measurements were conducted in both warp and weft directions using the stationary voltage method, i.e,. the volume electrical resistivity method [9, 10].

A schematic representation of the apparatus is shown in Figure 1.



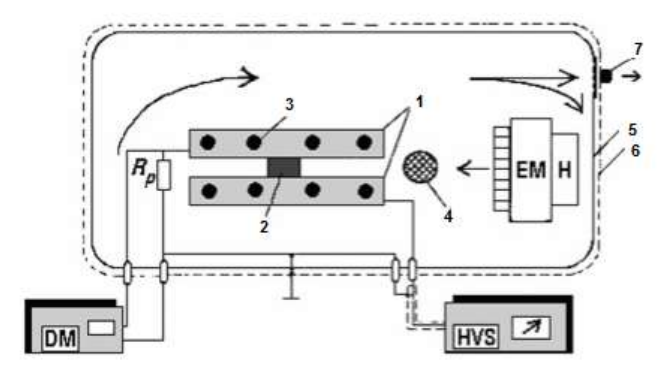


Figure 1. Schematic representation of the apparatus for determining the volume electrical resistivity of fabrics.

The fabric sample (2), with unknown electrical resistivity (Rx), is placed between the electrode plates (1) and fixed in position using tightening screws (3). The silver-coated electrode plates (1) are connected to a high-voltage source (HVS). Air humidity and temperature inside the chamber are monitored via a digital measuring device (4). The entire sample holding system is enclosed within a transparent chamber (5), which is externally covered with a metallic mesh (6), forming a Faraday cage. Humidity variation within the chamber is regulated using a humidifier (H), as well as by adjusting the aperture opening (7), which connects the chamber to the surrounding atmosphere where the measurements are conducted. Air circulation is achieved using an electric motor with a turbine wheel (EM). Voltage measurements are carried out using a digital measuring device (DM), Philips PM 2528 model.

The voltage method is based on measuring the voltage (Um) across a resistor with known resistance (Rp). This Rp is connected in series with the fabric sample of unknown electrical resistivity (Rx). The volume electrical resistivity (Rx) of the fabric sample is calculated using the following equation [5]:

$$R_x \approx \frac{R_p R_i}{R_p + R_i} \cdot \frac{E}{U_m}$$
 where: $E = 1200 \text{ V}$, $R_p = 1,64 \text{ M}\Omega \text{ i}$ $R_i = 10 \text{ M}\Omega$.

RESULTS AND DISCUSSION

The results of sample preparation indicated that both the thickness and mass of the bonded fabrics were lower than the sum of the individual layers' thickness and surface masses. The reduction of surface mass after frontal bonding usually resulted from heat- and pressure-induced densification, volatilization of moisture/finishes, fiber shrinkage or melting, and fiber loss from the surface. This can be observed by comparing the measurement results presented in Tables 1, 2, and 3. The thickness of



the frontally bonded fabric F1I was 0.131 mm less than the combined thickness of fabrics F1 and interlining I. Similarly, the thickness of F2I was 0.116 mm less than the sum of F2 and I, and the thickness of F3I was 0.146 mm less than the sum of F3 and I. The difference in thickness observed after frontal bonding of fabrics F1, F2, and F3 can be attributed to the specific bonding conditions applied during the process.

Frontal bonding is a process of adhering the fusible interlining to the base fabric. The essence of this process lies in selecting an appropriate interlayer, i.e., a compatible thermoplastic, based on the fibre composition of the base fabric, and experimentally determining optimal bonding conditions such as temperature, pressure, and dwell time in the press. Under the influence of temperature, the thermoplastic melted and penetrated the pores of the fabrics, yarns, and fibres, and then solidified upon cooling over a specified period.

These process parameters must be properly maintained; otherwise, an inadequate bond may occur, manifesting as thermoplastic penetration onto the face side of the fabric's insufficient adhesion. This process reduces the pore size within the textile structure and decreases the thickness, affecting the resulting stability of the fabrics. A reduction in the fabric's pore size can influence air and moisture permeability, which is an important factor in determining the volume electrical resistivity.

Differences in the electrical resistivity of fabrics with the same fibre composition, measured in the warp and weft directions, originate from the structural and physical-mechanical properties of the fabric and the yarns used in its construction.

Lower electrical resistivity measured in the warp direction, compared to the values measured in the weft direction, can be partially attributed to a greater number of parallel threads acting as charge carriers along the direction of the applied voltage.

Table 4. Volume electrical resistivity values of the tested fabrics

| R, GΩ | 2 | | | | | | | | |
|-------|-----------------------|-----------------------------|-------------------|----------------------------------|-------|------|------|------|------|
| Samp | Sample Surface Fabric | | | φ, (%) (Humidity in the chamber) | | | | | |
| | | mass (gm ⁻²) | thickness (mm) | 40 | 45 | 50 | 55 | 60 | 65 |
| F1 | Warp | 179 | 0.450 | 6040 | 4640 | 3600 | 2780 | 2380 | 1850 |
| | Weft | | | 6700 | 4980 | 3980 | 3220 | 2730 | 2000 |
| F2 | Warp | 264 | 0.580 | 16900 | 11480 | 9300 | 7550 | 6400 | 5170 |
| | Weft | | | 17560 | 12130 | 9760 | 8310 | 7180 | 5560 |
| F3 | Warp | 226 | 0.680 | 5120 | 3390 | 2910 | 2580 | 2370 | 2160 |
| | Weft | | | 8460 | 5040 | 4400 | 4050 | 3770 | 3350 |
| | | | | | | | | | |
| I | Warp | 99 | 0.435 | 209 | 73.8 | 47.4 | 38.0 | 32.7 | 27.0 |
| | Weft | | | 293 | 115 | 74.2 | 56.9 | 47.9 | 39.6 |
| | | | | | | | | | |
| F1I | Warp | 273 | 0.754 | 302 | 113 | 91.1 | 71.3 | 59.8 | 52.8 |
| | Weft | | | 431 | 206 | 160 | 137 | 116 | 96.6 |
| F2I | Warp | 360 | 0.899 | 890 | 394 | 318 | 221 | 176 | 139 |
| | Weft | | | 1130 | 461 | 356 | 242 | 193 | 156 |
| F3I | Warp | 319 | 0.889 | 535 | 293 | 239 | 206 | 184 | 168 |
| | Weft | | | 851 | 548 | 449 | 387 | 359 | 321 |



The results of the average volume resistivity values of the fabrics are presented. At RH of 40%, the lowest electrical resistivity was obtained in the base fabrics made from raw silk (F3), while the highest was found in the fabrics composed of synthetic and El fibres (F2). At 65% RH, fabric F1 exhibited the lowest resistivity, whereas F2 remained the fabric with the highest value. The raw silk fabric (F3) lost its advantage over the PES fabric (F1), which can be explained by the approximately twice lower density of the warp and weft of the silk fabric compared to the PES fabric (Table 1).

Frontal bonding reduces the resistivity by an order of magnitude, approximately to the level of the fusible interlining, which improves wearing comfort by reducing the tendency to accumulate static electricity. This can be attributed to the fusible interlining (71.2% Co and 28.8% PES), which, as a conductive component, assumes the role of charge transfer medium in the bond structure.

Based on the results presented in Table 4, the influence of fibre composition on the volume electrical resistivity of the tested fabrics is evident. Fabrics made from cellulose-based fibres exhibited the lowest resistivity, followed by the frontally bonded base fabrics, then those made from protein-based fibres (silk), while the highest was measured in fabrics composed of synthetic and elastane fibre blends.

The amount of moisture a textile material can absorb depends on its fibre composition. Due to their high content of hydroxyl groups, natural cellulose fibres behave as highly hydrophilic substances that form hydrogen bonds with water molecules. As water penetrates the cellulose structure, limited swelling and volumetric contraction occur, which can be explained by the dipole field in which negatively charged OH groups in cellulose attract the positively charged parts of water molecules [11, 12].

Protein fibres also possess good sorption capacities. Although silk exhibits a strong tendency to generate static electricity (comparable to PES) under dry conditions, its main protein component – fibroin rapidly absorbs moisture from the air due to high sorption ability, especially at higher RH levels. This leads to fibre swelling and a corresponding decrease in resistivity. Nevertheless, PES fabric (F1) still shows lower resistivity values, primarily due to its higher structural density.

Figures 2 to 8 illustrate the volume electrical resistivity of the base fabrics, fusible interlining, and frontally bonded fabrics as a function of RH within the testing chamber.



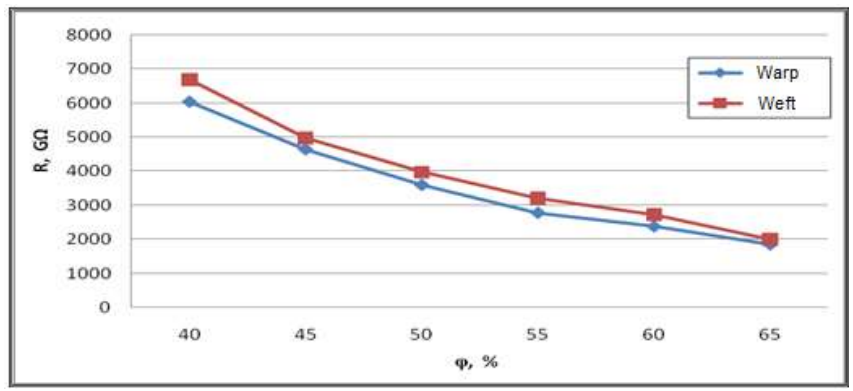


Figure 2. Dependence of the volume electrical resistivity of fabric F1 (100% PES) on air humidity

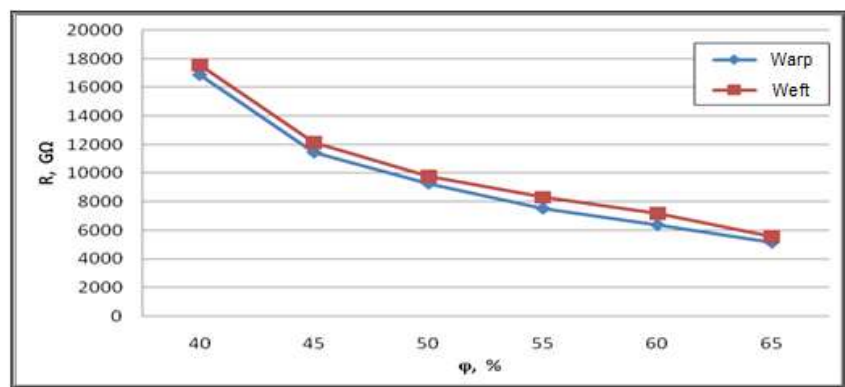


Figure 3. Dependence of the volume electrical resistivity of fabric F2 (96.1% PES and 3.9% elastane) on air humidity

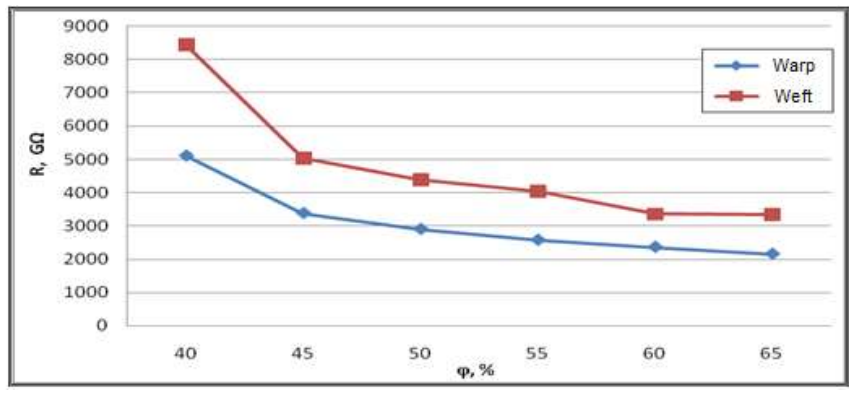


Figure 4. Dependence of the volume electrical resistivity of fabric F3 (100% silk) on air humidity



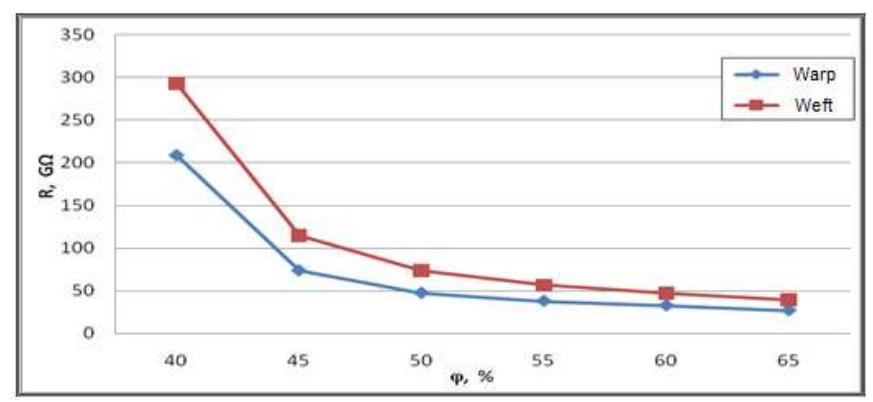


Figure 5. Dependence of the volume electrical resistivity of fabric I (71.2% cotton and 28.8% PES) on air humidity

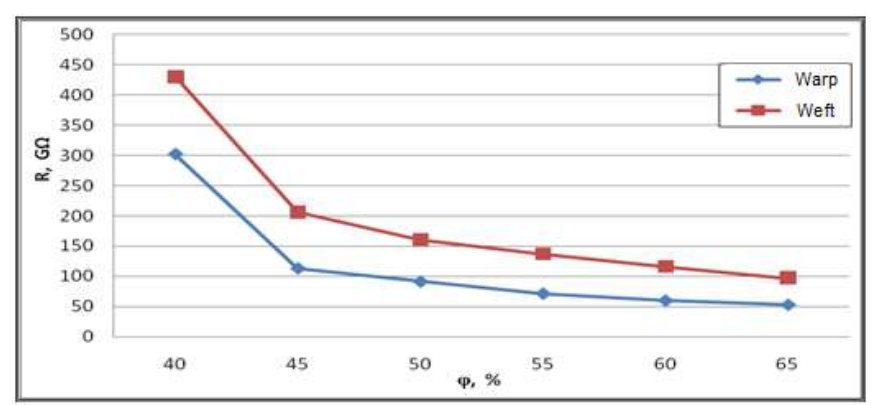


Figure 6. Dependence of the volume electrical resistivity of frontally bonded fabric F1I on air humidity

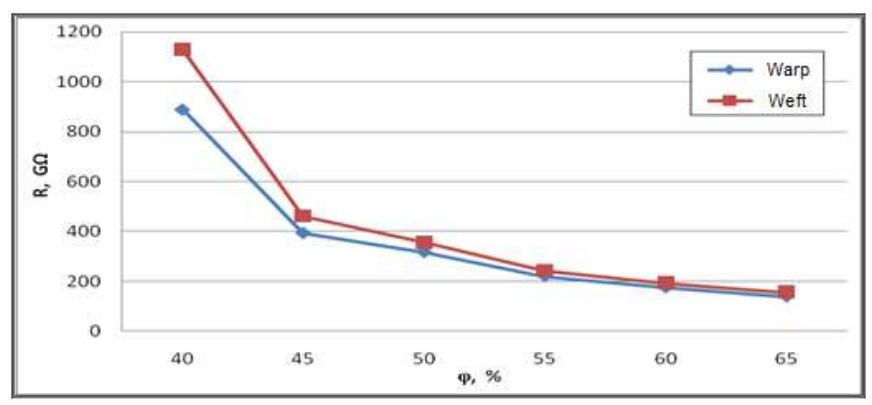


Figure 7. Dependence of the volume electrical resistivity of frontally bonded fabric F2I on air humidity



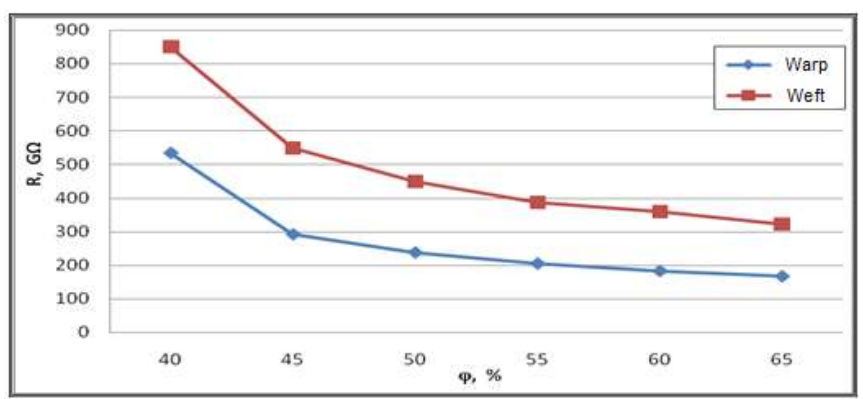


Figure 8. Dependence of the volume electrical resistivity of frontally bonded fabric F3I on air humidity

Observing figures 2 to 4, which depict the volume electrical resistivity of base fabrics as a function of air humidity, the silk F3 exhibits the largest difference between warp and weft resistivity values. This is attributed to the significant difference in fineness of these yarns. This discrepancy persists at humidity levels and is also evident in frontally bonded silk fabric F3I, as shown in Figure 8.

CONCLUSION

The obtained results demonstrated that the volume electrical resistivity primarily depends on the fibre composition and structural characteristics of the fabric. When the RH is reduced from 50% to 40%, the smallest increase in resistivity is observed in fabric F3 (100% silk). However, when RH is increased to 65%, the largest reduction in resistivity occurs in fabric T1 (PES), which can be attributed to the fact that fabric has approximately half the warp and weft density compared to the PES fabric. The highest electrical resistivity was measured in fabric F2, composed of synthetics and El fibres. The lowest resistivity was observed in the fusible interlining I (Co/PES), made of cellulose-based fibres. Frontal bonding of basic fabrics significantly reduced electrical resistance at 65% humidity, most notably in fabrics F2 (37 times in the warp direction and 35 times in the weft direction). At 40% humidity, the most significant reduction was seen in fabric F1 (20 times in the warp direction and 15 times in the weft direction). Based on these results, it can be concluded that frontal bonding with a fusible interlining significantly improves the performance of PES fabrics. Lowering the relative humidity of the environment in which the textile material is located by 25% increases the electrical resistance of the textile material sample several times. This highlights the importance of conditioning textile samples in an environment of precisely controlled humidity before measurement, to ensure accurate and reproducible results.



References

- [1] Antić, S., & Kostić, M. (2012). Određivanje atributa tekstilnih materijala u funkciji kvaliteta i komfora odeće. *Tekstilna industrija*, *60*(1), 5-13. https://scindeks.ceon.rs/article.aspx?artid=0040-23891201005A
- [2] Asanovic, K., Cerovic, D., Mihailovic, T., Kostic, M., Reljic, M. (2015). Quality of clothing fabrics in terms of their comfort properties, Indian Journal of Fibre & Textile Research, 40 (4), 363-372. Ray ID: 957e58710c55e297
- [3] Cerović, D., Asanović, K., Dojčilović, J., Mihajlidi, T., & Mihailović, T. (2008). Uticaj sirovinskog sastava i vlažnosti vazduha na elektrofizička svojstva tkanina, Beograd, XLVI Savetovanje Srpskog hemijskog društva, 21. februar, 146. ISBN 978-86-7132-035-1
- [4] Asanović, K., Mihailović, T., Kostić, M., Gajić, I., & Ivanovska, A. (2020). Uticaj termičkog fiksiranja međupostave na kvalitet odevnih tkanina ocenjen sa aspekta njihovih električnih otpornosti. *Tekstilna industrija*, 68(4), 4-11. https://doi.org/10.5937/tekstind2004004A
- [5] Kramar A., Asanović K., Obradović B., Kuraica M., Kostić M. (2018). Electrical Resistivity of Plasma Treated Viscose and Cotton Fabrics with Incorporated Metal Ions, Fibers and Polymers, 19 (3), 571-579. https://doi.org/10.1007/s12221-018-7716
- [6] Asanović, K. A., Mihailović, T. V., & Kostić, M. M. (2017). Kompresija odevnih tkanina pre i posle termičkog fiksiranja međupostave. *Tekstilna industrija*, 65(4), 11-17. https://scindeks.ceon.rs/dialogs/howToCite.aspx?articleId=004023891704011
- [7] Asanovic, K., Mihajlidi, T., Milosavljevic, S., Cerovic, D., & Dojcilovic, J. (2007). Investigation of the electrical behavior of some textile materials, *Journal of Electrostatics*, 65 (3), 162-167. https://doi.org/10.1016/j.elstat.2006.07.008
- [8] Mihajlidi, T., Asanović, K., Simić, D., Simić, M., & Ostojić, S. (2000). Određivanje električne otpornosti tekstilnih površina, *Tekstilna industrija*, 48 (11-12), 5-8. https://scindeks.ceon.rs/article.aspx?query=ISSID%26and%262574&page=3&sort=8&stype=0&backurl=%2fissue.aspx%3fissue%3d2574
- [9] Mihajlidi, T., Asanović, K., Simić, M., Simić, D., & Nikolić, D. (2002). Određivanje električne otpornosti tekstilnih materijala naponskom metodom. *Tekstilna industrija*, 50(8-10), 27-32. https://scindeks.ceon.rs/dialogs/howToCite.aspx?articleId=0040-23890210027M
- [10] Kramar, A., Asanović, K., Obradović, B., Kuraica, M., Kostić, M. (2018). Electrical resistivity of plasma treated viscose and cotton fabrics with incorporated metal ions, Fibers and Polymers, 19 (3), 571-579. https://doi.org/10.1007/s12221-018-7716-z
- [11] Georgijev, N., Nikolić, T., Radivojević, D., & Ristić, I. (2007). *Tekstilna vlakna*, Leskovac, VSŠT ISBN 978-86-81087-28-2
- [12] Škundrić, P., Kostić, M., Medović, A., Mihajlović, T., Asanović, K., & Sretković, Lj. (2008). Tekstilni materijali, Beograd, TMF, ISBN 978-86-7401-249-9



Izvod

UTICAJ RELATIVNE VLAŽNOSTI VAZDUHA NA ZAPREMINSKE ELEKTRIČNE OTPORNOSTI TKANINA NAMENJENIH ZA GORNJU ODEĆU

Slađana Antić <u>ID</u>, Suzana Đorđević <u>ID</u>, Sandra Stojanović <u>ID</u>, Tanja Nikolić <u>ID</u>, Svetomir Golubović <u>ID</u>

Akademija strukovnih studija Južna Srbija, Odsek Visoka tehnološko umetnička škola, Leskovac, Srbija

Električna otpornost tekstilnih tkanina intenzivno zavisi od sadržaja vlage u ispitivanom uzorku, što u velikoj meri opredeljuje relativna vlažnost sredine u kojoj se nalazi. Molekuli vode su u izvesnom stepenu jonizovani, tako da joni vode koji se nalaze oko tekstilnog materijala neutralizuju naelektrisanje na njegovoj površini. Sa druge strane zavisno od sirovinskog sastava, vlakna sorbuju različitu količinu vlage iz sredine koja ih okružuje što utiče na povećanje njihove elektroprovodnosti. Ovaj rad prikazuje rezultate ispitivanja zapreminske električne otpornosti za tri tkanine različitog sirovinskog sastava namenjenih za izradu ženskog blejzera (F1 - 100% PES, F2 -96.1% PES i 3.9% Elastan, F3 -100% Svila). Kod blejzera neki krojevi trebaju biti ojačani lepljivom međupostavom, tako da je iskazana potreba za dvoslojnim uzorcima. Ispitivanja su izvršena na lepljivu međupostavu (I - 71.2% Pamuk i 28.8% PES) i frontalno fiksiranim tkaninama (F1I, F2I i F3I). Električne otpornosti uzoraka merene su u pravcu osnove i potke, kod vlažnosti u komori od 40 do 65% u razmacima po 5 jedinica. Najmanju električnu otpornost kod vlažnosti od 40% poseduje F3, dok najveću F2. Kod vlažnosti od 65% najmanju otpornost pokazuje F1. a najvišu F2. tkanina od svile gubi prednost nad tkaninom od PES-a, što se može objasniti njenim konstruktivnim svojstvima. Može se zaključiti, da sniženje relativne vlažnosti sredine u kojoj se nalazi tekstilni materijal za 25% povećava njegovu električnu otpornost nekoliko puta.

Ključne reči: tkanina, sirovinski sastav, elektična otpornost.



UDK 677.494.7.072 : 677.017 DOI: 10.46793/NovelTDS16.198G

EFFECT OF TOW BREAK CONDITIONS ON THE PROPERTIES OF HIGH-BULK ACRYLIC YARN

Ferhan Gebes^{1,*} ID, İlter Sevilen¹ ID, Kenan Yıldırım² ID

¹ Ormo Yün İplik R&D Department, Fatih Mahallesi Gölyolu Harmansazı Mevkii,
Orhangazi/Bursa, Turkey,

² Bursa Technical University, EANSF Polymer Materials Engineering Department,
Yıldırım/Bursa, Turkey.

Synthesized in the 1890s and defined as a fiber containing a minimum of 85% acrylonitrile molecules by weight, acrylic fiber is primarily used in the clothing industry, in apparel products such as sweaters, dresses, suits and children's clothing. Acrylic fibers are similar to wool in terms of high elongation and elastic recovery. These elastic properties ensure that fabrics made from acrylic and wool have a soft handle. High-bulk acrylic yarn is used for hand knitting yarn due to the soft touch. It is produced by blending relax and un-relax acrylic fiber in specific proportions and spinning them into yarn. The relaxation properties of acrylic fiber are affected by tow breaking process parameters. There are 3 main effective process parameters in the tow breaking process, including oven temperature, draw ratio and breaking tension. In this study, the effect of draw ratio on the properties of acrylic yarn in the tow breaking process was investigated. According to the results, draw ratio affected hairiness and unevenness in relaxed acrylic yarns, whereas tensile strenght and softness were unaffected.

Keywords: tow breaking process, high-bulk acrylic yarn, relax and un-relax acrylic fiber, temperature, draw ratio.

INTRODUCTION

The first reported synthesis of acrylonitrile and polyacrylonitrile (PAN) dates back to the 1890s [1, 2]. Acrylic fiber is defined by the Federal Trade Commission as a fiber containing at least 85% acrylonitrile by weight [3-6]. Modacrylic fiber was defined by the

* Author address: Ferhan Gebes, Ormo Yün İplik R&D Department, Fatih Mahallesi Gölyolu Harmansazı Mevkii, No:20 16800, Orhangazi/Bursa, Turkey e-mail address: fgebes@ormo.com.tr.



same commission as a fiber containing 35-85% acrylonitrile group by weight [2, 3, 6]. With the development of staple fiber processes, acrylic fibers became a major competitor in markets where wool fibers were widely used. By 1963, the carpet and sweater markets accounted for almost 50% of the total acrylic production. The growth rate in the United States and Western Europe declined rapidly in the 1970s. This was due to the maturation of the wool substitute market and the loss of market share to nylon in carpets and to polyester in apparel industry. In the 1970s, acrylic fiber production capacity increased rapidly in Japan, Eastern Europe and developing countries [2]. This rapid growth had been driven by the advantages of acrylics, including their special properties such as wool-like appearance and handle, as well as the economic benefits provided by acrylonitrile's relatively low cost and ease of dyeability [3, 5]. In 2003, Turkey's annual acrylic fiber production capacity was approximately 277,000 tons. Aksa ranked second globally with a 9% market share. Additionally, Aksa operated the largest single - site production facility among all acrylic fiber manufacturers worldwide [2, 7, 8]. Currently, Aksa stands as Turkey's only acrylic fiber manufacturer and the world's largest in terms of production capacity. In 2023, Aksa announced that it had reached an annual acrylic fiber production capacity of 355,000 tons per year. Acrylic fibers are produced in various lengths depending on their end - use applications, including staple (discontinuous), filament (continuous), and tow forms [2, 4, 5, 9-12]. Due to their hydrophobic surface yet water - absorbing cross - section, they are predominantly used in staple form [9-12]. Depending on the intended application, staple fiber length may range from 25 mm to 150 mm. Fiber fineness ranges from 1 to 22 dtex, with 1.3 dtex, 2.2 dtex, and 3.3 dtex being the most commonly used values. The tow form is typically sold in packages of up to 2.2 million kilotex, depending on customer specifications [2, 5, 13, 14].

The cross – sectional appearance of acrylic fibers varies depending on the drawing conditions [3]. The surface of acrylic fibers is fibrillar, and the size of the fibrils varies according to the spinning process and the type of solvent used during this process [2]. The longitudinal cross -sectional appearance of acrylic fibers is smooth, crimped, and striated [4].

Acrylic fibers are similar to wool in terms of their high elongation and elastic recovery. These elastic properties contribute to a soft handle in fabrics made from both acrylic and wool. Although the tensile strength of acrylic is significantly lower than that of other synthetic fibers, it is higher than that of wool [2, 4, 5].

Polyacrylonitrile fibers are hydrophobic [3]. The moisture content of the fiber, a key factor affecting wear comfort, is approximately 2%, which is lower than that of cotton fibers (7%) and wool fibers (14%), resulting in lower comfort performance [2,5]. Due to their low moisture absorption, acrylic fibers also exhibit low electrical conductivity [2, 5, 9-12]. Among the prominent chemical properties of acrylic fibers are their strong resistance to sunlight and microorganisms [2-5]. One study found that acrylic fibers resist degradation eight times longer than olefin fibers, five times more than cotton and wool, and nearly four times more than nylon [2, 15]. Additionally, acrylic fibers show resistance to the majority of biological and chemical agents [2-4].

The main markets for acrylic fibers are apparel, home textiles, and outdoor fabrics. In the apparel sector, they are used in various knitted outerwear products such as sweaters, dresses, suits and children's clothing. Another important market for acrylic includes hand - knitting yarn, deep - pile fabrics and short socks [2, 5, 9-12].



Polyacrylonitrile fibers are also used in the production of blankets, rugs and carpets due to their good heat retention capacity (similar to wool), high resilience, low specific gravity and wrinkle resistance. In addition, due to these properties, they are utilized in places where wool fibers are especially used, in the production of knitwear and curtains, as well as in outdoor applications such as sunshades, tents and tarps, and in automotive upholstery (such as car covers), owing to their excellent resistance to sunlight [2, 3, 5].

MATERIALS AND METHODS

Within the scope of the study, 4 different machine drawing ratios were applied to 5-denier relax – un-relax acrylic tow in the tow breaking machine. The two drawing zones and the oven temperature were kept constant. The oven temperature was set to 130 $^{\circ}$ C, while the 4th drawing zone (E₄) and the 5th drawing zone (E₅) were adjusted to 1.32 and 1.47, respectively, as shown in Figure 1.

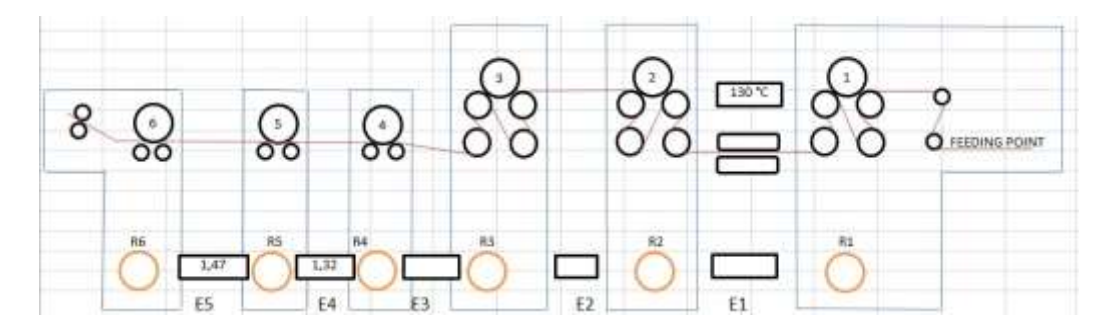


Figure 1. The oven temperature and the drawing zones in the tow breaking machine.

The fibers, in bump form, were dyed using the H. Krantz Marchinenbalt - 51 Aachen (2003) brand machine. The dyeing conditions are presented in Figure 2.



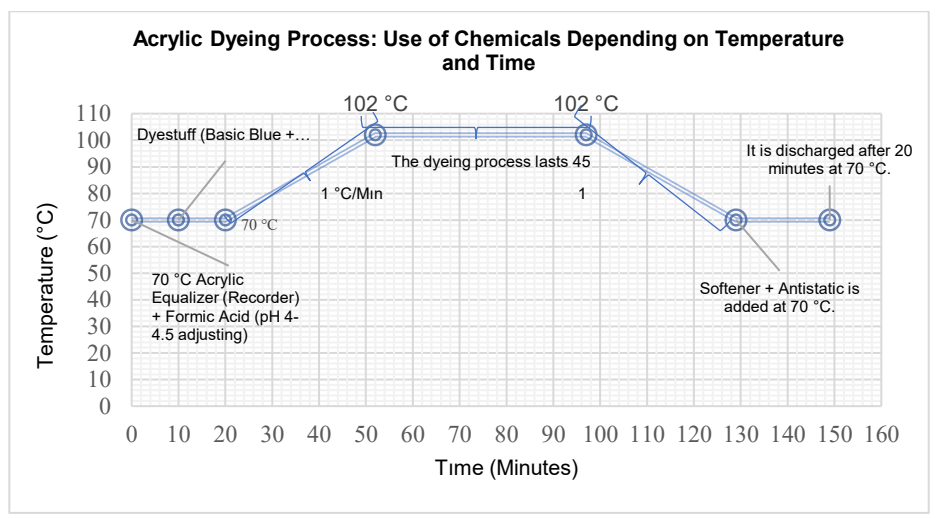


Figure 2. The conditions for dyeing acrylic fiber [16]

Following the dyeing process, the fibers were subjected to a dewatering treatment through vibration – assisted squeezing in a centrifuge machine (Oğuz Machine, 2000 model) operating at a rotational speed of 1200-1500 rpm (turns/min) for 45 minutes. Subsequently, drying was carried out in an RF – type drying machine (Sonar, 2004 model) at a temperature of 50 °C and a line speed of 18 meters per minute.

After these pre – treatment steps, the fibers were converted into drawing sliver form through a four-passage drawing process using GC 30 (NSC N. Scumberger, 2015 model) drawing machines.

The drawing slivers, which were thinned and homogeneously blended through the drafting process, were processed into single – ply yarn with a linear density of 12 Nm using a semi-worsted ring spinning system on an HDB (Houget Duesberg Bosson, 1992) model machine. During the spinning process, a twist of 184 Z-twist per meter was imparted to yarn.

Single-ply yarns were made into bobbins form using a 2005 model Japanese Muratec yarn cleaning machine, which simultaneously transferred the yarn and repaired ring - spinning breaks through air splicing.

There-ply hand knitting yarn was produced by plying on a HMX 132 (HemaksCo, 2021) model automatic plying machine at a speed of 450 rpm. The plied yarns were then twisted using a Volkmann (2002) model multi-ply twisting machine with the two-for-one technique, imparting 120 S-direction twist per meter, at a speed of 45 m/min and the spindle speed to 5400 rpm.

The yarns were heat-set in a Superba fixation machine using steam at 96-104 $^{\circ}$ C, providing twist stabilization and volume enhancement. They were then converted into cake form suitable for balling. Finally, the cakes were transformed into balls using a Gökhan Machine (2023) model balling machine.

To evaluate the physical and performance characteristics of the yarn samples, the following tests were conducted:



- Tensile strength and elongation were measured using the I.V. Calderara tensile tester in accordance with TS EN ISO 2062.
- Hairiness and unevenness were assessed using the Premier IQ5 device based on ASTM D1425 and ASTM D5647 standards,
- Boiling water shrinkage was determined according to ASTM D2259,
- Pilling behavior was evaluated in accordance with EN ISO 12945-1,
- Handle assessment was carried out based on expert tactile evaluation.

RESULTS AND DISCUSSION

The effects of draw ratio variation, resulting from the modification of the drawing rollers in the tow breaking machine, on the properties of acrylic yarns are presented in Table 1. An increase in the draw ratio from 1.3 to 1.47 led to a noticeable rise in the boiling water shrinkage values. This increase was attributed to the denser packing of the fibers and the enhancement of the yarn's bulk properties. This phenomenon can be explained by the water absorption properties of the staple structure used in acrylic fiber production, where moisture is absorbed through the fiber cross-section. The resistance of the fiber's outer surface to water affects the inward progression of moisture, promoting fiber swelling and consequently contributing to an increase in yarn bulk [9-12].

However, when the draw ratio was increased from 1.47 to 1.59 and subsequently to 1.64, a decrease in the boiling water shrinkage values was observed. This reduction was associated with the increased tension imposed on the fibers at higher draw ratios, which led to a loss in bulk properties. According to the available literature, the cross-sectional morphology of acrylic fibers changes depending on the drawing conditions, and this structural transformation significantly affects the bulk characteristics of the fiber [3]. In this context, as the draw ratio increases, the differential tension between the drawing rollers intensifies, resulting in a more stretched and flattened fiber structure. Consequently, the fiber's ability to create bulk is diminished, leading to a decline in the overall bulkiness of the yarn.

Variations in the draw ratio did not result in a significant change in yarn hairiness. This finding is consistent with the literature, which indicates that the surface characteristics of fibers are influenced more by the spinning method and the solvents used during processing than by the drawing conditions [2].

With the increase in the draw ratio, an enhancement in yarn tensile strength was observed, accompanied by a reduction in elongation. This can be attributed to the improved fiber alignment during drawing, which enhances tensile strength but simultaneously reduces elasticity due to increased structural rigidity. According to the literature, acrylic fibers exhibit higher tensile strength than wool, making them more durable; however, they are generally weaker compared to other synthetic fibers [2, 4, 5].



Table 1. Evaluation of all yarn and fabric properties at different machine draw ratios across tow, single yarn, plied yarn, ball, and fabric forms

| Single yarri, piled yarri | , ball, and fabric forn 1,30 (R1:39 – | 1,47 (R1:44 – | 1,59 (R1:46 – | 1,64 (R1:46 – |
|----------------------------|--|---------------|---------------|---------------|
| Machine draw ratio | R2:30) | R2:30) | R2:29) | R2:28) |
| | 21 | 25 | 23 | 23 |
| | 22 | 25 | 24 | 25 |
| Boiling water shrinkage | 23 | 26 | 24 | 23 |
| (tow) | 21 | 26 | 25 | 24 |
| | 22 | 26 | 25 | 24 |
| | 14,76 | 14,6 | 14,84 | 13,96 |
| Yarn hairiness (HI) | 14,54 | 13,8 | 14,5 | 14,84 |
| ram namness (m) | 14,44 | 13,76 | 14,62 | 14,87 |
| | 12,85 | 12,7 | 14,46 | 12,68 |
| Yarn unevenness CVm | 12,66 | 13,02 | 13,81 | 13,8 |
| (%) | | | | |
| . , , | 13,02 | 14,32 | 14,22 | 13,76 |
| TI: (0/50) | 0 | 0 | 20 | 0 |
| Thin (-%50) | 10 | 10 | 0 | 0 |
| | 10 | 20 | 0 | 10 |
| | 20 | 0 | 0 | 0 |
| Thick (+%50) | 20 | 0 | 0 | 0 |
| | 0 | 0 | 20 | 0 |
| | 30 | 60 | 0 | 20 |
| Neps (+%200) | 20 | 20 | 20 | 40 |
| | 50 | 30 | 20 | 10 |
| | 540 | 700 | 540 | 620 |
| | 380 | 700 | 780 | 540 |
| | 600 | 540 | 620 | 700 |
| | 700 | 540 | 540 | 860 |
| | 540 | 620 | 700 | 680 |
| Tensile strength | 540 | 620 | 540 | 700 |
| | 620 | 540 | 700 | 720 |
| | 620 | 680 | 700 | 780 |
| | 780 | 700 | 620 | 620 |
| | 700 | 620 | 620 | 700 |
| | 11 | 12 | 11 | 8 |
| | | | | 11 |
| | 8 | 12 | 11 | 9 |
| | 11 | 9 | 10 | |
| | 10 | 10 | 9 | 12 |
| Tensile elongation | 13 | 13 | 12 | 11 |
| 3 | 11 | 11 | 10 | 10 |
| | 13 | 9 | 11 | 8 |
| | 12 | 10 | 12 | 12 |
| | 13 | 13 | 10 | 10 |
| | 14 | 13 | 12 | 10 |
| Pilling – nope count | 0 | 0 | 1 | 2 |
| (fabric) 7200 turns | 0 | 1 | 1 | 2 |
| (Iddilo) 1200 tullis | 0 | 0 | 1 | 2 |
| Dilling numerical tast | 0 | 0 | 1 | 2 |
| Pilling - numerical test | 0 | 1 | 1 | 2 |
| result (fabric) 7200 turns | 0 | 0 | 1 | 2 |



| Pilling - picture test result (fabric) 7200 turns | 5 5 5 | 5 5 5 | 5 5 5 | 5 5 5 |
|--|-------------|-------------|-------------|-------------|
| Handling (based on | 5/5/4/3 | 5/5/5/5 | 5/5/4/3 | 3/3/3/3 |
| evaluations by 3 experts | 4/4/4/3 | 4/4/5/4 | 5/4/4/4 | 4/4/5/4 |
| using 4 skeins from each test sample) | 4/4/5/3 | 5/5/5/5 | 4/5/4/4 | 4/4/5/4 |

CONCLUSION

In this study, the effects of variations in the draw ratio – resulting from modifications to the drawing rollers of the tow breaking machine – on the properties of acrylic yarns were investigated. An increased draw ratio led to a rise in yarn tensile strength, while a reduction was observed in elongation at break. However, yarn hairiness was not significantly influenced by changes in the draw ratio.

The most prominent change was observed in the boiling water shrinkage, which was directly associated with its bulkiness characteristics. Increasing the draw ratio up to 1.47 resulted in a higher boiling water shrinkage, indicating the development of a bulkier fiber structure. However, when the draw ratio exceeded 1.47 and reached 1.59 and 1.64, a decrease in boiling water shrinkage was recorded, suggesting a loss in the fiber's bulk properties. These findings revealed that the volumetric response of acrylic fibers to the draw ratio had a threshold: while moderate increases enhanced bulkiness, exceeding this critical value led to a deterioration in bulk-related properties.

The obtained results revealed that the variation in draw ratio had significant effects not only on the strength of the yarn but also on the volumetric structure of the fiber. In particular, the adjustment of the draw ratio through the modification of the drawing rollers used in the tow breaking machine should be considered a critical process parameter in the production of acrylic yarns targeted for high bulk properties.

Acknowledgment

This study was supported by the Scientific and Technological Research Council of Turkey TÜBİTAK under the scope of the TEYDEB 1505 University–Industry Collaboration Support Program (Project No: 5240040), and was carried out in collaboration with ORMO Yün İplik Sanayi ve Ticaret A.Ş. and Bursa Technical University.

References

- [1] Moureau C. Annals of Chemistry and Physics, 1893. 2(7), 186.
- [2] Mark HF. *Encyclopedia of Polymer Science and Technology*.3rd ed. Acrylic Fibers, (Vol 1, pp. 135-136), (Vol 9, pp. 1-35), (Vol 10, pp. 616-617). Wool, 3rd ed. (Vol 12, pp. 546-580).
- [3] Babaoğul M, Şener A, Öztop H. *Tekstil Lifleri; Temel Özellikleri, Kullanım ve Bakım*, Yün, 2010. pp. 111-145, 209, Akrilik ve Modakrilik Lifler, 2010. pp. 235-240.



- [4] Dalgıç D. Fabric performances of high bulk acrylic and wool blends. Master's thesis, Afyon Kocatepe University, Institute of Science, Department of Textile Engineering, 2009.
- [5] Lukens RP. *Polymers: Fibers and Textiles, A Compendium,* 1960. pp. 1-45, pp. 505-536.
- [6] US Federal Trade Commission. *Rules and Regulations under the Textiles Fiber Products Identification Act.*, 1960. pp. 4.
- [7] Tiyek İ, Bozdoğan F. The importance of coagulation bath in acrylic fiber production. *Journal of Engineering Sciences*. 2005, 11(3), 319-323.
- [8] Bozdoğan F, Karacan İ, Tiyek İ. Characterisation of structure and properties of a selection of polyacrylonitrile (PAN)-based acrylic fibers produced in Turkey. *Ege Üniversitesi Tekstil ve Konfeksiyon Araştırma ve Uygulama Merkezi Yayınları*, 2004. pp. 81. ISBN 975-483-636-1.
- [9] Çolak S. S. Effect of production parameters of cut acrylic fiber and blended yarns on yarn and fabric properties. Master's thesis, Bursa Uludag University, Graduate School of Natural and Applied Sciences, Department of Textile Engineering, 2020.
- [10] Yavaşcaoğlu A. Investigation of the properties of fabrics woven from acrylic blended yarns. PhD thesis. Bursa Uludag University, Graduate School of Natural and Applied Sciences, Department of Textile Engineering, 2018.
- [11] Süpüren Mengüç G. A Research on yarn and fabric characteristics of acrylic/wool/angora blends. *Textile and Apparel.* 2016, 26(1), 40-47.
- [12] Bahtiyari İ, Akça C, Duran K. Novel Usage of Wool. *Textile and Apparel.* 2008, 1, 4-8.
- [13] Needles HL. Handbook of Textile Fibers, Dyes and Finishes, 1981.
- [14] Moncrieff RW. Man-Made Fibers. 1975.
- [15] Teige W. Chemiefasern/Textilind. 1983, 33(85), 636.
- [16] Gebeş F. Investigation of the effects of wool fiber ratio in yarn composition on yarn properties. Master's thesis, Bursa Technical University, Department of Polymer Materials Engineering, 2024.

Izvod

UTICAJ PROCESNIH PARAMETARA RROIZVODNJE NA SVOJSTVA AKRILNE PREĐE VELIKE GUSTINE

Ferhan Gebes^{1,*} <u>ID</u>, İlter Sevilen¹ <u>ID</u>, Kenan Yıldırım² <u>ID</u>

¹Ormo Yün İplik Odeljenje za istraživanje i razvoj, Fatih Mahallesi Gölyolu Harmansazı Mevkii, Orhangazi/Bursa, Turska,

²Tehnički univerzitet u Bursi, EANSF Odsek za inženjerstvo polimernih materijala, Yıldırım/Bursa, Turska.

Sintetisano 1890-ih i definisano kao vlakno koje sadrži najmanje 85% molekula akrilonitrila po težini, akrilno vlakno se prvenstveno koristi u industriji odeće, u odevnim



proizvodima kao što su džemperi, haljine, odela i dečija garderoba. Akrilno vlakno je slično vuni po svojoj elastičnosti. Zbog ovih elastičnih svojstava, tkanine napravljene od akrila i vune su meke na dodir. Zbog svoje mekoće, akrilna pređa velike gustine koristi se za ručno pletenje. Ona se proizvodi kombinovanjem relaksiranih i nerelaksiranih akrilnih vlakana u određenim razmerama i njihovim upredanjem. Proces istezanja utiče na relaksaciona svojstva akrilne pređe. Postoje 3 glavna parametra ovog procesa, uključujući temperaturu, stepen istezanja i prekidnu silu pređe. U ovoj studiji istraživan je uticaj stepena istezanja na svojstva akrilne pređe. Prema rezultatima ove studije, stepen istezanja uticao je na svojstva relaksiranih akrilnih vlakana, uključujući maljavost i neravnomernost, dok su zatezna čvrstoća i mekoća ostali nepromenjeni.

Ključne reči: Istezanje, akrilna pređa velike gustine, relaksirana i nerelaksirana akrilna vlakna, temperatura, stepen istezanja





UDK 640.4 (497-15)

DOI: 10.46793/NovelTDS16.209C

HOSPITALITY 4.0 IN THE WESTERN BALKANS: TECHNOLOGICAL INNOVATION FOR A SUSTAINABLE FUTURE

Drago Cvijanović¹ ID, Aleksandra Vujko^{2,*} ID, Božo Ilić² ID

¹Faculty of Hotel Management and Tourism in Vrnjačka Banja, University of Kragujevac, Sebia

² Faculty of Tourism and Hospitality Management, Singidunum University, Belgrade, Serbia

³ Academy of Vocational Studies Šumadija, Department Aranđelovac, Serbia

This study investigates the relationship between hotel location and employee familiarity with the concept and technologies of Hospitality 4.0 across five Western Balkan countries: Albania, Bosnia and Herzegovina, Montenegro, North Macedonia, and Serbia. Using a structured questionnaire and chi-square tests on a sample of 250 hotel employees, the research examines five key variables: familiarity with Hospitality 4.0, understanding of associated technologies, managerial support for its principles, perceived transformative impact, and alignment with future tourism trends. The findings reveal statistically significant associations between country and all five variables (p < 0.001 in most cases), indicating that national context significantly influences both awareness and adoption of Hospitality 4.0. The respondents from Albania and Bosnia and Herzegovina demonstrated the highest levels of familiarity and organizational support, while Montenegro and North Macedonia exhibited lower levels of awareness and engagement. Serbia showed internal disparities, with both high and low levels of agreement. These results point to uneven progress in digital transformation within the hospitality sector in the region. The study underscores the need for targeted policy interventions, industry training programs, and cross-country knowledge sharing to support a cohesive transition toward Hospitality 4.0. This research contributes to understanding regional dynamics of technological adoption in hospitality and offers practical insights for advancing innovation in hotel management.

Keywords: Hospitality 4.0; Western Balkans; hotel industry; digital transformation; smart tourism; innovation; chi-square analysis; regional development

* Author address: Aleksandra Vujko, Faculty of Tourism and Hospitality Management, Singidunum University, Belgrade, Sebia e-mail address: avujko@singidunum.ac.rs



INTRODUCTION

The hospitality industry is undergoing a transformative phase known as Hospitality 4.0, characterized by the integration of advanced technologies and innovative practices aimed at enhancing customer experiences while simultaneously fostering sustainable development [1]. This evolution is not merely a response to changing consumer preferences; it is a proactive approach to redefining service delivery in a sector that is increasingly influenced by digitalization. As the industry navigates the complexities of a post-pandemic world, the significance of Hospitality 4.0 becomes apparent, illuminating pathways toward operational efficiency, personalized customer interactions, and environmentally responsible practices [2].

Hospitality 4.0 represents a paradigm shift in the way the hospitality industry operates, integrating cutting-edge technologies to enhance service delivery and customer experiences. At its core, Hospitality 4.0 is defined by its incorporation of digital tools and data-driven strategies to streamline operations and elevate guest satisfaction [3]. This evolution encompasses a wide scope of innovations, including the Internet of Things (IoT), cloud computing, and augmented reality (AR), all of which contribute to a more interconnected and responsive hospitality ecosystem [4]. According to Vongvisitsin & Tung [5], hotels are now utilizing IoT devices to provide guests with personalized room controls, allowing them to adjust lighting, temperature, and entertainment systems through their smartphones. The impact of Hospitality 4.0 on customer experience is profound, as it not only facilitates a more seamless and enjoyable stay but also enables service providers to anticipate and cater to individual preferences. This shift is evident in the use of mobile applications that allow guests to check in remotely, access room keys digitally, and even order room service with a few taps, thereby enhancing convenience and efficiency in service delivery [6].

Central to the success of Hospitality 4.0 are the technological innovations that drive its implementation, prominently featuring Artificial Intelligence (AI) and Machine Learning. These technologies are revolutionizing customer service by enabling businesses to offer personalized experiences that were previously unattainable. According to Vujko et al., [7], AI-powered chatbots provide instant support to guests, answering queries and resolving issues in real-time, which significantly enhances customer satisfaction. According to Skorupan et al., [8], machine learning algorithms analyze vast amounts of customer data to generate tailored recommendations, whether for dining options, local attractions, or personalized deals. This level of personalization not only fosters loyalty among guests but also enhances operational efficiency, as businesses can optimize marketing strategies based on consumer behavior patterns. According to Valdez-Juárez et al., [9], data analytics plays a crucial role in refining operational processes; for instance, hotels can utilize predictive analytics to forecast demand and manage inventory more effectively, ensuring that resources are allocated efficiently and reducing waste.

The intersection of technology and sustainability is a pivotal aspect of Hospitality 4.0, as the industry seeks to mitigate its environmental impact while enhancing service delivery. Technological advancements are instrumental in promoting sustainable practices, with energy-efficient systems and smart building technologies leading the way. According to



Stylos et al., [10], hotels are increasingly adopting smart thermostats and lighting systems that adjust according to occupancy, significantly reducing energy consumption. According to Ogiemwonyi et al., [11], waste reduction technologies, such as smart recycling bins equipped with sensors that monitor waste levels, empower establishments to manage resources more effectively and minimize landfill contributions. Initiatives like these not only improve operational sustainability but also resonate with environmentally conscious consumers, who are increasingly prioritizing eco-friendly practices in their travel choices [12]. By integrating these innovative technologies, the hospitality sector can align itself with global sustainability goals, ensuring a more responsible and resilient future.

The research started from the starting hypothesis of the paper H: that hotel stakeholders with a higher level of recognition of the Hospitality 4.0 concept demonstrate greater readiness for its implementation. The aim of this study is to explore how well hotel stakeholders recognize the key components of Hospitality 4.0 and to assess their readiness—technological, financial, and organizational—for integrating smart, digital, and automated solutions aligned with the Hospitality 4.0 paradigm. According to this, the main objective of the paper is to evaluate the level of awareness, understanding, and preparedness of hotel stakeholders regarding the concept of Hospitality 4.0 and its potential implementation within hotel operations.

MATERIAL AND METHODS

To fulfill the aim of exploring how well hotel stakeholders recognize the key components of Hospitality 4.0 and assessing their technological, financial, and organizational readiness for integrating smart, digital, and automated solutions, this study employed a quantitative research design. A total of 73 hotel managers and owners participated in the research. The study was conducted across prominent mountain destinations in the Western Balkans, a region comprising Albania, Bosnia and Herzegovina, Montenegro, North Macedonia, and Serbia. Known for its rich cultural heritage and complex sociopolitical history, the Western Balkans is a growing tourism region with increasing interest in digital transformation [13].

The hotels included in the study were selected based on their recognition and popularity among tourists, ensuring the sample reflected the most frequented and competitive establishments in the region. Geographically, the study covered hotels located on Korab Mountain (Albania and North Macedonia), Radomire Village and Tomor Mountain (Albania), Zlatibor, Tara, Kopaonik, and Stara Planina (Serbia), Brezovica (Kosovo and Metohija), Durmitor (Montenegro), and Jahorina (Bosnia and Herzegovina).

Participants received a structured questionnaire via email, consisting of 10 Likert-scale statements. These statements were grouped to measure two primary dimensions:

Recognition of the Hospitality 4.0 concept — including awareness of its technologies (e.g., IoT, AI, robotics) and strategic importance (I am familiar with the concept of Hospitality 4.0 and its relevance to the hotel industry; I understand the technologies commonly associated with Hospitality 4.0 (e.g., AI, IoT, robotics, smart rooms); Our hotel management has discussed or introduced the principles of Hospitality 4.0.; I believe that Hospitality 4.0 represents a significant



shift in how hotels operate and deliver services; Hospitality 4.0 aligns with current trends and future demands in the tourism and hotel industry).

Responses were measured using a five-point Likert scale, ranging from Strongly Disagree (1) to Strongly Agree (5). The data were analyzed using descriptive statistics to summarize stakeholders' levels of recognition and readiness. To examine potential associations between the location of the hotel (by country or region) and the observed levels of readiness and concept recognition, the Pearson Chi-Square test was employed. This allowed the identification of statistically significant variations based on geographic context.

RESULTS AND DISCUSSION

The results reveal that the implementation of Hospitality 4.0 in the Western Balkans remains uneven, with varying degrees of technological awareness and organizational readiness among hotel stakeholders. These disparities suggest that while the potential for digital transformation exists, systemic barriers—such as limited investment, insufficient training, and policy support—must be addressed to fully leverage the benefits of Hospitality 4.0 in the region.

Familiarity with the Concept of Hospitality 4.0

The first statement, "I am familiar with the concept of Hospitality 4.0 and its relevance to the hotel industry," reveals statistically significant variation across the countries (χ^2 = 72.298, df = 16, p < 0.001). The respondents from Albania and Bosnia and Herzegovina (BiH) are more likely to strongly agree or agree with the statement, in contrast to those from Montenegro, North Macedonia, and Serbia, where a higher proportion of respondents selected disagree, strongly disagree, or no opinion. This implies uneven dissemination or adoption of the Hospitality 4.0 concept across the region. In Serbia, despite having the largest sample size (28.8%), there is a notable concentration of negative or neutral responses. The high percentage of "no opinion" in North Macedonia and Serbia may indicate a knowledge gap or lack of exposure to digital transformation strategies in the hospitality sector.

- Implication: There is a need for targeted awareness and capacity-building initiatives, particularly in countries where technological innovation is still perceived as peripheral to hotel operations.

Understanding of Technologies Associated with Hospitality 4.0

The second item, "I understand the technologies commonly associated with Hospitality 4.0 (e.g., AI, IoT, robotics, smart rooms)," also shows significant differences (χ^2 = 52.935, df = 16, p < 0.001). Albania again stands out with a high level of strong agreement, indicating a relatively advanced understanding of Hospitality 4.0 technologies. Montenegro and Bosnia and Herzegovina (BiH), in contrast, show higher levels of uncertainty or disagreement, reflecting a potential lack of technical training or limited exposure to practical applications of such technologies. Serbia shows a more polarized distribution, with the respondents both agreeing and disagreeing, suggesting internal disparities in hotel innovation practices.



- Implication: These results highlight a potential skills gap that could hinder the adoption of smart solutions in hotel management, especially in countries still lagging in digital innovation infrastructure or education.

Organizational Support for Hospitality 4.0 Principles

The third statement, "Our hotel management has discussed or introduced the principles of Hospitality 4.0," yielded the strongest statistical result (χ^2 = 81.403, df = 16, p < 0.001), confirming a highly significant relationship between the country and whether the management fosters discussion on innovation. The respondents from Serbia and Albania reported higher agreement, suggesting some progress toward institutional adoption in those countries.

However, BiH and Montenegro show concerning levels of either no opinion or disagreement, pointing to a disconnect between frontline staff and upper management on innovation priorities. The very high proportion of "strong disagree" in North Macedonia (50%) raises concern about the complete lack of strategic engagement with digital transformation in that context.

- Implication: For Hospitality 4.0 to take root, top-down initiatives must be paired with inclusive, organization-wide discussions. Institutional inertia or lack of communication can stall progress, even in environments with technically capable staff.

Perceived Transformative Impact of Hospitality 4.0

The fourth statement, "I believe that Hospitality 4.0 represents a significant shift in how hotels operate and deliver services," maintains statistical significance (χ^2 = 44.340, df = 16, p < 0.001), although to a slightly lesser degree. A strong affirmative trend is observed in BiH and Albania, where Hospitality 4.0 is more likely to be perceived as transformative. The respondents from Serbia show a divided perception, with some recognizing the shift and others expressing disagreement or no opinion. Again, Montenegro and North Macedonia appear less convinced of the importance of digital transformation.

- Implication: Belief in the relevance of Hospitality 4.0 appears to correlate with prior exposure to or engagement in technology-driven service delivery. This confirms the role of experiential learning and national digital ecosystems in shaping staff attitudes.

Alignment with Industry Trends and Future Demands

The statement "Hospitality 4.0 aligns with current trends and future demands in the tourism and hotel industry," is also statistically significant ($\chi^2 = 30.547$, df = 16, p = 0.015), though the strength of association is weaker than previous items. While the majority of the respondents from BiH and Montenegro agree with the alignment, disagreement is strongest among the respondents from Serbia. The notable level of "no opinion" responses in North Macedonia again indicates either ambivalence or insufficient understanding.

-Implication: Perceptions of alignment with future trends may depend not only on internal management decisions but also on national tourism strategies and the visibility of digital innovations within a country's broader hospitality and tourism ecosystem.



| | | | | | .0 by Hotel Lo otel is located | | | Total |
|---|-----------------------------|--|---|--|--|---------------------------------------|------------------------------|--|
| | | | Albania | BiH | Montenegro | North Macedonia | Serbia | |
| I am | Strongly | Count | 4 | 3 | 0 | 0 | 0 | 7 |
| familiar with | agree | % of Total | 5,5% | 4,1% | 0,0% | 0,0% | 0,0% | 9,6% |
| the concept | Agree | Count | 1 | 4 | 7 | 0 | 3 | 15 |
| of | | % of Total | 1,4% | 5,5% | 9,6% | 0,0% | 4,1% | 20,5% |
| Hospitality | No | Count | 0 | 0 | 1 | 9 | 10 | 20 |
| 4.0 and its | opinion | % of Total | 0,0% | 0,0% | 1,4% | 12,3% | 13,7% | 27,4% |
| relevance to the hotel | Disagree | Count | 0 | 3 | 4 | 5 | 8 | 20 |
| industry. | | % of Total | 0,0% | 4,1% | 5,5% | 6,8% | 11,0% | 27,4% |
| madou y. | Strongly | Count | 6 | 5 | 0 | 0 | 0 | 11 |
| | disagree | % of Total | 8,2% | 6,8% | 0,0% | 0,0% | 0,0% | 15,1% |
| Total | | Count | 11 | 15 | 12 | 14 | 21 | 73 |
| | | % of Total | 15,1% | 20,5% | 16,4% | 19,2% | 28,8% | 100,0% |
| | | Value | df | | tic Significance (2 | -sided) | | |
| Pearson Chi- | Square | 72,298 ^a | 16 | ,000 | | | | T |
| | | | | | otel is located | T | | Total |
| | | | Albania | BiH | Montenegro | North Macedonia | Serbia | |
| 1 | Strongly | Count | 6 | 3 | 0 | 4 | 2 | 15 |
| understand | agree | % of Total | 8,2% | 4,1% | 0,0% | 5,5% | 2,7% | 20,5% |
| the | Agree | Count | 4 | 8 | 2 | 1 | 4 | 19 |
| technologie | | % of Total | 5,5% | 11,0% | 2,7% | 1,4% | 5,5% | 26,0% |
| s commonly | No | Count | 1 | 4 | 8 | 4 | 2 | 19 |
| associated with | opinion | % of Total | 1,4% | 5,5% | 11,0% | 5,5% | 2,7% | 26,0% |
| Hospitality | Disagree | Count | 0 | 0 | 2 | 5 | 7 | 14 |
| 4.0 (e.g., | | % of Total | 0,0% | 0,0% | 2,7% | 6,8% | 9,6% | 19,2% |
| AI, IoT, | Stronglydi | Count | 0 | 0 | 0 | 0 | 6 | 6 |
| robotics, smart rooms). | sagree | % of Total | 0,0% | 0,0% | 0,0% | 0,0% | 8,2% | 8,2% |
| Total | | Count | 11 | 15 | 12 | 14 | 21 | 73 |
| | | % of Total | 15,1% | 20,5% | 16,4% | 19,2% | 28,8% | 100,0% |
| | | Value | df | | tic Significance (2 | | | 100,011 |
| Pearson Chi- | Square | 52,935 ^a | 16 | .000 | g (= | | | |
| | | | | , | otel is located | | | Total |
| | | | Albania | BiH | Montenegro | North Macedonia | Serbia | Total |
| Our hotel | Strongly | Count | 2 | 4 | 2 | 1 | 8 | 17 |
| manageme | agree | % of Total | 2,7% | 5,5% | 2,7% | 1,4% | 11,0% | 23,3% |
| nt has | Agree | Count | 8 | 0 | 0 | 1,470 | 2 | 11 |
| discussed | Agree | % of Total | 11,0% | 0,0% | 0,0% | 1,4% | 2,7% | |
| | No | % of Total | | | | | | 15,1% |
| or | No | i Count | 0 | 10 | 3 | 0 | 2 | 15 |
| or introduced | oninian | | 0.001 | 40 === | 4 407 | 0.00/ | | 20,5% |
| or introduced the | opinion | % of Total | 0,0% | 13,7% | 4,1% | 0,0% | 2,7% | |
| or introduced the principles of | opinion Disagree | | 0,0% | 13,7% | 7 | 0,0% 5 | 2,7% | 18 |
| or introduced the principles of Hospitality | | % of Total | | | | | | |
| or introduced | | % of Total Count | 1 | 1 | 7 | 5 | 4 | 18 |
| or introduced the principles of Hospitality | Disagree | % of Total Count % of Total Count | 1 1,4% 0 | 1 1,4% 0 | 7 9,6% 0 | 5 6,8% 7 | 4 5,5% 5 | 18 24,7% 12 |
| or introduced the principles of Hospitality 4.0. | Disagree | % of Total Count % of Total Count % of Total % of Total | 1 1,4% 0 0,0% | 1 1,4% 0 0,0% | 7 9,6% 0 0,0% | 5 6,8% 7 9,6% | 4 5,5% 5 6,8% | 18 24,7% 12 16,4% |
| or introduced the principles of Hospitality 4.0. | Disagree | % of Total Count % of Total Count | 1 1,4% 0 | 1 1,4% 0 | 7 9,6% 0 | 5 6,8% 7 | 4 5,5% 5 | 18 24,7% 12 |
| or introduced the principles of Hospitality | Disagree | % of Total Count % of Total Count % of Total Count % of Total Count % of Total | 1 1,4% 0 0,0% 11 15,1% | 1 1,4% 0 0,0% 15 20,5% | 7 9,6% 0 0,0% 12 16,4% | 5 6,8% 7 9,6% 14 19,2% | 4 5,5% 5 6,8% 21 | 18 24,7% 12 16,4% 73 |
| or introduced the principles of Hospitality 4.0. | Disagree Strongly disagree | % of Total Count % of Total Count % of Total Count % of Total Count % of Total Value | 1 1,4% 0 0,0% 11 15,1% | 1 1,4% 0 0 0,0% 15 20,5% Asympto | 7 9,6% 0 0,0% 12 | 5 6,8% 7 9,6% 14 19,2% | 4 5,5% 5 6,8% 21 | 18 24,7% 12 16,4% 73 |
| or introduced the principles of Hospitality 4.0. | Disagree Strongly disagree | % of Total Count % of Total Count % of Total Count % of Total Count % of Total | 1 1,4% 0 0,0% 11 15,1% df | 1 1,4% 0 0,0% 15 20,5% Asympto | 7 9,6% 0 0,0% 12 16,4% tic Significance (2 | 5 6,8% 7 9,6% 14 19,2% | 4 5,5% 5 6,8% 21 | 18 24,7% 12 16,4% 73 100,0% |
| or introduced the principles of Hospitality 4.0. | Disagree Strongly disagree | % of Total Count % of Total Count % of Total Count % of Total Count % of Total Value | 1 1,4% 0 0,0% 11 15,1% df | 1 1,4% 0 0,0% 15 20,5% Asympto | 7 9,6% 0 0,0% 12 16,4% | 5 6,8% 7 9,6% 14 19,2% | 4 5,5% 5 6,8% 21 | 18 24,7% 12 16,4% 73 |



| I believe that | Strongly agree | % of Total | 6,8% | 8,2% | 1,4% | 2,7% | 5,5% | 24,7% | |
|------------------------|--|------------|-------------|-----------------------------------|--------------------------|--------------------|--------|--------|--|
| Hospitality | Agree | Count | 0 | 1 | 5 | 2 | 5 | 13 | |
| 4.0 | | % of Total | 0,0% | 1,4% | 6,8% | 2,7% | 6,8% | 17,8% | |
| represents | No | Count | 0 | 1 | 4 | 8 | 3 | 16 | |
| a significant | opinion | % of Total | 0,0% | 1,4% | 5,5% | 11,0% | 4,1% | 21,9% | |
| shift in how hotels | Disagree | Count | 2 | 3 | 0 | 0 | 9 | 14 | |
| operate and | | % of Total | 2,7% | 4,1% | 0,0% | 0,0% | 12,3% | 19,2% | |
| deliver | Strongly | Count | 4 | 4 | 2 | 2 | 0 | 12 | |
| services. | disagree | % of Total | 5,5% | 5,5% | 2,7% | 2,7% | 0,0% | 16,4% | |
| Total | | Count | 11 | 15 | 12 | 14 | 21 | 73 | |
| | | % of Total | 15,1% | 20,5% | 16,4% | 19,2% | 28,8% | 100,0% | |
| | | Value | df | Asymptotic Significance (2-sided) | | | • | | |
| Pearson Chi-S | Pearson Chi-Square 44,340 ^a | | | ,000 | | | | | |
| | | | The place v | where the ho | ere the hotel is located | | | Total | |
| | | | Albania | BiH | Montenegro | North Macedonia | Serbia | | |
| Hospitality | Strongly agree | Count | 1 | 5 | 2 | 4 | 0 | 12 | |
| 4.0 aligns | | % of Total | 1,4% | 6,8% | 2,7% | 5,5% | 0,0% | 16,4% | |
| with current | Agree | Count | 5 | 5 | 6 | 1 | 4 | 21 | |
| trends and future | _ | % of Total | 6,8% | 6,8% | 8,2% | 1,4% | 5,5% | 28,8% | |
| demands in | No | Count | 4 | 1 | 1 | 5 | 3 | 14 | |
| the tourism | opinion | % of Total | 5,5% | 1,4% | 1,4% | 6,8% | 4,1% | 19,2% | |
| and hotel | Disagree | Count | 0 | 3 | 3 | 2 | 10 | 18 | |
| industry. | _ | % of Total | 0,0% | 4,1% | 4,1% | 2,7% | 13,7% | 24,7% | |
| | Strongly | Count | 1 | 1 | 0 | 2 | 4 | 8 | |
| | disagree | % of Total | 1,4% | 1,4% | 0,0% | 2,7% | 5,5% | 11,0% | |
| Total | | Count | 11 | 15 | 12 | 14 | 21 | 73 | |
| | | % of Total | 15,1% | 20,5% | 16,4% | 19,2% | 28,8% | 100,0% | |
| | Value | | | Asymptotic Significance (2-sided) | | | | • | |
| Pearson Chi-S | Square | 30,547a | 16 | ,015 | | | | | |

The results across all five items indicate that national context significantly influences attitudes and knowledge related to Hospitality 4.0. The consistent statistical significance (p < 0.001 in most cases) confirms that the country in which a hotel operates plays a major role in shaping awareness, organizational integration, and perceived value of technological innovation in hospitality. This points to several policy and managerial recommendations: National tourism authorities should invest in raising awareness of Hospitality 4.0 principles through conferences, training, and public-private partnerships; Hotel management must foster innovation cultures, ensuring that employees at all levels are informed, trained, and empowered to participate in digital transformation. Cross-border collaboration and knowledge sharing could help less advanced markets

learn from more proactive countries in the region, such as Albania or BiH.

CONCLUSION

In conclusion, Hospitality 4.0 embodies a crucial evolution within the hospitality industry, driven by technological innovation and a commitment to sustainability. As the sector adapts to the demands of modern travelers, it is evident that advancements such as Al, data analytics, and smart technologies are central to enhancing customer experiences and improving operational efficiencies. Moreover, the integration of sustainable practices through these technological innovations not only addresses environmental concerns but



also meets the growing expectations of eco-conscious consumers. As the hospitality industry continues to evolve in the face of ongoing challenges, embracing the principles of Hospitality 4.0 will be essential for creating a sustainable and customer-centric future. This transformative journey highlights the potential of technology not only to redefine service delivery but also to pave the way for a more sustainable and responsible hospitality landscape.

The findings of this study highlight a significant disparity in awareness and readiness for Hospitality 4.0 among hotel stakeholders across five Western Balkan countries. While Albania and Bosnia and Herzegovina show relatively higher levels of familiarity and openness to digital transformation in hospitality, other countries—particularly Montenegro, North Macedonia, and Serbia—exhibit a mix of limited knowledge, uncertainty, and organizational hesitation. These regional differences reflect broader structural and developmental disparities in digital infrastructure, investment capacities, and education systems.

Practical implications include the need for targeted capacity-building initiatives such as national training programs, transnational cooperation, and cross-sectoral workshops that bridge the knowledge and technological gaps. Policy-makers should facilitate access to funding for technological upgrades and support public-private partnerships aimed at fostering innovation. Hotel managers are encouraged to engage in strategic planning and workforce reskilling to improve technological readiness and adapt to emerging customer expectations.

From an operational perspective, a proactive integration of Hospitality 4.0 technologies—such as AI, IoT, and robotics—could help hotels streamline operations, enhance guest experience, and increase competitiveness, particularly in post-pandemic recovery contexts where digital touchpoints have become increasingly critical.

Limitations of this study include the relatively small and uneven sample size across countries, which may affect generalizability. In addition, the reliance on self-reported data may introduce subjectivity and social desirability bias. Future research should expand the sample, include qualitative interviews with hotel managers and IT specialists, and explore longitudinal data to monitor the evolution of Hospitality 4.0 adoption over time in the region.

Acknowledgement:

This research is supported by the Ministry of Science, Technological Development and Innovation of the Republic of Serbia by the Decision on the scientific research funding for teaching staff at the accredited higher education institutions in 2025 (No. 451-03-137/2025-03/200375 of February 4, 2025).

References

[1] Alam SS, Kokash HA, Ahsan MN, Ahmed S. Relationship between technology readiness, Al adoption and value creation in hospitality industry: Moderating role of technological turbulence. *International Journal of Hospitality Management*. 2025, 127, 104133. https://doi.org/10.1016/i.ijhm.2025.104133



- [2] Fakfare P, Manosuthi N, Lee J-S, Han H, Jin M. Customer word-of-mouth for generative Al: Innovation and adoption in hospitality and tourism. *International Journal of Hospitality Management*. 2025, 126, 104070. https://doi.org/10.1016/j.ijhm.2024.104070
- [3] Shang D, Wu W, Ji Y. Understanding employee digital learning engagement and innovative work behavior in hospitality sectors: A machine learning based multistage approach. *International Journal of Hospitality Management*. 2025, 125, 103985. https://doi.org/10.1016/j.ijhm.2024.103985
- [4] Martin-Rios C, Ciobanu T. Hospitality innovation strategies: An analysis of success factors and challenges. *Tourism Management*. 2019, 70, 218-229. https://doi.org/10.1016/j.tourman.2018.08.018
- [5] Vongvisitsin TB, Tung VWS. Technology start-ups in tourism and hospitality: A networked social capital theory perspective from early-stage start-up founders. *Tourism Management*. 2025, 106, 104996. https://doi.org/10.1016/j.tourman.2024.104996
- [6] Maiti M, Kayal P, Vujko A. A study on ethical implications of artificial intelligence adoption in business: Challenges and best practices. *Future Business Journal*. 2025, 11:34. https://doi.org/10.1186/s43093-025-00462-5
- [7] Vujko A, Papović Z, Cvijanović D. Artificial intelligence and its influence on sustainable travel agencies business: The role of chatbots in creating tourist arrangements. *Ekonomika*. 2025, 71(1), 1-15. https://doi.org/10.5937/ekonomika2501001V
- [8] Skorupan A, Vujko A, Bjelić K. The hotel industry role in terms of achieving tourism destination sustainability: Challenges and best practices. *Serbian Journal of Engineering Management*. 2025, 10(1), 68-78. https://doi.org/10.5937/SJEM2501068S
- [9] Valdez-Juárez LE, Ramos-Escobar EA, Rui-Zamora JA, Borboa-Álvarez EP. Drivers and pressures of industry 4.0 that generate marketing innovation and affect the innovative performance of Mexican SMEs: From the perspective of open innovation. *Journal of Open Innovation: Technology, Market, and Complexity*. 2025, 11(2), 100541. https://doi.org/10.1016/j.joitmc.2025.100541
- [10] Stylos N, Fotiadis AK, Shin DD, Huan T-C. Beyond smart systems adoption: Enabling diffusion and assimilation of smartness in hospitality. *International Journal of Hospitality Management*. 2021, 98, 103042. https://doi.org/10.1016/j.ijhm.2021.103042 [11] Ogiemwonyi O, Alam MN, Hago IE, Azizan NA, Hashim F, Hossain MS. Green innovation behaviour: Impact of industry 4.0 and open innovation. *Heliyon*. 2023, 9(6), e16524. https://doi.org/10.1016/j.heliyon.2023.e16524
- [12] Caiado RGG, Machado E, Santos RS, Thomé AMT, Scavarda LF. Sustainable I4.0 integration and transition to I5.0 in traditional and digital technological organisations. *Technological Forecasting and Social Change*. 2024, 207, 123582. https://doi.org/10.1016/j.techfore.2024.123582
- [13] Knežević M, Pindžo R, Ćulić M, Kovačić S, Dunjić M, Vujko A. Sustainable (re)development of tourism destinations as a pledge for the future a case study from the Western Balkans. *GeoJournal of Tourism and Geosites*. 2024, 56(4), 1564-1575. https://doi.org/10.30892/gtg.56413-1327



Izvod

HOSPITALITY 4.0 NA ZAPADNOM BALKANU: TEHNOLOŠKE INOVACIJE ZA ODRŽIVU BUDUĆNOST

Drago Cvijanović¹ ID, Aleksandra Vujko² ID, Božo Ilić² ID

¹Fakultet za hotelijerstvo i turizam u Vrnjačkoj Banji, Univerzitet u Kragujevcu, Srbija ² Fakultet za turistički i hotelijerski menadžment, Univerzitet Singidunum, Beograd, Srbija

³ Akademija strukovnih studija Šumadija, Departman Aranđelovac, Srbija

Ova studija istražuje odnos između lokacije hotela i upoznatosti zaposlenih sa konceptom i tehnologijama Hospitality 4.0 u pet zemalja Zapadnog Balkana: Albaniji, Bosni i Hercegovini, Crnoj Gori, Severnoj Makedoniji i Srbiji. Korišćenjem strukturisanog upitnika i hi-kvadrat testova na uzorku od 250 zaposlenih u hotelijerstvu, istraživanje analizira pet ključnih varijabli: upoznatost sa Hospitality 4.0, razumevanje povezanih tehnologija, podršku menadžmenta za principe Hospitality 4.0, percipirani transformativni uticaj i usklađenost sa budućim trendovima u turizmu. Rezultati pokazuju statistički značajne veze između zemlje i svih pet varijabli (p < 0,001 u većini slučajeva), što ukazuje da nacionalni kontekst značajno utiče na svest i usvajanje koncepta Hospitality 4.0. Ispitanici iz Albanije i Bosne i Hercegovine pokazali su najviši nivo upoznatosti i organizacione podrške, dok su Crna Gora i Severna Makedonija pokazale niže nivoe svesti i angažovanosti. U Srbiji su primećene unutrašnje razlike, sa izraženim visokim i niskim nivoima saglasnosti. Ovi rezultati ukazuju na neujednačen napredak u digitalnoj transformaciji sektora hotelijerstva u regionu. Studija naglašava potrebu za cilianom politikom, programima obuke u industriji i međuzemaliskom razmenom znanja kako bi se podržao kohezivan prelaz ka Hospitality 4.0. Ovo istraživanje doprinosi razumevanju regionalne dinamike usvajanja tehnologije u hotelijerstvu i nudi praktične uvide za unapređenje inovacija u upravljanju hotelima.

Ključne reči: Hospitality 4.0; Zapadni Balkan; hotelska industrija; digitalna transformacija; pametni turizam; inovacije; hi-kvadrat analiza; regionalni razvoj





- 1. Dr. Anita Tarbuk, Full Professor, Faculty of Textile Technology, University of Zagreb, Zagreb, Croatia
- 2. Dr. Tihana Dekanić, Associate Professor, Faculty of Textile Technology, University of Zagreb, Zagreb, Croatia
- 3. Dr. Sandra Flinčec Grgac, Full Professor, Faculty of Textile Technology, University of Zagreb, Zagreb, Croatia
- 4. Dr. Igor Jordanov, Full Professor, Faculty of Technology and Metallurgy, Institute of Textile Engineering, Ss. Cyril and Methodius University in Skopje, North Macedonia
- Dr. Emilija Toshikj, Associate Proffessor, Ss. Cyril and Methodius University in Skopje, Faculty of Technology and Metallurgy, Department of Textile Engineering, Skopje, North Macedonia
- 6. Dr. Ljubica Tasic, Associate professor, Institute of Chemistry, University of Campinas, Sao Paulo, Brazil
- 7. Dr. Zou Xiaobo, Full Professor, School of Food and Biological Engineering, Jiangsu University, Jiangsu, China
- 8. Dr. Marcela-Elisabeta Barbinta-Patrascu, Associate professor, Faculty of Physics, University of Bucharest, Bucharest, Romania
- 9. Dr. Snežina Andonova, Full Professor, Faculty of Engineering, South-West University "Nefil Rilski", Blagoevgrad, Bulgaria
- Dr. Jelka Geršak, Full Professor, Research and Innovation Centre for Design and Clothing Science, University of Maribor, Faculty of Mechanical Engineering, Slovenia
- 11. Dr. Svjetlana Janjić, Full Professor, University of Banja Luka, Faculty of Technology, Banja Luka, Bosnia and Herzegovina
- 12. Dr. Mirjana Petronijević, Senior Scientific Associate, University of Novi Sad, Faculty of Technology, Novi Sad, Serbia
- 13. Dr. Aleksandra Zarubica, Full Professor, University of Niš, Faculty of Natural Sciences and Mathematics, Department of Chemistry, Niš, Serbia
- 14. Dr. Miloš Kostić, Senior Scientific Associate, The Faculty of Sciences and Mathematics, University of Niš, Serbia
- 15. Dr. Marija Kodrić, Innovation Center, University of Nis, Niš, Serbia
- Dr. Olivera Stamenković, Full Professor, Faculty of Technology, University of Niš, Leskovac, Serbia
- 17. Dr. Dragan Đorđević, Full Professor, Faculty of Technology, University of Niš, Leskovac, Serbia
- 18. Dr. Sandra Konstantinović, Full Professor, Faculty of Technology, University of Niš, Leskovac, Serbia
- 19. Dr. Bojana Danilović, Full Professor, Faculty of Technology, University of Niš, Leskovac, Serbia
- 20. Dr. Nada Nikolić, Full Professor, Faculty of Technology, University of Niš, Leskovac, Serbia

- 21. Dr. Dušan Trajković, Full Professor, Faculty of Technology, University of Niš, Leskovac. Serbia
- 22. Dr. Saša Savić, Associate Professor, Faculty of Technology, University of Niš, Leskovac, Serbia
- 23. Dr. Milan Kostič, Assistant Professor, Faculty of Technology, University of Niš, Leskovac, Serbia
- 24. Dr. Nenad Ćirković, Assistant Professor, Faculty of Technology, University of Niš, Leskovac, Serbia
- 25. Dr. Tatajana Šarac, Assistant Professor, Faculty of Technology, University of Niš, Leskovac, Serbia
- 26. Dr. Jovana Stepanović Profirovič, , Assistant Professor, Faculty of Technology, University of Niš, Leskovac, Serbia
- 27. Dr. Slobodan Glišić, College Lecturer, Academy of applied studies Southern Serbia, Department of Leskovac, Business School, Leskovac, Sebia
- 28. Dr. Dragana Ilić, Professor of Vocational Studies, Academy of Applied Studies Southern Serbia, Department of Leskovac, Business School, Leskovac, Sebia